



Kasdi Merbah University - Ouargla

Faculty of Applied Sciences

Department of Process Engineering

Dissertation Submitted in Partial Fulfillment of the Requirement for the Degree
of PhD in Process Engineering, Option: Process and environment

**Valorization of Date Palm By-Products from some
Cultivars: Environmental Application**

**Valorization des sous-produits de certaines variétés de palmier
dattier: Application environnementale**

Presented by the Candidate: Hind Bouafia

Defended and Approved in: 15/02/2026

Board of Examiners:

Pr Nasreddine Chennuf	University of Ouargla	President
Pr Mohamed Lamine Sekirifa	University of Ouargla	Supervisor
Dr Youcef Touil	University of Ouargla	Co-supervisor
Dr Hicham Siboukeur	University of Ouargla	Examiner
Pr Abdelhamid Khalaf	University of Ouargla	Examiner
Pr Salah Eddine LAOUINI	University of Elouad	Examiner
Dr Laid ZEGHOUD	University of Elouad	Examiner

Academic Year: 2025/2026

Dedication

I would like to dedicate this work to.....

My mother KABDI FAFIHA

My father's pure soul TAHAR

My Husband GOUDJIL MOHAMMED and my kids KINANE and MISK

My Sisters WARDA, SOUMIA and Brother MOHAMMED

My aunt BOUAFIA FATIHA

All my family

All my Friends

Hind Bouafia

Acknowledgment

I would like to express my sincere gratitude to my supervisor, Professor **SEKIRIFA MOHAMED LAMINE** at the University of KASDI MERBAH Ouargla, for his invaluable guidance, continuous support, and insightful advice throughout the development of this thesis. His dedication and encouragement were instrumental in shaping my research.

I am also deeply thankful to my co-supervisor **TOUIL YUCEF** for his persistent counsel and unwavering commitment that greatly facilitated the completion of this work.

My heartfelt thanks go to the members of the examination committee: Professors for their time, constructive feedback, and thoughtful evaluations.

I am grateful to the staff and engineers of the *Laboratoire de Biogéochimie des Milieux Désertiques* at KASDI MERBAH University of *Ouargla* for their technical assistance and collaborative spirit.

Special appreciation is extended to the *Research Center for Physico-Chemical Analysis*, especially its director **BELKHALFA HAKIM** for the generous provision of facilities and resources essential to this research.

I would also like to thank **Mr. GADJA OMAR** engineer at the *Laboratoire de Géologie du Sahara*, for his valuable services and technical support.

My sincere thanks are given to the *National Agency for Water Resources (ANRH Ouargla)*, particularly to the laboratory manager **MASSAOUDI SALIMA** for their cooperation and facilitation in conducting the necessary analyses.

Finally, I wish to thank everyone who contributed, whether materially or morally, to the successful completion of this thesis. Above all, I am profoundly grateful to my mother and my husband, whose encouragement and steadfast support were fundamental to my perseverance and success in this endeavor. Thank you all.

Abstract

This study investigates the use of agricultural date palm by-products (leafy fronds and empty fruit bunches of three cultivars *Ghars*, *Degla* and *Takermost*) as sustainable, low-cost biosorbents for the removal of methylene blue dye from aqueous solutions. The research encompasses chemical modifications—using KOH and H₂SO₄ treatments—of the adsorbent materials, their physicochemical characterization, and systematic adsorption experiments to elucidate the key factors influencing adsorption efficiency and mechanisms. Among the modifications, KOH treatment notably enhanced the adsorption capacities, with maximum capacity reaching approximately 4.48 mg/g and dye removal efficiency exceeding 99%. This was linked to the increased surface functional groups and porosity, as confirmed by FTIR, XRD, and SEM analyses.

Adsorption was affected by pH, temperature, contact time, and initial concentration, adapting to the Freundlich and Temkin isotherm models, indicative of heterogeneous and cooperative adsorptive interactions. Kinetic analyses consistently aligned with a pseudo-second-order model. Thermodynamic studies revealed spontaneous and exothermic adsorption under ambient conditions. The multistep adsorption mechanism encompasses surface adsorption, external film diffusion, and intraparticle diffusion, which are influenced by the adsorbent type, chemical modification, and dye concentration.

It was observed that there are differences among the palm cultivars *Degla*, *Ghars*, and *Takermost*, highlighting the impact of cultivar variation on adsorption performance

Bioadsorptive membranes were prepared from KOH-modified empty fruit bunch biomass (*Ghars* cultivar) combined with sodium alginate for use in treating drainage water in the region between *Said Otba* and *Ain El Beida* in the Wilaya of *Ouargla*. These membranes effectively reduced the biochemical oxygen demand by 50%, the chemical oxygen demand by 23.3%, and the total suspended solids by 36%.

Key words: Date palm biomass, Cultivar, Chemical modification, Adsorption, Methylene blue removal, Bioadsorptive membrane.

Résumé

Cette étude examine l'utilisation des sous-produits agricoles de palmier dattier (les palmes et les régimes de trois cultivars *Ghars*, *Degla* et *Takermost*) comme biosorbants durables et à faible coût pour l'élimination du colorant bleu de méthylène à partir de solutions aqueuses. Elle inclut des modifications chimiques des matériaux sorbants (traitement au KOH et au H₂SO₄), leur caractérisation physico-chimique, ainsi que des expériences d'adsorption systématiques afin de déterminer les facteurs clés influant sur l'efficacité et le mécanisme d'adsorption. Parmi les traitements appliqués, celui au KOH a nettement amélioré la capacité d'adsorption, avec une capacité maximale d'environ 4,48 mg/g et un taux d'élimination du colorant dépassant 99 %. Cette amélioration s'explique par l'augmentation des groupes fonctionnels en surface et de la porosité, comme l'ont confirmé les analyses FTIR, DRX et MEB.

L'adsorption a été influencée par le pH, la température, le temps de contact et la concentration initiale, suivant les modèles d'isothermes de Freundlich et Temkin, témoignant d'interactions adsorptives hétérogènes et coopératives. Les analyses cinétiques se sont systématiquement conformées au modèle pseudo-second ordre. Les études thermodynamiques ont révélé une adsorption spontanée et exothermique dans des conditions ambiantes. Le mécanisme d'adsorption multistep englobe l'adsorption superficielle, la diffusion à travers la couche externe et la diffusion intraparticulaire, influencés par le type d'adsorbant, la modification chimique et la concentration en colorant.

Il a été observé qu'il existe des différences entre les cultivars de palmier *Degla*, *Ghars* et *Takermost*, mettant en évidence l'influence de la variation des cultivars sur la performance de l'adsorption.

Des membranes bioadsorptives ont été préparées à partir de biomasse de régimes vides modifiée au KOH (cultivar *Ghars*) combinée à d'alginate de sodium, destinées au traitement des eaux de drainage dans la région située entre *Saïd Attaba* et *Ain El Beyda* dans la wilaya de *Ouargla*. Ces membranes ont réduit efficacement la demande biochimique en oxygène de 50%, la demande chimique en oxygène de 23,3% et les matières en suspension totales de 36%.

Mots-clés : Biomasse de palmier dattier, Cultivar, Modification chimique, Adsorption, Élimination du bleu de méthylène, Membrane bioadsorptive.

الملخص

بحثت هذه الدراسة استخدام مخلفات النخيل الزراعية (الجريد والعراجين لثلاث أصناف غرس، *نقلة* و*تكرموست*) كميزات حيوية مستدامة ومنخفضة التكلفة لإزالة صبغة أزرق الميثيلين من المحاليل المائية. تشتمل الدراسة على التعديلات الكيميائية - بالمعالجات KOH و H_2SO_4 - للمواد الممتازة و التوصيف الفيزيائي والكيميائي لها والتجارب المنهجية للامتزاز لتوضيح العوامل الرئيسية المؤثرة على كفاءة وآلية الامتزاز. من بين التعديلات، عززت المعالجة بـ KOH بشكل ملحوظ قدرات الامتزاز، حيث وصلت السعة القصوى إلى حوالي 4.48 ملغم/غرام مع كفاءة إزالة صبغة تجاوزت 99%، ويُعزى ذلك إلى زيادة مجموعات الوظائف السطحية والمسامية، كما تم تأكيده من خلال تحاليل FTIR و XRD و SEM.

تأثرت عملية الامتزاز بعوامل مثل درجة الحموضة، ودرجة الحرارة، ومدة التلامس، وتركيز الصبغة الابتدائي، متوافقة مع نماذج الامتزاز متساوي الحرارة لفرندليش وتيمكين، والتي تشير إلى تفاعلات امتزازية غير متجانسة وتعاونية. أظهرت الدراسات الحركية توافقاً مستمراً مع نموذج الامتزاز من الدرجة الثانية الزائف. كشفت الدراسات الحرارية أن الامتزاز كان تلقائياً وطارداً للحرارة في الظروف المحيطة. تشمل آلية الامتزاز متعددة المراحل الامتزاز السطحي، والانتشار عبر الغشاء الخارجي، والانتشار داخل الجزيئات، والتي تتأثر بنوع المادة الممتازة، والتعديل الكيميائي، وتركيز الصبغة.

لوحظ أن هناك فروق بين أصناف النخيل *نقلة*، *غرس*، و*تكرموست*، مما يبرز تأثير اختلاف الصنف على أداء الامتزاز.

تم تحضير أغشية حيوية مازة معدة من كتلة العرجون المعدلة بـ KOH (صنف الغرس) إضافة إلى ألجينات الصوديوم، لاستخدامها في معالجة مياه الري بالمنطقة الواقعة بين سعيد عتبة وعين البيضاء بولاية ورقلة، حيث خفضت هذه الأغشية بشكل فعال الطلب البيوكيميائي على الأكسجين بنسبة 50%، والطلب الكيميائي على الأكسجين بنسبة 23.3%، والمواد العالقة الكلية بنسبة 36%.

الكلمات المفتاحية: كتلة نخيل التمر، الصنف، التعديل الكيميائي، الامتزاز، إزالة الأزرق الميثيلين، الغشاء الممتز الحيوي.

Table of Contents

Subjects	Page
Dedication	I
Acknowledgment	II
English Abstract	III
French Abstract	IV
Arabic Abstract	V
Table of Contents	VI
List of Tables	XII
List of Figures	XIII
Nomenclature	XVI
General Introduction	1
Chapter 1: Bibliographic Summary	
Introduction	5
I. General overview of water	5
I.1. Water: description, molecular composition, structure, and stability	5
I.2. The essential role of water in life and ecosystems	7
I.3. Physical properties and chemical behavior of water	8
I.3.1. Physical properties of water	9
I.3.2. Chemical behavior of water	10
II. Fundamentals of water pollution	10
II.1. Definition and scope of water pollution	10
II.2. Types of water pollution	10

II.3. Sources of water contamination	11
II.4. Pollution indicators and water quality parameters	12
II.5. Impacts of water pollution	13
II.5.1. Human health impacts	13
II.5.2. Ecological impacts	14
II.5.3. Economic implications	14
III. Synthetic dyes as emerging water pollutants	14
III.1. Classification of synthetic dyes	14
III.2. Industrial applications of synthetic dyes	15
III.3. Pathways of dye discharge into aquatic systems	15
III.4. Environmental and health hazards of dye pollution	16
III.4.1. Environmental impact	16
III.4.2. Health hazards	17
III.5. Overview of dye removal techniques	18
III.5.1. Adsorption techniques	18
III.5.2. Chemical methods	19
III.5.3. Biological methods	20
III.5.4. Membrane filtration and electrochemical methods	20
IV. Adsorption as a green approach for dye removal	21
IV.1. Definition of adsorption	21
IV.2. Fundamental mechanisms of adsorption	21
IV.3. Types of Adsorption	22
IV.3.1. Physisorption	22
IV.3.2. Chemisorption	22

IV.3.3. Interplay and transition between physisorption and chemisorption	23
IV.4. Influencing parameters	23
IV.4.1. Adsorbent properties	23
IV.4.2. Dye properties	24
IV.4.3. Solution chemistry	24
IV.5. Adsorption thermodynamics	25
IV.6. Isotherm models applied to dye adsorption	25
IV.6.1. Adsorption capacity and removal efficiency	26
IV.6.2. Types of curve for adsorption	26
IV.6.3. Adsorption isotherms models	27
IV.6.3.1. Langmuir isotherm	27
IV.6.3.2. Freundlich isotherm	28
IV.6.3.3. Temkin isotherm	28
IV.7. Adsorption kinetics	29
IV.7.1. The intraparticle and external film diffusion models	29
IV.7.2. Pseudo-first-order model	30
IV.7.3. Pseudo-second-order model	30
V. Date palm waste as a sustainable bioadsorbent for dye removal	31
V.1. Biological and morphological characteristics of Phoenix dactylifera L.	31
V.1.1. Taxonomy and origin	31
V.1.2. Plant structure	31
V.1.3. Environmental adaptations	32

V.2. Comparative analysis of date palm cultivars: <i>Ghars</i>, <i>Degla</i>, and <i>Takermost</i>	33
V.2.1. Morphological characteristics of palms and fruits	33
V.2.2. Fruit Quality and Physicochemical Properties	34
V.2.3. Biochemical and nutritional profiles	35
V.2.4. Agronomic and ecological implications	35
V.3. Date palm production and waste: global, African, and Algerian perspectives	36
V.4. Adsorption capacities of date palm-based adsorbents	37
Conclusion	38
Chapter 2: Review of Adsorption Studies Using Raw and Modified Plant Wastes for Water Treatment: With Emphasis on Date Palm Biomass	
Introduction	40
I. Adsorption using raw plant-based wastes	40
II. Biochar derived from plant wastes: thermal conversion and adsorptive applications	44
III. Chemically Modified Plant Wastes for Water Treatment	47
Conclusion	50
Chapter 3: Modifications of Date Palm By-Products (Materials and Methods)	
Introduction	52
I. Biomass collection area	52
II. Chemicals	53
III. Preparation of adsorbents	54
IV. Characterization of adsorbents	56
IV.1. FTIR analysis	56
IV.2. XRD and XRF analysis	56

IV.3. SEM analysis	57
V. Batch adsorption studies	57
V.1. Adsorbate	57
V.2. Contact time effect	57
V.3. Initial dye concentration effect	58
V.4. pH effect	58
V.5. Temperature effect	58
Conclusion	58
Chapter 4: Results and Discussion	
Introduction	61
I. Fourier Transform Infrared Spectroscopy (FTIR) analysis	62
II. X-ray Diffraction (XRD) / X-ray Fluorescence (XRF) analysis	65
III. Scanning Electron Microscopy (SEM) analysis	70
IV. Fundamental study of the adsorption of MB on date palm biomasses	74
IV.1. Factors affecting the adsorption procedure	74
IV.1.1. Effect of pH	74
IV.1.2. Effect of contact time	78
IV.1.3. Effect of temperature	81
IV.1.4. Effect of initial concentration	87
IV.2. Adsorption equilibrium	91
IV.2.1. Adsorption isotherms	91
IV.2.2. Modeling results	95
IV.2.3. Adsorption kinetics	101
IV.2.4. Adsorption mechanism	111

Conclusion	120
Chapter 5: Application of Modified Date Palm Biomass for Wastewater Treatment	
Introduction	122
I. Degradation and Pollution of Water Resources in Ouargla Region	122
II. Advances in Adsorptive Membranes for Wastewater Treatment and Desalination	123
III. Materials and methods	124
III.1. Materials	124
III.2. Preparation of alginate-KOH-FBG adsorptive membrane	124
III.3. Location of sampling point	125
III.4. Filtration system design	128
IV. Results and discussion	128
Conclusion	131
General Conclusion	133
References	137

List of Tables

Table N°	Title	Page
Table I.1	Physical properties of liquid water	9
Table III.1	List of chemicals	53
Table IV.1	The crystallinity index CI_{XRD} of each sample	67
Table IV.2	Thermodynamic parameters for adsorption of MB onto raw and modified leafy fronds of three cultivars	86
Table IV.3	Thermodynamic parameters for adsorption of MB onto raw and modified empty fruit bunch of three cultivars	87
Table IV.4	Langmuir, Freundlich, and Temkin Constants for adsorption of MB onto raw and modified leafy fronds of three cultivars at 25 °C using the linear method	100
Table IV.5	Langmuir, Freundlich, and Temkin Constants for adsorption of MB onto raw and modified empty fruit bunch of three cultivars at 25 °C using the linear method	101
Table IV.6	Pseudo-first-order and pseudo-second-order adsorption rate constants and calculated $q_{e,cal}$ values of MB onto raw and modified leafy fronds of three cultivars at 25 °C	109
Table IV.7	Pseudo-first-order and pseudo-second-order adsorption rate constants and calculated $q_{e,cal}$ values of MB onto raw and modified empty fruit bunch of three cultivars at 25 °C	110
Table IV.8	External film and intraparticle diffusion parameters of MB adsorption onto raw and modified leafy frond of three cultivars at 25 °C	118
Table IV.9	External film and intraparticle diffusion parameters of MB adsorption onto raw and modified empty fruit bunch of three cultivars at 25 °C	119
Table V.1	Physicochemical parameters of effluent and filtrate	130

List of Figures		
Figure N°	Title	Page
Figure I.1	Water molecule	6
Figure I.2	Immediate and secondary effects of textile dyes on different materials and environments	16
Figure I.3	Dye removal techniques	19
Figure I.4	System of isotherm classification	27
Figure I.5	Diagrammatic representation of date palm structure	32
Figure I.6	Fruits of three cultivars <i>Degla</i> , <i>Ghars</i> and <i>Takermost</i>	35
Figure III.1	Geographical map of biomass sampling area	53
Figure III.2	Modification of date palm biomasses of three cultivars plan	55
Figure III.3	(a) Raw leafy fronds of <i>Takermost</i> cultivar (RLT), (b) H ₂ SO ₄ modified leafy fronds of <i>Takermost</i> cultivar (H ₂ SO ₄ -LT), (c) KOH modified leafy fronds of <i>Takermost</i> cultivar (KOH-LT)	56
Figure IV.1	The FTIR spectra of raw and modified leafy fronds of three cultivars	63
Figure IV.2	The FTIR spectra of raw and modified empty fruit bunch of three cultivars	64
Figure IV.3	XRD patterns of all samples	66
Figure IV.4	XRF spectra of raw and modified leafy fronds of three cultivars	68
Figure IV.5	XRF spectra of XRD of raw and modified empty fruit bunch of three cultivars	69
Figure IV.6	SEM images of RLG, H ₂ SO ₄ -LG and KOH-LG	71
Figure IV.7	SEM images of RFBG, H ₂ SO ₄ -FBG and KOH-FBG	72
Figure IV.8	SEM images of RLG, H ₂ SO ₄ -LG, KOH-LG, RFBG, H ₂ SO ₄ -FBG and KOH-FBG after adsorption of MB	73
Figure IV.9	Effect of pH on the adsorption of MB onto raw and modified leafy fronds of three cultivars (C ₀ = 30 mg/l, m = 1 g, V=50 ml, agitation speed =200 rpm, T=25 ± 1 °C, contact time =1 h)	76
Figure IV.10	Effect of pH on the adsorption of MB onto raw and modified empty fruit bunch of three cultivars (C ₀ = 30 mg/l, m = 1 g, V=50 ml, agitation speed =200 rpm, T=25 ± 1 °C, contact time =1 h)	77

Figure IV.11	Effect of contact time on the adsorption of MB onto raw and modified leafy fronds of three cultivars ($C_0 = 30$ mg/l, $m = 1$ g, $V=50$ ml, agitation speed =200 rpm, $T=25 \pm 1$ °C, $pH=5.4$)	79
Figure IV.12	Effect of contact time on the adsorption of MB onto raw and modified empty fruit bunch of three cultivars ($C_0 = 30$ mg/l, $m = 1$ g, $V=50$ ml, agitation speed =200 rpm, $T=25 \pm 1$ °C, $pH=5.4$)	80
Figure IV.13	Effect of temperature on the adsorption of MB onto raw and modified leafy fronds of three cultivars ($C_0 = 30$ mg/l, $m = 1$ g, $V=50$ ml, agitation speed =200 rpm, contact time =1 h, $pH=5.4$)	81
Figure IV.14	Effect of temperature on the adsorption of MB onto raw and modified empty fruit bunch of three cultivars ($C_0 = 30$ mg/l, $m = 1$ g, $V=50$ ml, agitation speed =200 rpm, contact time =1 h, $pH=5.4$)	83
Figure IV.15	Plot of $\ln K_d$ vs. $1/T$ for estimation of thermodynamic parameters for the adsorption of MB onto raw and modified leafy fronds and empty fruit bunch of three cultivars	85
Figure IV.16	Effect of initial concentration on the adsorption of MB onto raw and modified leafy fronds of three cultivars ($m = 1$ g, $V=50$ ml, agitation speed =200 rpm, contact time =1 h, $T=25 \pm 1$ °C)	89
Figure IV.17	Effect of initial concentration on the adsorption of MB onto raw and modified empty fruit bunch of three cultivars ($m = 1$ g, $V=50$ ml, agitation speed =200 rpm, contact time =1 h, $T=25 \pm 1$ °C)	90
Figure IV.18	Adsorption isotherms of MB onto raw leafy fronds and empty fruit bunch of three cultivars	92
Figure IV.19	Adsorption isotherms of MB onto H_2SO_4 -modified leafy fronds and empty fruit bunch of three cultivars	93
Figure IV.20	Adsorption isotherms of MB onto KOH -modified leafy fronds and empty fruit bunch of three cultivars	94
Figure IV.21	Langmuir isotherm plots for adsorption of MB onto raw and modified leafy fronds and empty fruit bunch of three cultivars	97
Figure IV.22	Freundlich isotherm plots for adsorption of MB onto raw and modified leafy fronds and empty fruit bunch of three cultivars	98
Figure IV.23	Temkin isotherm plots for adsorption of MB onto raw and modified leafy fronds and empty fruit bunch of three cultivars	99
Figure IV.24	Pseudo-first-order plot for adsorption of MB onto raw leafy fronds and empty fruit bunch of three cultivars	103

Figure IV.25	Pseudo-first-order plot for adsorption of MB onto H₂SO₄-modified leafy fronds and empty fruit bunch of three cultivars	104
Figure IV.26	Pseudo-first-order plot for adsorption of MB onto KOH-modified leafy fronds and empty fruit bunch of three cultivars	105
Figure IV.27	Pseudo-second-order plot for adsorption of MB onto raw leafy fronds and empty fruit bunch of three cultivars	106
Figure IV.28	Pseudo-second-order plot for adsorption of MB onto H₂SO₄-modified leafy fronds and empty fruit bunch of three cultivars	107
Figure IV.29	Pseudo-second-order plot for adsorption of MB onto KOH-modified leafy fronds and empty fruit bunch of three cultivars	108
Figure IV.30	External film diffusion plot for adsorption of MB onto raw leafy fronds and empty fruit bunch of three cultivars	112
Figure IV.31	External film diffusion plot for adsorption of MB onto H₂SO₄-modified leafy fronds and empty fruit bunch of three cultivars	113
Figure IV.32	External film diffusion plot for adsorption of MB onto KOH-modified leafy fronds and empty fruit bunch of three cultivars	114
Figure IV.33	Intraparticle diffusion plot for adsorption of MB onto raw leafy fronds and empty fruit bunch of three cultivars	115
Figure IV.34	Intraparticle diffusion plot for adsorption of MB onto H₂SO₄-modified leafy fronds and empty fruit bunch of three cultivars	116
Figure IV.35	Intraparticle diffusion plot for adsorption of MB onto KOH-modified leafy fronds and empty fruit bunch of three cultivars	117
Figure V.1	Preparation of alginate-KOH-FBG adsorptive membrane plan	126
Figure V.2	Sampling point of drainage water	127
Figure V.3	Location of sampling point	127
Figure V.4	Filtration system setup	129

Nomenclature

ABA	ABscisic Acid
ANRH	National Agency for Water Resources (Agence Nationale des Ressources Hydriques)
AOPs	Advanced Oxidation Processes
B	Temkin constant related to the adsorption heat (J/mol)
BOD₅	Biochemical Oxygen Demand (mg/l)
C	Intercept relates to the boundary layer thickness
C₀	Initial concentration of adsorbate (mg/l)
C_e	Residual concentration of adsorbate (mg/l)
CI_{XRD}	Crystallinity Index (%)
COD	Chemical Oxygen Demand (mg/l)
EC	Electrical Conductivity ($\mu\text{s}/\text{cm}$)
FTIR	Fourier Transform Infrared Spectroscopy
H₂SO₄-FBD	H ₂ SO ₄ modified empty Fruit Bunch <i>Degla</i>
H₂SO₄-FBG	H ₂ SO ₄ modified empty Fruit Bunch <i>Ghars</i>
H₂SO₄-FBT	H ₂ SO ₄ modified empty Fruit Bunch <i>Takermost</i>
H₂SO₄-LD	H ₂ SO ₄ modified Leafy frond <i>Degla</i>
H₂SO₄-LG	H ₂ SO ₄ modified Leafy frond <i>Ghars</i>
H₂SO₄-LT	H ₂ SO ₄ modified Leafy frond <i>Takermost</i>
K_d	Equilibrium constant
K_{efd}	Rate constant of external film diffusion model (min^{-1})
K_F	Freundlich adsorption constant related to adsorption capacity [$(\text{mg} \cdot \text{g}^{-1}) \cdot (\text{l} \cdot \text{mg}^{-1})^{1/n}$]
K_{id}	Rate constant of intraparticle diffusion model ($\text{mg} \cdot \text{g}^{-1} \cdot \text{min}^{-1/2}$)
K_L	Langmuir adsorption constant related to affinity (l/mg)
KOH-FBD	KOH modified empty Fruit Bunch <i>Degla</i>
KOH-FBG	KOH modified empty Fruit Bunch <i>Ghars</i>
KOH-FBT	KOH modified empty Fruit Bunch <i>Takermost</i>
KOH-LD	KOH modified Leafy frond <i>Degla</i>
KOH-LG	KOH modified Leafy frond <i>Ghars</i>
KOH-LT	KOH modified Leafy frond <i>Takermost</i>
K_T	Temkin equilibrium binding constant (l/g)
k₁	Pseudo-first-order rate constant (min^{-1})
k₂	Pseudo-first-order rate constant ($\text{g} \cdot \text{mg}^{-1} \cdot \text{min}^{-1}$)
LCAs	Low-Cost Adsorbents
m	Adsorbent mass (g)
MB	Methylene Blue

n	Value indicates adsorption intensity
PFO	Pseudo-first-order
pH	potential of Hydrogen
PSO	Pseudo-second-order
q_e	Adsorption capacity at equilibrium (mg/g)
q_{e,cal}	Calculated adsorption capacity at equilibrium (mg/g)
q_m	Monolayer or maximal adsorption capacity (mg/g)
q_t	Adsorption capacity at time t (min)
R	Universal gas constant=8.314.10 ⁻³ (kJ/mol.K)
R²	Correlation coefficient
RE	Removal Efficiency (%)
RFBD	Raw empty Fruit Bunch <i>Degla</i>
RFBG	Raw empty Fruit Bunch <i>Ghars</i>
RFBT	Raw empty Fruit Bunch <i>Takermost</i>
RLD	Raw Leafy frond <i>Degla</i>
RLG	Raw Leafy frond <i>Ghars</i>
RLT	Raw Leafy frond <i>Takermost</i>
ROS	Reactive Oxygen Species
SEM	Scanning Electron Microscopy
T	Temperature (°C or K)
t	Time (min)
TDS	Total Dissolved Solids (mg/l or ppm)
TSS	Total suspended solids (mg/l)
UV-Vis	UltraViolet-Visible
v	Solution volume (l)
VOCs	Volatile Organic Compounds
XRD	X-ray Diffraction
XRF	X-ray Fluorescence
ΔG°	Standard Gibbs free energy change (kJ/mol)
ΔH°	Standard enthalpy change (kJ/mol)
ΔS°	Standard entropy change (kJ/mol.K)
θ	Angle between the incident X-ray beam and the crystallographic planes within a sample
λ_{max}	Wavelength at which a molecule absorbs light most efficiently (nm)

General Introduction

Water is essential for life and supports ecosystems, human health, and socioeconomic development globally. It plays a crucial role in biological processes and is vital for agriculture, industry, and domestic use. However, freshwater resources are increasingly stressed by population growth, urbanization, and industrialization, leading to higher demand and declining water quality. Currently, over 2 billion people worldwide lack access to safe drinking water, highlighting the critical need for improved water management and pollution control [1].

Water pollution occurs when harmful organic and inorganic substances contaminate water bodies, negatively affecting aquatic life, biodiversity, and human health. Synthetic dyes, mainly from industries such as textiles, leather, paper, and food, pose a major environmental hazard due to their stability, toxicity, non-biodegradability, and ability to color water intensely even at low concentrations. This coloration reduces light penetration and disrupts photosynthesis in aquatic environments. Additionally, many dyes and their breakdown products are carcinogenic and mutagenic, posing serious health risks [2; 3].

Various physicochemical and biological methods, such as coagulation-flocculation, chemical oxidation, membrane filtration, and biological treatment, have been used to remove dyes and other pollutants from wastewater. However, these methods often face challenges such as high costs, incomplete removal, sludge production, and operational complexity. Adsorption has gained attention as an effective, economical, and eco-friendly alternative, which works by accumulating contaminants on adsorbent surfaces through physical or chemical means. It offers simplicity, high efficiency, and the possibility of adsorbent regeneration. Although activated carbon is the standard adsorbent, its high cost and energy demands have encouraged research into low-cost, sustainable adsorbents from agricultural waste [4; 5].

Date palm (*Phoenix dactylifera* L.) cultivation is economically and culturally significant, particularly in the arid and semi-arid regions of the Middle East and North Africa (MENA), including *Algeria*, which ranks among the top producers globally (out). The extensive cultivation of date palms generates considerable quantities of lignocellulosic waste, primarily fronds (leaves) and empty fruit bunches (rachis), which are often disposed of by open burning or landfilling, contributing to environmental pollution and resource wastage. Valorizing these residues represents a strategic opportunity to promote sustainable agricultural waste management, aligned with circular economy principles [6-8].

Owing to their lignocellulosic composition, which is rich in cellulose, hemicellulose, lignin, and functional groups (hydroxyl and carboxyl), date palm residues have demonstrated

promising adsorption potential for various pollutants, including synthetic dyes. Both raw and chemically modified date palm biomass have been explored to enhance adsorption capacity through acidic or alkaline treatments that modify surface chemistry and increase porosity and active binding sites [9; 10].

Despite the growing literature on the use of date palm biomass, most studies have focused on single cultivars or ignored comparative analyses between different cultivars and biomass types. Moreover, the influence of chemical modifications (acidic vs. alkaline) on adsorption efficacy across cultivars remains unexplored. Addressing this research gap is critical for optimizing adsorbent selection and treatment protocols that are suitable for local environmental applications.

This study aimed to valorize the by-products of date palms -specifically the leafy fronds and empty fruit bunches-from three cultivars: *Ghars*, *Degla*, and *Takermost*, collected from the *Ouargla* region in southern *Algeria*, for the removal of methylene blue dye from aqueous solutions.

While previous research in this domain has primarily emphasized the effects of parameters such as pH, temperature, initial pollutant concentration, and contact time on adsorption performance, this study introduces two pivotal factors for investigation:

- The type of chemical treatment applied to the biomass (acidic with H₂SO₄ vs. alkaline with KOH)
- The inherent influence of cultivar type on adsorption capacity and dye removal efficiency
- Evaluation of the practical application of these adsorbents for the treatment and purification of real contaminated waters, such as drainage water.

This approach allows for a comprehensive understanding of how genetic and chemical factors synergistically affect adsorption properties and offers insights into the tailored development of effective bioadsorbents.

This work is guided by the following key questions:

1. To what extent can raw and chemically modified date palm by-products from different cultivars effectively remove methylene blue and potentially other contaminants from aqueous solutions?

2. How do the type of chemical modification and cultivar origin influence the structural, chemical, and adsorption characteristics of these biomasses?
3. How do operational environmental conditions (pH, temperature, pollutant concentration, and contact time) interact with adsorbent properties to optimize the removal efficiency?
4. What are the adsorption mechanisms, kinetics, and thermodynamic parameters governing the uptake process of these materials?
5. Can these biosorbents be successfully developed into practical and scalable materials (e.g., bioadsorptive membranes) for real-world water purification applications, such as irrigation water treatment?

This dissertation is structured into five key chapters, each addressing critical aspects of the research:

The first provides a bibliographic overview of the molecular nature of water, its environmental importance, pollution challenges with emphasis on dyes, and the fundamentals of adsorption alongside valorization of date palm agricultural wastes.

The second chapter focuses on global research on adsorption by raw and chemically modified biomass, particularly date palm residues, and discusses their adsorption capacities, surface properties, modification methods, and gaps, particularly regarding cultivar influence.

The third section describes the collection and preparation of date palm biomass from *Ouargla*, chemical modifications, characterization techniques (FTIR, XRD, XRF, SEM), and the experimental design for adsorption studies.

The fourth section presents the physicochemical characterization and adsorption results, analyzing mechanisms, kinetics, isotherms, thermodynamics, and comparing cultivars and treatment effects on adsorption efficacy.

The fifth chapter demonstrates the fabrication of a sodium alginate-based bioadsorptive membrane incorporating KOH-modified biomass and assesses its performance for removing contaminants from drainage water.

Finally, a general conclusion summarizes the key scientific findings, confirms the viability of valorized date palm by-products for environmental remediation, and recommends avenues for further development and scale-up.

Chapter 1

Bibliographic Summary

Introduction:

Water pollution, particularly from synthetic dyes, poses significant environmental and health risks owing to their toxicity and persistence. Adsorption has emerged as a sustainable and cost-effective method for dye removal, leveraging the abundant and renewable nature of agricultural waste materials. Among these, date palm waste (*Phoenix dactylifera L.*) stands out because of its lignocellulosic composition, which offers rich functional groups and porous structures ideal for adsorption. This chapter explores the potential of date palm residues as bioadsorbents by examining their morphological and chemical properties, adsorption mechanisms, and comparative efficacy across cultivars. By valorising this agricultural byproduct, we addressed both waste management challenges and water pollution mitigation, aligning with circular economy principles and sustainable environmental practices.

I. General overview of water

I.1. Water: description, molecular composition, structure, and stability

Water is a fundamental inorganic compound with the chemical formula H_2O . It is a transparent, tasteless, odorless, and nearly colorless liquid under ambient conditions. Universally recognized as essential for life, water is also notable as the most abundant compound on Earth's surface, existing naturally in all three physical states: solid (ice), liquid, and gas (vapor) [11; 12].

Each water molecule comprises two hydrogen atoms covalently bonded to a single oxygen atom (H-O-H) [11; 13]. The hydrogen atoms are attached at an angle of approximately 104.5° (figure I.1), making the molecule “bent” rather than linear. Oxygen is more electronegative than hydrogen, resulting in an uneven sharing of electrons and creating a polar molecule with distinct partial charges, with oxygen being slightly negative and hydrogen slightly positive [13; 15]. This polarity underpins the unique solvent capabilities of water and its ability to dissolve many ionic and polar substances.

At the molecular level, the structure of water is defined by its polarity and hydrogen bonding. Each water molecule can form up to four hydrogen bonds: two via its hydrogen atoms and two via the lone electron pairs [16; 14]. This allows for the creation of a highly dynamic, tetrahedral, three-dimensional network in the liquid state, where bonds are constantly forming and breaking on the picosecond scale.

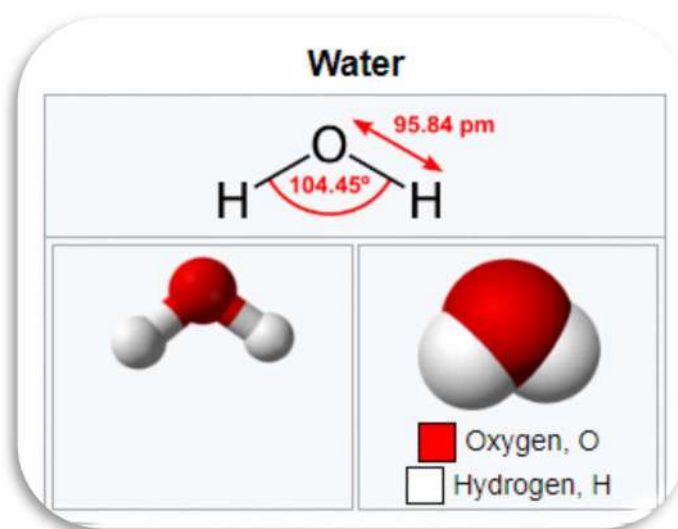


Figure I.1: Water molecule [14].

In ice (the solid phase), these hydrogen bonds arrange each molecule into a rigid hexagonal lattice, maintaining space between molecules, which explains why solid water is less dense (ice floats on water) [17].

The variability and strength of these hydrogen bonds confer water with “anomalous” physical properties, such as high boiling and melting points, high heat capacity, surface tension, and density anomalies near freezing [18; 19].

The stability of water can be considered from several perspectives: molecular, structural, and environmental.

- **Molecular stability:** The covalent O-H bonds within each molecule are strong and require high energy to break.
- **Structural stability:** In clusters, the extensive hydrogen-bond network of water stabilizes both small molecular aggregates and bulk phases. Water clusters (oligomers) often form stable cyclic or cage-like geometries, maximizing hydrogen bonding [19; 20].
- **Environmental stability:** Water’s resilience is evident in its ability to resist rapid temperature changes (high specific heat), buffer pH changes (as both acid and base), and resist phase changes, except under substantial temperature or pressure variations [18; 15].

Furthermore, the stability of water at interfaces, such as mineral or biological surfaces, and in confined environments (e.g., within proteins or clathrates) shows that the properties and

structures of water can adapt while maintaining remarkably robust hydrogen-bond networks [20; 21].

I.2. The essential role of water in life and ecosystems

Water is unparalleled in its significance for both living organisms and the environment. As the most abundant substance on Earth, water constitutes approximately 65–90% of the mass of living organisms and covers approximately 70% of the Earth's surface, thereby sustaining all known forms of life [22; 23]. Its centrality arises from its unique molecular and physical properties, which underpin the connectivity among living systems and ecosystem processes.

At the cellular and organismal levels, water fulfills various indispensable biological functions. It is the primary medium through which nutrients, waste products, and signaling molecules are transported throughout the body. The polarity and hydrogen-bonding capacity of water make it an exceptional solvent, enabling the complex chemistry of life to proceed efficiently [22; 24; 25].

Water is also central to the following:

- **Cellular homeostasis and osmoregulation:** Regulation of the internal environment and ensuring that cells maintain optimal turgidity and function [26].
- **Thermoregulation:** Facilitating heat dissipation in animals via sweating and transpiration in plants [23; 24].
- **Biochemical reactions:** Water acts as a reactant and medium for a vast range of enzymatic and metabolic reactions, including hydrolysis and condensation processes essential for cellular metabolism and macromolecular synthesis [22; 27; 28].
- **Molecular structure and stability:** Promoting the three-dimensional folding and stability of proteins and nucleic acids, largely as a result of hydrophilic and hydrophobic interactions driven by the structure [25; 27].
- **Acid–Base balance:** Buffering physiological systems and providing a reservoir for protons and hydroxide ions, which is vital for maintaining pH balance [24; 27].

Indeed, humans, like all animals, cannot survive for more than a few days without water, given its central role in both macro- and micro-physiological contexts [24; 26].

The role of water in the environment is equally profound. The ecosystem structure, function, and resilience fundamentally depend on water availability and quality [29; 30]. Key functions include:

- **Provisioning services:** Supplying drinking water, irrigation, and habitat for aquatic and terrestrial species, often mediated via surface and groundwater systems [29; 30].
- **Regulation and maintenance:** Enabling ecosystem services, such as flood regulation, nutrient cycling, waste filtration, and microclimate stabilization. For example, wetlands act as sponges and filters, moderating floods and purifying water before it re-enters aquifers or streams [29; 30].
- **Biodiversity habitats:** They provide the primary environment for aquatic life and play a crucial role at the interface between ecosystems. Freshwater habitats, such as rivers, lakes, and wetlands, support a disproportionate share of global biodiversity and vital life stages (e.g., spawning and migration) for many species [30; 31].
- **Support for energy flow and nutrient cycling:** Water transports organic and inorganic materials, driving food webs and supporting ecosystem productivity from local (e.g., riparian buffer zones) to global scales [30; 31].

Life on Earth almost certainly originated in water, with the early oceans serving as cradles for the chemical evolution that gave rise to the first living cells [32; 33]. Water's unusual physical traits, such as its high heat capacity, high surface tension, the anomaly of ice floating on liquid water, and solvent properties, create stable and supportive environments for life. These properties also buffer against abrupt environmental changes, fostering the resilience of both organisms and ecosystems [25].

Thus, water is not merely a passive backdrop for biological and ecological processes; rather, it is an active participant and determinant of structure, function, and resilience in life and ecosystems across scales. Consequently, preserving water resources is paramount for sustaining life and ensuring the continued functioning of planetary ecosystems [24; 22; 31].

1.3. Physical properties and chemical behavior of water

Water is a unique substance with distinct physical and chemical properties that are crucial for life and natural processes. The physical properties of a liquid are largely influenced by its molecular structure, which includes hydrogen bonding and dipolar characteristics. These properties affect the behavior of water in different states and its interactions with other

substances. Chemically, water acts as a universal solvent and participates in numerous reactions essential for biological and environmental systems. Table I.1 lists the most important physical properties of water at different temperatures.

Table I.1: Physical properties of liquid water [37]

<i>Temperature (°C)</i>	<i>Density (g/cm³)</i>	<i>Surface Tension (g/s²)</i>	<i>Dynamic Viscosity (g/cm/s)×10⁻²</i>	<i>Heat of Vaporization (cal/g)</i>	<i>Specific Heat (cal/g/°C)</i>	<i>Thermal Conductivity (cal/cm/s/°C)×10⁻³</i>
-10	0.99794	–	–	603.0	1.02	–
-5	0.99918	76.4	–	–	–	–
0	0.99987	75.4	1.7921	597.3	1.0047	1.34
4	1.00000	–	–	–	–	–
5	0.99999	74.8	1.5188	594.5	1.0037	1.37
10	0.99973	74.2	1.3077	591.7	1.0013	1.40
15	0.99913	73.4	1.1404	588.9	0.9998	1.42
20	0.99823	72.7	1.0050	586.0	0.9988	1.44
25	0.99708	71.9	0.8937	583.2	0.9983	1.46
30	0.99568	71.1	0.8007	580.4	0.9980	1.48
35	0.99506	70.3	0.7225	577.6	0.9979	1.50
40	0.99225	69.5	0.6560	574.7	0.9980	1.51
45	0.99024	68.7	0.5988	571.9	0.9982	1.53
50	0.98807	67.9	0.5494	569.0	0.9985	1.54

1.3.1. Physical properties of water

- ***Molecular structure and hydrogen bonding:*** Water molecules are dipolar, with a partial negative charge near the oxygen atom and a partial positive charge near hydrogen atoms. This polarity allows water molecules to form hydrogen bonds, which are stronger than van der Waals forces and contribute to water's unique properties [34; 35].
- ***Density and phase changes:*** Water has its maximum density at 4°C, which causes ice to float. This property is crucial for aquatic life, as it prevents bodies of water from freezing. Water's ability to exist in all three states—solid, liquid, and gas—under Earth's conditions is vital for the water cycle and climate regulation [36; 37].
- ***Surface tension and viscosity:*** Water's high surface tension is due to hydrogen bonding, which also affects its viscosity. These properties are important for processes like capillarity, which allows water to move through soil and plant tissues [34; 38].

- **Thermal properties:** Water has a high specific heat capacity, which means it can absorb a lot of heat without a significant increase in temperature. This property helps stabilize earth's climate and supports life by moderating temperature fluctuations [37; 39].

1.3.2. Chemical behavior of water

- **Solvent Properties:** Water is known as the "universal solvent" because it can dissolve a wide range of substances. This ability is due to its polarity, which allows it to interact with various ions and molecules, facilitating chemical reactions in biological and environmental systems [40; 41].
- **Reactivity and ionization:** Water can ionize into hydrogen and hydroxide ions, which is fundamental to acid-base chemistry. This ionization is crucial for maintaining pH balance in biological systems and for various chemical processes [37; 42].
- **Hydrogen bond network:** The extensive hydrogen bond network in water contributes to its anomalous properties, such as its high boiling and melting points compared to other similar-sized molecules. This network also plays a role in the solvation of ions and molecules, affecting their reactivity and stability [41; 43].

II. Fundamentals of water pollution

II.1. Definition and scope of water pollution

Water pollution is broadly defined as the contamination of water bodies by harmful substances, resulting in significant adverse changes in water quality and ecosystem health [2; 44]. This phenomenon encompasses the introduction of chemical, physical, or biological components that compromise the beneficial uses of water, including drinking, habitat provision, irrigation, and recreation [45]. Pollutants responsible for such degradation include toxic chemicals, heavy metals, organic compounds, and pathogens, which may originate from both natural processes and anthropogenic activities [2; 44].

II.2. Types of water pollution

There are diverse types of water pollution, each with distinct sources and impacts on the environment. Understanding these types and their sources is essential for developing effective strategies to mitigate water pollution and protect water quality in the future:

- **Point source pollution:** This type of pollution originates from identifiable sources, such as industrial discharges, wastewater treatment plants, and oil spills. These sources release pollutants directly into water bodies, making it easier to monitor and regulate [2].
- **Nonpoint source pollution:** Unlike point source pollution, nonpoint source pollution originates from diffuse sources, such as agricultural runoff, urban runoff, and atmospheric deposition. It is challenging to control due to its widespread nature and variability [2; 46].
- **Groundwater pollution:** This occurs when pollutants infiltrate the soil and contaminate underground water reserves. Common sources include agricultural chemicals, industrial waste, and leachate from landfills [2].
- **Surface water pollution:** This type involves the contamination of rivers, lakes and oceans. It is often caused by industrial effluents, agricultural runoff, and urban wastewater, leading to issues like eutrophication and habitat destruction [2; 47].

II.3. Sources of water contamination

- **Industrial activities:** Industries such as mining, manufacturing, and chemical processing release a variety of pollutants, including heavy metals, organic compounds, and toxic chemicals, into water bodies [48].
- **Agricultural practices:** The use of fertilizers, pesticides, and animal waste in agriculture contributes significantly to water pollution. These substances can lead to nutrient loading and the proliferation of harmful algal blooms [49].
- **Domestic waste:** Household waste, including sewage and detergents, often ends up in water bodies, introducing pathogens and organic pollutants that degrade the water quality [2; 46].
- **Urban runoff:** Urban areas contribute to water pollution through stormwater runoff, which carries pollutants such as oil, heavy metals, and debris from roads and buildings into nearby water bodies [50].
- **Natural Sources:** Although less common, natural events such as volcanic eruptions and sedimentation from heavy rainfall can contribute to water pollution. However, these are typically minor compared to anthropogenic sources [44].

II.4. Pollution indicators and water quality parameters

Water quality parameters are critical indicators of the health and usability of water resources. These parameters encompass a range of physical, chemical, and biological characteristics that determine the suitability of water for various uses, including drinking, agriculture, and industrial applications. Understanding these parameters is essential for effective water management and for controlling pollution:

- **pH:** The pH level of water indicates its acidity or alkalinity, which can affect aquatic life and the solubility of its chemical constituents. The pH values typically range from 6.81 to 8.33 across different water sources, with deviations that can potentially harm the ecosystems [51; 52].
- **Total Dissolved Solids (TDS):** measures the concentration of dissolved substances in water, affecting its taste and suitability for consumption. TDS levels can vary significantly, from 93 ppm in rainwater to 815 ppm in bore water [51; 53].
- **Turbidity:** This parameter measures the cloudiness of water, which can indicate the presence of suspended particles in the water. High turbidity levels, such as those consistently between 4-5 NTU, can exceed recommended limits and impact water quality [51; 54].
- **Hardness:** Water hardness, primarily due to calcium and magnesium ions, affects its suitability for domestic and industrial applications. Hardness levels can range from soft to very hard, with sea water exhibiting the highest hardness at 76.2 mg/l as CaCO₃ [51; 55].
- **BOD:** Biochemical Oxygen Demand (BOD) measures the total amount of dissolved oxygen consumed by microorganisms while breaking down organic substances, such as food waste or sewage. In rural ponds, elevated levels of phosphate, animal manure, and domestic sewage from dispersed sources can increase the organic load, resulting in higher BOD [52].
- **COD:** specifically measures the amount of organic material in a water sample that can be chemically oxidized using a strong oxidizing agent. It is commonly used to assess the potential for both organic and inorganic substances in water bodies, wastewater, and industrial discharges to oxidize. Thus, COD is a reliable indicator of water pollution levels. An increase in the concentration of organic and inorganic materials resulted in a higher COD value [52].

- **TSS:** Total suspended solids, also called non-filterable solids, refer to particles that cannot pass through a filter with 1-micron-sized pores. To determine the amount of TSS, a measured volume of sewage was filtered through a glass fiber filter apparatus, and the residue left on the filter was dried and weighed. The dry weight of the residue represented the concentration of suspended solids in the sample [52].
- **Nutrients (Nitrates and Phosphates):** Nitrates and phosphates are essential nutrients for the growth of aquatic plants; however, their excessive concentrations can lead to serious environmental issues, such as eutrophication and water pollution. Nitrates are mainly produced through nitrification processes, and agricultural activities, fertilizer use, and sewage significantly increase their levels in surface waters. When concentrations exceed safe limits, such as the 10 mg/l maximum set by the U.S. Environmental Protection Agency for drinking water; they pose health risks. Therefore, continuous monitoring of nitrate and phosphate levels is crucial for pollution management and limiting harmful algal blooms in aquatic environments [52; 54; 56].

II.5. Impacts of water pollution

Water pollution, caused by the introduction of harmful substances into water bodies, leads to the deterioration of water quality. This poses significant risks to human health, disrupts ecosystems, and threatens economic stability worldwide.

II.5.1. Human health impacts

- Water pollution is a significant public health threat, contributing to over 50 diseases and responsible for 80% of diseases and 50% of child deaths worldwide [57; 58].
- Contaminated water is a vector for waterborne diseases such as cholera, typhoid, and dysentery, with millions of cases reported annually [59; 2].
- Chronic exposure to pollutants such as arsenic, nitrates, and heavy metals can lead to severe health issues, including cancer, organ damage, and developmental disorders [57; 58].
- Diarrhea, primarily caused by enteroviruses in polluted water, is the most common waterborne illness and significantly impacts child health [58].

II.5.2. Ecological impacts

- Water pollution disrupts aquatic ecosystems, leading to the death of organisms, loss of biodiversity, and degradation of ecosystem services [59; 60].
- Eutrophication, caused by excessive nutrients, results in overabundant algal growth, alters aquatic environments, and depletes oxygen levels, which can lead to fish kills [2].
- Pollutants such as pesticides, heavy metals, and industrial waste accumulate in aquatic organisms, causing acute and chronic effects, including immune suppression and metabolic reduction in fish species [60].
- Biological magnification leads to increased concentrations of pollutants as they move up the food chain, affecting top predators and potentially humans [2].

II.5.3. Economic implications

- The economic costs of water pollution are substantial, including expenses related to pollution control, remediation, and healthcare for pollution-related diseases [61].
- Water pollution affects industries reliant on clean water, such as fisheries and tourism, leading to economic losses and reduced livelihoods for communities dependent on these sectors [61].
- Effective water pollution management, including wastewater treatment and pollution prevention measures, is crucial for economic sustainability and development [60].

III. Synthetic dyes as emerging water pollutants

Synthetic dyes are crucial components in various industries because of their vibrant colors and cost-effectiveness compared to natural dyes. They are primarily used in textiles but also find applications in food, medicine, cosmetics, and other fields. Synthetic dyes are classified based on their chemical structure and the type of fiber with which they are used. Their industrial applications are vast and diverse.

III.1. Classification of synthetic dyes

- **Chemical structure:** Synthetic dyes are classified based on their chemical structure, which determines their color properties and applications. Common classes of dyes include azo, anthraquinone, and phthalocyanine dyes. Azo dyes, characterized by the presence of one or more azo groups (-N=N-), are the most widely used in the textile industry [62].

- **Fiber type:** Dyes are classified according to the type of fiber they are intended for. For example, cellulose fibers use direct, reactive, and vat dyes; wool uses acid and mordant dyes; and synthetic fibers like polyester use disperse dyes [63].
- **Functional properties:** Some synthetic dyes are designed with additional functional properties, such as UV-absorbency, antimicrobial activity, and water repellency. These functional dyes are used in technical textiles for enhanced performance [64].

III.2. Industrial applications of synthetic dyes

- **Textile industry:** The textile industry is the largest consumer of synthetic dyes, utilizing them for coloring fabrics. The industry uses a wide range of dyes to achieve various shades and fastness properties, with an annual production of approximately 7×10^5 tons [62; 65].
- **Non-Textile applications:** Beyond textiles, synthetic dyes are used in non-textile applications such as food coloring, cosmetics, and pharmaceuticals. They serve as acid-base indicators, color filters for displays, and in ink-jet printing [66].
- **Technical textiles:** In technical textiles, dyes with additional properties, such as antimicrobial and UV protection, are used to enhance the functionality of the fabric, making them suitable for specialized applications [64].

III.3. Pathways of dye discharge into aquatic systems

- **Industrial effluents:** The textile industry is a primary source of dye discharge, with a significant portion of dyes lost during the dyeing process and directly entering water bodies as effluents. This industry alone accounts for a substantial amount of dye pollution owing to the high volume of water used and the variety of dyes applied [67; 68].
- **Urban and agricultural runoff:** Dyes can also enter aquatic systems through urban runoff, which carries dyes from surfaces such as roads and roofs into stormwater systems, and agricultural runoff, which transports dyes from products such as fertilizers and seed coatings [69].
- **Groundwater contamination:** Dyes can infiltrate groundwater through processes such as advection, dispersion, and retardation, which are influenced by geological conditions and groundwater flow. This contamination is particularly concerning because it affects drinking water sources [69].

III.4. Environmental and health hazards of dye pollution

The environmental and health hazards of dye pollution are significant, stemming from the extensive use of synthetic dyes in various industries, particularly textiles. While essential for fabric coloration, these dyes pose severe risks to ecosystems and human health owing to their chemical composition and persistence in the environment. The discharge of dye-laden effluents into water bodies leads to pollution that affects aquatic life, soil quality and air purity (figure I.2).

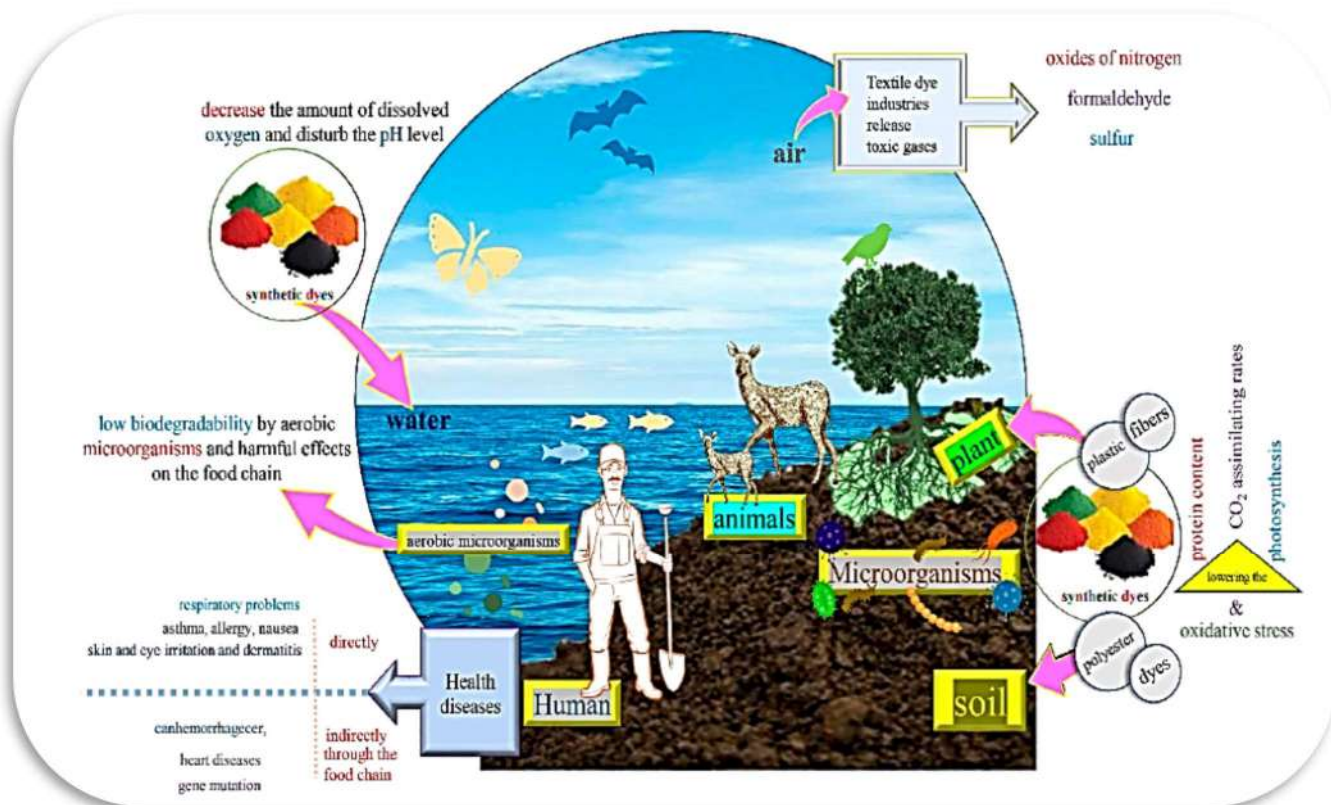


Figure I.2: Immediate and secondary effects of textile dyes on different materials and environments [65].

III.4.1. Environmental impact

- **Aquatic ecosystems:**

Industrial dye effluents exert significant detrimental effects on receiving water bodies, such as rivers, lakes, ponds, streams, and seas, spreading toxicity over wide areas and harming various forms of aquatic life. These wastewaters contain multiple toxic substances, notably dyes that are potent colorants, highly visible, and recalcitrant, persisting even at concentrations above 1 mg/L, with typical textile effluent dye concentrations reaching up to 300 mg/L. The pronounced dark coloration and elevated turbidity of these effluents impede sunlight penetration into water,

thereby inhibiting photosynthesis in aquatic plants. This reduction in photosynthetic activity not only decreases dissolved oxygen levels but also disturbs water pH. These changes collectively reduce primary food production, hinder the degradation of contaminants by aerobic microorganisms, and disrupt the aquatic food web, ultimately leading to widespread ecological imbalances. Water bodies are particularly vulnerable to such pollution, and contamination is often not immediately apparent because pollutants may persist in sediments and aquatic organisms long after the water appears clear [65; 70].

- ***Soil contamination:***

Textile industry effluents, comprising both liquid and solid wastes, often contain a broad spectrum of hazardous substances, including heavy metals, toxic chemicals, dyes, plastics, polyesters, fibers, yarns, and other polymeric compounds. When these contaminants are discharged into the environment, they lead to significant soil pollution, particularly affecting local landfill habitats and agricultural fields, a situation that is especially acute in developing countries. The accumulation of these pollutants in the soil causes long-term ecological damage by altering the soil pH and introducing chemical stressors that inhibit plant growth. The negative effects of these pollutants on plants include oxidative stress, reduced protein content, impaired photosynthesis, and decreased CO₂ assimilation rates, all of which collectively compromise soil health and agricultural productivity [65; 71; 72].

- ***Air pollution:***

Textile dye industries emit a range of toxic gases and pollutants during the dyeing process, including sulfur compounds, formaldehyde, nitrogen oxides, volatile organic compounds (VOCs), particulate matter, and dust, which are characterized by unpleasant odors. The release of these substances significantly contributes to air pollution, adversely affecting local air quality and, by extension, global atmospheric conditions. Such emissions not only pose risks to human health—affecting workers and consumers—but also have detrimental consequences for animals, the environment, and final textile products [65; 71].

III.4.2. Health hazards

- ***Human health risks:*** Exposure to dyes and their byproducts, whether through direct contact in the workplace or via environmental contamination in air and water, poses substantial health risks to humans. These risks include skin and eye irritation, respiratory problems, asthma, allergies, and dermatitis, which may arise from the direct

inhalation of dust or volatile compounds generated during textile processing. Beyond these immediate effects, certain dye products and by-products, especially azo dyes, known for breaking down into carcinogenic aromatic amines, are associated with more severe and long-lasting health outcomes. Such compounds have been implicated in diseases affecting vital organs, including the brain, kidney, liver, and heart, as well as critical physiological systems, such as the respiratory, immune, and reproductive systems. Indirect exposure through the food chain can result in chronic diseases, such as cancer, tuberculosis, hemorrhages, gene mutations, and cardiovascular disorders, underscoring the broad and potentially persistent threat posed by these chemicals to human health [65; 73; 74].

- **Toxicity and Mutagenicity:** Dyes can exhibit genotoxicity, causing DNA damage that may result in heritable genetic changes in the exposed cells. This is a significant concern for workers in dye manufacturing and processing industries [73].
- **Bioaccumulation and Biomagnification:** Dyes can accumulate in organisms and magnify through the food chain, leading to higher concentrations in top predators, including humans. This can exacerbate the toxicological effects on health [75].

III.5. Overview of dye removal techniques

Dye removal from wastewater is a critical environmental challenge owing to the toxic and persistent nature of dyes used in various industries. Several techniques have been developed to address this issue, each with its own advantages and limitations. This overview explores the primary methods for dye removal, including adsorption, chemical, biological, and advanced oxidation processes (figure I.3), and highlights their effectiveness and potential for sustainable wastewater treatment:

III.5.1. Adsorption techniques

Adsorption is a highly efficient and widely used method for removing various dyes from wastewater, owing to its simplicity and effectiveness. Traditionally, activated carbon has been the primary adsorbent due to its high performance; however, its cost has motivated researchers to explore alternative low-cost adsorbents (LCAs) such as bentonite clay, fly ash, industrial waste, agricultural by-products, and natural substances, including rice husk-based carbon,

bottom ash, shrimp shells, and other waste biomasses. These materials are successful in dye removal by accumulating dye molecules on their surfaces, a process influenced by surface chemistry, pore structure, and electrostatic interactions, thereby broadening the practical and sustainable application of adsorption technologies for wastewater treatment [65; 76; 77].

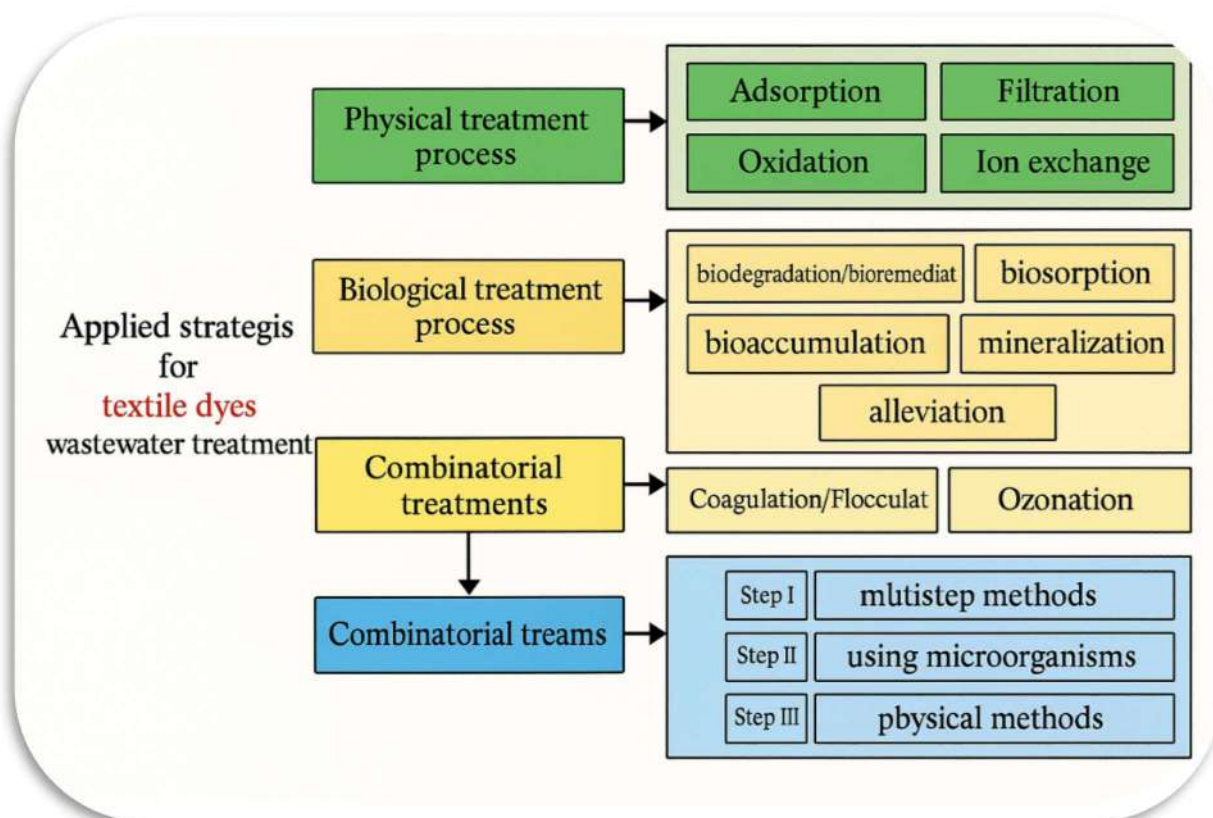


Figure I.3 : Dye removal techniques [65].

III.5.2. Chemical methods

Chemical treatment methods, such as coagulation, flocculation, precipitation, and advanced oxidation processes (AOPs), are widely used for removing dyes from textile wastewater because of their effectiveness in breaking down complex dye molecules. Coagulation and flocculation employ chemicals such as aluminum sulfate, iron salts, and lime to precipitate and remove suspended materials and specific dyes (e.g., crystal violet, Direct Red 28, Acid Yellow, and Acid Red 73). However, these are considered simple pretreatment steps that often require additional processes to address the residual soluble contaminants. Advanced oxidation processes, including ozonation and Fenton reactions, are notable for their ability to generate highly reactive radicals that mineralize dyes, such as Reactive Red 120, Acid Blue 92, Rhodamine B, and Crystal Violet, into less harmful substances. Ozonation, in particular, offers

advantages such as the absence of sludge generation and no change in wastewater volume when applied in the gas state. However, its efficiency is influenced by factors such as the pH, salt concentration, and temperature. Moreover, chemical treatments can be costly and may produce secondary pollutants, highlighting the necessity for careful operational control and possible integration with other treatment methods to achieve complete contaminant removal [65; 78; 79].

III.5.3. Biological methods

Biological treatments for dye removal utilize microorganisms, fungi, and enzymes to degrade or transform dye molecules, making these approaches environmentally friendly and potentially cost-effective. These methods include both aerobic and anaerobic degradation processes, with techniques such as biosorption, in which biological materials adsorb dye molecules, and bioaccumulation. Bioremediation can occur naturally through indigenous microbes found in wastewater or be induced by isolating and cultivating specific microorganisms for large-scale applications. Key contributors to dye degradation are bacteria and fungi, which secrete a range of degrading enzymes (e.g., oxidoreductases, hydrolases, oxygenases, peroxidases, and laccases) that can break down resistant dye compounds into harmless or beneficial products. Notably, extracellular laccases from fungi, such as *Neurospora crassa* and *Phanerochaete chrysosporium*, have been effective in degrading various dyes, whereas certain bacteria, such as *Bacillus subtilis*, *Proteus sp.*, *Streptococcus sp.*, and *Lysinibacillus sp.*, have shown the ability to decolorize and detoxify dyes, such as crystal violet, methylene blue, and Remazol red. Although biological treatments generate minimal secondary pollution and can be integrated with other technologies, their efficiency is often limited by the specific conditions required for microbial activity, the possibility of incomplete degradation, and challenges such as slow processing times and the inhibitory effects of high concentrations of toxic pollutants on the growth of microbes [65; 77; 79; 80].

III.5.4. Membrane filtration and electrochemical methods

Membrane filtration is a highly effective membrane-based separation technology that is widely used for dye removal and water reclamation from industrial wastewater. Techniques such as reverse osmosis, ultrafiltration, and nanofiltration operate by passing contaminated water through membranes with different pore sizes, physically separating the dyes, and yielding reusable water. Advanced implementations often combine membrane filtration with other treatments, such as electro-Fenton reactions or iron nanoparticle reduction, to enhance the dye

removal efficiency. Although membrane filtration (particularly with nanomembranes) offers excellent performance, it is associated with several operational challenges, including membrane fouling, irreversible membrane changes, the production of insoluble wastes, and sometimes the generation of foul odors, necessitating additional post-treatment processes and increasing operational costs. In parallel, electrochemical methods such as electrocoagulation employ electrical currents to coagulate and remove dye particles, offering high removal rates but often requiring substantial energy input and careful management to control costs and by-products. Overall, both membrane and electrochemical approaches provide powerful options for dye removal, but their practical application is limited by their cost and the need for further treatment to mitigate secondary issues [5; 65; 79].

IV. Adsorption as a green approach for dye removal

IV.1. Definition of adsorption

Adsorption is a surface-based separation process in which molecules or ions (adsorbates) from a fluid phase accumulate on the surface of a solid material (adsorbent) owing to physical or chemical interactions. This phenomenon is characterized by the preferential concentration of the adsorbate at the interface, resulting in the formation of an adsorbed layer on the solid surface, and is governed by the equilibrium relationships described by adsorption isotherms [81; 82].

IV.2. Fundamental mechanisms of adsorption

The adsorption mechanism involves the accumulation of molecules or ions (adsorbates) from a fluid phase onto the surface of a solid material (adsorbent), driven by various physical and chemical interactions. At the atomic level, unbalanced forces at the surface of the adsorbent attract adsorbate species, resulting in their preferential concentration at the interface between the two phases. These interactions may include van der Waals forces, hydrogen bonding, electrostatic interactions, and, in certain cases, chemical bonding (chemisorption). The nature and strength of these interactions determine whether adsorption is physical (physisorption), characterized by weak, reversible attractions and low adsorption energies, or chemical, involving the formation of stronger, often irreversible bonds. Adsorption proceeds until equilibrium is achieved between the adsorbed and unadsorbed phases, as described quantitatively by adsorption isotherms, such as the Langmuir and Freundlich models. The efficiency and selectivity of the adsorption process are further influenced by the properties of

the adsorbent, such as surface area, porosity, and surface chemistry, which facilitate the transport and binding of adsorbate species to available active sites [81; 83].

IV.3. Types of Adsorption

Adsorption is a surface phenomenon in which molecules accumulate at the interface of a solid or liquid and is primarily categorized into two types: physisorption and chemisorption. These processes are distinguished by the nature of the forces involved and the energy changes associated with adsorption. Physisorption involves weak van der Waals forces, whereas chemisorption involves stronger chemical bonds. Understanding these types of adsorption is crucial for applications in catalysis, environmental chemistry and materials science.

IV.3.1. Physisorption

Physisorption, a fundamental type of adsorption, is predominantly governed by weak van der Waals forces, including dipole-dipole interactions and dispersion forces comparable to those responsible for maintaining cohesion in the liquid state [84; 85]. The energetic requirements for physisorption are relatively low, typically in the range of 0.03–3 kJ/mol, which accounts for the generally reversible nature of the process and its preference for low temperature conditions [86]. From a thermodynamic perspective, physisorption is frequently described by linear partition isotherms, which are particularly applicable to the adsorption of neutral organic molecules by molecular-association colloids [87]. A classical example illustrating physisorption is the adsorption of rare gases onto solid surfaces, a process that underpins various technological applications where reversibility is crucial, such as in gas storage and separation systems [85].

IV.3.2. Chemisorption

Chemisorption is characterized by the formation of chemical bonds, either covalent or ionic, between the adsorbate and the adsorbent, a process that fundamentally relies on electron sharing or transfer [88; 85]. The enthalpic demands of chemisorption are markedly higher than those of physisorption, typically ranging from 40 to 400 kJ/mol, which reflects the strength and specificity of the chemical interactions [86]. Such substantial energy involvement frequently renders chemisorption irreversible and restricts its occurrence to specific environmental conditions. The adsorption behavior in chemisorption is effectively modeled by site-limited isotherms, which capture the empirical constraints associated with the adsorption capacity of

mineral colloids or the cation-exchange behavior of humic substances [87]. Chemisorption is thus fundamental to a variety of industrial and environmental processes, playing an essential role in heterogeneous catalysis, where the interaction must result in the formation of a reactive surface species, as well as in phenomena such as corrosion and the adsorption of diatomic gases (e.g., O₂, N₂, and H₂) on transition metal surfaces [85; 89].

IV.3.3. Interplay and transition between physisorption and chemisorption

The complex dynamics of adsorption underscore the importance of both physisorption and chemisorption in achieving equilibrium. This is exemplified in systems such as CO adsorption on Au(111), where molecules are initially captured in a metastable chemisorption state before transitioning to a physisorption state [90]. The interplay between these adsorption types is particularly significant in environmental and materials science. For example, the adsorption of nitric oxide on metal-organic frameworks involves both mechanisms, which is crucial for understanding their reactivity and storage properties [91].

IV.4. Influencing parameters

The adsorption process for dye removal from aqueous solutions is influenced by several parameters, including:

IV.4.1. Adsorbent properties

The adsorption capacity of an adsorbent is strongly influenced by its surface area, pore structure, chemical composition, and particle size. High surface area and appropriate pore size distribution, as observed in polymeric adsorbents with functional amino groups, significantly enhance the uptake of reactive dyes [92]. Likewise, the surface area of polypyrrole–polyethyleneimine nano-adsorbents is a major factor governing their effectiveness in adsorbing methylene blue. The presence of specific functional groups on the adsorbent surface, such as the incorporation of polyethyleneimine in polypyrrole, introduces additional chelating sites that facilitate stronger chemical interactions with dye molecules [93]. Furthermore, the surface chemistry, as seen in fluorinated carbon fibers, also plays a vital role in determining adsorption performance [94]. In addition, reducing the particle size of adsorbents has been shown to enhance adsorption efficiency due to the increased surface area available for interaction, thereby promoting more effective dye removal [95].

IV.4.2. Dye properties

The adsorption behavior of dyes is significantly influenced by their molecular structure, charge, solubility and concentration. Dyes with distinct molecular characteristics and charges, such as cationic methylene blue, exhibit strong adsorption onto negatively charged adsorbents because of electrostatic attraction [93]. Similarly, the adsorption efficiency of dyes such as methyl violet and reactive orange is modulated by their specific molecular features [96]. Furthermore, the initial dye concentration in the solution plays a crucial role; higher concentrations can lead to surface saturation of the adsorbent, thereby decreasing the adsorption efficiency [97]. Additionally, dye solubility determines its availability in the solution phase and influences its overall uptake by the adsorbent [98].

IV.4.3. Solution chemistry

Solution chemistry, including pH, temperature, and coexisting ions, is crucial for dye adsorption. The pH affects both dye ionization and adsorbent charge, with a low pH favoring anionic dye adsorption and optimal methylene blue uptake occurring at approximately pH 6.2. Higher temperatures typically enhance the adsorption efficiency by increasing the dye mobility. The presence of other ions can compete with dyes for adsorption sites, reducing the overall efficiency, especially in complex solutions [93; 99].

IV.5. Adsorption thermodynamics

In adsorption studies, the evaluation of thermodynamic parameters provides essential insights into the spontaneity, heat effects, and disorder changes associated with the adsorption process. The primary parameters considered were the standard Gibbs free energy change (ΔG°), enthalpy change (ΔH°), entropy change (ΔS°), and equilibrium constant (Kd).

The Gibbs free energy change (ΔG°) is a reliable indicator of adsorption spontaneity. A negative ΔG° value at a given temperature indicates that the adsorption process is thermodynamically favorable and proceeds spontaneously [100; 101]. The relationship between ΔG° , the equilibrium constant (Kd), and temperature is given by the following equation:

$$\Delta G^\circ = -RT \ln Kd = \Delta H^\circ - T \Delta S^\circ \quad (1)$$

Where R is the universal gas constant and T is the absolute temperature in Kelvin. The equilibrium constant (Kd) reflects the extent of adsorption at equilibrium and is derived from

the ratio of the adsorbed amount to the remaining concentration in the solution at equilibrium. A higher K_d value indicates a stronger adsorption affinity between the adsorbate and the adsorbent surface [102].

The enthalpy change (ΔH°) represents the heat exchange during the adsorption process. A positive ΔH° value indicates an endothermic process in which heat is absorbed and adsorption is favored at higher temperatures. Conversely, a negative ΔH° indicates an exothermic process, in which adsorption is favored at lower temperatures and heat is released [103; 104]. The Van't Hoff equation is as follows:

$$\ln K_d = \left(\frac{\Delta S^\circ}{R} \right) - \left(\frac{\Delta H^\circ}{RT} \right) \quad (2)$$

One can determine ΔH° and ΔS° from the slope and intercept of a linear plot of $\ln K_d$ versus $1/T$.

Entropy change (ΔS°) provides information about the disorder at the solid–solution interface during adsorption. A positive ΔS° suggests increased randomness, often attributed to the release of water molecules or structural changes in the adsorbed phase, thereby favoring the adsorption process. In contrast, a negative ΔS° indicates a more ordered system after adsorption [103].

A ΔG° value between 0 and -20 kJ/mol is indicative of electrostatic interactions between the adsorption sites and the ion being adsorbed (physical adsorption), whereas values that are more negative, specifically in the range of -80 to -400 kJ/mol, suggest that the adsorption process entails charge sharing or transfer from the surface of the adsorbent to the adsorbing ion, leading to the formation of a coordinate bond (chemisorption) [100; 104].

IV.6. Isotherm models applied to dye adsorption

Understanding adsorption isotherms is critical for analyzing the interactions between dyes and adsorbents, interpreting adsorption capacity, and modeling removal efficiency. The accurate selection and application of adsorption isotherm models enables researchers to diagnose the adsorption mechanism, evaluate the effectiveness of adsorbents, and facilitate the scale-up and practical design of treatment processes.

IV.6.1. Adsorption capacity and removal efficiency

Adsorption capacity, commonly denoted as q_e , indicates the maximum amount of dye that can be held by a given mass of adsorbent and is often measured in mg/g [105]:

$$q_e = \frac{C_0 - C_e}{m} \times V \quad (3)$$

Where: C_0 : is the initial concentration of adsorbate (mg/l).

C_e : is the residual concentration of adsorbate (mg/l).

m : is adsorbent mass (g).

V : the solution volume (l).

The removal efficiency (RE %) indicates the percentage of the initial dye concentration removed from the aqueous solution, providing a practical assessment of the adsorbent performance [105] :

$$RE(\%) = \frac{C_0 - C_e}{C_0} \times 100 \quad (4)$$

IV.6.2. Types of curve for adsorption

The classification of isotherm shapes provides mechanistic insights into the adsorption process. Giles et al. developed a widely adopted system that divided isotherm curves into four main classes (figure I.4):

- **S-type (sigmoidal)**: Characterized by cooperative adsorption, where adsorption becomes easier as more dye is adsorbed; often observed when adsorbed molecules interact attractively, promoting cluster formation.
- **L-type (Langmuir-like)**: The most common type, indicating monolayer adsorption with decreasing site availability as coverage increases.
- **H-type (high affinity)**: Represents systems with very strong adsorbent-adsorbate interactions, resulting in nearly complete adsorption at low solute concentrations; often observed with high-affinity and ionic adsorptions.

- **C-type (constant partition or linear):** Shows constant partitioning between the adsorbate and adsorbent, suggesting unrestricted multilayer adsorption or the continual creation of new sites as the dye moves into the micropores [106; 107].

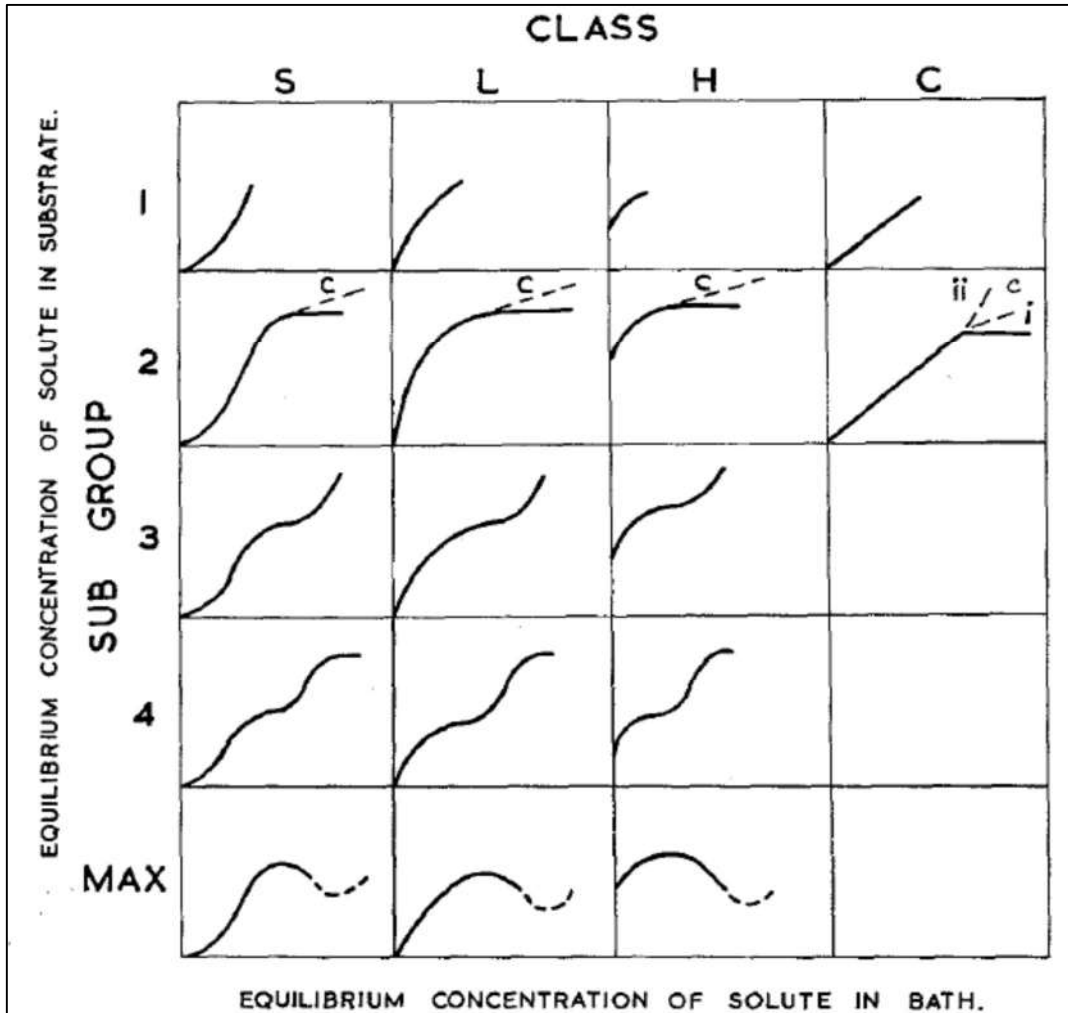


Figure I.4: System of isotherm classification [106].

IV.6.3. Adsorption isotherms models

In our study, we employed the most extensively utilized isotherm models to assess the adsorption efficacy, including Langmuir, Freundlich, and Temkin.

IV.6.3.1. Langmuir isotherm:

The Langmuir model assumes that adsorption occurs on a homogeneous surface via monolayer coverage without adsorbate-adsorbate interactions. This is mathematically expressed as:

$$\frac{C_e}{q_e} = \frac{C_e}{q_m} + \frac{1}{q_m K_L} \quad (5)$$

Where: q_m : is the monolayer or maximal adsorption capacity (mg/g).

K_L : is the Langmuir adsorption constant related to affinity (l/mg).

The model fits well with L-type isotherms and is prevalent in systems where monolayer adsorption dominates, providing direct measures of q_{max} and site affinity [108; 109].

IV.6.3.2. Freundlich isotherm:

The Freundlich model describes adsorption on heterogeneous surfaces, allowing multilayer formation at sites with varying affinities. The isotherm is represented as follows:

$$\log q_e = \log K_F + \frac{1}{n} \log C_e \quad (6)$$

Where: K_F : is the Freundlich adsorption constant related to adsorption capacity [(mg. g⁻¹) (l.mg⁻¹)^{1/n}].

n : indicates adsorption intensity; values of n are described as follows:

- $n=1$, linear adsorption.
- $n<1$, adsorption process with chemical interaction.
- $n>1$, adsorption process with physical interaction.
- Favorable adsorption process is declared when $0 < 1/n < 1$, and a cooperative adsorption process occurs when $1/n > 1$ [108].

IV.6.3.3. Temkin isotherm:

Temkin's approach considers indirect adsorbate-adsorbent interactions, proposing that the heat of adsorption decreases linearly with coverage due to adsorbent-adsorbate interactions. Its linearized form is:

$$q_e = B \ln C_e + B \ln K_T \quad (7)$$

Where: K_T : Temkin equilibrium binding constant (l/g).

B : Temkin constant related to the adsorption heat (J/mol).

It is especially useful in systems where interaction energies are not constant, offering corrections to models like Langmuir and Freundlich, particularly for systems approaching the transition between physical and chemical adsorption [108; 107].

IV.7. Adsorption kinetics

Understanding adsorption kinetics is critical for characterizing the transfer of adsorbate molecules from a solution to the surface of an adsorbent. Kinetic models not only provide insights into the adsorption mechanism but also inform the design and operation of adsorption systems for water and wastewater treatment, catalysis, and materials science. Among the plethora of kinetic approaches, intraparticle and extraparticle diffusion models, as well as pseudo-first-order (PFO) and pseudo-second-order (PSO) kinetic models, are widely employed and form the foundation of modern adsorption sciences.

IV.7.1. The intraparticle and external film diffusion models

Adsorption in porous materials typically proceeds through multiple resistance steps: external (film or boundary layer) diffusion, intraparticle diffusion within the pores, and surface adsorption. The external film diffusion model describes the movement of solute across the boundary layer surrounding the adsorbent whereas the intraparticle diffusion model, most classically represented by the Weber–Morris equation, captures the migration of adsorbate within the pores of the adsorbent [110- 112].

The Weber–Morris intraparticle diffusion model [112] and external film diffusion model [113] are expressed as follows, respectively:

$$q_t = K_{id}t^{0.5} + C \quad (8)$$

$$-\ln\left(1 - \frac{q_t}{q_e}\right) = K_{efd}t + C \quad (9)$$

Where: q_t : is the adsorption capacity at time t (min).

K_{id} ($\text{mg g}^{-1} \text{min}^{-1/2}$) and K_{efd} (min^{-1}): are the rate constants of intraparticle diffusion and external film diffusion models, respectively.

C : is the intercept relates to the boundary layer thickness.

If the plot of q_t versus $t^{0.5}$ is linear and passes through the origin, intraparticle diffusion is the sole rate-limiting step of the reaction. However, multi-linear plots indicate that more than one process (often film diffusion, surface adsorption, and intraparticle diffusion) may operate simultaneously [114; 112].

IV.7.2. Pseudo-first-order model

The pseudo-first-order kinetic model, originally proposed by Lagergren (1898), assumes that the rate of occupation of adsorption sites is proportional to the number of unoccupied sites [115]. Its differential form is as follows:

$$\ln(q_e - q_t) = \ln q_e - k_1 \cdot t \quad (10)$$

Where: k_1 : is the pseudo-first-order rate constant (min^{-1}).

This model often adequately describes the initial stages of adsorption but may not fit well for systems where intraparticle diffusion or chemisorption is dominant [110; 116].

IV.7.3. Pseudo-second-order model

The pseudo-second-order (PSO) kinetic model, formalized by Ho and McKay (1999) and earlier discussed by Blanchard et al. (1984), postulates that adsorption follows a second-order mechanism, possibly involving chemisorption or complexation with two available sites [110; 111]. Its rate equation is:

$$\frac{t}{q_t} = \frac{t}{q_e} + \frac{1}{k_2 q_e^2} \quad (11)$$

k_2 : is the pseudo-first-order rate constant ($\text{g mg}^{-1} \text{min}^{-1}$).

Despite initial interpretations suggesting a chemisorption-driven mechanism, subsequent studies have highlighted that the PSO model often fits well even when the underlying process is diffusion-controlled, especially in systems with heterogeneous pore structures [116; 117].

V. Date palm waste as a sustainable bioadsorbent for dye removal

V.1. Biological and morphological characteristics of of *Phoenix dactylifera* L.

V.1.1. Taxonomy and origin

Phoenix dactylifera L., commonly known as the date palm, is a member of the Arecaceae family and is the type species of the genus *Phoenix* [118]. This species is particularly notable because of its long-standing cultural and economic importance across arid regions. The evolutionary origin of the date palm is widely believed to be centered in the Fertile Crescent region, near present-day Iraq, as reflected by both archaeological and genetic evidence [119]. The genus *Phoenix* comprises approximately 14 species; however, *P. dactylifera* is the only widely cultivated and economically significant species adapted for fruit production [120].

V.1.2. Plant structure

The date palm is an arborescent monocotyledonous perennial plant characterized by a single erect stem reaching heights of up to 30 m, crowned by a dense canopy of pinnate leaves (figure I.5) [121]. A stable chromosome number important for breeding and genetic improvement programs. The reproductive biology of date palms includes a dioecious system, where male and female flowers occur on separate plants, which underlines the necessity for cross-pollination, often facilitated manually or naturally by wind and insects. Inflorescences emerge from leaf axils and bear hundreds of flowers, making pollination efficiency critical for yield [122].

The root system of *Phoenix dactylifera* plays a vital role in absorption and anchorage, comprising five root categories across four topological orders that are essential for plant stability and nutrient uptake [123]. Notably, its roots contain pneumatodes-air-filled structures derived from a generative layer-characterized by crystal-containing plastids and wall outgrowths within young aerenchymatous tissues [124]. Date palms exhibit pronounced dimorphism in inflorescence morphology; female inflorescences possess longer spikelets, averaging 62 spikelets per rachis with approximately 55 flowers each, whereas male inflorescences are more complex, with 236 spikes per rachis and 81 flowers per spike. Inflorescences develop acrotonically from the leaf axils at the apex of the plant [125]. Its leaves are covered with epicuticular waxes, formed at the three-to four-leaf stage, in two morphological patterns, “filaments” and “tubes,” varying by cultivar; these waxes function to reduce transpiration and protect against environmental stresses [126].

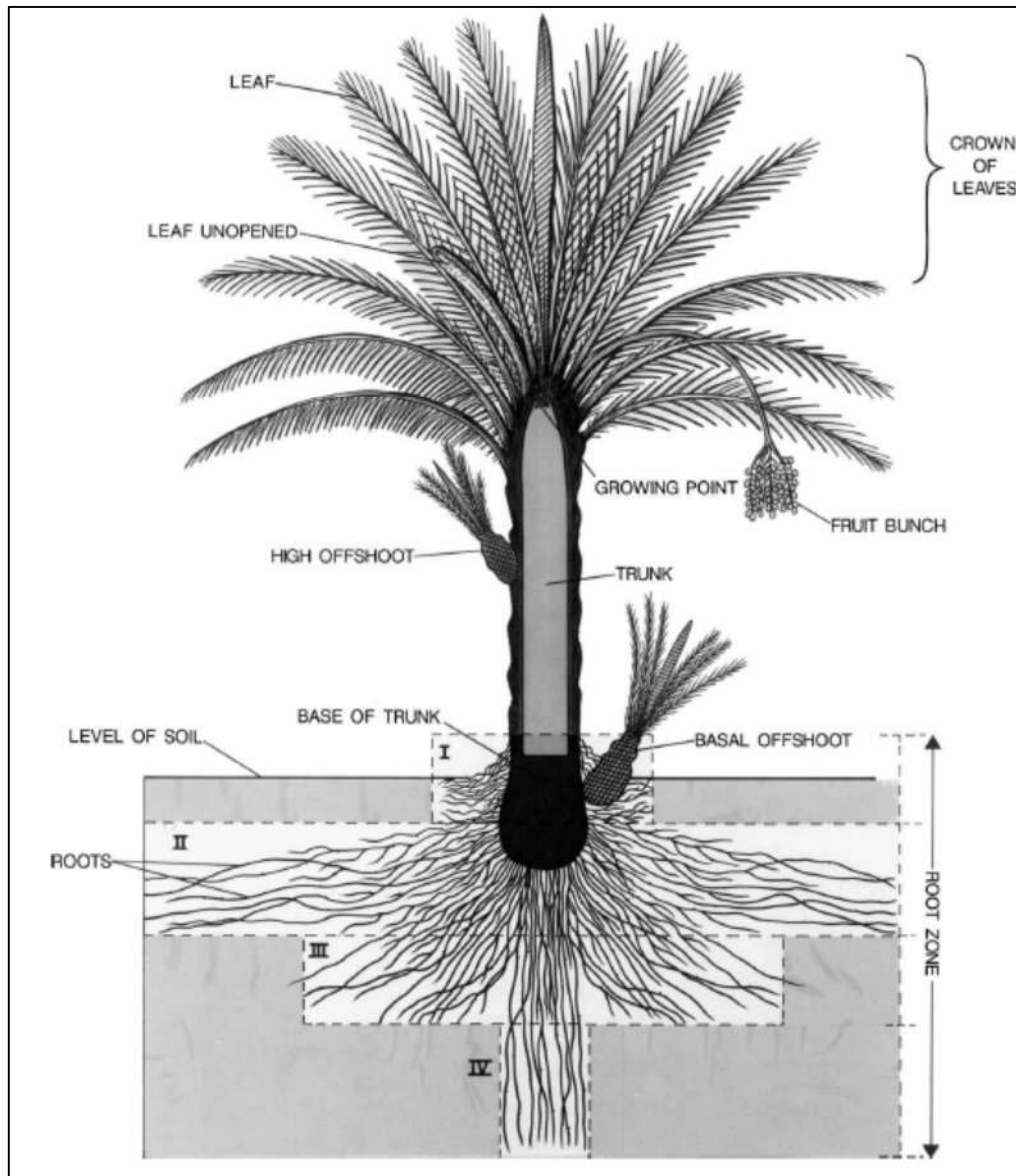


Figure I.5: Diagrammatic representation of date palm structure [118].

Phoenix dactylifera has a distinct genetic structure with two primary gene pools: oriental and occidental. This genetic diversity is shaped by isolation and intraspecific gene flow, with no evidence of interspecific hybridization in the cultivated gene pool [127].

V.1.3. Environmental adaptations

Date palms (*Phoenix dactylifera*) exhibit multifaceted adaptations to abiotic stress, enabling their survival in harsh arid environments. Their drought tolerance mechanisms largely rely on osmotic adjustment, where root osmotic strength increases via the accumulation of organic osmolytes, such as sugars and amino acids, which surpass mineral osmolytes in maintaining cellular turgor and metabolic function under water scarcity. Concurrently, leaf membrane remodeling mitigates oxidative damage and preserves photosynthetic efficiency during drought

stress [128]. Seasonal metabolic shifts further modulate water relations and drought responses, highlighting the temporal complexity of stress adaptation [129].

Regarding salinity tolerance, although not a strict halophyte, date palms manage moderate salinity through selective ion uptake and compartmentalization, preventing toxic accumulation in sensitive tissues [130]. The enhancement of salinity resilience has been documented with biostimulants, such as arbuscular mycorrhizal fungi, which improve nutrient uptake and stress response pathways [131; 132].

Temperature adaptation aligns with its native habitat, optimally growing between 32 and 38°C during the day and minimally 7°C at night, with physiological processes such as photosynthesis and respiration finely tuned to this range [121].

Nutrient and soil preferences favor sandy or loamy textures with slightly alkaline pH (7.5–8.5), supported by a deep, efficient root system that accesses groundwater vital for survival in arid zones [119; 121].

Molecularly, the resilience of a species is underpinned by biochemical networks, notably involving abscisic acid (ABA) signaling; ABA receptors regulate water-use efficiency and stress responses [133]. Additionally, the rapid detoxification of reactive oxygen species (ROS) by antioxidant mechanisms reduces cellular damage under drought and salinity stress [128]. These concerted physiological, biochemical, and molecular strategies underscore the remarkable capacity of date palms to withstand multiple abiotic stressors characteristic of their native desert environments.

V.2. Comparative analysis of date palm cultivars: *Ghars*, *Degla*, and *Takermost*

Phoenix dactylifera L. exhibits broad cultivar diversity, particularly in North African oases such as Algeria and Tunisia. Among the numerous cultivars, *Ghars*, *Degla* (including *Deglet Nour*), and *Takermoust* stand out because of their distinct morphological and fruit characteristics, which influence their agricultural value, adaptability, and commercial importance.

V.2.1. Morphological characteristics of palms and fruits

- ***Ghars*:** *Ghars* palms generally produce fruits of medium size with moderate pulp-to-seed ratios. Morphologically, the palm exhibits a relatively compact spathe structure with shorter spathes than *Degla* cultivars [134]. *Ghars* dates tend to have shorter and

narrower spathes and fewer flowers per spike. In terms of leaf biochemical profile, *Ghars* leaves have a high total sugar content ($74.54 \pm 6.92\%$) but comparatively lower protein and flavonoid levels than *Degla* cultivars [135].

- ***Degla***: *Degla* is notable for its large fruit size, with some reports indicating the highest spathe weight and diameter across the male palms studied, suggesting that vigorous tree morphology supports abundant fruit production [134; 136]. Morphologically, *Degla* palms produce longer and wider fruits with higher pulp weight (up to 21.63 g per fruit) and larger physical dimensions (length up to 4.90 cm, diameter ~2.85 cm) [136]. The leaves of this cultivar show high protein ($39.09 \pm 4.58\%$) and phenolic contents, attributed to their biochemical robustness [135].
- ***Takermost***: is Common in Algerian oases and exhibits intermediate morphological traits between *Ghars* and *Degla* cultivars. Detailed biometric data are less frequently reported; however, *Takermoust* fruits tend to have smaller average size and weight relative to *Degla* but may display higher acidity levels and slightly lower sugar content than *Deglet Nour*. Morphological differentiation includes variations in fruit pulp consistency and seed dimensions, which are often indicative of adaptation to specific local environments [136].

V.2.2. Fruit Quality and Physicochemical Properties

- *Ghars* fruits are characterized by moderate moisture and sugar content, and the cultivar is regarded as having a good balance but is generally considered less prestigious commercially than *Degla*. The sugar composition favors reducing sugars, correlating with a neutral to slightly basic pH and relatively high moisture content [136].
- *Degla* fruits are widely valued for their high total sugar content (often $> 70\%$), moderate acidity, and long shelf life, which is partly attributable to their lower moisture content relative to that of highly succulent cultivars. The physicochemical profile renders them highly suitable for both fresh consumption and processing [136]. Their high phenolic and flavonoid contents also contribute to antioxidant properties that are beneficial for nutrition and storage [135].
- *Takermost* fruits tend to have lower sugar levels and higher acidity than *Degla* fruits, thus exhibiting a distinctive taste profile. They also show variations in water content and firmness, which may require adapted postharvest treatments to ensure quality [136].



Figure I.6: Fruits of three cultivars *Degla*, *Ghars* and *Takermost*

V.2.3. Biochemical and nutritional profiles

Biochemical profiling of male palm leaflets [135] indicates:

- *Degla Beida* (closely related to *Degla*) exhibited the highest protein and flavonoid concentrations, suggesting enhanced metabolic activity and resilience in metabolic pathways relevant to fruit quality.
- *Ghars* showed the highest total sugar content in leaves but lower protein and phenolic contents, indicating a differential resource allocation strategy.
- The biochemical profile of *Takermost* is less documented but is hypothesized to present intermediate values reflecting its phenotypic and agronomic characteristics.

V.2.4. Agronomic and ecological implications

The morphological and biochemical differences among these cultivars have direct implications for their agronomic management and commercial utility.

- *Degla* cultivars, especially *Deglet Nour*, are widely plantation-favored for their superior fruit size and quality, although their genetic uniformity can increase susceptibility to diseases such as *Bayoud* (*Fusarium oxysporum f.sp. albedinis*) [137].
- Although less commercially dominant, *Ghars* palms present valuable genetic diversity and adaptability, making them important cultivars for sustainable oasis ecosystem management [134].
- *Takermost*, with moderate fruit and tree size and distinct flavor profiles, contributes to agro-biodiversity, which is important for genetic resource conservation and niche market exploitation [136].

Collectively, the *Ghars*, *Degla*, and *Takermost* cultivars represent a spectrum of date palm diversity in Algerian oases, differentiated by their morphological, physicochemical, and biochemical profiles. *Degla* excels in fruit size and commercial desirability, *Ghars* in genetic and biochemical diversity, and *Takermost* reflects intermediate traits that are valuable for local adaptation.

V.3. Date palm production and waste: global, African, and Algerian perspectives

Date palm cultivation (*Phoenix dactylifera* L.) represents a critical agricultural sector in arid and semi-arid regions worldwide, underpinning the socio-economic fabric of several communities. Global date production is estimated at approximately 7.9 million metric tons annually, with countries in the Arab world accounting for approximately 5.4 million tons, underscoring the region's preeminence in date palm agriculture [138]. Egypt, Iran, and Saudi Arabia continue to dominate the global output, cumulatively contributing to nearly half of the total production [6]. Despite substantial fruit yields, date palm cultivation generates considerable quantities of biomass waste, estimated at approximately 12 million metric tons annually, which largely remains underutilised owing to limited economically feasible valorization pathways [139].

In Africa, North African countries are the foremost date producers, with Egypt, Tunisia, and Algeria recognised as key contributors to the continent's date supply. However, date production in these regions is frequently undermined by pest infestations, diseases such as bayoud, and insufficient access to optimised marketing channels, all of which dampen yield quality and constrain economic profitability [138]. Moreover, environmental pressures and traditional cultivation practices necessitate concerted research and development interventions to sustain this sector.

Algeria occupies a prominent position in date production, ranking as the fourth largest producer worldwide. The expansion of date cultivation acreage in Algeria is particularly noteworthy. For example, in the province of Bechar, output surged dramatically from a modest 2,446 tons in 2015 to 59,781.3 tons by 2021, alongside an increase in the cultivated area to approximately 13,918.5 hectares. The varietal composition prominently features ‘*Ghars*’, a soft date favoured locally, and the dry date cultivar ‘*Degla Beida*’, both integral to Algeria’s date industry and export portfolio [140]. The importance of maintaining cultivar diversity is underscored by concerns over genetic erosion driven by monocultures and pest susceptibilities [137].

Date palm biomass waste in Algeria, encompassing seeds, press cakes, leaf litter, and pruning residues, holds significant potential as a resource for bioenergy and agricultural applications [6]. The accumulation of lignocellulosic date palm residues is substantial; however, their prevalent disposal through open-air burning contributes to environmental pollution and greenhouse gas emissions. To address this, innovative strategies such as biomass gasification have been proposed, which convert agricultural residues into clean energy, reducing environmental footprints and generating economic value [7]. Furthermore, the conversion of date palm waste into biochar offers multifaceted benefits, including improved soil fertility, carbon sequestration, and enhanced water retention, which are vital for sustainable oasis agriculture amid climatic challenges [141].

In conclusion, while global and African date palm production continues to grow, maximising the sustainable use of the vast biomass residues generated is imperative. Algeria exemplifies both the opportunities and challenges in this domain, highlighting the necessity for integrated agronomic management, waste valorization technologies, and environmental safeguards to ensure the long-term viability of its date palm agroecosystems.

V.4. Adsorption capacities of date palm-based adsorbents

The utilisation of agricultural waste biomass, including date palm residues (*Phoenix dactylifera* L.), for pollutant adsorption has emerged as a promising sustainable approach for environmental remediation. Agricultural waste, composed mainly of lignocellulosic materials, can be transformed into effective adsorbents through physical and chemical modifications, enhancing their adsorption capability by increasing the number of active sites and improving porosity [142; 143].

The adsorption mechanisms involved in pollutant uptake by date-palm-derived adsorbents generally include electrostatic interactions, complexation, ion exchange, and van der Waals forces. The heterogeneous chemical composition of date palm biomass, which is rich in cellulose, hemicellulose, lignin, and extractives, provides diverse functional groups (e.g. hydroxyl, carboxyl, and phenolic) that can bind dyes, heavy metals, and organic pollutants through multiple interactions [144]. Moreover, chemical treatments, such as acid or base modification and the production of activated carbon or biochar, optimise the surface chemistry and textural properties, thereby improving the adsorption capacity and selectivity [145].

Thus, date palm waste represents a valuable feedstock for creating low-cost, efficient adsorbents with broad applicability in treating industrial effluents laden with dyes, heavy metals, and organic pollutants. The valorization of such biomass not only addresses waste management challenges but also contributes to circular economy objectives by transforming agro-industrial residues into functional environmental materials [139; 6].

Further a comprehensive review of adsorption comparative studies of date palm adsorbents will be presented in the subsequent chapter to deepen the understanding in this area.

Conclusion

The utilisation of date palm by products as a bioadsorbent presents a promising solution for pollutants removal, combining environmental sustainability and technical efficacy. Its lignocellulosic structure, enhanced by chemical modifications, enables efficient adsorption through diverse mechanisms, such as electrostatic interactions and ion exchange. Comparative studies of cultivars, such as *Ghars*, *Degla*, and *Takermoust*, highlight the influence of morphological and biochemical traits on adsorption performance. This approach not only mitigates water pollution but also repurposes agricultural waste, thereby contributing to the circular economy. Future research should focus on optimising pretreatment methods and scaling up applications to maximise the environmental and economic benefits of date-palm-based adsorbents.

Chapter 2

Review of Adsorption Studies Using Raw and Modified Plant Wastes for Water Treatment: With Emphasis on Date Palm Biomass

Introduction

Water pollution caused by a range of organic and inorganic contaminants is a serious environmental and public health issue, prompting the search for affordable and sustainable treatment solutions to address this problem. Plant-based wastes, especially the abundant date palm residues in regions such as the Middle East and North Africa, are being increasingly explored as low-cost, eco-friendly adsorbents. Numerous studies have shown that both raw and chemically modified date palm waste can effectively remove pollutants, such as heavy metals, antibiotics, and dyes, from water. The adsorption capacities of these materials are enhanced through chemical or thermal processing, which alters their surface and chemical characteristics.

The literature shows that date palm waste is a highly effective adsorbent, with its performance influenced by factors such as pH, pollutant concentration, adsorbent dose, contact time, temperature, and chemical modifications. Various adsorption models have been employed to understand these underlying mechanisms. However, most studies overlook the specific impact of different date palm cultivars and their unique properties on pollutant removal efficiency, marking a gap in the current research.

This chapter reviews recent research on the use of plant waste, particularly raw and modified date palm residues, for water treatment, examining adsorption mechanisms, modification methods, and current trends. It identifies key research gaps, particularly regarding the effects of different date palm cultivars (*Degla, Ghars, and Takermoust*). This review forms the basis for further studies aimed at optimizing adsorption efficiency through cultivar selection and operational parameters.

I. Adsorption using raw plant-based wastes

The use of raw plant-based wastes as adsorbents in wastewater treatment is becoming increasingly popular because of their low cost, wide availability, and positive environmental impact. Agricultural by-products serve as a source of these materials, which have demonstrated significant effectiveness in removing contaminants such as heavy metals, dyes, and pharmaceutical residues from water. Their natural adsorptive properties, which can be further improved through chemical treatments, facilitate the removal process. This method not only helps address water pollution but also supports sustainable waste management by repurposing plant waste.

In a comparative study by *Olabanji et al.* (2014), raw okra and sugarcane waste were evaluated as bioadsorbents for the removal of heavy metals from aqueous solutions. The findings revealed that raw okra waste exhibited superior adsorption efficiency, achieving removal rates of 65.10% for Pb(II) and 57.80% for Ni(II), outperforming sugarcane waste in this regard. This study also highlighted the effective retention of Cd(II) and Zn(II) ions, underscoring the broad applicability of okra waste in multi-metal systems. The adsorption behavior conformed well to the Freundlich isotherm model, suggesting a heterogeneous surface and a multilayer adsorption process. These results confirm the potential of low-cost, unmodified plant residues as promising materials for heavy metal remediation in wastewater [146].

Thaçi et al. (2022) evaluated the adsorption performance of various raw agro-waste materials for removing Pb^{2+} , Cu^{2+} , and Zn^{2+} ions from aqueous solutions. Among the tested biosorbents, maize cob showed high efficiency, especially for Zn^{2+} (92.6%) and Cu^{2+} (66%), while wheat bran exhibited the highest Pb^{2+} removal (93.7%). Olive waste also demonstrated promising adsorption properties, achieving up to 97% removal of Pb^{2+} and 62% of Cu^{2+} . In addition, coffee waste achieved one of the highest Pb^{2+} removal efficiencies (97.5%), confirming its potential as a low-cost natural adsorbent. These results highlight the effectiveness of unmodified plant-based residues as viable alternatives for heavy metal removal from wastewater treatment [147].

Gupta et al. (2018) investigated the adsorption performance of potato plant wastes, namely potato stem powder (PSP) and potato leaf powder (PLP), for the removal of cationic dyes such as methylene blue (MB) and malachite green (MG) from aqueous solutions. The surface morphology and functional groups of the raw materials contributed significantly to their adsorption ability. The optimal pH and temperature for dye removal were 7 and 303 K, respectively. The adsorption kinetics followed the pseudo-second-order and intraparticle diffusion models, while the equilibrium data fit well to both the Langmuir and Freundlich isotherms. PLP exhibited the highest adsorption capacity, reaching 52.6 mg/g for MB. Thermodynamic analysis confirmed the exothermic and spontaneous nature of the process, indicating the feasibility of using raw potato waste as a low-cost biosorbent for dye removal from wastewater [148].

El-Shafie et al. (2023) explored the potential of using raw watermelon rinds (WMR) as a green, low-cost, and non-conventional bioadsorbent for the removal of acridine orange (AO) dye from aqueous solutions. The study included both raw and thermally treated samples; however, attention to the raw form revealed its applicability in pollutant removal without requiring

complex processing steps. Characterization of the raw WMR showed the presence of functional groups capable of interacting with dye molecules, and experimental findings confirmed its adsorption efficiency, albeit at a lower level than that of the thermally treated forms. This highlights the potential of utilizing unmodified agricultural residues as effective and economical alternatives for wastewater treatment [149].

Raw date palm wastes have also been utilized as agricultural by-products for pollutant adsorption, particularly in regions abundant in date palm cultivation, owing to their availability and favorable physicochemical properties.

Mirzadeh et al. (2022) evaluated the potential of raw date palm fibers for the removal of two common pharmaceutical contaminants: tetracycline (TC) and ciprofloxacin (CIP). The adsorption experiments, conducted in batch mode, assessed the effects of pH, biosorbent dose, contact time, temperature, initial antibiotic concentration, and the presence of salt. The raw date palm waste achieved removal efficiencies exceeding 84% for TC and 66% for CIP at initial concentrations of 80 and 150 mg/L, respectively. The kinetic data were best fitted to the pseudo-second-order model, and the equilibrium adsorption was described by the Langmuir isotherm for TC and the Dubinin–Radushkevich (D–R) isotherm for CIP. The thermodynamic parameters confirmed that the adsorption process was spontaneous and endothermic, supporting the potential of raw date palm biomass as a cost-effective and environmentally friendly adsorbent for the removal of antibiotics from contaminated water [150].

Another study demonstrated the efficiency of palm fibers and petioles, both considered solid agricultural waste from date palm trees, as effective biosorbents for the removal of lead ions (Pb^{2+}) from contaminated water. The adsorption capacity increased with contact time and was highest at pH 4.5. The process was influenced by the adsorbent dose, particle size, and ionic strength. The equilibrium data fit the Langmuir, Freundlich, and D–R isotherms, and the kinetics followed a pseudo-second-order model. The thermodynamic parameters indicated a spontaneous process, supporting the potential of these materials for large-scale water treatment applications [151].

Date palm trunk (DPT) fiber was investigated as a low-cost and effective adsorbent for Cu^{2+} removal from aqueous solutions. Maximum adsorption occurred at pH 5, with a dose of 5 g/l and particle size of 75 μm . Adsorption increased with Cu^{2+} concentration up to 100 mg/l but declined in efficiency at higher concentrations. The Langmuir isotherm best described the

equilibrium data, indicating monolayer adsorption, while the kinetics followed a pseudo-second-order model, suggesting chemisorption ($E = 14.59 \text{ kJ/mol}$). These results highlight the potential of DPT fiber as an economical material for copper removal, although further studies are needed to assess its performance in complex wastewater matrices [152].

Date palm leaf base (LB) was used as a low-cost adsorbent for the removal of Congo Red (CR) dye from aqueous solutions. This study examined the effects of temperature and pH on dye removal efficiency. The results indicated that the percentage of CR removal increased with increasing temperature and decreased with increasing pH. Equilibrium data were better described by the Langmuir isotherm model, which suggests monolayer adsorption, than by the Freundlich model. The thermodynamic parameters showed that the adsorption process was exothermic ($\Delta H^\circ < 0$) and non-spontaneous across the studied temperature range ($\Delta G^\circ > 0$). This study highlights the potential of using date palm waste, specifically the leaf base, as an effective dye-removal material for contaminated water [153].

Date palm leaf fibers were investigated as low-cost and effective adsorbents for the removal of methylene blue (MB) from aqueous solutions. The adsorbent demonstrated high efficiency, with over 80% dye removal occurring within the first two minutes. The adsorption equilibrium data were well described by the Freundlich and Temkin isotherm models, while the kinetic behavior followed the pseudo-second-order model, with the calculated and experimental adsorption capacities in close agreement. These findings confirm the potential of raw date palm leaves as a sustainable alternative to activated carbon for treating dye-contaminated industrial wastewater [154].

Although the use of raw plant-based waste as adsorbents presents numerous advantages, there are challenges and considerations that must be addressed. The adsorption capacity can vary significantly based on the type of plant waste and targeted pollutants. Additionally, the efficiency of raw adsorbents may be lower than that of chemically modified or activated forms, suggesting a potential need for further treatment or modification to enhance their performance. Despite these challenges, the integration of plant-based adsorbents into wastewater treatment processes offers a promising pathway for sustainable and cost-effective environmental management.

II. Biochar derived from plant wastes: thermal conversion and adsorptive applications

The use of biochar derived from plant waste has gained significant attention owing to its potential to enhance adsorption capabilities in environmental applications. Biochar, a carbon-rich material produced through pyrolysis, can be modified physically or chemically to improve its adsorption properties for various pollutants, including nutrients, heavy metals and organic contaminants. This approach not only aids in waste management but also contributes to environmental sustainability by effectively utilizing plant waste.

Natrayan et al. (2023) examined the efficiency of biochars synthesized from peanut shells and various agricultural wastes in the adsorption of lead (Pb) from industrial effluents. The results demonstrated that higher pH values led to precipitation phenomena, while increasing temperatures enhanced the chemical reactivity between biochars and Pb^{2+} ions, indicating an endothermic adsorption process. The adsorption capacity decreased with higher initial Pb concentrations, likely due to the saturation of active sites, whereas increased adsorbent dosage and agitation speed significantly improved the removal efficiency by exposing more active zones for interaction. Additionally, extended contact time positively influenced Pb adsorption, and kinetic studies confirmed the chemical stability and effectiveness of the developed biochars in capturing Pb^{2+} ions from aqueous media [155].

Nguyen et al. (2023) evaluated the performance of engineered biochars derived from various agricultural by-products for the removal of the emerging antibiotic contaminant oxytetracycline (OTC) from aqueous solutions. Among the tested materials, coir-derived biochar demonstrated the highest adsorption efficiency, achieving 93% removal in batch experiments and sustaining its performance over eight reuse cycles. Durian peel and straw biochars also exhibited notable adsorption capacities, whereas biochars from rice husks and macadamia nut shells were comparatively less effective. The primary adsorption mechanism was attributed to pore-filling interactions facilitated by van der Waals forces within the micro- and mesoporous structures of the biochars. These findings highlight the potential of tailored agricultural waste biochars for treating pharmaceutical-contaminated water [156].

He et al. (2024) investigated the adsorption performance of biochar derived from lavender straw (LBC) for the removal of methylene blue (MB) from aqueous solutions. The study reported a

high maximum adsorption capacity of $305.27 \text{ mg}\cdot\text{g}^{-1}$ under optimal conditions, including a dosage of $1.0 \text{ g}\cdot\text{l}^{-1}$, pH 8.0, contact time of 360 min, and temperature of 318 K. The adsorption process was characterized as spontaneous, endothermic, and entropy-driven, with mechanisms involving electrostatic interactions, pore-filling, and hydrogen bonding. In addition, LBC exhibited excellent reusability, retaining adsorption capacities exceeding $200 \text{ mg}\cdot\text{g}^{-1}$ after five regeneration cycles. These findings support the potential of LBC as an efficient and sustainable adsorbent for treating dye-contaminated wastewater [157].

Activated biochar from date palm waste has shown strong potential for removing various water pollutants, owing to its high surface area, porosity, and functional groups. Several studies have highlighted the effectiveness of biochar in adsorbing heavy metals, dyes, and organic compounds, confirming its value as a sustainable treatment material.

Many studies have demonstrated the high efficiency of biochar derived from date palm seeds in removing chlorinated volatile organic compounds (CVOCs) from water. Remmani et al. reported that the optimized biochar outperformed commercial activated carbon, achieving adsorption capacities of 86.68 mg/g for TCE and 85.97 mg/g for PCE. This superior performance was attributed to its high surface area, microporosity, and nanotubular structure. Adsorption followed pseudo-second-order kinetics, indicating chemisorption, and both Langmuir and Freundlich isotherms fitted the data well. These results highlight the potential of date palm waste for producing cost-effective and sustainable adsorbents for wastewater treatment [158].

Mahmoud et al. (2024) evaluated biochar derived from date palm leaf midribs using a two-step pyrolysis method for the removal of Cu(II) from wastewater. The biochar exhibited a high adsorption capacity and retained over 85% efficiency after five reuse cycles, demonstrating strong reusability and stability. Optimal adsorption occurred at pH 6, with a dosage of 1 g/l and 360 min contact time. Kinetic and isotherm models indicated that the process involved chemisorption, with monolayer and multilayer adsorption mechanisms. Thermodynamic analyses confirmed the spontaneity and exothermic nature of adsorption, reinforcing the potential of date palm biochar as a sustainable and cost-effective solution for heavy metal remediation in wastewater [159].

Zubair et al. (2020) conducted a comprehensive study on biochars derived from date palm fronds waste, a significant biomass source in Saudi Arabia, where over 25 million palm trees

produce large volumes of residues. This study assessed the effects of pyrolysis temperature and duration on the physicochemical properties of biochars and their adsorption performance for both cationic (methylene blue, crystal violet) and anionic dyes (methyl orange, Eriochrome Black T). Biochars produced at 700 °C for 4 h exhibited the highest BET surface area (431.82 m²/g) and adsorption capacities, reaching up to 934.57 mg/g for crystal violet. The adsorption kinetics followed the pseudo-second-order model, while the Redlich–Peterson isotherm best described the equilibrium data. The sorption mechanisms were attributed to electrostatic forces, π – π interactions, and surface complexation effects. This study highlights the strong potential of date palm biochars as cost-effective and sustainable adsorbents for treating dye-contaminated wastewater [160].

Aichour et al. (2021) evaluated biochar derived from date palm petioles (DPB) for the removal of methyl orange (MO) dye from wastewater. Batch adsorption experiments were conducted to assess the effects of dye concentration, pH, temperature, and contact time. The DPB exhibited a high adsorption capacity and could be reused for up to three cycles with consistent performance. This study highlights the simplicity, low cost, and effectiveness of date palm biomass-based biochars for dye remediation in wastewater [161].

Khadhri et al. (2018) investigated activated carbon produced from date palm petioles using NaOH activation for the removal of indigo carmine dye. The resulting material exhibited a high surface area (655 m²/g) and mesoporous structure, favoring adsorption in both batch and continuous systems. In batch mode, adsorption followed pseudo-second-order kinetics and the Langmuir isotherm, indicating a chemisorption-enhanced physisorption mechanism. In the continuous mode, the Thomas and Yoon–Nelson models effectively described the fixed-bed performance. The activated carbon maintained its efficiency over three reuse cycles, demonstrating its potential as a low-cost and eco-friendly adsorbent for dye removal [162].

Although biochar offers numerous environmental benefits, challenges remain in optimizing its production and application. Variability in feedstock composition and processing conditions can lead to differences in biochar properties, affecting its performance. Future research should focus on standardizing production methods and exploring new activation techniques to enhance the adsorptive capabilities of biochar. Additionally, large-scale production and cost-reduction strategies are essential for the broader adoption of biochar technologies.

III. Chemically modified plant wastes for water treatment

Addressing the challenge of water pollution requires both innovative and sustainable solutions. The utilization of chemically modified plant waste as adsorbents for water treatment has emerged as a promising strategy, leveraging abundant agricultural and industrial byproducts as low-cost raw materials. Native plant residues often possess inherent limitations in adsorption capacity because of their chemical and structural characteristics. However, targeted chemical modifications, such as alkalization, acidification, esterification, and carbonization, can significantly alter surface properties, increase the density of functional groups, and improve porosity, thereby greatly enhancing pollutant removal performance [163]. These modified biosorbents have demonstrated efficacy in removing heavy metals, dyes, and other hazardous pollutants from aqueous systems, often rivaling conventional commercial adsorbents but at a fraction of their cost [164]. Additionally, this approach contributes to resource recovery and waste valorization, aligning with the principles of green chemistry and the circular economy. As research continues to refine modification protocols and elucidate adsorption mechanisms, chemically modified plant wastes are poised to play an increasingly central role in sustainable water treatment technologies.

Fathy et al. (2013) investigated the effect of alkali-acid pretreatment on rice straw (RS) to enhance its adsorption capacity for methylene blue (MB) dye. The raw RS showed limited adsorption efficiency, whereas chemical modification with citric acid and EDTA significantly improved its performance. Adsorption was influenced by factors such as pH, contact time, initial dye concentration, and salt content, with optimal uptake at higher pH values and adsorbent doses. The process followed pseudo-second-order kinetics and fitted well with the Langmuir and Redlich–Peterson isotherms. This study confirmed the potential of treated RS as a cost-effective and sustainable adsorbent for dye-laden wastewater [165].

Kovacova et al. (2020) examined the effect of alkaline modification on the adsorption performance of four types of wooden sawdust for Cu(II) and Zn(II) removal. Treatment with NaOH and KOH significantly enhanced the adsorption efficiency from 20% to 46.5%, which was attributed to the increased –OH functional groups, as confirmed by FTIR analysis. Despite their compositional differences, all the sawdust types exhibited similar metal removal capacities. The Langmuir model best described the adsorption behavior, suggesting monolayer adsorption at equilibrium. Ion exchange and hydrogen bonding have been proposed as key

mechanisms. These findings highlight the potential of both raw and modified sawdust as low-cost adsorbents for the removal of heavy metals from water [166].

Castro et al. (2020) evaluated bio-adsorbents derived from chemically modified fruit peels—banana, orange, and granadilla—for the removal of Zn(II) ions from synthetic wastewater. The peels were treated with NaOH and calcium acetate to enhance their adsorption capacity. The results showed that the removal efficiency increased with higher concentrations of modifying agents, reaching up to 97.13% for orange peels. Adsorption followed pseudo-second-order kinetics and was best described by the Langmuir isotherm model. This improved performance was attributed to the increased number of binding sites, particularly in the cellulose-rich peels. These findings support the potential of agro-industrial waste as low-cost, sustainable adsorbents for the removal of heavy metals [167].

Jawad et al. (2020) synthesized sulfuric acid-treated coconut shell (SATCS) and evaluated its efficiency for methylene blue (MB) dye removal. Under optimal conditions (0.1 g/100 ml dosage, pH 8, 303 K), the adsorbent achieved a maximum capacity of 50.6 mg/g. Adsorption followed a chemisorption-dominated heterogeneous mechanism involving electrostatic interactions, hydrogen bonding, and π - π interactions. This study highlights the potential of SATCS as a low-cost and effective biosorbent for treating dye-contaminated wastewater [168].

Building on the promising performance of various chemically modified agricultural wastes, particular attention has been directed toward date palm-derived biosorbents, whose chemical functionalization has further enhanced their capacity to remove a range of pollutants from aqueous media.

In this context, multiple investigations, such as those by *Siva Kumar et al.* (2024), have highlighted the improved adsorption capabilities of date palm-derived biomasses after chemical modifications using agents such as sodium hydroxide and citric acid. These modifications significantly enhanced the removal efficiencies of organic contaminants, such as phenol and 2,4,6-trichlorophenol, with Langmuir model predictions revealing adsorption capacities exceeding 120 mg/g in some cases. These findings underscore the potential of modified date palm fibers and stones as efficient, eco-friendly, and low-cost adsorbents for wastewater purification [142].

Siva Kumar *et al.* (2023) investigated the adsorption performance of raw and NaOH-modified date palm fiber (RDPF and NaOH-CMDPF) for phenol removal from aqueous solutions. The adsorption efficiency was influenced by parameters such as pH, contact time, adsorbent dose, and initial phenol concentration. The modified fiber exhibited a notably higher monolayer adsorption capacity (89.67 mg/g) compared to the raw material (45.62 mg/g), with both fitting well to Langmuir, Freundlich, D–R, and pseudo-second-order models. These findings highlight the potential of chemically treated date palm waste as an effective, low-cost, and sustainable biosorbent for the treatment of phenol-contaminated wastewater [9].

Moreover, recent findings by Hafeez *et al.* (2019) demonstrated the effectiveness of acid-treated *Phoenix dactylifera L.* seeds as biosorbents for the removal of Zn^{2+} ions, a hazardous heavy metal prevalent in industrial effluents, such as those from the fertilizer and galvanizing sectors. Through optimization via response surface methodology, the study revealed a maximum uptake of 26.84 mg/g under acidic conditions (pH \approx 3.5), highlighting the crucial role of chemical modification and operational parameters in enhancing the adsorption efficiency of date-palm-based materials for heavy metal remediation [169].

In addition to phenol and heavy metal pollutants such as Zn^{2+} and 2,4,6-TCP, several recent studies have explored the application of chemically modified date palm biomass for the efficient removal of toxic mercury ions. For instance, Rajamohan *et al.* (2014) reported that protonated *Phoenix dactylifera* biomass achieved a remarkable 92% mercury removal under optimized conditions (pH 7.0, 3 g/L dosage), with kinetics following a pseudo-second-order model and a maximum uptake of 46.73 mg/g. These findings reinforce the versatility and potential of date-palm-based biosorbents for treating various classes of contaminants through tailored chemical modifications [170].

Yadav *et al.* (2014) investigated the potential of chemically modified date palm trunk (DPT) grafted with diethylenetriamine and triethylamine via epichlorohydrin crosslinking for the removal of hexavalent chromium from aqueous media. The modified adsorbent (MDPT) exhibited a high adsorption capacity, reaching 89.3 mg/g at 100 mg/L Cr(VI), and achieved up to 99.95% removal at an optimum pH of 3.5 and dosage of 1.2 g/L. The adsorption followed pseudo-second-order kinetics and was best described by the Langmuir isotherm, indicating monolayer sorption with a maximum capacity of 129.8 mg/g. Reusability tests confirmed the stability of the material over four cycles, with minimal performance loss. These findings

highlight the efficacy of grafted DPT as a cost-effective and regenerable biosorbent for Cr(VI) remediation [171].

In conclusion, chemical modifications such as alkalization and acidification significantly enhanced the pollutant removal performance of date palm waste, making it an effective biosorbent for various contaminants. However, the environmental impact and economic feasibility of these modifications must be carefully evaluated to ensure sustainable and cost-effective water-treatment solutions. Further research on optimizing these processes and exploring alternative modification techniques could provide more sustainable options for large-scale applications.

Conclusion:

This review clarifies how plant and date palm wastes, whether raw or chemically modified, can be used to treat water and remove various pollutants, such as pharmaceuticals, dyes, and heavy metals. Research has shown that chemically modifying these wastes makes them more effective for adsorption. This method is also characterized by being inexpensive, sustainable, and reusable.

Despite these advances, a clear research gap persists regarding the influence of date palm cultivars (e.g., *Degla*, *Ghars*, and *Takermost*) on adsorption behavior and efficiency. There is a shortage of studies addressing how the physical and chemical compositions of different cultivars translate into variations in pollutant removal. Moreover, most existing studies have investigated traditional process variables in isolation, without systematically integrating date palm cultivars as a decisive factor. A better understanding of how cultivar variations interact with operational variables, such as pH, temperature, adsorbent dose, contact time, and initial pollutant concentration, could enable the design of more effective, locally adapted adsorbent materials with renewable and sustainable properties.

The current chapter sets the stage for the next, which describes the experimental methods used to evaluate the efficacy of raw and chemically treated date palm by-products in removing methylene blue from water. The following sections cover the material collection, chemical modification, surface characterization, and adsorption experiments, focusing on the effect of cultivar and modifications on several factors such as contact time, dye concentration, pH, and temperature to provide scientific solutions for water treatment.

Chapter 3

Modifications of Date Palm By-Products (Materials and Methods)

Introduction

This chapter outlines the materials, reagents, and experimental procedures employed to investigate the adsorption performance of chemically modified and unmodified date palm by-products for the removal of methylene blue from aqueous solutions. The study includes the collection and preparation of raw materials, their chemical treatment, and the characterization techniques used to analyze surface and structural modifications. Furthermore, it presents the batch adsorption protocols designed to evaluate the influence of key operational parameters such as contact time, initial dye concentration, pH, and temperature on adsorption efficiency.

I. Biomass collection area

The date palm by-products utilized in this study, including leafy fronds and empty fruit bunches, were sourced from three distinct cultivars: *Degla*, *Ghars*, and *Takermost*. These samples were collected from AinMoussa Region in the Ouargla Oasis (32° 03' 04.1'' N, 5° 20' 12.1'' E), located in the southeastern Algerian Sahara (Figure III.1) which lies between the lines of longitude and latitude shown in the table below in November 2021. This region is known for its unique environmental conditions (hot and dry), which may influence the properties and characteristics of the date palm by-products and making it an ideal source of raw biomass for valorization. The selection of these particular cultivars was based on their prevalent cultivation (under arid and semi-arid climatic conditions) and their significance in local agricultural practices. The samples were manually harvested, classified by cultivar and palm part, and then transported to the laboratory for cleaning, drying and further chemical modification.

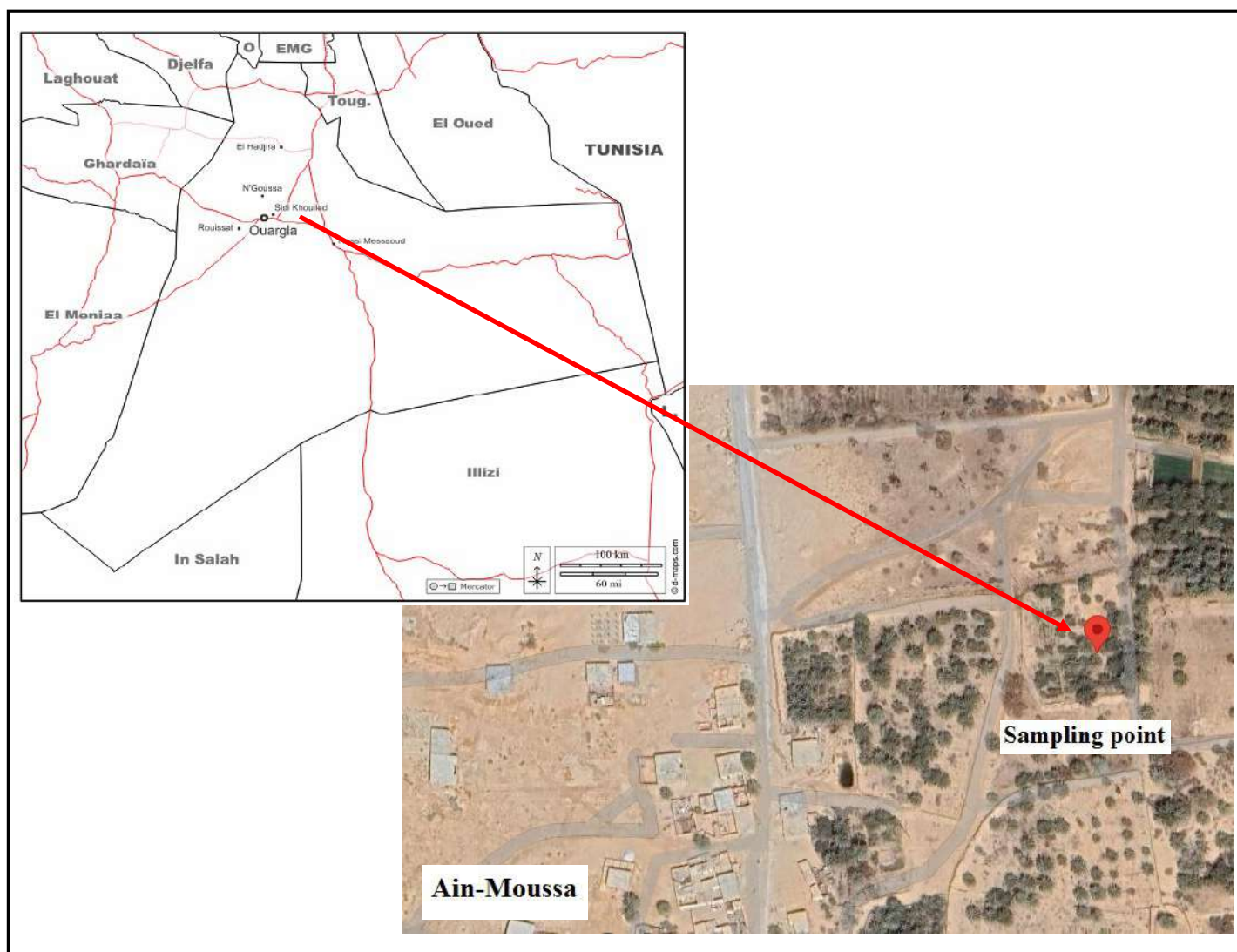


Figure III.1: Geographical map of biomass sampling area [173].

II. Chemicals

The chemicals used in this study are listed in the table III.1:

Table III.1: List of chemicals

<i>Name</i>	<i>Chemical formula</i>	<i>Purity</i>	<i>Supplier</i>
<i>Potassium hydroxide</i>	<i>KOH</i>	<i>85%</i>	<i>BIOCHEM Chemopharma</i>
<i>Sulfuric acid</i>	<i>H₂SO₄</i>	<i>98%</i>	<i>BIOCHEM Chemopharma</i>
<i>Methylene blue</i>	<i>C₁₆H₁₈N₃ClS</i>	<i>-</i>	<i>BIOCHEM Chemopharma</i>
<i>Sodium hydroxide</i>	<i>NaOH</i>	<i>97%</i>	<i>BIOCHEM Chemopharma</i>
<i>Hydrochloric acid</i>	<i>HCl</i>	<i>37%</i>	<i>BIOCHEM Chemopharma</i>

III. Preparation of adsorbents

For preparation of modified adsorbents from date palm by-products which were planted in the area mentioned above, the obtained samples went through the following stages:

- **Cutting samples**

The samples were cut into small pieces without grinding so that we could purify them well.

- **Washing samples**

The samples were washed with distilled water several times to get rid of all contaminants.

- **Grinding and sieving samples**

Before grinding with a stone grinder, the samples were air-dried for one day, then were sieved to obtain a fine powder ($d < 400 \mu\text{m}$)

- **Modifying samples**

Each sample was divided into three equal portions for subsequent modifications:

- The first portion was dried in a vacuum oven at $110 \text{ }^\circ\text{C}$ for 24 h. It was stored in a sealed glass container prior to use for adsorption studies. Before adsorption experiments no chemical or physical treatment was performed on dried raw pulverized particles.
- The second portion was acid modified to increase the adsorption property of the adsorbent. 100 grams of sample and 500 ml of 0.5 M solution of H_2SO_4 were taken in a beaker and the resulting mixture was stirred for two hours (150 rpm), then allowed to soak for 24 h. After this the content of the beaker was filtered and extensively washed with distilled water to eliminate the excessive acid which was tested by measuring the pH which should be between 6-7 (neutralization) and refiltered through a Whatman filter paper. Then it was dried for 24 hours at $110 \text{ }^\circ\text{C}$ and finally stored in a sealed glass container for later use.
- The third portion underwent alkaline treatment using 0.5 M KOH, following the same protocol as the acid treatment.

A total of 18 samples were obtained from the combination of date palm by-products, cultivars, and modification methods. The entire process is summarized in figure III.2.

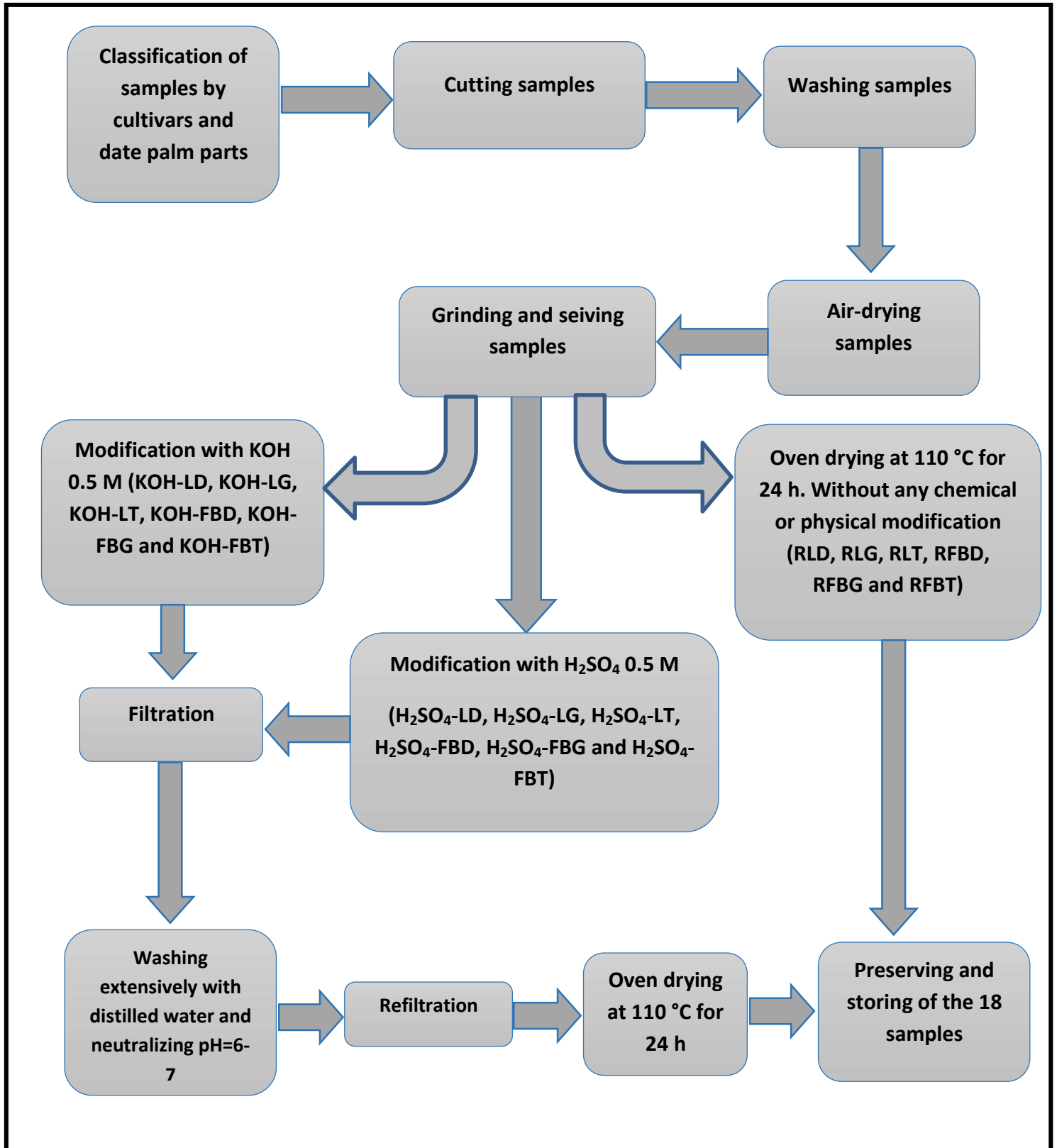


Figure III.2: Modification of date palm biomasses of three cultivars plan

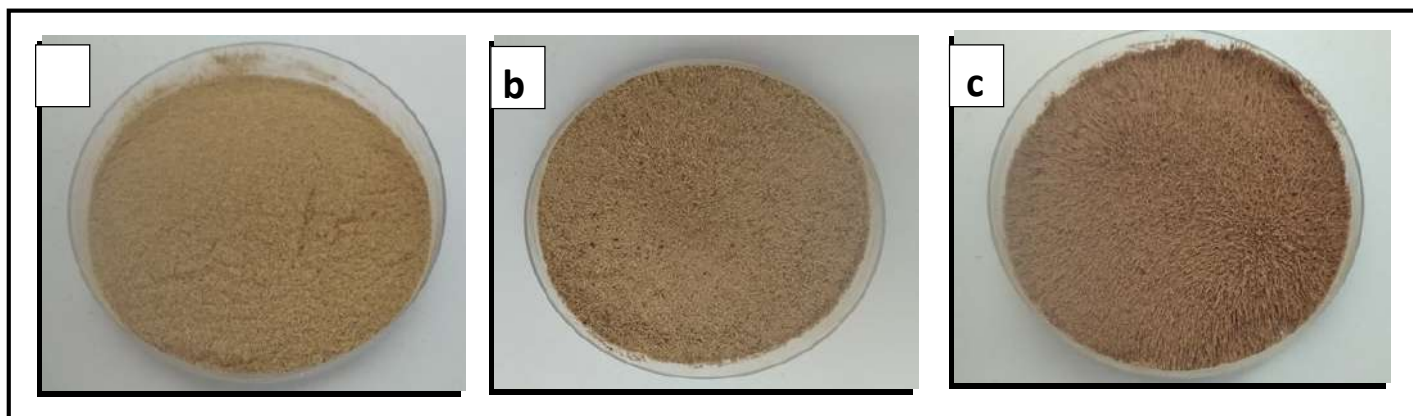


Figure III.3: (a) Raw leafy fronds of *Takermost* cultivar (RLT), (b) H_2SO_4 modified leafy fronds of *Takermost* cultivar (H_2SO_4 -LT), (c) KOH modified leafy fronds of *Takermost* cultivar (KOH-LT)

IV. Characterization of adsorbents

In order to better understand the physicochemical characteristics of the date palm by-products before and after modification, several characterization techniques were employed. These include **Fourier Transform Infrared Spectroscopy (FTIR)**, **X-ray Diffraction (XRD)** /**X-ray Fluorescence (XRF)** and **Scanning Electron Microscopy (SEM)**. These tools provided complementary information necessary to support the adsorption study.

IV.1. FTIR analysis

FTIR was used to identify the functional groups present on the surface of the materials, which are responsible for the adsorption interaction.

For this work, samples were characterized using FTIR SHIMADZU 8300 with thin and transparent KBr pellets, obtained by compressing under vacuum finely ground biomass with KBr. The IR absorption range used for our samples is between 4000 and 400 cm^{-1} .

IV.2. XRD and XRF analysis

XRD provided information about crystallinity and structural changes induced the chemical modifications. X-ray Fluorescence (XRF) is a method used to identify and measure the elements present in a material, it works by exposing a sample to X-rays, which interact with the atoms and cause them to emit specific fluorescent X-rays. By analyzing this emitted fluorescence, the elemental makeup of the sample can be determined. The powdered sample ($<150\text{ }\mu\text{m}$) was analyzed using the BTX II X-ray diffraction system (Olympus), equipped with a Cu X-ray tube (30 kV , $330\text{ }\mu\text{A}$) and a cooled 2D CCD detector. The sample was loaded into

the analysis cell and scanned over a 2θ range of 5° – 55° . Diffractograms were processed via X Powder to identify crystalline phases. XRF analysis, performed with the integrated SDD detector, revealed key elements including K, Cr, Fe, and Cu in the 3–12 keV range.

IV.3. SEM analysis

SEM allowed visualization of surface morphology, giving insight into texture, porosity and the effects of surface modification.

The surface morphology of samples was examined using a Zeiss EVO 15 SEM. Samples were gold-coated for 60 seconds after mounting on conductive stubs. Imaging was performed at 20.00 kV under varying magnifications to observe surface texture and particle characteristics.

V. Batch adsorption studies

To assess the adsorption capacity of both untreated and chemically modified palm biomass, a series of batch experiments were conducted. These experiments aimed to examine the effect of various operational parameters, including contact time, initial dye concentration, pH, and temperature, on the efficiency of methylene blue removal.

V.1. Adsorbate

The dye selected for this study was methylene blue (MB), a cationic compound with the chemical formula $C_{16}H_{18}N_3SCl$ and a molecular weight of 319.86 g/mol, obtained from BIOCHEM Chemopharma. A stock solution with a concentration of 1000 mg/l was prepared. Working solutions of varying concentrations were then prepared by appropriate dilution of the stock solution.

MB adsorption experiments were conducted to evaluate the adsorption capacity of the samples. After the adsorption process was completed, the residual dye concentration in solution was determined by measuring the absorbance at the maximum wavelength ($\lambda_{max} = 664$ nm) using a UV-Vis spectrophotometer (OPTIZEN POP).

V.2. Contact time effect

The effect of contact time on MB adsorption was investigated by adding 1 gram of each sample to 50 ml of methylene blue solution at initial concentrations of 10, 30, 50, 70, and 90 mg/L. The experiments were conducted at a constant temperature of $25^\circ C$. The mixtures were

agitated for varying contact times of 5, 10, 15, 30, 40, 60, 90, and 120 minutes. After filtration, the residual dye concentrations in the filtrates were determined using UV-Visible spectrophotometry.

V.3. Initial dye concentration effect

The effect of initial dye concentration on the adsorption of MB was examined by preparing solutions with concentrations of 10, 30, 50, 70, and 90 mg/L. A fixed mass of 1 g of each adsorbent sample was added to 50 ml of dye solution. The mixtures were agitated for 60 minutes at a constant temperature of 25 °C. Following filtration, the remaining dye concentrations were measured using UV-Vis spectrophotometry.

V.4. pH effect

The influence of solution pH on methylene blue adsorption was investigated over a pH range of 3 to 13 (specifically at pH values of 3, 5, 7, 9, 11, and 13). The pH was adjusted using 0.2 M hydrochloric acid (HCl) or 0.2 M sodium hydroxide (NaOH) solutions. For each test, 1 g of adsorbent was added to 50 ml of MB solution at an initial concentration of 30 mg/l. The mixtures were agitated for 60 minutes at a constant temperature of 25 °C. After filtration, the residual dye concentration was determined using UV-Vis spectrophotometry.

V.5. Temperature effect

The effect of temperature on the adsorption of methylene blue was evaluated at different temperatures: 25 °C, 35 °C, 45 °C, and 55 °C. For each experiment, 1 g of the adsorbent was added to 50 ml of dye solution with an initial concentration of 30 mg/l. The mixtures were agitated for 60 minutes under controlled conditions. After filtration, the remaining dye concentration in the solution was measured using UV-Vis spectrophotometry. This investigation aimed to assess the thermodynamic behavior of the adsorption process.

Conclusion

The methodology described in this chapter provides a comprehensive framework for evaluating the adsorption efficiency of different palm biomass-based adsorbents. The systematic preparation, modification, and characterization of the materials, coupled with controlled batch adsorption experiments, establish a solid foundation for interpreting the results presented in the subsequent chapter. The combination of physicochemical analyses and adsorption trials allows for a better understanding of how surface modifications and operational conditions influence the removal of methylene blue from aqueous solution.

Chapter 4

Results and Discussion

Introduction

This chapter presents a comprehensive discussion of the results obtained from the characterization and adsorption studies carried out on raw and chemically modified date palm biomass. A suite of analytical techniques, namely Fourier-transform infrared spectroscopy (FTIR), X-ray diffraction (XRD), X-ray fluorescence (XRF), and scanning electron microscopy (SEM), was employed to investigate the structural, elemental, and morphological alterations resulting from acidic and alkaline modifications. The adsorption behavior of methylene blue was systematically evaluated under varying experimental conditions, including solution pH, contact time, temperature, and initial dye concentration. To elucidate the adsorption mechanisms and quantify the interaction between the dye molecules and the biomass surface, several isotherm and kinetic models were applied. Special emphasis was placed on comparing the performance of the three date palm cultivars and biomass types to critically assess the influence of chemical treatments on their adsorption efficiencies.

I. Fourier Transform Infrared Spectroscopy (FTIR) analysis

Fourier Transform Infrared Spectroscopy (FTIR) was employed to examine the surface functional groups present in both the raw and chemically modified date palm biomass of three cultivars. This analysis is essential for comprehending the chemical modifications induced by acidic and alkaline treatments, as well as the interactions between the adsorbent surface and methylene blue molecules during the adsorption process.

The spectra of the raw (unmodified) samples of leafy fronds (Figure IV.1) displayed characteristic absorption bands around $\sim 3400\text{ cm}^{-1}$, corresponding to O–H stretching vibrations of hydroxyl groups [174], $\sim 2920\text{ cm}^{-1}$ for C–H stretching of aliphatic chains [105], $\sim 1730\text{ cm}^{-1}$ attributed to C=O stretching of carboxylic or ester groups, and ~ 1600 for C=C aromatic ring vibrations [175]. The band at 1246 cm^{-1} corresponds to the syringyl ring and C–O stretching vibrations typically found in lignin and xylan structures, while the band at 1156 cm^{-1} is associated with the C–O–C asymmetric stretching vibrations present in cellulose and hemicellulose [174].

Acid treatment resulted in a noticeable reduction in peak intensities [176]. The broadening and increased intensity of the O–H stretching band ($\sim 3400\text{ cm}^{-1}$) suggests an enrichment of surface hydroxyl groups ($\text{H}_2\text{SO}_4\text{-LT}$). These observations confirm the efficacy of acid treatment in altering the surface chemistry of biomass, potentially enhancing its adsorption performance.

Alkaline treatment improves biomass surface properties by hydrolyzing ester bonds and removing acetyl groups and amorphous components (e.g., lignin and hemicellulose) [163]. FTIR spectroscopy results confirmed the disappearance of C=O and C–O band intensities along with slight peak shifts after potassium hydroxide (KOH) treatment, demonstrating the resulting chemical and structural modifications of the material.

Similar spectral features were observed in both raw and modified empty fruit bunch samples (Figure IV.2), with the appearance of a characteristic absorption peak at 2920 cm^{-1} , attributed to C–H stretching vibrations in aliphatic groups [175].

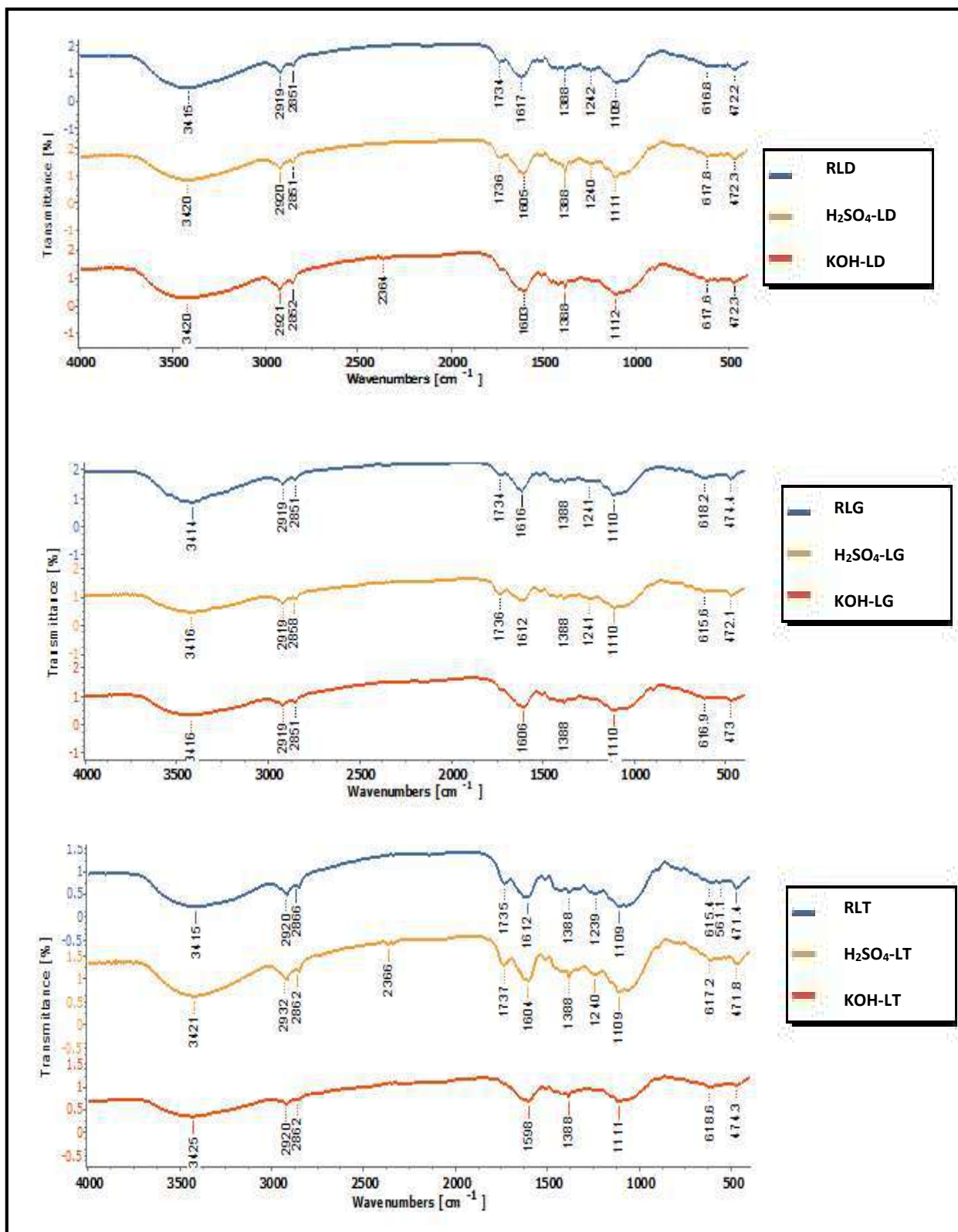


Figure IV.1: The FTIR spectra of raw and modified leafy fronds of three cultivars

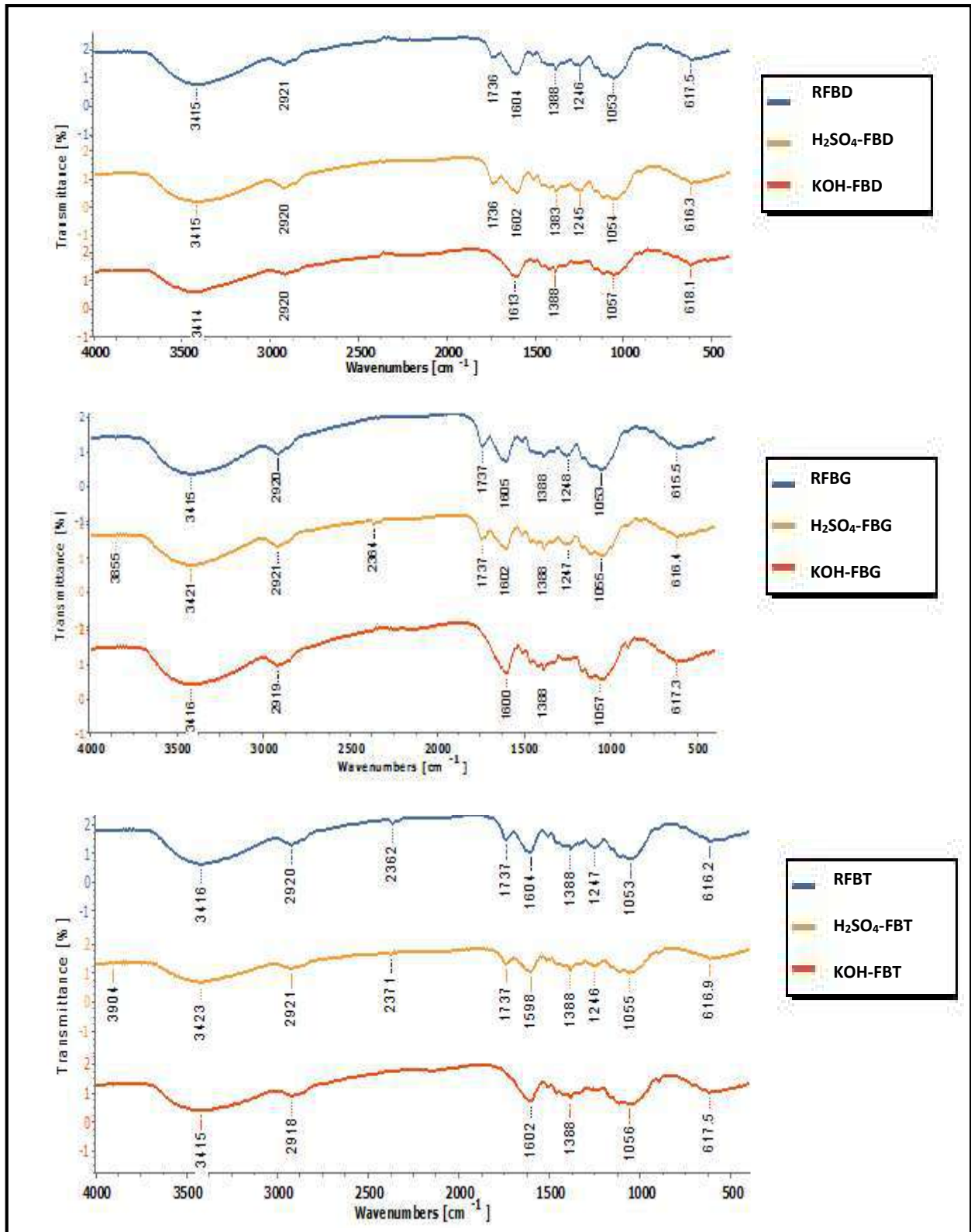


Figure IV.2: The FTIR spectra of raw and modified empty fruit bunch of three cultivars

II. X-ray Diffraction (XRD) / X-ray Fluorescence (XRF) analysis

A comparative analysis of the X-ray diffraction (XRD) and X-ray fluorescence (XRF) data for 18 date palm biomass samples, comprising three cultivars (*Degla*, *Ghars*, and *Takermost*) subjected to alkaline (KOH), acidic (H₂SO₄), and unmodified conditions, revealed distinct trends in crystallinity and inorganic elemental composition.

The patterns XRD of all samples are displayed in Figure IV.3, while Table IV.1 displays the crystallinity index (CI) data.

The crystallinity index (CI) was calculated using the integration method. This method uses a straight-line background, taking the highest 2θ values as a reference. It compares the area under the full pattern with the area under the crystalline peaks using the following equation [177]:

$$\text{Crystallinity index } CI_{XRD} (\%) = 100 \times \frac{\text{Area crystalline XRD peaks}}{\text{Area under all XRD peaks}} \quad (12)$$

From Table IV.1, it can be concluded that KOH-modified samples generally exhibited the highest CI values, particularly in leafy frond parts (e.g., KOH-LD: 51.53%, KOH-LG: 49.86%), compared to their raw counterparts (RLD: 42.61%, RLG: 43.00%). Acidic modification with H₂SO₄ also enhanced CI, although the magnitude of the increase varied by sample and was sometimes less pronounced than that with KOH. Empty fruit bunch (FB) samples displayed lower overall CI values (e.g., RFBD: 26.32%, KOH-FBD: 32.84%) than leafy fronds, likely reflecting inherent anatomical differences and higher amorphous content.

Figure IV.4 and IV.5 show the XRF spectra of raw and modified leafy fronds and empty fruit bunch of three cultivars. XRF analysis identified potassium (K), calcium (Ca), copper (Cu), iron (Fe), chromium (Cr) and manganese (Mn) as the predominant inorganic elements in the biomass [178], with K being particularly abundant in the raw samples. Both KOH and H₂SO₄ treatments resulted in a marked reduction in K and Mn concentrations, attributable to their solubilization and removal during processing. Conversely, Ca and Cr tended to become relatively enriched in the by-products, particularly after modification.

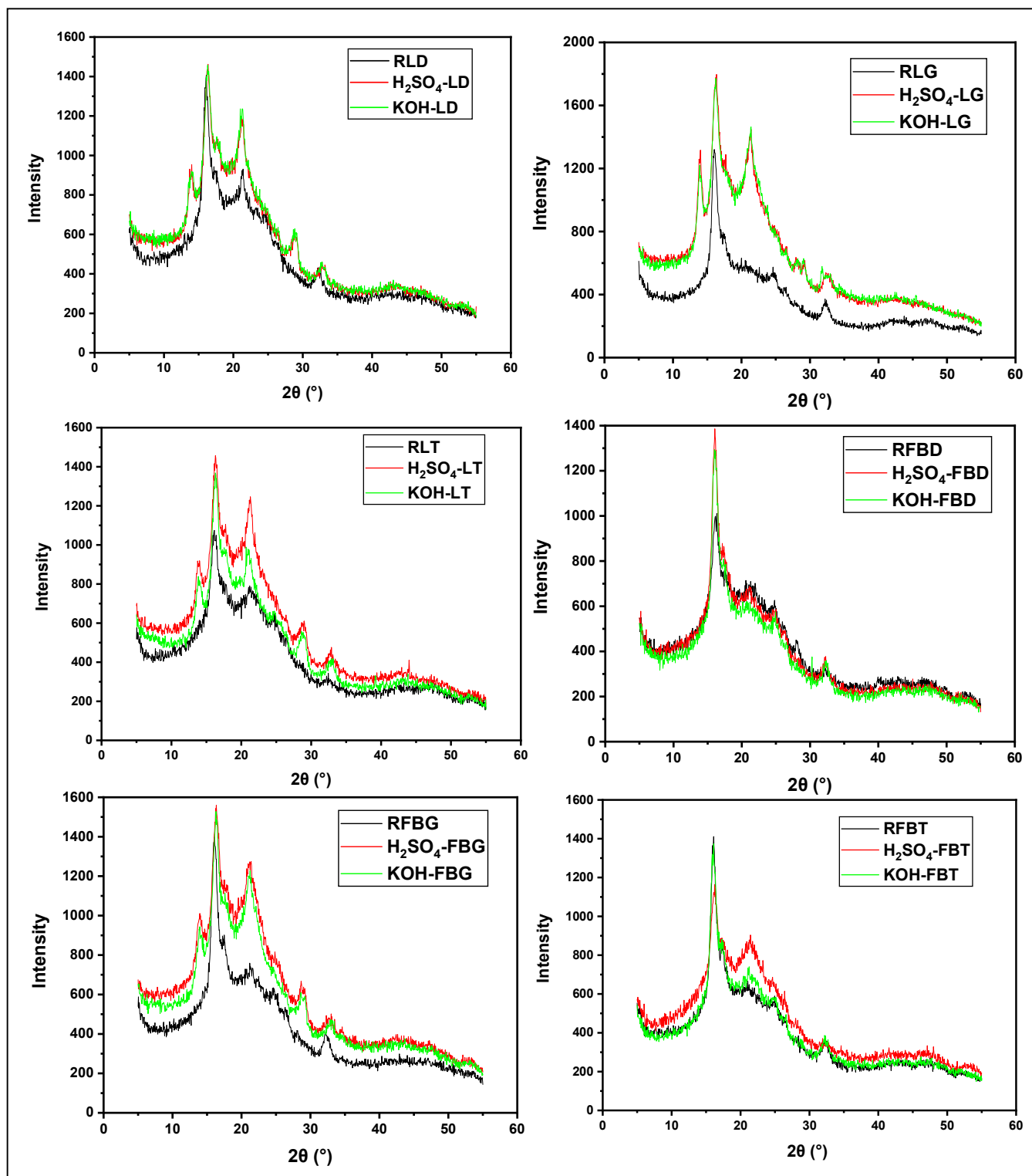


Figure IV.3: XRD patterns of all samples

Table IV.1: The crystallinity index CI_{XRD} of each sample.

<i>Sample</i>	<i>The crystallinity index CI_{XRD} (%)</i>
<i>RLD</i>	<i>42.61</i>
<i>H₂SO₄-LD</i>	<i>48.31</i>
<i>KOH-LD</i>	<i>51.53</i>
<i>RLG</i>	<i>43.00</i>
<i>H₂SO₄-LG</i>	<i>48.37</i>
<i>KOH-LG</i>	<i>49.86</i>
<i>RLT</i>	<i>40.74</i>
<i>H₂SO₄-LT</i>	<i>49.64</i>
<i>KOH-LT</i>	<i>45.15</i>
<i>RFBD</i>	<i>26.32</i>
<i>H₂SO₄-FBD</i>	<i>29.59</i>
<i>KOH-FBD</i>	<i>32.84</i>
<i>RFBG</i>	<i>40.66</i>
<i>H₂SO₄-FBG</i>	<i>51.17</i>
<i>KOH-FBG</i>	<i>50.20</i>
<i>RFBT</i>	<i>28.33</i>
<i>H₂SO₄-FBT</i>	<i>41.03</i>
<i>KOH-FBT</i>	<i>42.30</i>

The extent of mineral removal and retention was influenced by both the type of chemical treatment and the cultivar, with *Ghars* and *Takermost* generally exhibiting higher CI and more pronounced increases post-modification than *Degla*.

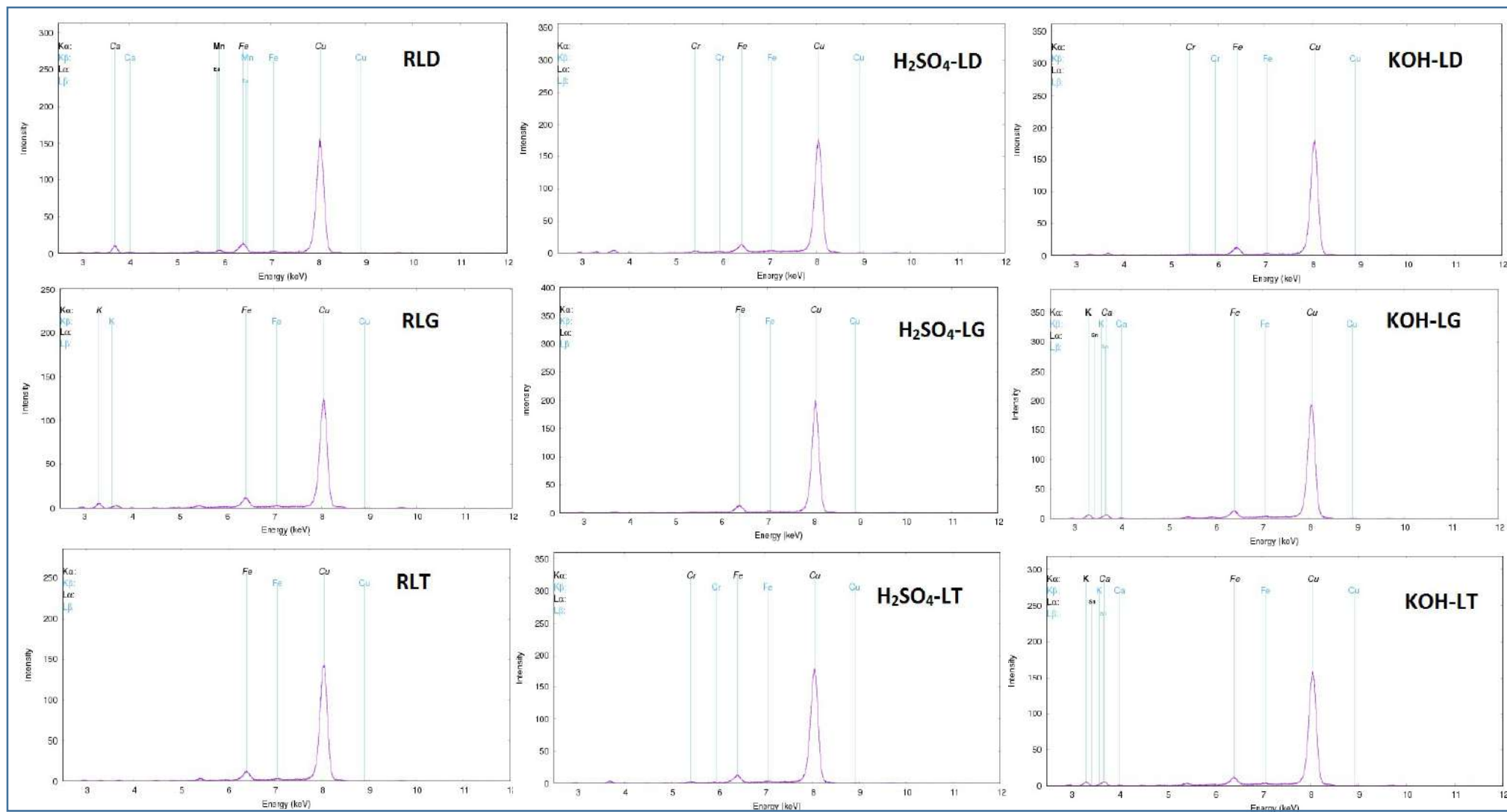


Figure IV.4: XRF spectra of raw and modified leafy fronds of three cultivars

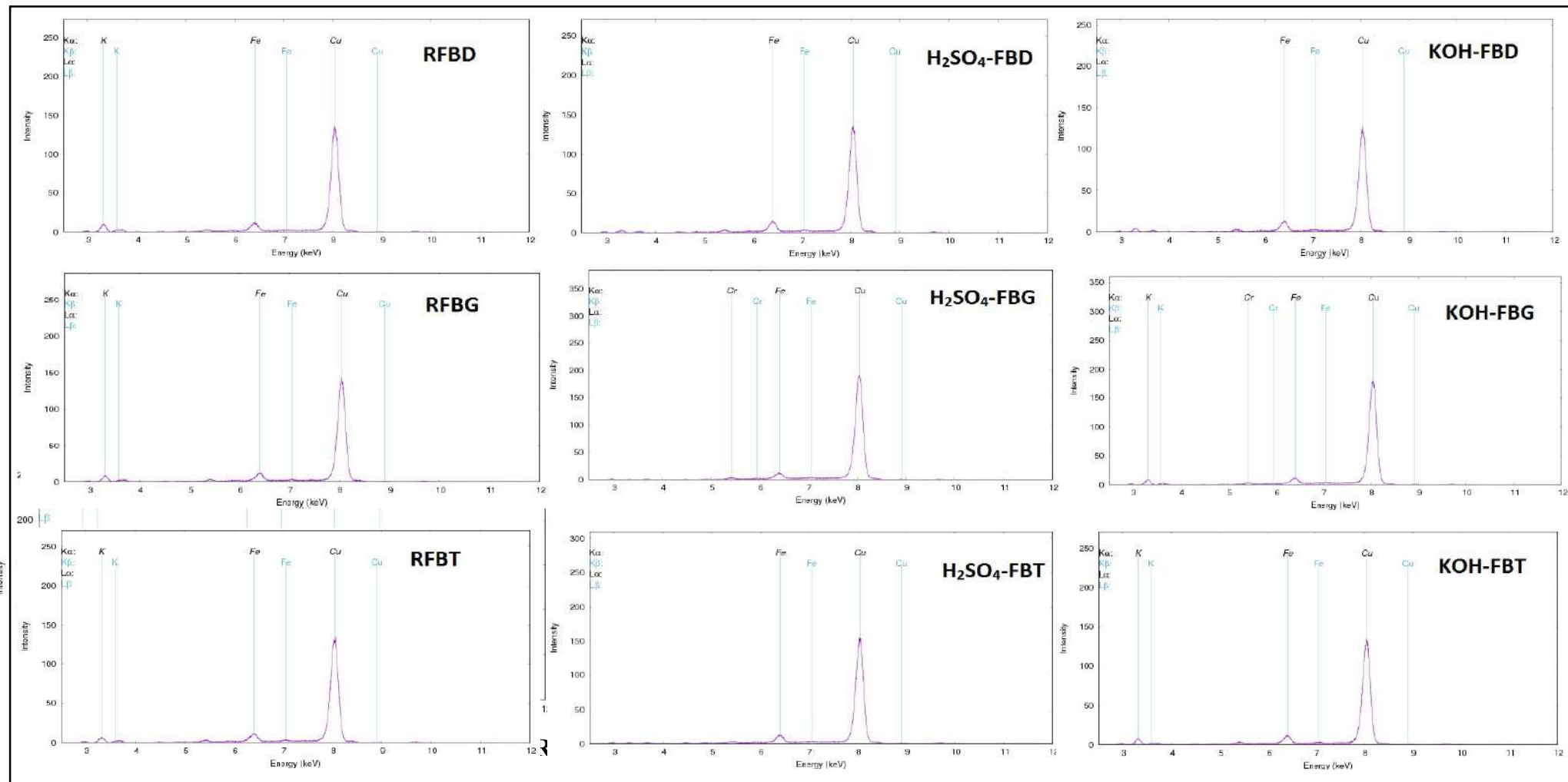


Figure IV.5: XRF spectra of XRD of raw and modified empty fruit bunch of three cultivars

These findings underscore the interplay between genetic background and chemical pretreatment in modulating the structural and compositional attributes of date palm biomass [179]. The observed trends are consistent with previous reports on lignocellulosic biomass, wherein alkaline pretreatment selectively removes amorphous components and certain minerals. This process improves the crystallinity of cellulose [180].

III. Scanning Electron Microscopy (SEM) analysis

The scanning electron microscopy (SEM) analysis conducted in this study specifically focused on the date palm biomass of the Ghars cultivar. This cultivar was chosen as a representative example to elucidate the morphological changes occurring before and after chemical modification, as illustrated in Figures IV.6 and IV.7, and also following methylene blue (MB) adsorption, which is displayed in Figure IV.8. It is essential to emphasize that the observations presented here pertain exclusively to this cultivar and are not intended to be generalized to all cultivars examined in the broader study.

Prior to MB adsorption, the raw Ghars biomass exhibited relatively smooth, compact surfaces with tightly bound fibers and limited visible porosity [161]. In contrast, the chemically modified samples (KOH and H₂SO₄) demonstrated increased surface roughness, enhanced porosity, and partial fiber separation, indicative of effective delignification and hemicellulose removal [181]. These modifications are known to increase the available surface area and create additional adsorption sites, thereby facilitating greater interactions with dye molecules [164].

Following MB adsorption, the SEM micrographs revealed the emergence of distinct surface deposits and increased particle aggregation across all Ghars samples, with previously open pores and fissures becoming partially or completely occluded by the adsorbed dye [104]. The treated samples, in particular, exhibited more pronounced surface coverage, suggesting a higher adsorption capacity consistent with their increased porosity and surface roughness.

The observed morphological changes, such as the reduction in visible pore volume and the formation of aggregated dye-biomass complexes, support the hypothesis that MB molecules are effectively immobilized within the porous matrix and on the exposed fiber surfaces [182].

These findings underscore the critical role of surface morphology and microstructural features in dictating adsorption efficiency, as enhanced roughness and porosity directly correlate with improved dye uptake. Moreover, the occlusion of pores and surface coverage adsorption provided visual confirmation of successful MB binding, corroborating the efficacy of chemical pretreatment strategies in optimizing biomass-based adsorbents for environmental remediation applications.

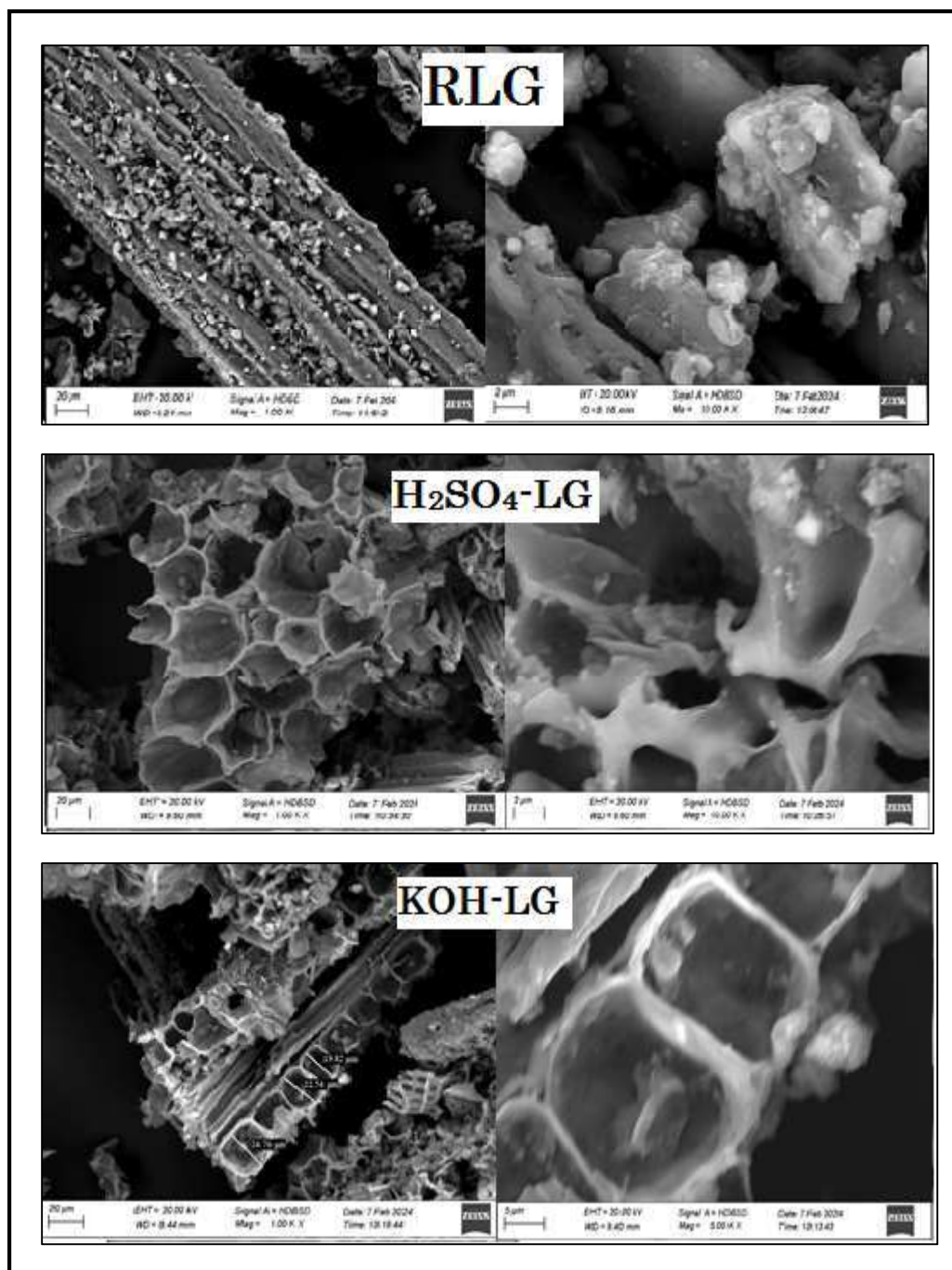


Figure IV.6: SEM images of RLG, H₂SO₄-LG and KOH-LG

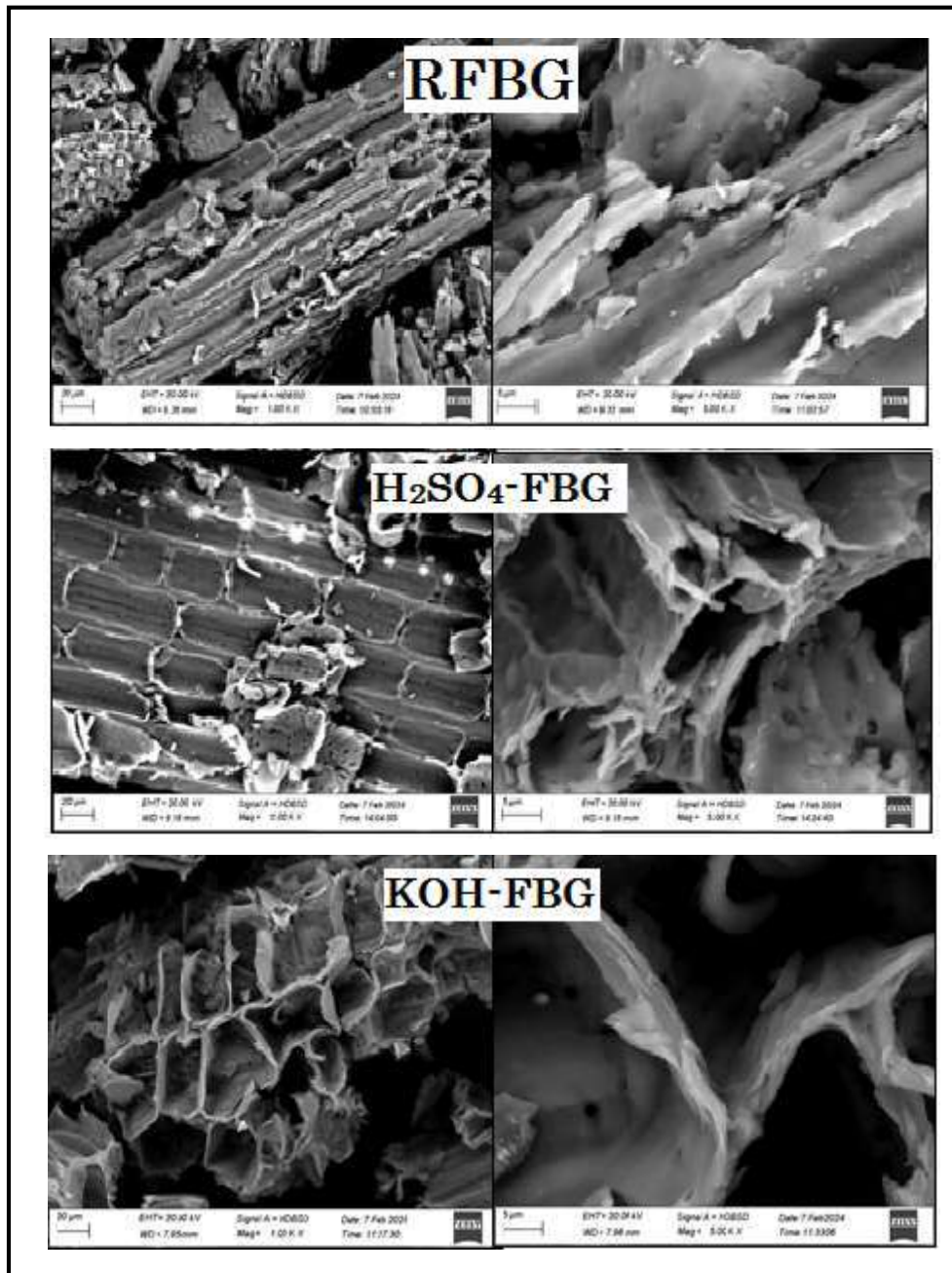


Figure IV.7: SEM images of RFBG, H₂SO₄-FBG and KOH-FBG

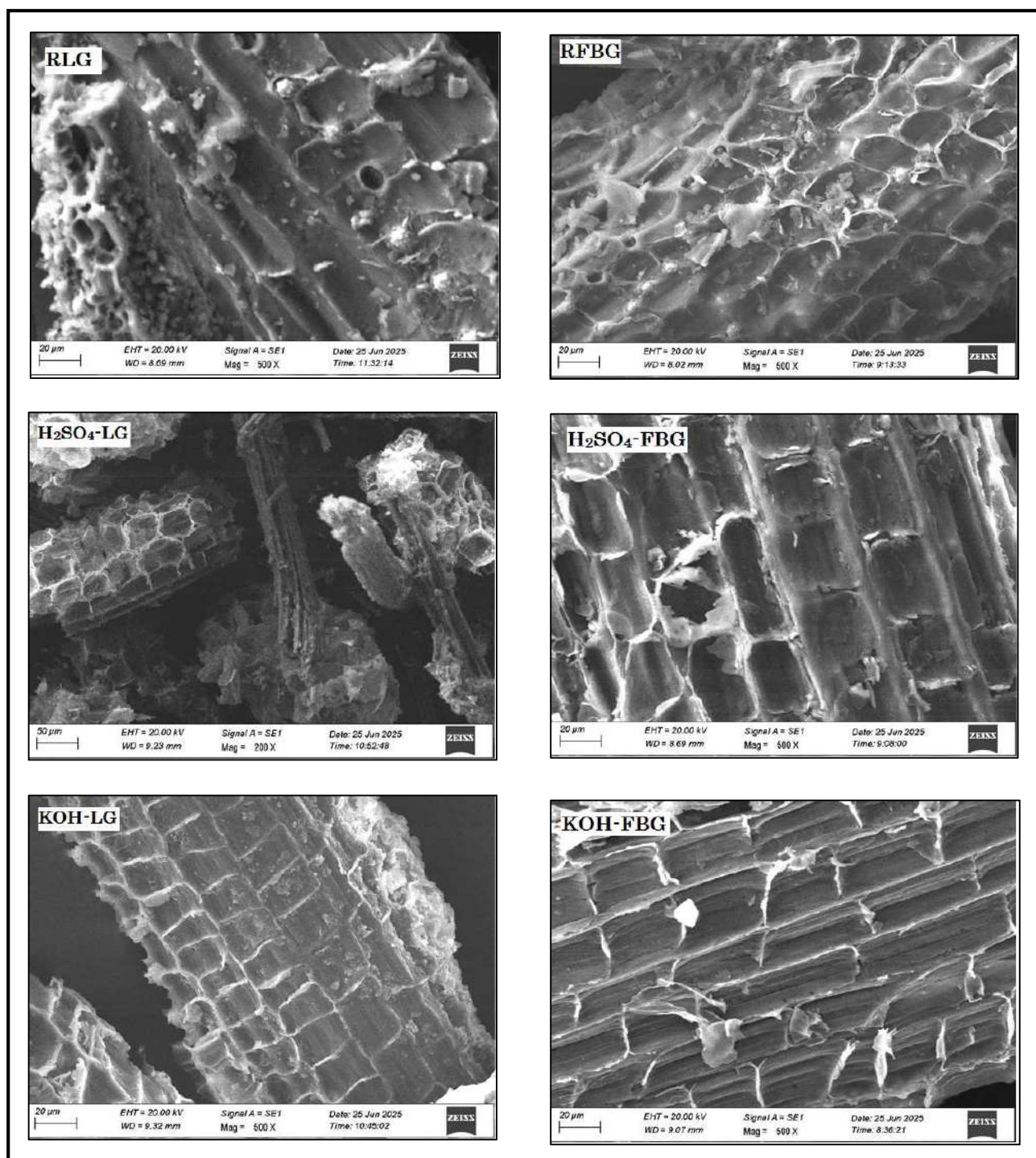


Figure IV.8: SEM images of RLG, H₂SO₄-LG, KOH-LG, RFBG, H₂SO₄-FBG and KOH-FBG after adsorption of MB

IV. Fundamental study of the adsorption of MB on date palm biomasses

IV.1. Factors affecting the adsorption procedure

IV.1.1. Effect of pH

The influence of pH on the adsorption of methylene blue (MB) onto various biomasses was systematically investigated to elucidate the adsorption mechanisms and optimize conditions for dye removal. pH is a critical factor in adsorption processes, as it affects both the surface charge of the adsorbent and the ionization state of the dye [164; 183], thereby influencing electrostatic interactions, hydrogen bonding, and overall adsorption efficiency [184]. In this study, batch adsorption experiments were conducted with an initial MB concentration of 30 mg/l, an adsorbent dosage of 1 g, a solution volume of 50 ml, agitation at 200 rpm, a temperature of 25 ± 1 °C, and the contact time fixed at 1 h. The pH was systematically varied to assess its impact, utilizing both raw and chemically modified samples of leafy fronds and empty fruit bunches from three date palm cultivars: *Degla*, *Ghars*, and *Takermost*, as depicted in Figures IV.9 and IV.10.

The removal efficiency of MB exhibited a significant dependence on pH across all sample types. Generally, adsorption capacity increased with rising pH, reaching a maximum at alkaline conditions particularly, with a removal efficiency approaching 100 %, before plateauing or slightly declining at the highest pH values. At elevated pH levels (pH >11), the adsorption of methylene blue (MB) onto the biomass diminishes due to the increased concentration of free hydroxyl ions (OH⁻) in the solution. These ions compete with MB molecules for the available adsorption sites on the adsorbent surface. Furthermore, the adsorbent surface acquires a more negative charge at higher pH values, either through the adsorption of OH⁻ ions or the ionization of weakly acidic functional groups. This enhanced negative charge further repels the cationic MB dye, resulting in reduced adsorption efficiency. The overall process is influenced by the pH-dependent nature of the surface charges and the dynamic interactions between MB, OH⁻ ions, and the adsorbent during the adsorption process [182; 185].

The modified samples consistently demonstrated superior performance compared to their raw counterparts across all cultivars and biomass types, suggesting that chemical modification enhances the availability of active sites and surface functional groups. Among the cultivars, *Degla* and *Takermost* exhibited superior adsorption performance relative to *Ghars*, with empty fruit bunches generally achieving higher removal

efficiencies than leafy fronds under identical conditions ($RE_{\max\text{KOH-LD}}=99.48\%$, $RE_{\max\text{KOH-FBD}}=99.24\%$, $RE_{\max\text{KOH-FBG}}=99.25\%$ and $RE_{\max\text{KOH-FBT}}=99.15\%$ at pH=7, $RE_{\max\text{KOH-LG}}=98.31\%$ at pH=9 and $RE_{\max\text{KOH-LT}}=98.55\%$ at pH=13) (see Figures IV.9 and IV.10).

The increase in methylene blue (MB) removal with rising pH is primarily attributed to the deprotonation of surface functional groups on the adsorbent, which generates a more negatively charged surface and enhances electrostatic attraction toward the cationic dye molecules [183; 186]. At lower pH values, competition between H^+ ions and MB cations for adsorption sites diminishes dye uptake. Maximum adsorption was generally observed in the mildly alkaline range (pH 7–11), consistent with previous studies [187]. Chemically modified samples, characterized by a higher density of oxygen-containing functional groups and increased porosity, demonstrated superior adsorption performance due to improved electrostatic interactions and greater accessibility of active sites (13- _batch_ and _fixed-bed_ colum fixed bed). While electrostatic attraction is the dominant mechanism at higher pH, additional interactions such as hydrogen bonding and π – π stacking, especially in modified adsorbents with aromatic or oxygenated groups, further contribute to the enhanced adsorption capacity, highlighting the importance of surface chemistry in optimizing dye removal [183; 187].

The findings indicate that the selection of biomass type and the chemical modification strategy should be specifically designed to optimize the advantageous surface chemistry and enhance adsorption efficiency under alkaline conditions.

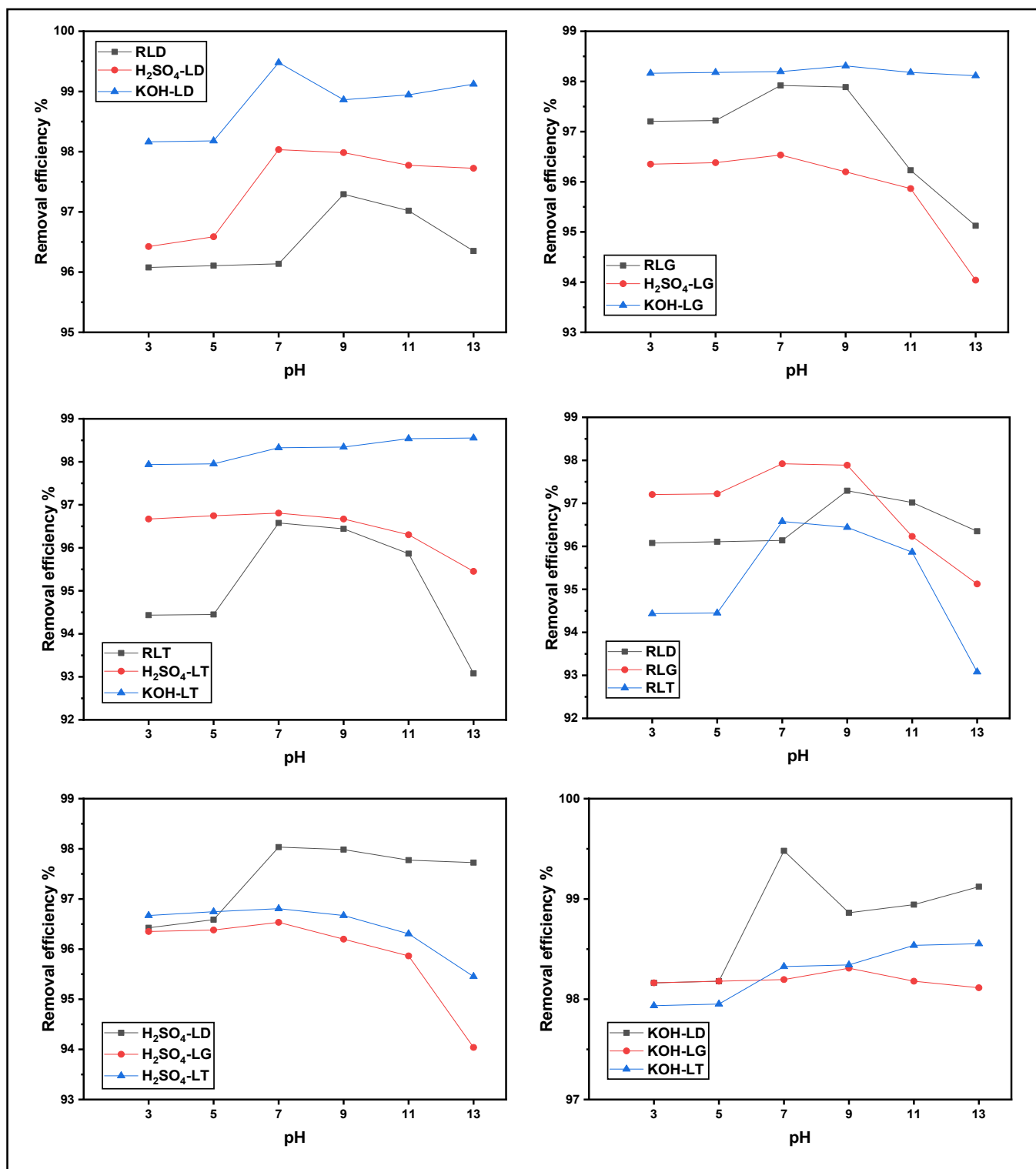


Figure IV.9: Effect of pH on the adsorption of MB onto raw and modified leafy fronds of three cultivars ($C_0 = 30 \text{ mg/l}$, $m = 1 \text{ g}$, $V=50 \text{ ml}$, agitation speed =200 rpm, $T=25 \pm 1 \text{ }^\circ\text{C}$, contact time =1 h).

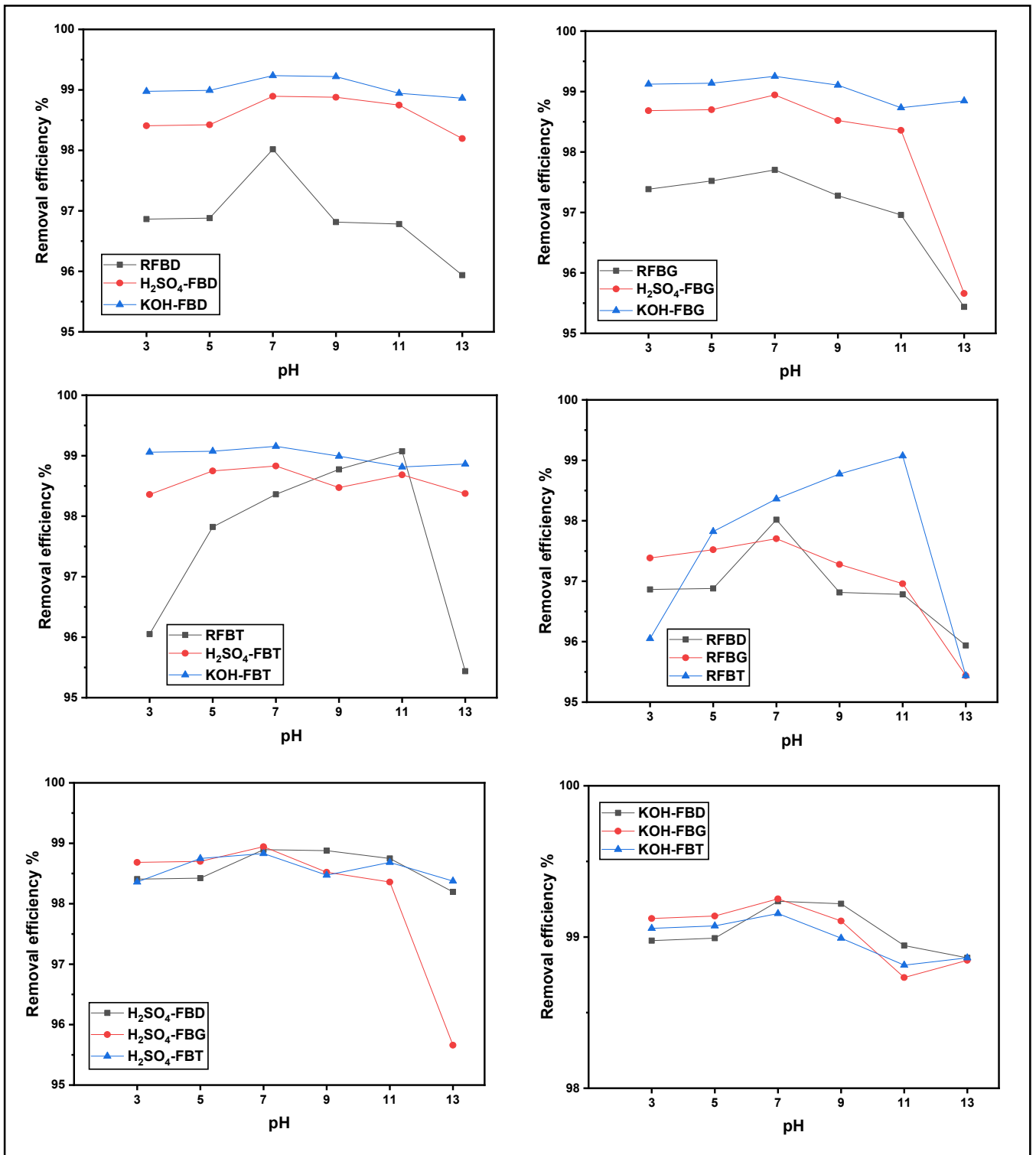


Figure IV.10: Effect of pH on the adsorption of MB onto raw and modified empty fruit bunch of three cultivars ($C_0 = 30 \text{ mg/l}$, $m = 1 \text{ g}$, $V=50 \text{ ml}$, agitation speed =200 rpm, $T=25 \pm 1 \text{ }^\circ\text{C}$, contact time =1 h).

IV.1.2. Effect of contact time

Figures (IV.11) and (IV.12) illustrate the impact of contact time on the adsorption of methylene blue (MB) onto date palm biomass derived from the *Ghars*, *Degla*, and *Takermost* cultivars. The removal efficiency was systematically examined under consistent experimental conditions, with measurements taken over a duration ranging from 5 to 120 minutes.

The adsorption of MB occurred rapidly during the first 60 min of the experiment, and then increased slightly until 120 min, when the highest amount of MB was adsorbed onto the biomass. The rapid initial uptake of MB, attributable to the abundance of available active sites on the adsorbent surfaces, followed by a gradual approach to equilibrium as these sites became saturated [188; 104].

All modified biomasses demonstrated a higher and more rapid rate of contaminant removal compared to the raw biomasses, with the samples modified with alkali exhibiting the most significant enhancement within the shortest equilibrium time, suggesting a more favorable surface structure or a higher density of functional groups conducive to MB adsorption. In the case of raw leafy fronds, RLG surpassed the other cultivars; conversely, in raw empty fruit bunches, RFBT exhibited the highest removal rate. For acid-modified biomasses, H₂SO₄-LD achieved the greatest removal efficiency in leafy fronds, whereas H₂SO₄-LT was superior in empty fruit bunches. Among the alkali-modified biomasses, KOH-FBD ($RE_{\max\text{KOH-LD}}=99.27\%$), and KOH-FBG ($RE_{\max\text{KOH-FBD}}=99.20\%$) displayed the best removal performance.

Applying chemical modifications to agricultural waste significantly accelerates the adsorption process, enabling faster contaminant removal and quicker equilibrium. This not only improves the efficiency and feasibility of wastewater treatment but also reduces operational costs, making chemically treated materials a practical and economical choice for water purification applications [189].

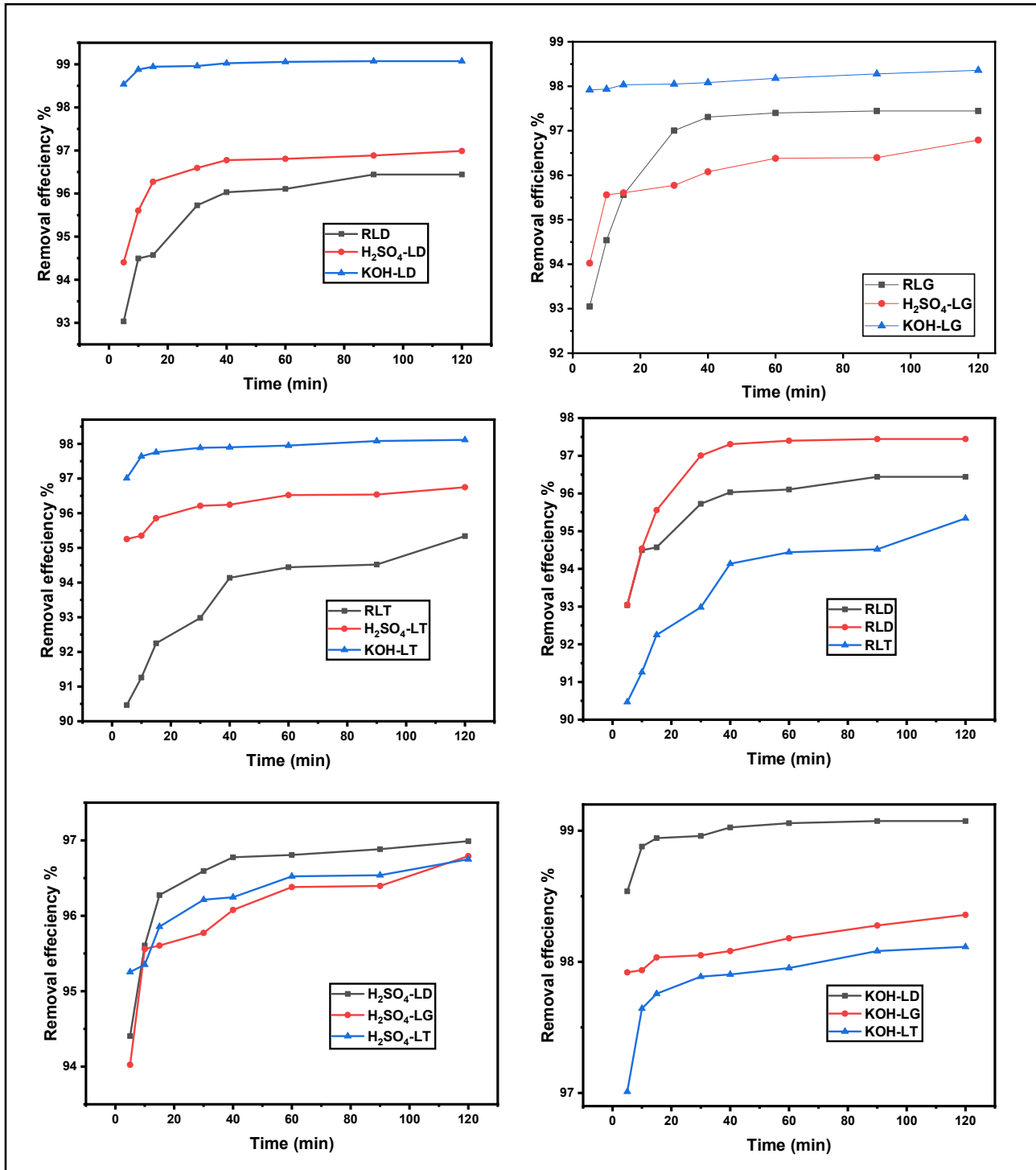


Figure IV.11: Effect of contact time on the adsorption of MB onto raw and modified leafy fronds of three cultivars ($C_0 = 30 \text{ mg/l}$, $m = 1 \text{ g}$, $V=50 \text{ ml}$, agitation speed =200 rpm, $T=25 \pm 1 \text{ }^\circ\text{C}$, $\text{pH}=5.4$).

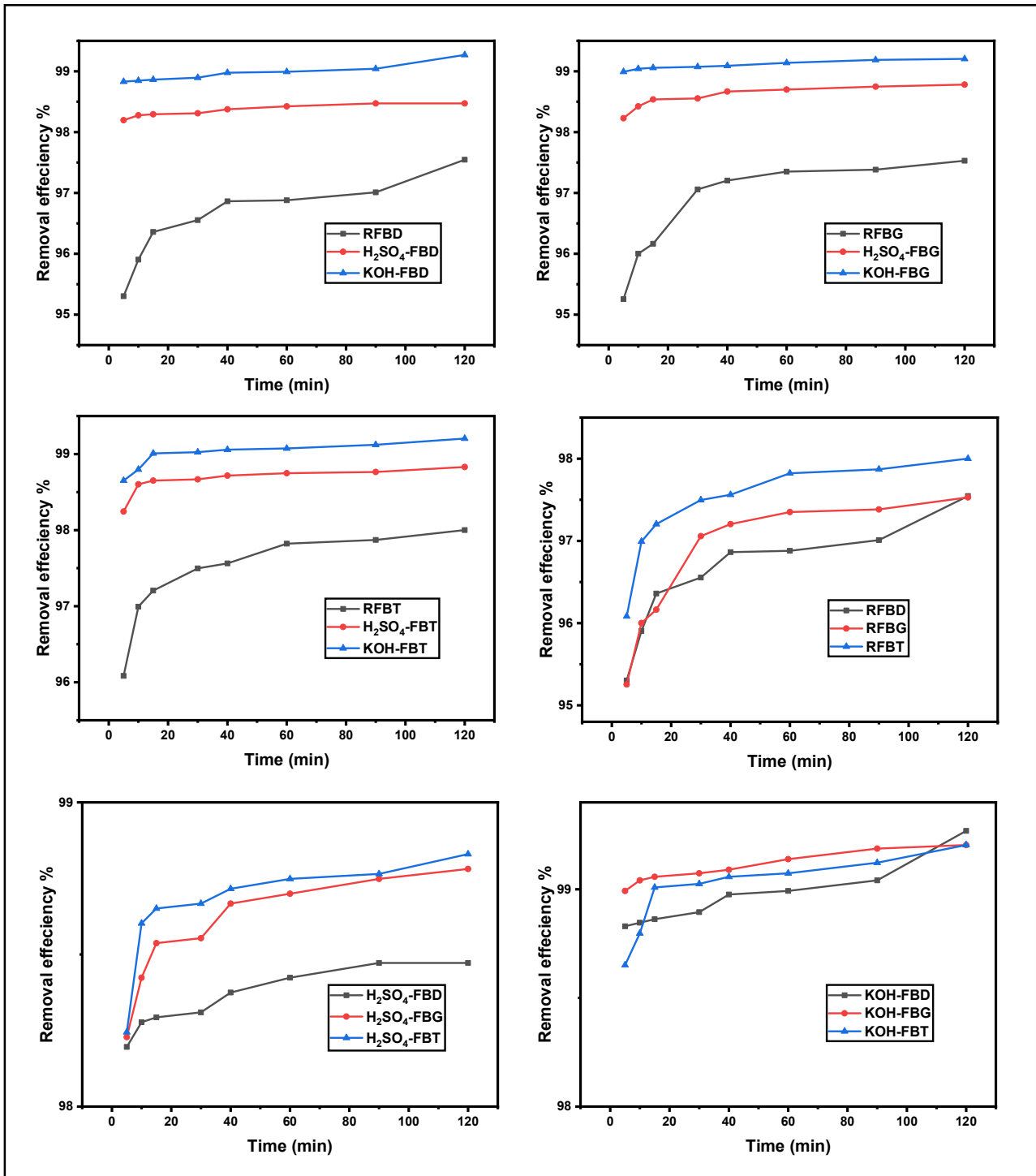


Figure IV.12: Effect of contact time on the adsorption of MB onto raw and modified empty fruit bunch of three cultivars ($C_0 = 30 \text{ mg/l}$, $m = 1 \text{ g}$, $V=50 \text{ ml}$, agitation speed =200 rpm, $T=25 \pm 1 \text{ }^\circ\text{C}$, $\text{pH}=5.4$).

IV.1.3. Effect of temperature

Temperature plays a pivotal role in the adsorption process, influencing both the capacity and rate of contaminant removal by various biomasses [164; 190]. Figures (IV.13) and (IV.14) show the effect of temperature on the adsorption of MB onto raw and modified leafy fronds and empty fruit bunch of three cultivars, respectively, at 25 °C, 35°C, 45°C, and 55 °C.

When comparing chemically modified biomasses (H₂SO₄- or KOH-modified) to their raw by-products, chemical modification typically enhanced the adsorption capacity at all temperatures, with alkaline-modified biomasses exhibiting the highest adsorption capacities in all biomasses. Acid and alkaline modifications introduce or expose additional functional groups and increase the surface area, making the modified biomasses more effective adsorbents than raw materials.

Regardless of the cultivar or treatment, the general trend of decreasing adsorption with increasing temperature persists, underscoring the exothermic nature of the process for these biosorbents. Generally, an increase in temperature results in a decrease in adsorption capacity for most physical adsorption systems, including dye removal. This is because higher temperatures boost the kinetic energy and solubility of dye molecules in the solution, promoting desorption and weakening the interactions between the adsorbate and the active sites of the adsorbent. This indicates that the adsorption process is exothermic. Consequently, elevated temperatures diminish the effectiveness of adsorbents in capturing contaminants [185; 190].

However, the biomass derived from the acid modification of leafy fronds, demonstrated an increasing removal efficiency with increasing temperatures, similar behavior reported by [191]. Biosorptive removal of pollutants is typically an endothermic process, in which increasing the temperature enhances adsorption by raising the surface activity and kinetic energy of the adsorbate. This effect is particularly evident with acid-modified biomass, as higher temperatures promote greater interaction between the adsorbate and adsorbent [164; 192; 193].

Among the cultivars, notable performance differences emerged, with certain varieties consistently excelling over others in specific treatments and palm parts. For example, in leafy fronds, one cultivar might demonstrate superior adsorption when alkaline-

modified, while another might perform better under acid modification or in its raw state, and so forth. Similar patterns were observed in empty fruit bunches, highlighting the impact of both genetic and anatomical factors on adsorption behavior.

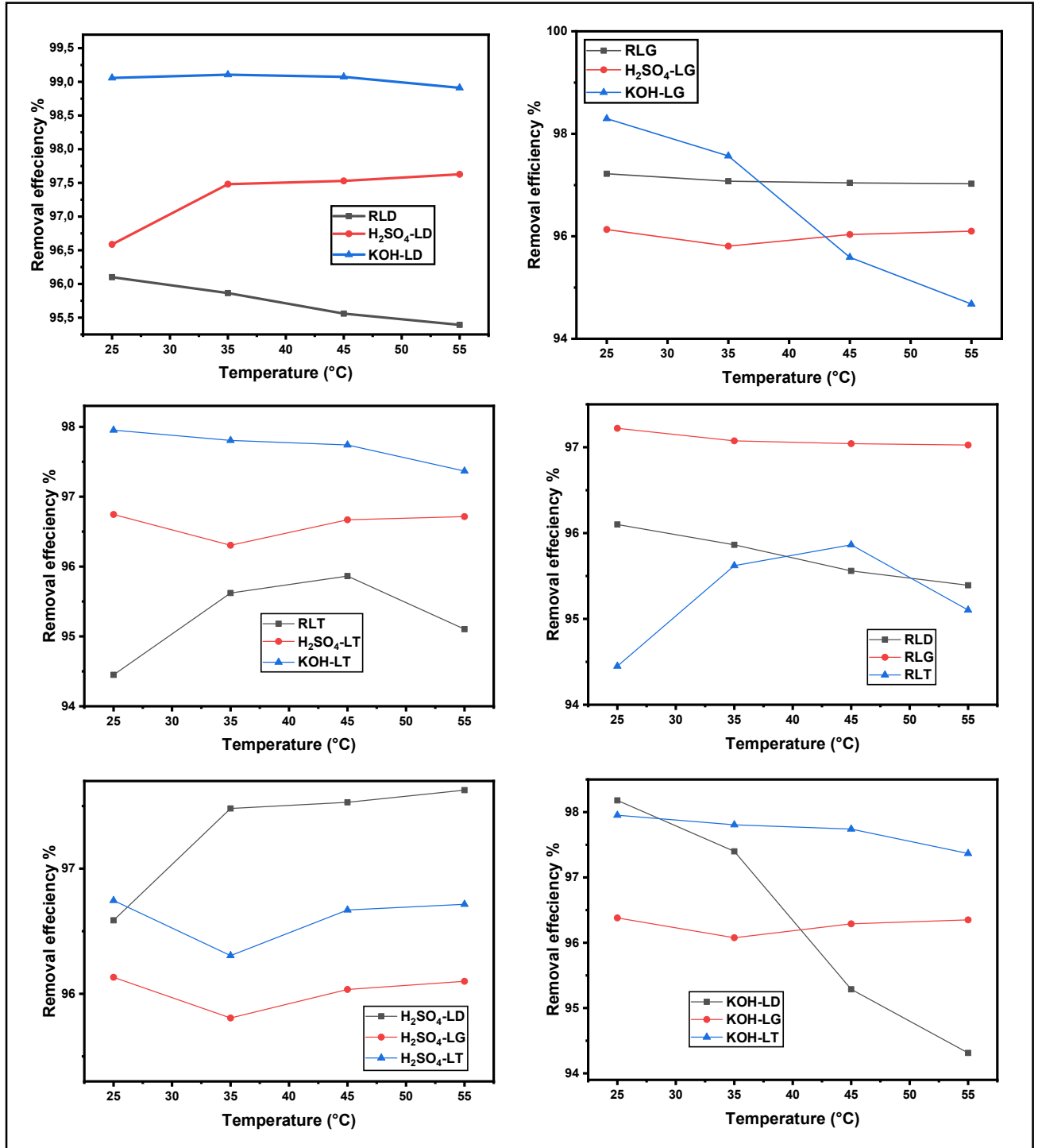


Figure IV.13: Effect of temperature on the adsorption of MB onto raw and modified leafy fronds of three cultivars ($C_0 = 30 \text{ mg/l}$, $m = 1 \text{ g}$, $V=50 \text{ ml}$, agitation speed =200 rpm, contact time =1 h, pH=5.4).

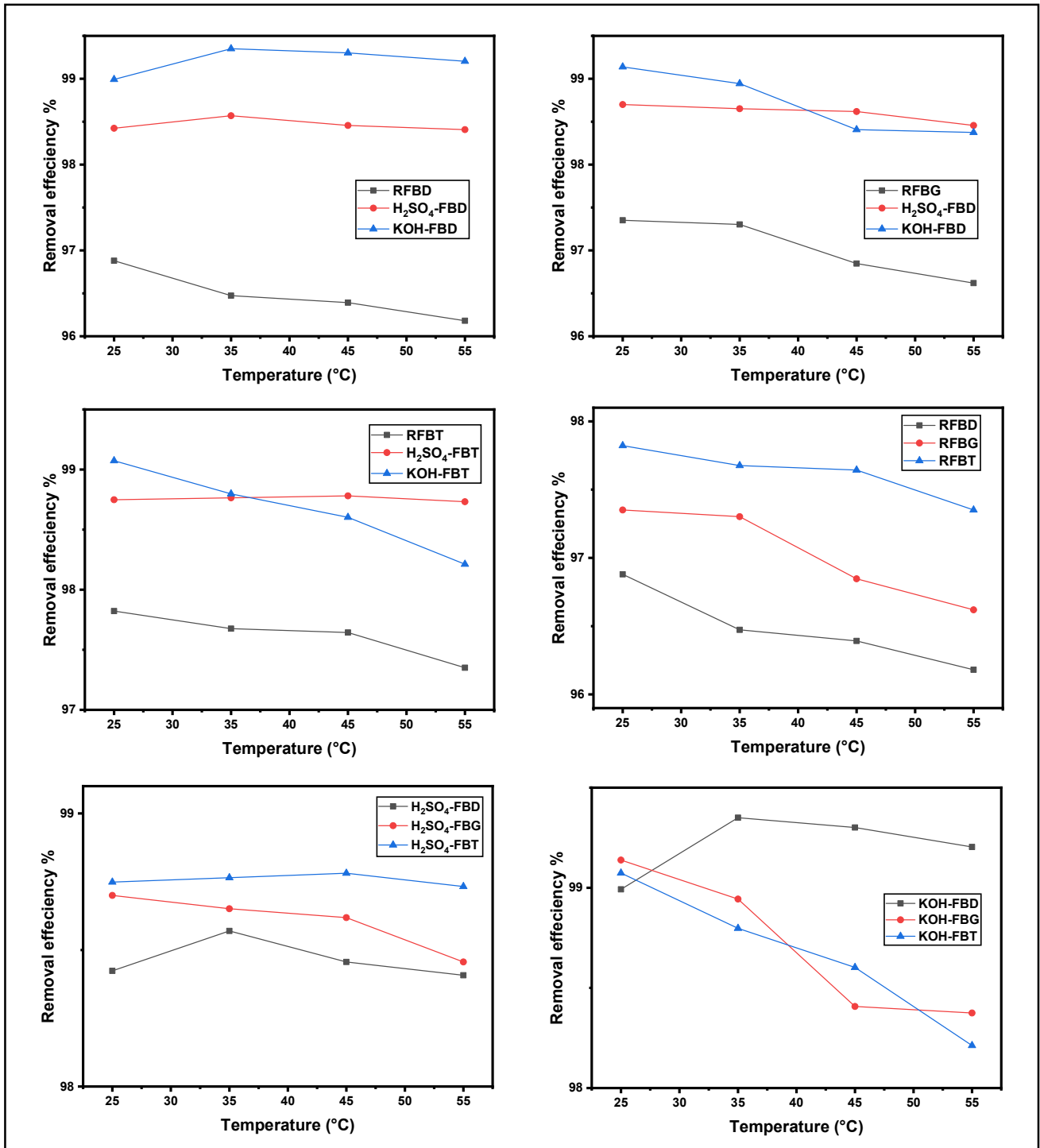


Figure IV.14: Effect of temperature on the adsorption of MB onto raw and modified empty fruit bunch of three cultivars ($C_0 = 30 \text{ mg/l}$, $m = 1 \text{ g}$, $V=50 \text{ ml}$, agitation speed =200 rpm, contact time =1 h, pH=5.4).

Thermodynamic parameters were evaluated to gain insight into the adsorption mechanisms. The changes in the Gibbs free energy (ΔG°), enthalpy (ΔH°), and entropy (ΔS°) were calculated based on the equations (1) and (2) in chapter 1. The values of ΔH° , ΔS° , and ΔG° were determined from the slope and intercept (equations (1) and (2)) obtained by plotting $\ln K_d$ against $1/T$ using the linear Van't Hoff equation (figure IV.15).

From tables IV.2 and IV.3, the negative ΔG° values obtained from the adsorption of MB by all adsorbents indicate that adsorption is a spontaneous and thermodynamically favorable process [187]. Electrostatic interactions between adsorption sites and the adsorbing ion (physical adsorption) are consistent with a ΔG° value between 0 and -20 kJ/mole [104].

For RLD, RLG, KOH-LD, KOH-LG, KOH-LT, RFBD, RFBG, H₂SO₄-FBG, KOH-FBG, RFBT and KOH-FBT, the Gibbs free energy change values become less negative or even positive as temperature increases from 298 K to 328 K, indicating a decrease in spontaneity of adsorption at higher temperatures.

Negative ΔH° values for most raw and modified adsorbents indicate that the adsorption of MB is exothermic, meaning that increasing temperature reduces adsorption capacity [194]. In contrast, acid-modified leafy fronds samples and KOH-FBD exhibit positive ΔH° suggesting an endothermic process where adsorption may be enhanced at higher temperatures, likely due to increased mobility of MB molecules and the creation of new active sites on the adsorbent surface [151; 195].

ΔS° values provide additional insight. Negative ΔS° values for raw and KOH-modified adsorbents indicate a decrease in randomness at the solid–liquid interface during adsorption, consistent with the exothermic nature of the process [148; 196; 197]. Conversely, positive ΔS° values for some H₂SO₄-modified samples suggest increased disorder, possibly due to structural changes in the adsorbent or desorption of water molecules from the surface [175; 195; 198; 199].

The results showed that temperature significantly affected the MB adsorption. Most raw and KOH-treated adsorbents exhibited spontaneous, exothermic behavior favoring

lower temperatures, whereas some H₂SO₄-treated samples benefited from higher temperatures owing to their endothermic nature, consistent with prior studies.

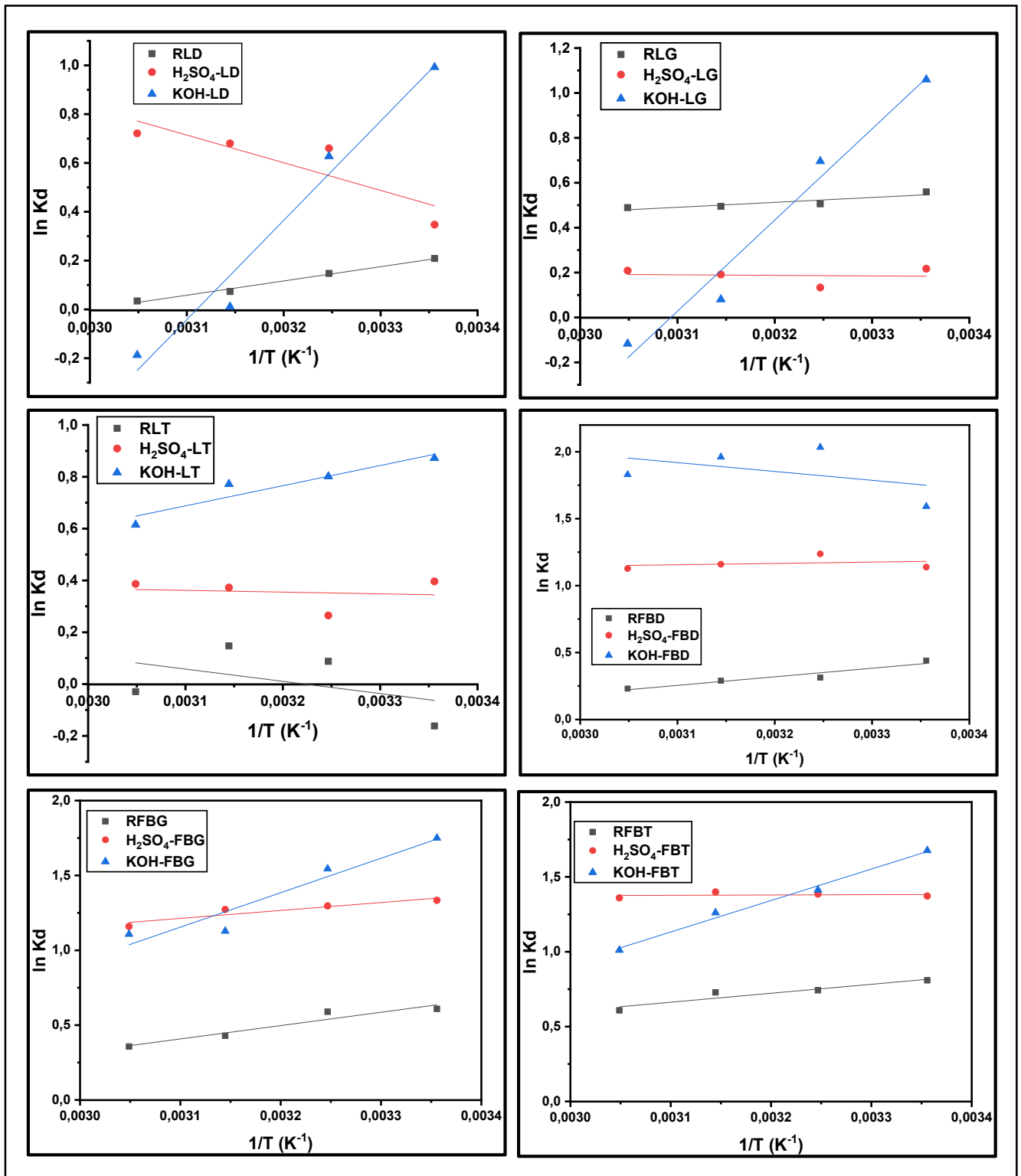


Figure IV.15: Plot of $\ln K_d$ vs. $1/T$ for estimation of thermodynamic parameters for the adsorption of MB onto raw and modified leafy fronds and empty fruit bunch of three cultivars

Table IV.2: Thermodynamic parameters for adsorption of MB onto raw and modified leafy fronds of three cultivars

<i>Adsorbent</i>	<i>T(K)</i>	ΔG° (kJ/mol)	ΔH° (kJ/mol)	ΔS° (kJ/mol.K)
<i>RLD</i>	298	-0,40	-4,87	-0,015
	308	-0,25		
	318	-0,10		
	328	0,05		
<i>H₂SO₄-LD</i>	298	-0,98	9,45	0,035
	308	-1,33		
	318	-1,68		
	328	-2,03		
<i>KOH-LD</i>	298	-2,35	-33,94	-0,106
	308	-1,29		
	318	-0,23		
	328	0,83		
<i>RLG</i>	298	-1,22	-1,82	-0,002
	308	-1,20		
	318	-1,18		
	328	-1,16		
<i>H₂SO₄-LG</i>	298	-0,38	0,21	0,002
	308	-0,41		
	318	-0,42		
	328	-0,44		
<i>KOH-LG</i>	298	-2,57	-33,86	-0,105
	308	-1,52		
	318	-0,47		
	328	0,58		
<i>RLT</i>	298	0,06	3,94	0,013
	308	-0,06		
	318	-0,19		
	328	-0,32		
<i>H₂SO₄-LT</i>	298	-0,93	0,56	0,005
	308	-0,98		
	318	-1,03		
	328	-1,08		
<i>KOH-LT</i>	298	-2,32	-6,49	-0,014
	308	-2,18		
	318	-2,04		
	328	-1,90		

Table IV.3: Thermodynamic parameters for adsorption of MB onto raw and modified empty fruit bunch of three cultivars

<i>Adsorbent</i>	<i>T(K)</i>	ΔG° (kJ/mol)	ΔH° (kJ/mol)	ΔS° (kJ/mol.K)
<i>RFBD</i>	298	-1,17	-5,34	-0,014
	308	-1,03		
	318	-0,89		
	328	-0,75		
<i>H₂SO₄-FBD</i>	298	-2,90	-0,82	0,007
	308	-2,97		
	318	-3,04		
	328	-3,11		
<i>KOH-FBD</i>	298	-4,32	5,51	0,033
	308	-4,65		
	318	-4,98		
	328	-5,31		
<i>RFBG</i>	298	-1,46	-7,42	-0,020
	308	-1,26		
	318	-1,06		
	328	-0,86		
<i>H₂SO₄-FBG</i>	298	-3,23	-4,42	-0,004
	308	-3,19		
	318	-3,15		
	328	-3,11		
<i>KOH-FBG</i>	298	-4,29	-19,19	-0,050
	308	-3,79		
	318	-3,29		
	328	-2,79		
<i>RFBT</i>	298	-1,94	-4,92	-0,010
	308	-1,84		
	318	-1,74		
	328	-1,64		
<i>H₂SO₄-FBT</i>	298	-3,46	-0,18	0,011
	308	-3,57		
	318	-3,68		
	328	-3,79		
<i>KOH-FBT</i>	298	-4,12	-17,53	-0,045
	308	-3,67		
	318	-3,22		
	328	-2,77		

IV.1.4. Effect of initial concentration

The initial concentration of methylene blue (MB) is pivotal in determining the efficiency of dye removal during adsorption. The MB concentration was varied from 10 mg/l to 90 mg/l. As observed in figures (IV.16) and (IV.17), the modified biomasses

showed higher dye removal values than their raw counterparts, especially the alkali-modified biomasses ($q_{e\text{KOH-LD}}= 4.473$ mg/g, $q_{e\text{KOH-LG}}= 4.449$ mg/g, $q_{e\text{KOH-LT}}= 4.447$ mg/g, $q_{e\text{KOH-FBD}}= 4.475$ mg/g, $q_{e\text{KOH-FBG}}= 4.476$ mg/g and $q_{e\text{KOH-FBT}}= 4.468$ mg/g at $C_0=90$ mg/l), and the cultivars showed different dye removal efficiencies among themselves.

Increasing the initial concentration of MB generally increased the percentage removal of the dye for both raw and modified adsorbents derived from leafy fronds and empty fruit bunches. Higher initial concentrations of MB increased the driving force for mass transfer, promoting greater adsorption uptake as more dye molecules were transported to the adsorbent sites. This results in more efficient dye removal due to the stronger interactions between MB and the adsorbent [200-202].

In contrast, the removal efficiencies of $\text{H}_2\text{SO}_4\text{-LG}$ and $\text{H}_2\text{SO}_4\text{-LT}$ decreased as the initial concentration increased because the limited number of adsorption sites became saturated more rapidly at higher concentrations [200; 203].

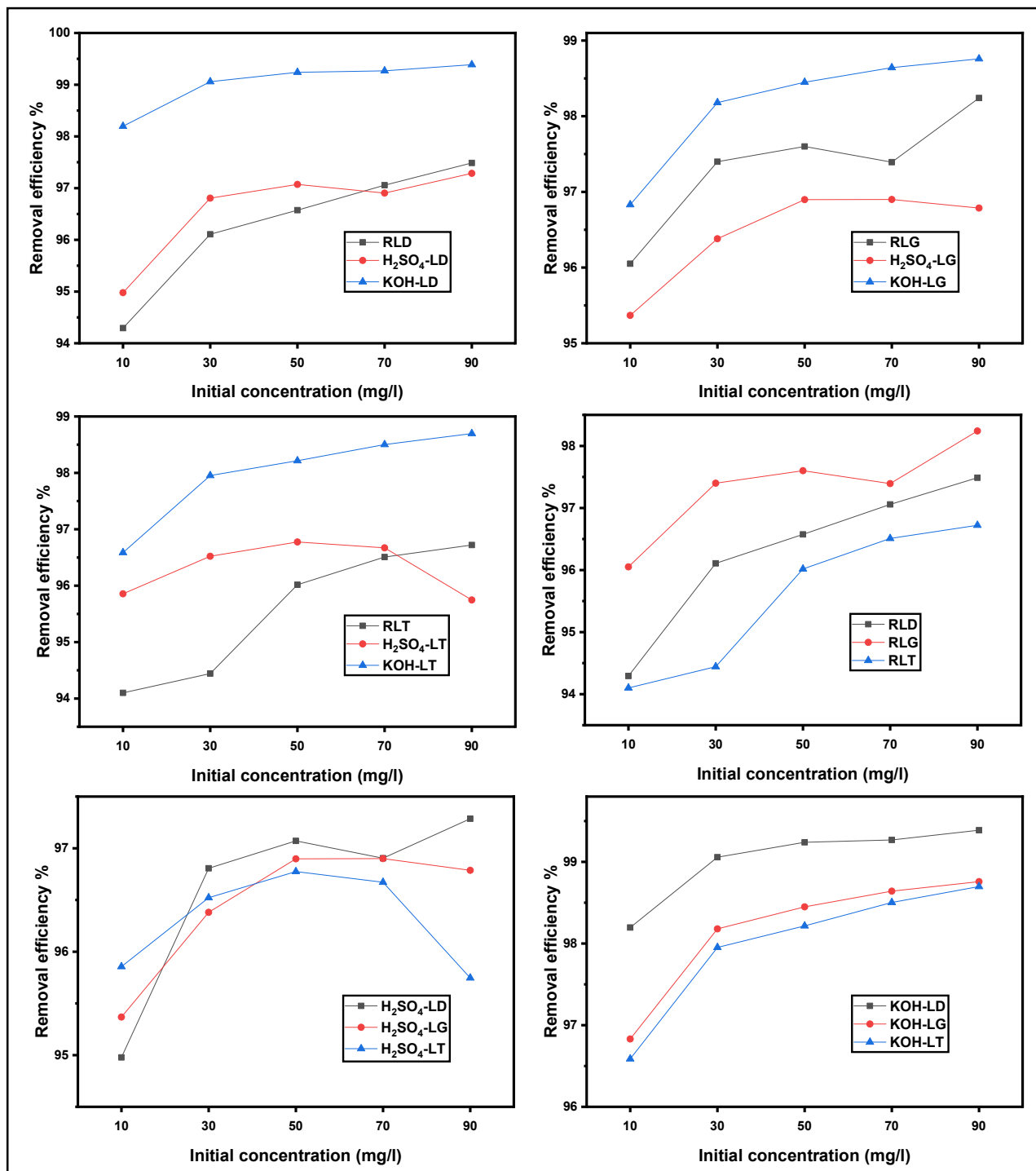


Figure IV.16: Effect of initial concentration on the adsorption of MB onto raw and modified leafy fronds of three cultivars (m = 1 g, V=50 ml, agitation speed =200 rpm, contact time =1 h, T=25 ± 1 °C)

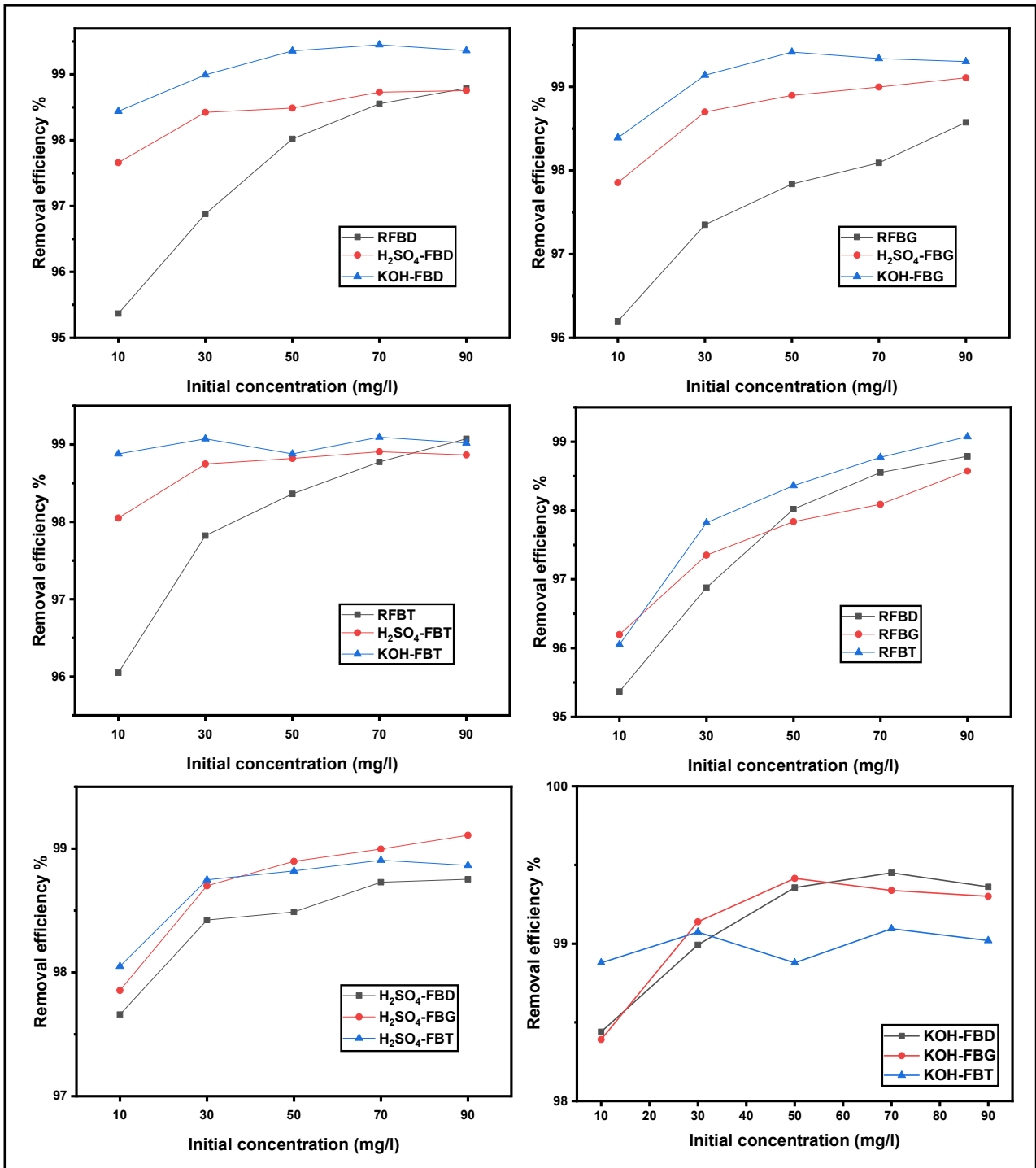


Figure IV.17: Effect of initial concentration on the adsorption of MB onto raw and modified empty fruit bunch of three cultivars ($m = 1 \text{ g}$, $V=50 \text{ ml}$, agitation speed =200 rpm, contact time =1 h, $T=25 \pm 1 \text{ }^\circ\text{C}$)

IV.2. Adsorption equilibrium

IV.2.1. Adsorption isotherms

The type of isotherm provides valuable insights into the adsorption mechanism, the nature of the adsorbent-adsorbate interaction, and the structural properties of the adsorbent. As shown in Figures (IV.18), (IV.19), and (IV.20), and following the classification by *Giles and Coll*, the adsorption isotherms of MB on RLD, RFBG, and KOH-FBT are categorized as S-type. This classification indicates significant cooperative adsorption or strong lateral interactions between the MB molecules on the adsorbent surface. The other adsorbents displayed type C isotherms, except for KOH-FBD, which exhibited a type L isotherm. For C isotherms, adsorption occurs through a partitioning mechanism into the bulk of the adsorbent, a behavior expected for highly porous or swellable materials, such as silica gel. In contrast, L-type isotherms exhibit a concave shape relative to the concentration axis, indicating the progressive saturation of the adsorbent surface as the concentration of MB increases. This behavior suggests that adsorption primarily occurs in a monolayer on energetically similar sites, with minimal interactions between the adsorbed molecules [106; 107].

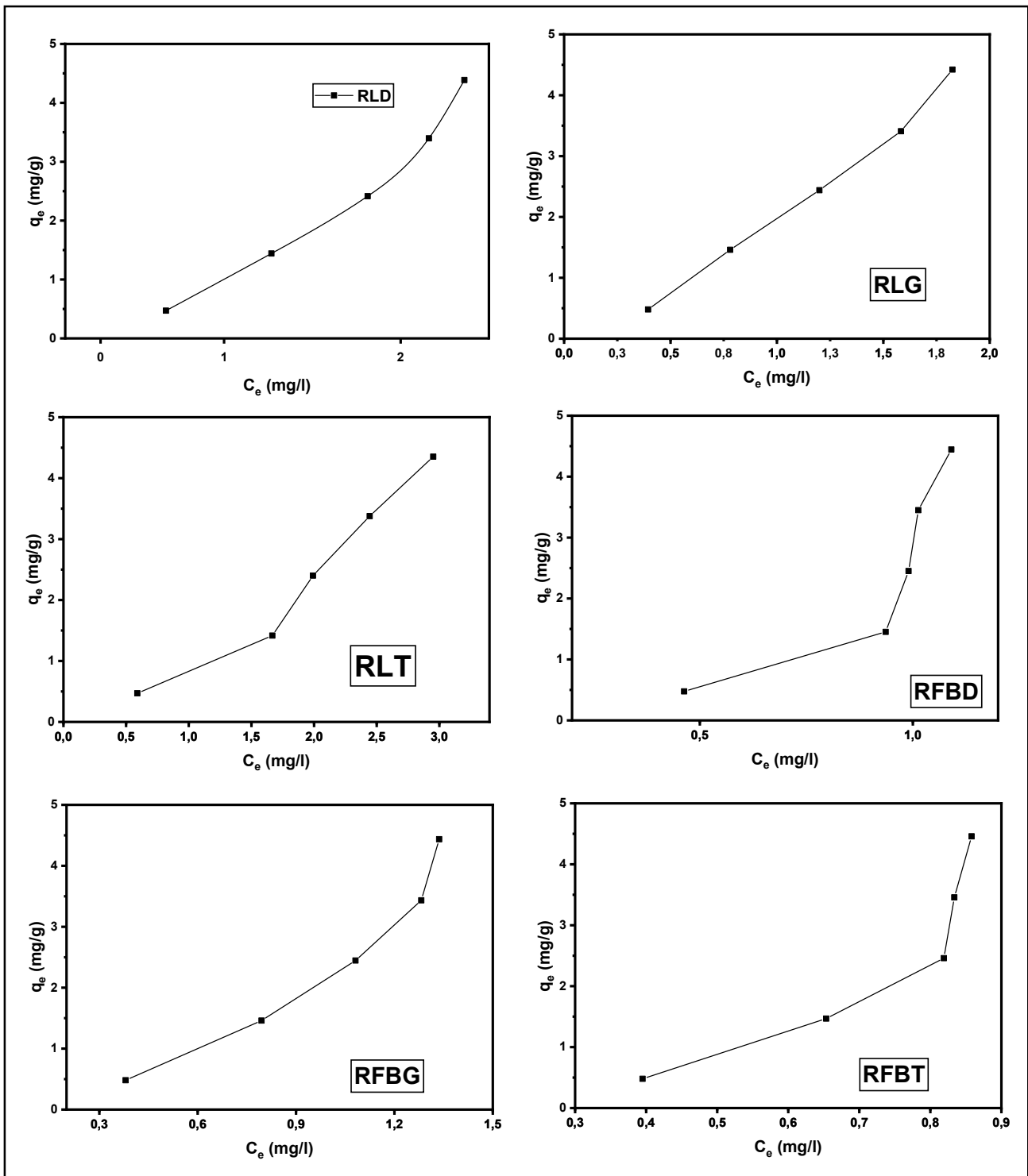


Figure IV.18: Adsorption isotherms of MB onto raw leafy fronds and empty fruit bunch of three cultivars

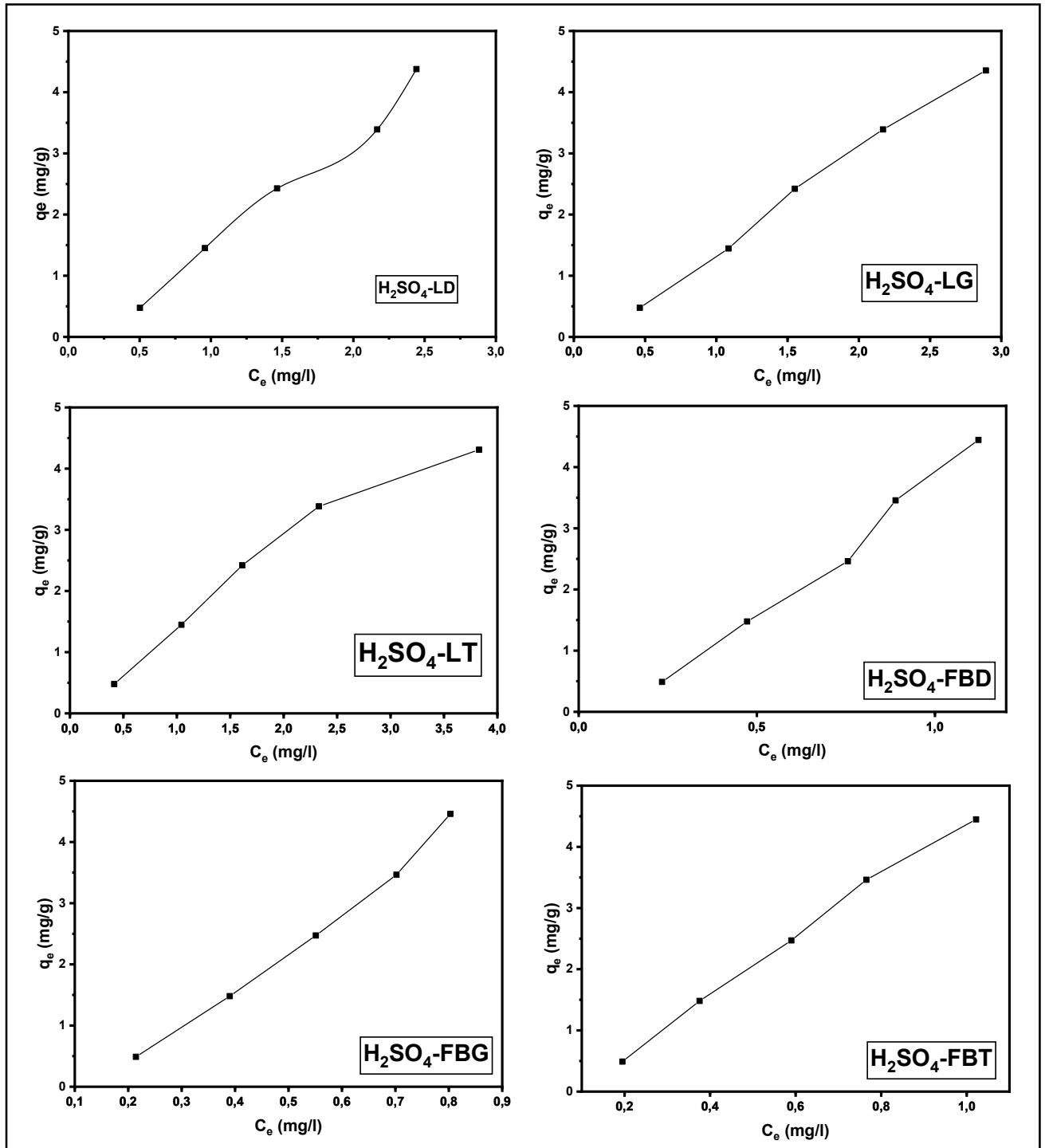


Figure IV.19: Adsorption isotherms of MB onto H_2SO_4 -modified leafy fronds and empty fruit bunch of three cultivars

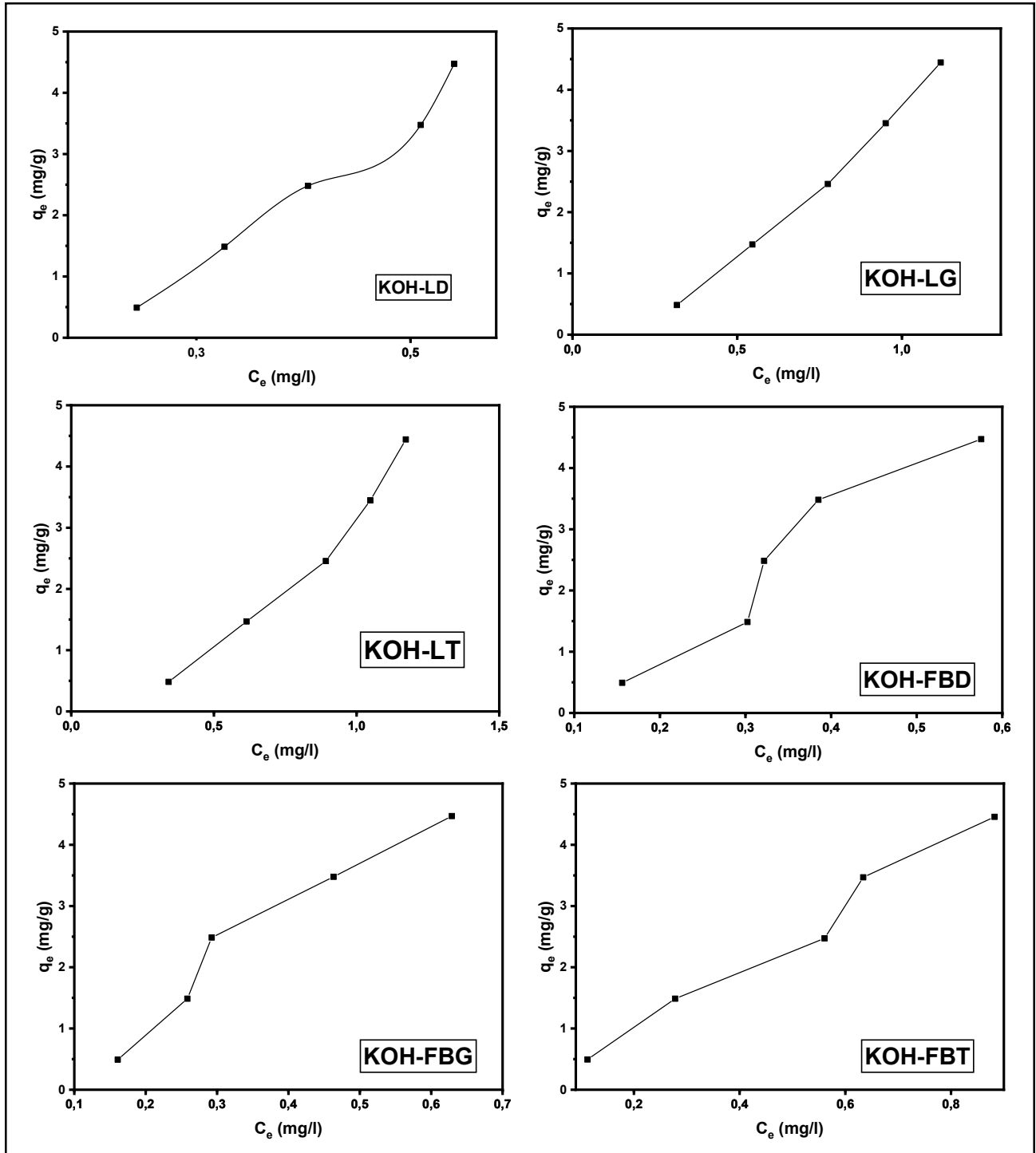


Figure IV.20: Adsorption isotherms of MB onto KOH-modified leafy fronds and empty fruit bunch of three cultivars

IV.2.2. Modeling results

Isotherm modeling serves as a crucial approach to understanding the adsorption mechanisms involved in dye removal via various adsorbents. In this study, isotherm models Langmuir, Freundlich, and Temkin were applied to analyze the adsorption of MB onto raw and chemically modified leafy fronds and empty fruit bunches of three cultivars, as demonstrated in Figures (IV.21), (IV.22) and (IV.23), and summarized in Tables IV.4 and IV.5.

Although the linearized Langmuir isotherm model sometimes produces relatively high correlation coefficients (R^2), the critical parameters derived, such as q_{\max} and K_L , are often negative for most adsorbents, including raw, H_2SO_4 -, and KOH-modified materials. The exception was H_2SO_4 -LT, which showed a positive q_{\max} (55.87 mg/g) value. Negative values for these parameters are physically implausible, as the adsorption capacity cannot be negative; suggesting that the Langmuir model does not adequately describe the adsorption behavior under the studied conditions, despite seemingly acceptable statistical indicators. This discrepancy likely arises from the foundational assumptions of the model, such as monolayer adsorption onto homogeneous surfaces, which do not align with the actual, potentially heterogeneous adsorption process observed. Consequently, isotherm models such as Freundlich or Temkin, which better accommodate surface heterogeneity and multilayer adsorption, were considered more suitable for representing the experimental data.

The Freundlich isotherm model, which is and is more flexible than the Langmuir model, effectively describes adsorption on heterogeneous surfaces and accounts for multilayer adsorption phenomena. The key parameters K_F (adsorption capacity) and n (adsorption intensity or surface heterogeneity) provide important mechanistic insights. In this study, all adsorbents exhibited positive K_F and n values, along with high correlation coefficients R^2 (its maximum values reach 0.9961 and 0.9967 for KOH-LT and H_2SO_4 -FBG, respectively), indicating an excellent fit to the experimental data and superior applicability compared to the Langmuir model. The values of n were consistently below 1 across samples, reflecting a cooperative adsorption process with chemical interaction [108; 204]. Notably, chemically modified adsorbents, such as those treated with KOH, demonstrated enhanced adsorption capacities, with K_F values of approximately 13.91 l/g and 14.85 l/g for KOH-LD and KOH-FBD, respectively, highlighting the positive impact of chemical activation on adsorbent performance.

The Temkin isotherm model posits that the heat of sorption for all molecules within a layer diminishes linearly with increasing coverage owing to interactions between the adsorbate and

adsorbent. The parameters B (associated with the heat of adsorption) and K_T (the binding equilibrium constant) were positive across all samples; however, the values of the latter for the adsorption process were relatively low, suggesting minimal interaction between the adsorbate molecules and the adsorbent. This observation corroborates the physical nature of the interaction between the adsorbate and adsorbent, as further evidenced by the Temkin constant B values being less than 8 kJ/mol. Notably, the K_T values increased in the KOH-modified biomasses, reaching a maximum of $K_T=9.87$ l/g for KOH-FBT. R^2 values exceeded 0.8 in most instances (except for RFBD, where $R^2=0.65$), indicating that the model adequately described the energetic heterogeneity of the adsorption process and that there was a uniform distribution of adsorbate on the adsorbent surface, however, the Freundlich isotherm remained the dominant isotherm, except for KOH-FBG [108].

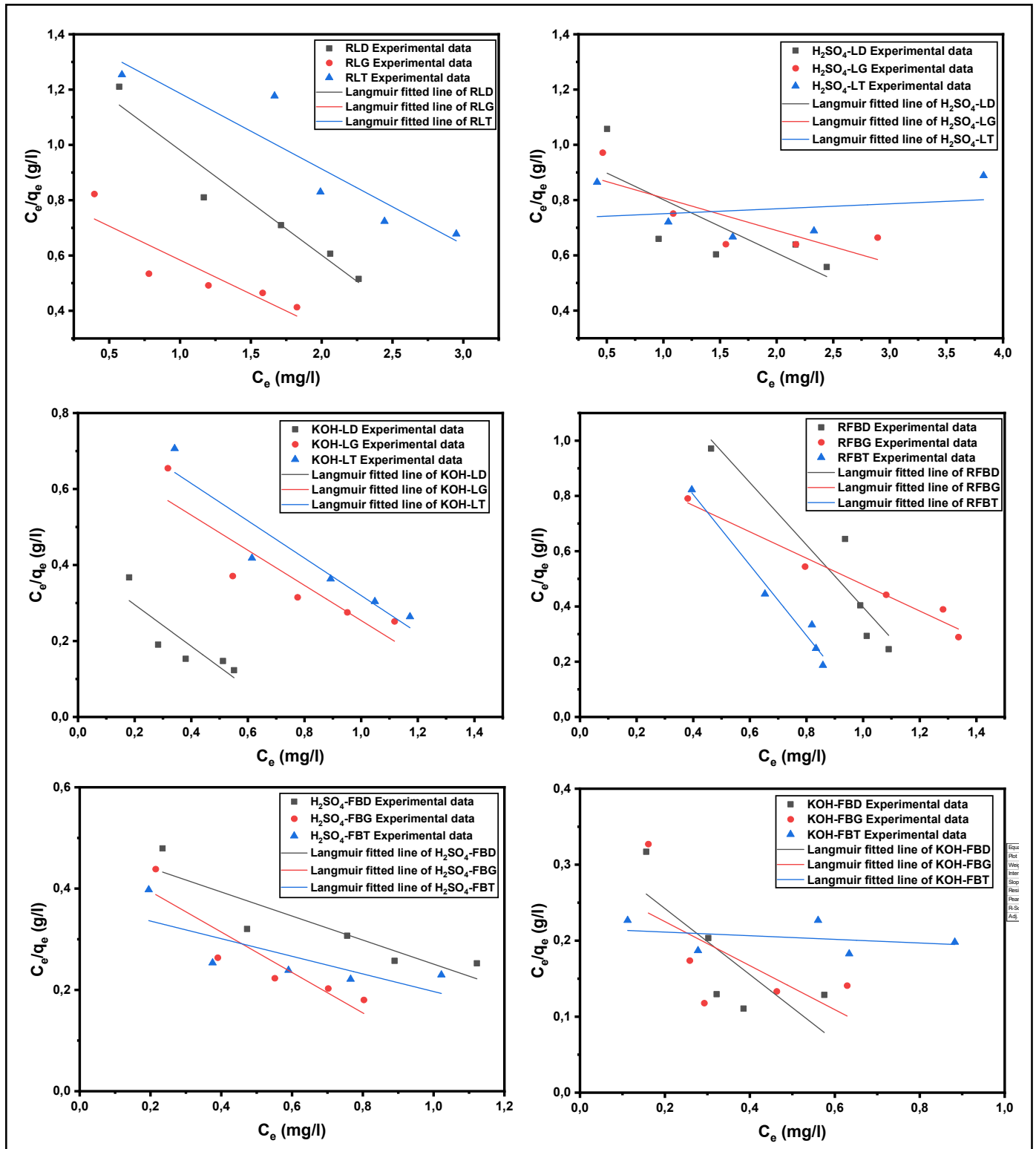


Figure IV.21: Langmuir isotherm plots for adsorption of MB onto raw and modified leafy fronds and empty fruit bunch of three cultivars

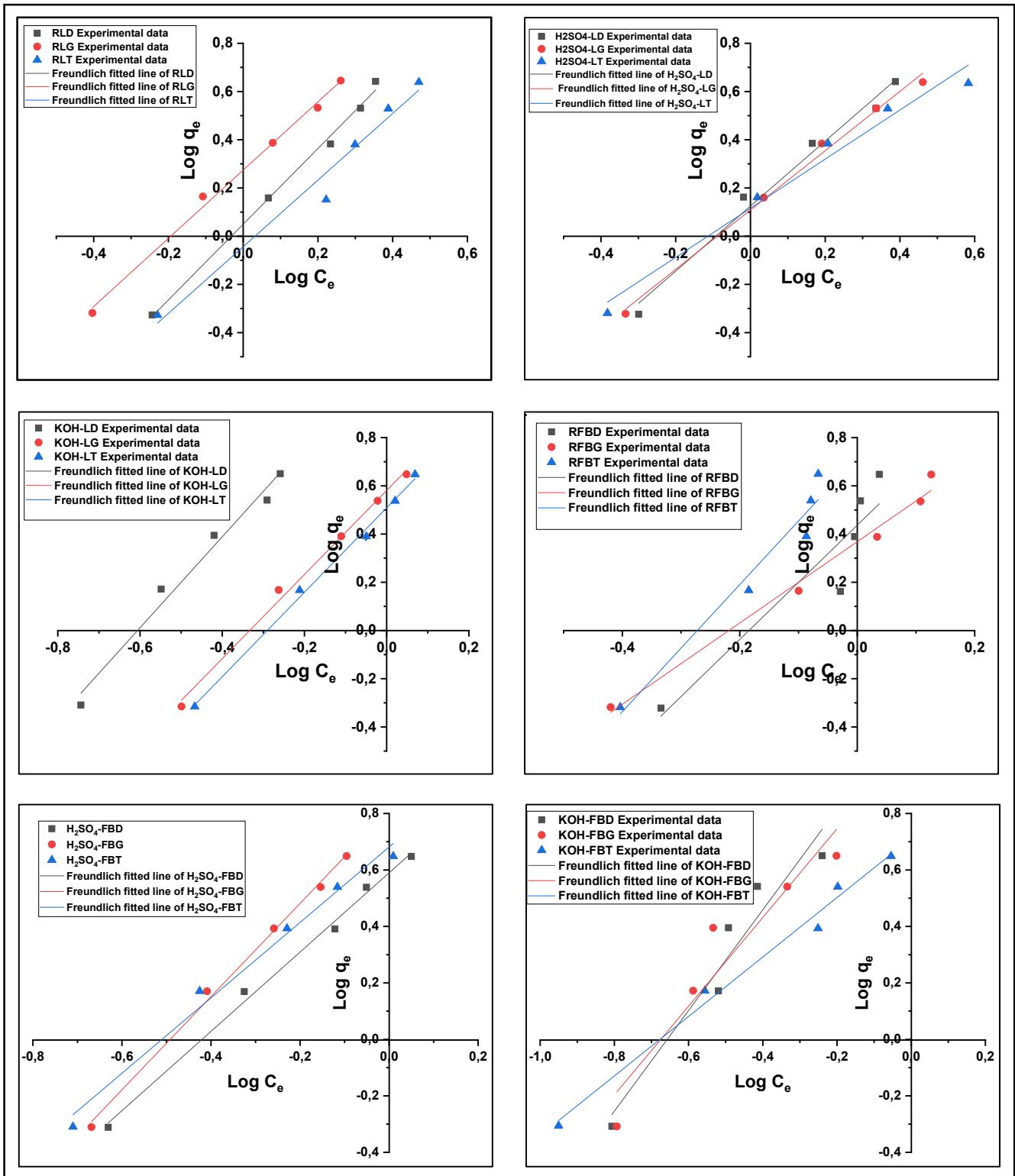


Figure IV.22: Freundlich isotherm plots for adsorption of MB onto raw and modified leafy fronds and empty fruit bunch of three cultivars

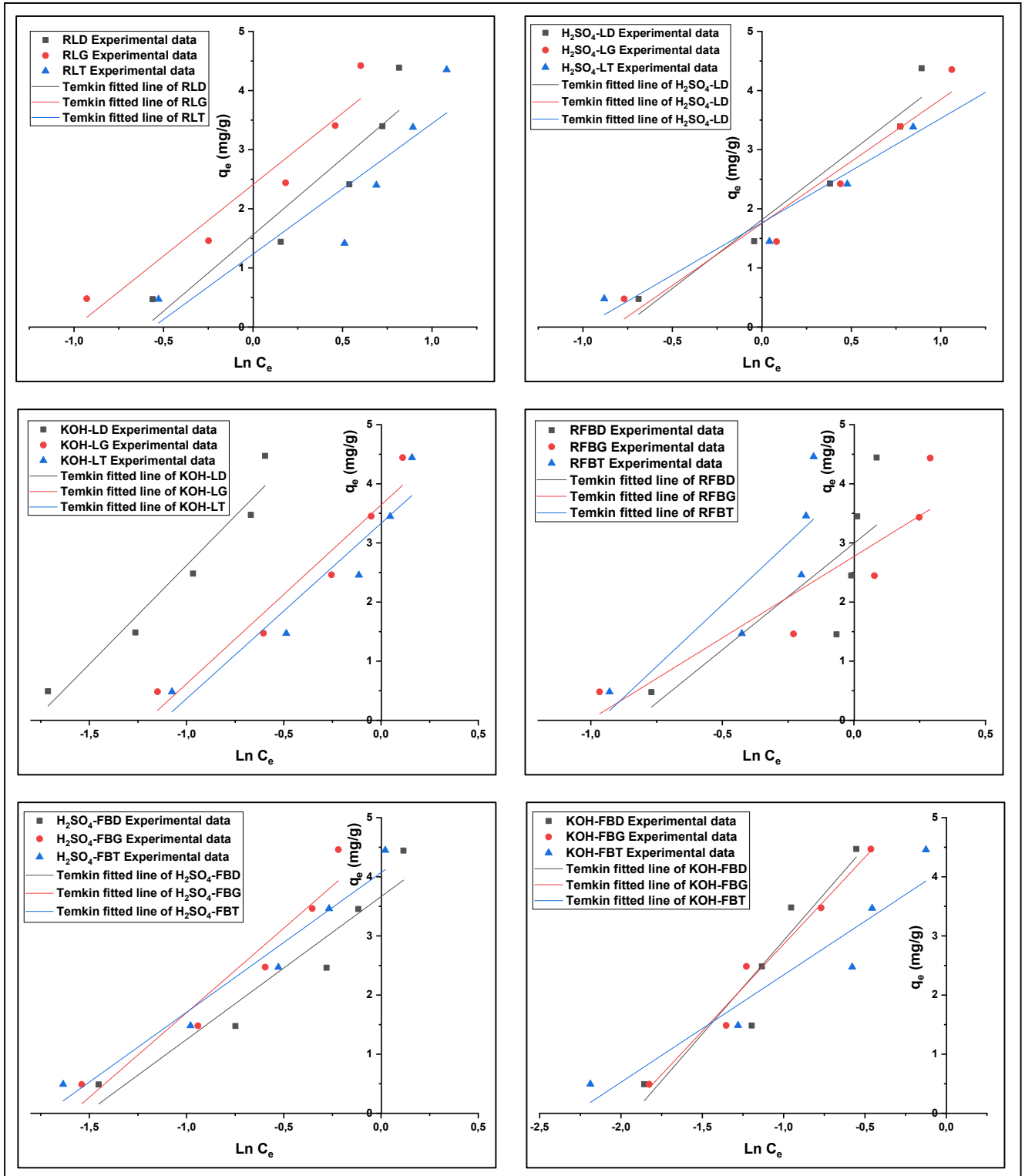


Figure IV.23: Temkin isotherm plots for adsorption of MB onto raw and modified leafy fronds and empty fruit bunch of three cultivars

Table IV.4: Langmuir, Freundlich, and Temkin Constants for adsorption of MB onto raw and modified leafy fronds of three cultivars at 25 °C using the linear method

Adsorbents	Langmuir isotherm constants			Freundlich isotherm constants			Temkin isotherm constants		
	q_{max} (mg/g)	K_L (l/mg)	R^2	K_F (l/g)	n	R^2	B (J/mol)	K_T (l/g)	R^2
<i>RLD</i>	Non calculable	-0,2789	0,9420	1,1214	0,6370	0,9955	2,5799	1,8306	0,8742
<i>RLG</i>	Non calculable	-0,2962	0,7854	1,8804	0,7069	0,9950	2,4185	2,7092	0,9263
<i>RLT</i>	Non calculable	-0,1873	0,8421	0,9044	0,7235	0,9725	2,2086	1,7482	0,81568
<i>H₂SO₄-LD</i>	Non calculable	-0,1940	0,6005	1,3333	0,7418	0,9836	2,3206	2,1849	0,9475
<i>H₂SO₄-LG</i>	Non calculable	-0,1273	0,6222	1,2844	0,8128	0,9939	2,0976	2,3055	0,9417
<i>H₂SO₄-LT</i>	55,8659	0,0244	0,0518	1,3063	0,9817	0,9770	1,7653	2,7139	0,9665
<i>KOH-LD</i>	Non calculable	-1,3521	0,7400	13,9126	0,5300	0,9805	3,3412	5,9545	0,9489
<i>KOH-LG</i>	Non calculable	-0,6456	0,8094	3,8109	0,5735	0,9947	3,0216	3,3357	0,9385
<i>KOH-LT</i>	Non calculable	-0,6061	0,8917	3,2272	0,5710	0,9961	2,9653	3,0752	0,8992

Table IV.5: Langmuir, Freundlich, and Temkin Constants for adsorption of MB onto raw and modified empty fruit bunch of three cultivars at 25 °C using the linear method

<i>Adsorbents</i>	<i>Langmuir isotherm constants</i>			<i>Freundlich isotherm constants</i>			<i>Temkin isotherm constants</i>		
	q_{max} (mg/g)	K_L (l/mg)	R^2	K_F (l/g)	n	R^2	B (J/mol)	K_T (l/g)	R^2
<i>RFBD</i>	<i>Non calculable</i>	-0,7396	0,8850	2,7335	0,4222	0,8850	3,5980	2,2973	0,6466
<i>RFBG</i>	<i>Non calculable</i>	-0,4992	0,9712	2,3360	0,5931	0,9868	2,7531	2,7356	0,8321
<i>RFBT</i>	<i>Non calculable</i>	-0,9698	0,9742	5,2234	0,3793	0,9544	2,6320	4,1775	0,7531
<i>H₂SO₄-FBD</i>	<i>Non calculable</i>	-0,4860	0,8057	3,8889	0,7124	0,9950	2,4149	4,5604	0,9196
<i>H₂SO₄-FBG</i>	<i>Non calculable</i>	-0,8423	0,8307	6,4777	0,6061	0,9967	2,8597	4,9275	0,9297
<i>H₂SO₄-FBT</i>	<i>Non calculable</i>	-0,4690	0,5875	4,7984	0,7490	0,9866	2,3617	3,3564	0,9605
<i>KOH-FBD</i>	<i>Non calculable</i>	-1,3205	0,5982	14,8518	0,5611	0,9342	3,1614	6,8500	0,9056
<i>KOH-FBG</i>	<i>Non calculable</i>	-1,0234	0,3941	11,4731	0,6369	0,9042	2,9402	7,1898	0,9788
<i>KOH-FBT</i>	<i>Non calculable</i>	-0,1109	0,1161	5,1605	0,9502	0,9882	1,8147	9,8712	0,9068

IV.2.3. Adsorption kinetics

The adsorption kinetics of MB onto raw and chemically modified leafy fronds and empty fruit bunches from three cultivars were systematically analyzed using both pseudo-first-order and pseudo-second-order kinetic models. The data are comprehensively represented in Figures IV.24–IV.29 and summarized in Tables IV.6 and IV.7.

The kinetic data revealed that the pseudo-second-order model fits the adsorption data significantly better than the pseudo-first-order model for all adsorbents and initial concentrations, as evidenced by the higher correlation coefficients (R^2), most of which are extremely close to or equal to 1 for the pseudo-second-order model (Tables IV.6 and IV.7), the

same was observed by [205]. This indicates that chemisorption is likely the rate-limiting step in the adsorption process, rather than simple physisorption, which aligns with the assumptions of the pseudo-second-order mechanism [110].

Raw adsorbents showed lower calculated equilibrium adsorption capacities $q_{e,cal}$ than the modified adsorbents. H_2SO_4 and KOH modification considerably enhanced the performance of both leafy fronds and empty fruit bunches, with KOH-modified samples exhibiting the highest $q_{e,cal}$ values in most cases ($q_{e,cal} = 4.4765$ mg/g, $q_{e,cal} = 4.4948$ mg/g and $q_{e,cal} = 4.4677$ mg/g, at $C_0 = 90$ mg/l for KOH-FBD, KOH-FBG and KOH-FBT respectively). The pseudo-first-order rate constants (k_1) were generally low, and the R^2 values were lower than those of the pseudo-second-order model, indicating the limited adequacy of this model in describing the adsorption kinetics under these conditions. In contrast, the pseudo-second-order rate constants (k_2) are much higher for the modified samples, especially those treated with KOH, demonstrating a faster uptake of MB and stronger sorbate-sorbent interactions after modification ($k_2 = 58.5210$ g.mg⁻¹ min⁻¹, $k_2 = 50.7405$ g.mg⁻¹ .min⁻¹ and $k_2 = 52.9676$ g.mg⁻¹ .min⁻¹, at $C_0 = 10$ mg/l for KOH-FBD, KOH-FBG, and KOH-LT, respectively). This demonstrates that chemical modification introduces more effective adsorption sites and possibly alters the surface charge, increasing the affinity toward MB molecules.

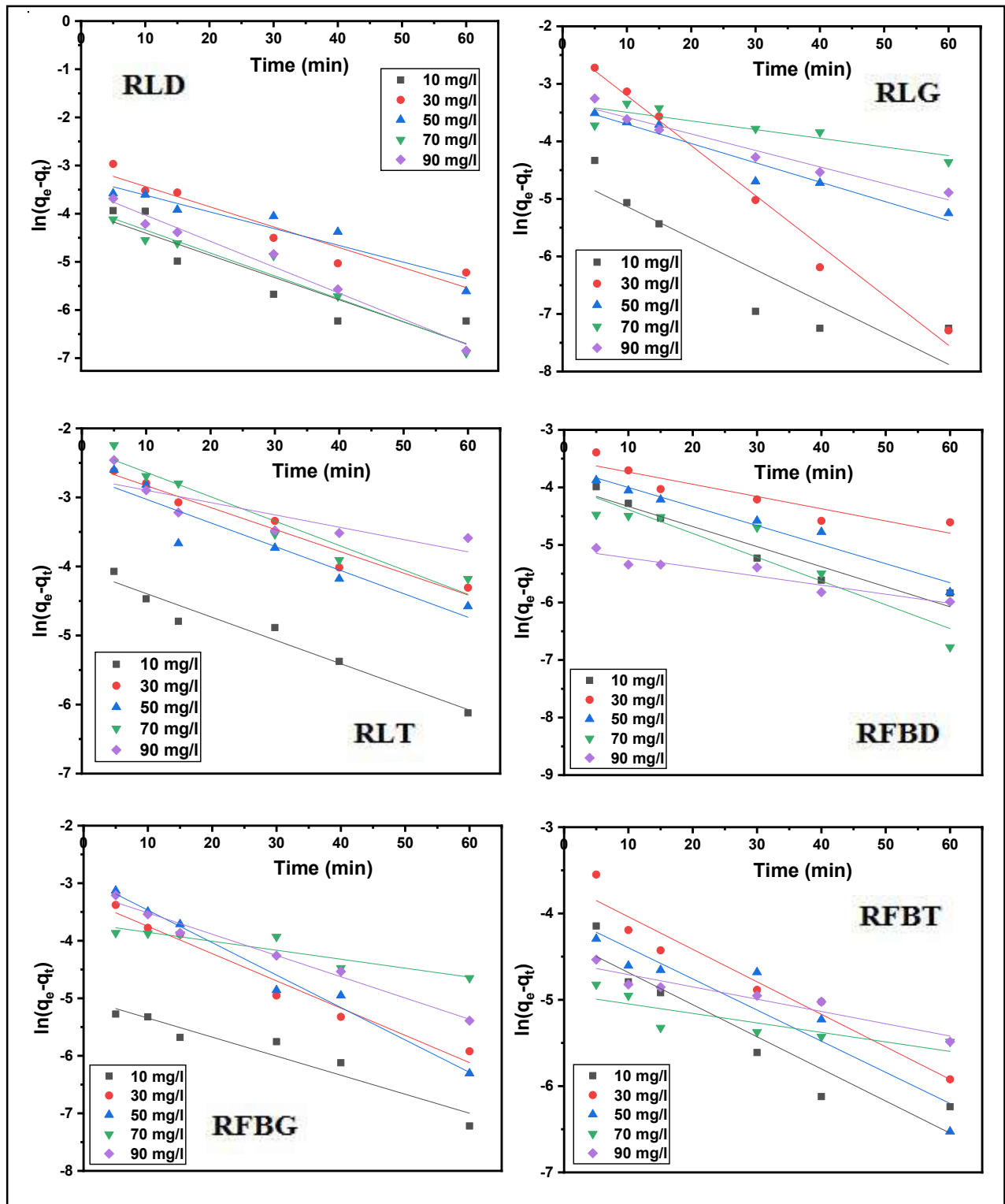


Figure IV.24: Pseudo-first-order plot for adsorption of MB onto raw leafy fronds and empty fruit bunch of three cultivars

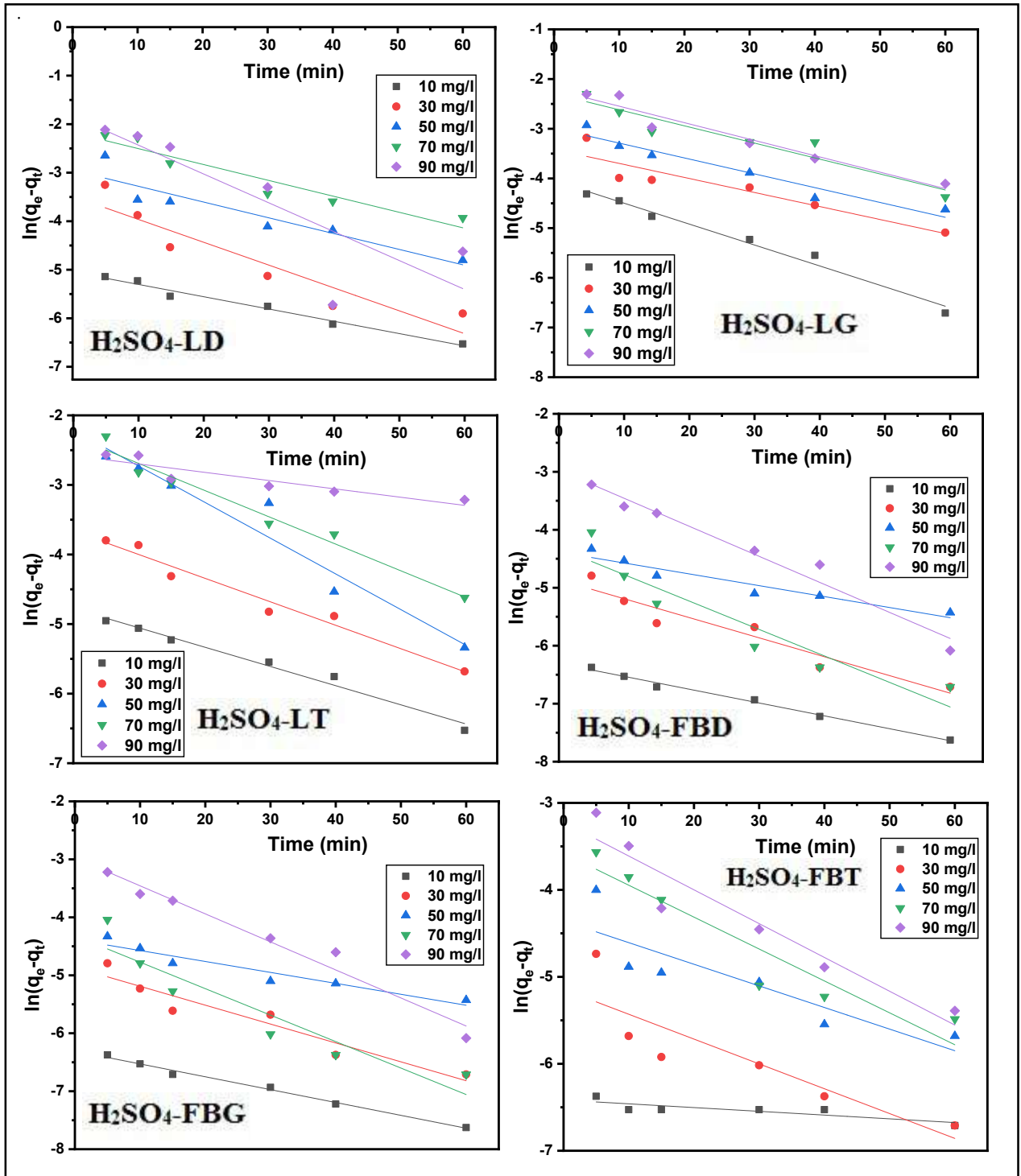


Figure IV.25: Pseudo-first-order plot for adsorption of MB onto H₂SO₄-modified leafy fronds and empty fruit bunch of three cultivars

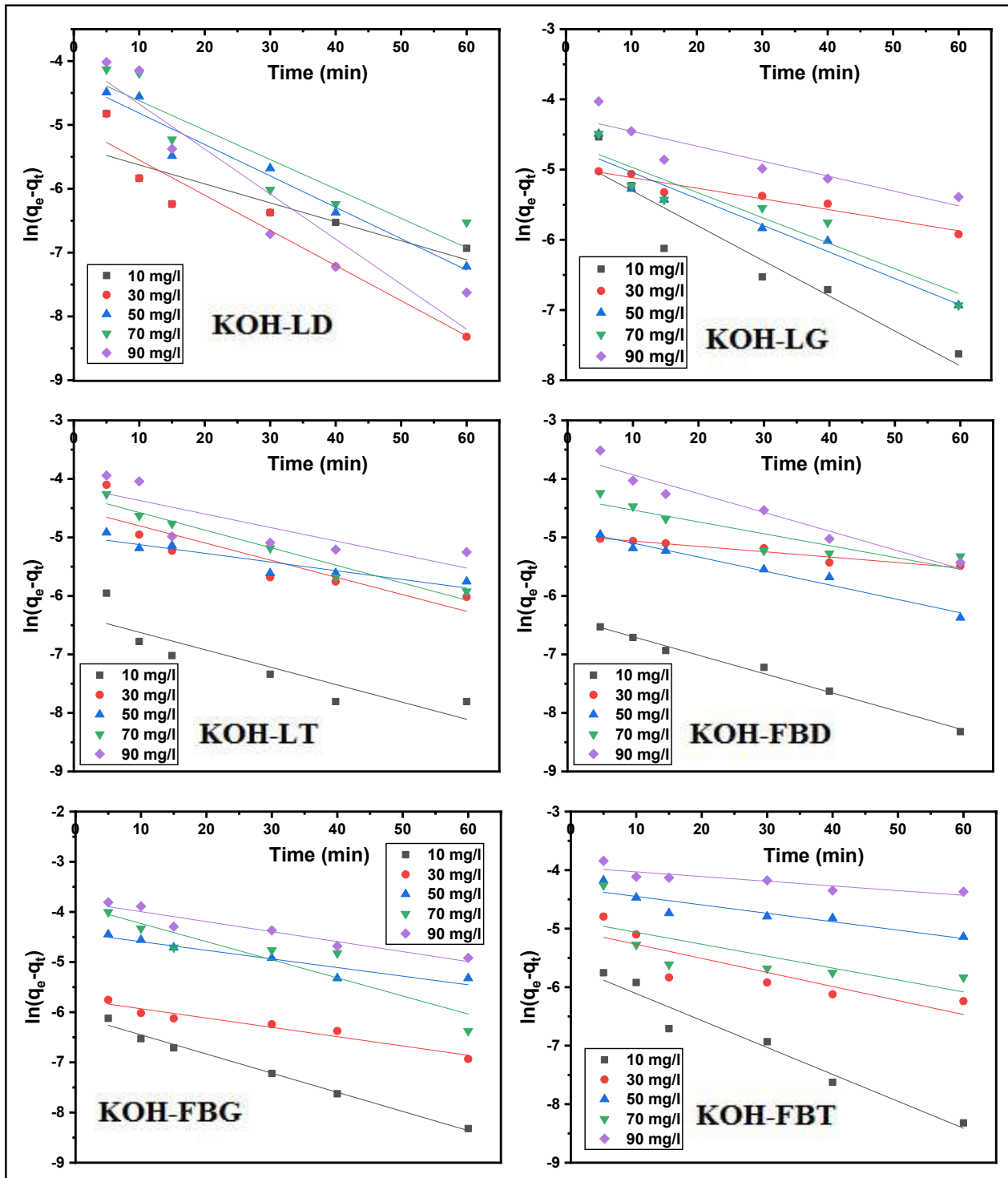


Figure IV.26: Pseudo-first-order plot for adsorption of MB onto KOH-modified leafy fronds and empty fruit bunch of three cultivars

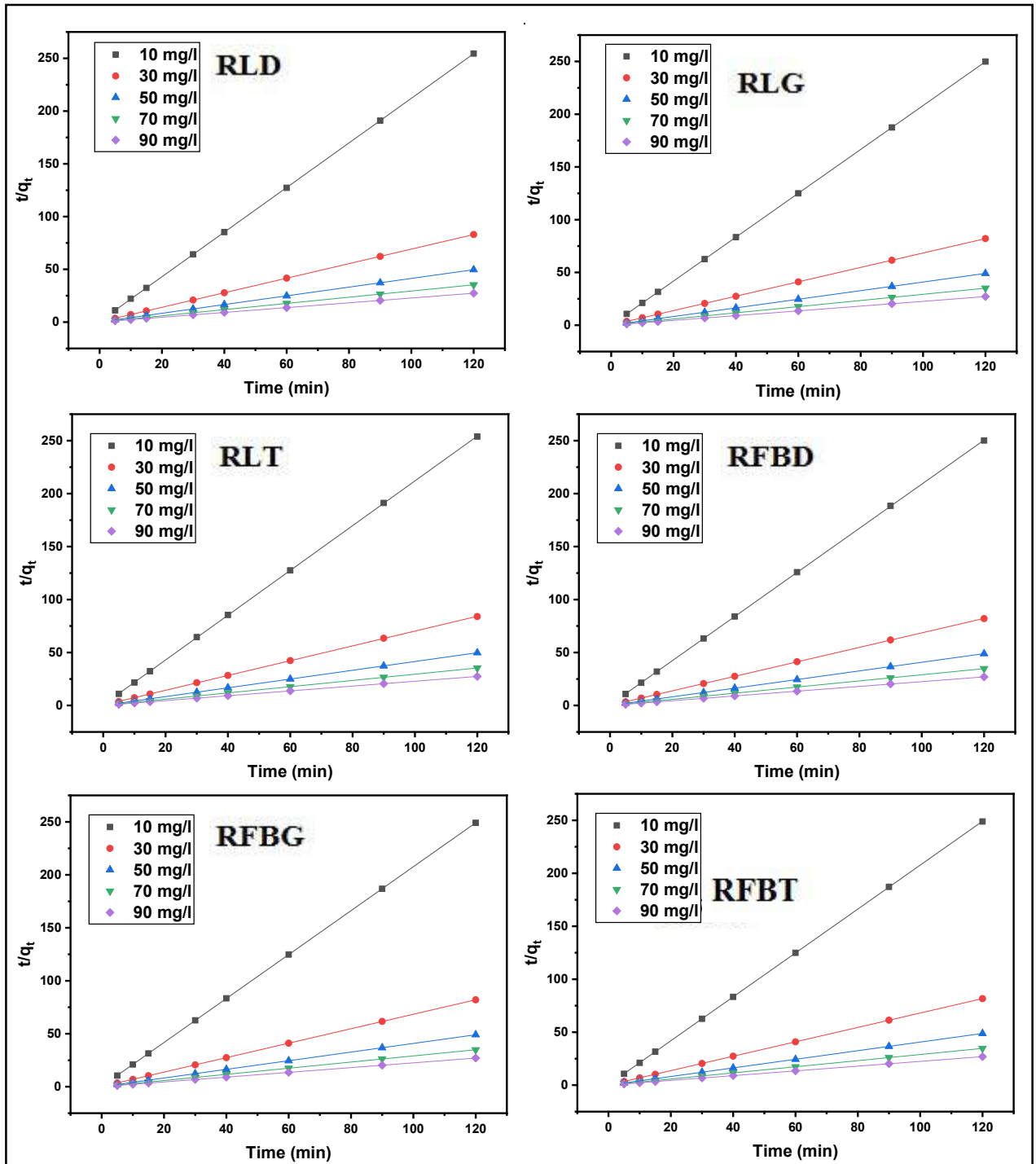


Figure IV.27: Pseudo-second-order plot for adsorption of MB onto raw leafy fronds and empty fruit bunch of three cultivars

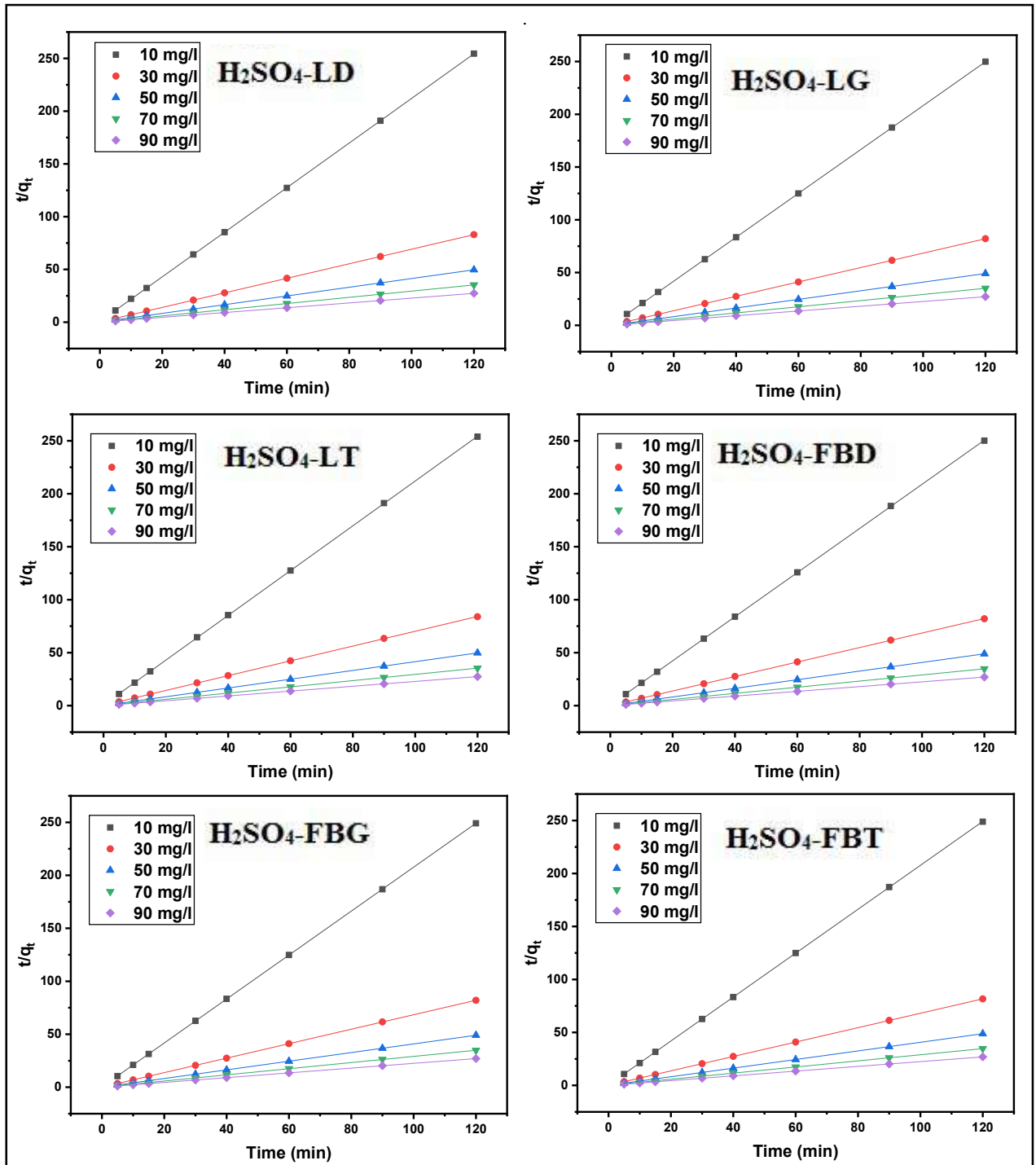


Figure IV.28: Pseudo-second-order plot for adsorption of MB onto H_2SO_4 -modified leafy fronds and empty fruit bunch of three cultivars

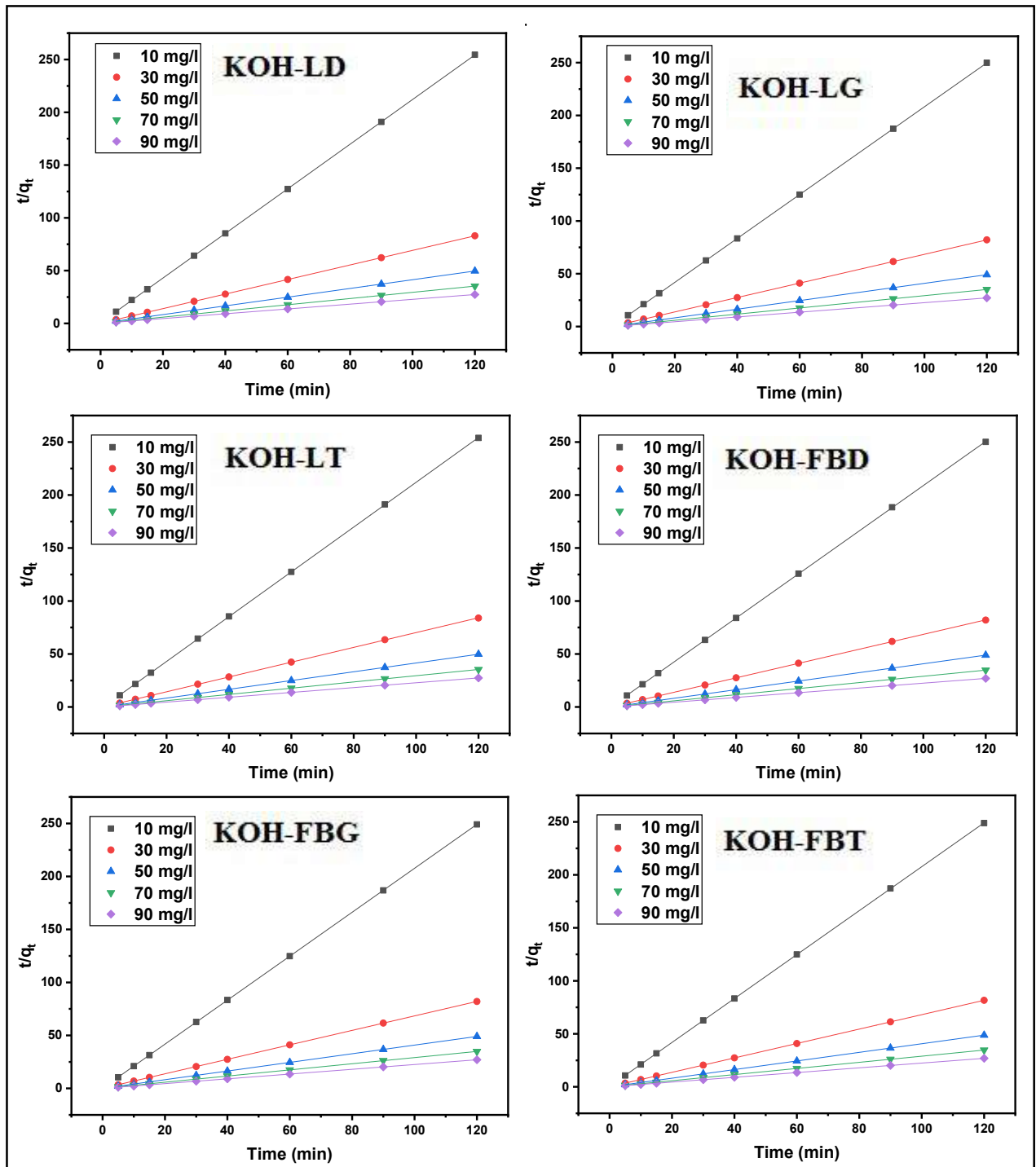


Figure IV.29: Pseudo-second-order plot for adsorption of MB onto KOH-modified leafy fronds and empty fruit bunch of three cultivars

Table IV.6: Pseudo-first-order and pseudo-second-order adsorption rate constants and calculated $q_{e,cal}$ values of MB onto raw and modified leafy fronds of three cultivars at 25 °C

Adsorbents	Pseudo-first-order				Pseudo-second-order		
	C_0 (mg/l)	$q_{e, cal}$ (mg/g)	k_1 (min^{-1})	R^2	$q_{e, cal}$ (mg/g)	k_2 ($g\ mg^{-1}\ min^{-1}$)	R^2
RLD	10	0,0194	0,0459	0,8318	0,4730	6,6545	1
	30	0,0491	0,0420	0,9182	1,4498	2,6141	1
	50	0,0381	0,0346	0,9134	2,4214	2,5652	1
	70	0,0210	0,0474	0,9514	3,4002	5,6942	1
	90	0,0305	0,0537	0,9784	4,3904	4,8305	1
RLG	10	0,0102	0,0549	0,8222	0,4809	15,8768	1
	30	0,0965	0,0868	0,9862	1,4657	2,6297	1
	50	0,0345	0,0335	0,9430	2,4474	3,0492	1
	70	0,0353	0,0151	0,7555	3,4246	1,7730	1
	90	0,0370	0,0286	0,9578	4,4301	2,6705	1
RLT	10	0,0173	0,0336	0,9541	0,4733	6,2094	0,9999
	30	0,0811	0,0317	0,9594	1,4321	1,2791	0,9999
	50	0,0683	0,0342	0,8737	2,4154	1,5571	1
	70	0,1020	0,0353	0,9378	3,3964	1,1372	1
	90	0,0661	0,0179	0,7180	4,3827	1,1716	0,9999
H_2SO_4 -LD	10	0,0064	0,0253	0,9798	0,4766	13,8784	1
	30	0,0306	0,0469	0,8714	1,4562	4,7281	1
	50	0,0523	0,0324	0,8619	2,4368	2,0771	1
	70	0,1139	0,0327	0,9166	3,4182	0,9151	0,9999
	90	0,1601	0,0593	0,7131	4,3975	0,9402	1
H_2SO_4 -LG	10	0,0175	0,0421	0,9822	0,4792	6,9431	1
	30	0,0329	0,0282	0,8656	1,4523	3,0143	0,9999
	50	0,0503	0,0299	0,9391	2,4350	1,9739	1
	70	0,1006	0,0323	0,9097	3,4099	1,0008	0,9999
	90	0,1092	0,0332	0,9444	4,3796	0,9476	1
H_2SO_4 -LT	10	0,0084	0,0275	0,9815	0,4813	10,6052	1
	30	0,0257	0,0337	0,9695	1,4520	4,3035	1
	50	0,1091	0,0513	0,9451	2,4298	1,3081	0,9999
	70	0,0996	0,0384	0,9727	3,4011	1,0832	0,9999
	90	0,0758	0,0119	0,8400	4,3427	0,9140	0,9999
KOH-LD	10	0,0048	0,0297	0,7214	0,4923	20,1994	1
	30	0,0067	0,0551	0,9253	1,4865	23,9706	1
	50	0,0132	0,0492	0,9502	2,4825	10,8320	1
	70	0,0156	0,0460	0,8474	3,4767	8,8293	1
	90	0,0189	0,0706	0,8858	4,4739	10,2170	1
KOH-LG	10	0,0082	0,0497	0,8872	0,4851	17,8171	1
	30	0,0070	0,0152	0,9403	1,4755	9,7888	1
	50	0,0095	0,0377	0,9251	2,4629	12,2755	1
	70	0,0100	0,03597	0,88466	3,4540	11,0002	1
	90	0,0144	0,0213	0,8181	4,4498	5,5743	1
KOH-LT	10	0,0018	0,0297	0,7786	0,4835	52,9676	1

	30	0,0110	0,0292	0,7684	1,4723	9,1132	1
	50	0,0069	0,0149	0,8656	2,4589	9,9637	1
	70	0,0139	0,0300	0,9524	3,4509	7,2578	1
	90	0,0160	0,0231	0,6541	4,4462	5,8615	1

Table IV.7: Pseudo-first-order and pseudo-second-order adsorption rate constants and calculated $q_{e,cal}$ values of MB onto raw and modified empty fruit bunch of three cultivars at 25 °C

Adsorbents	C_0 (mg/l)	Pseudo-first-order			Pseudo-second-order		
		$q_{e, cal}$ (mg/g)	k_1 (min^{-1})	R^2	$q_{e, cal}$ (mg/g)	k_2 ($g\ mg^{-1}\ min^{-1}$)	R^2
RFBD	10	0,0186	0,0349	0,9350	0,4803	6,1367	0,9999
	30	0,0296	0,0213	0,8493	1,4627	2,9518	0,9999
	50	0,0255	0,0331	0,9642	2,4551	4,0007	1
	70	0,0188	0,0414	0,8836	3,4518	5,9776	1
	90	0,0063	0,0157	0,8974	4,4478	11,7010	1
RFBG	10	0,0066	0,0331	0,9236	0,4822	14,7572	1
	30	0,0377	0,0473	0,9692	1,4646	3,8248	1
	50	0,0547	0,0564	0,9832	2,4506	3,0376	1
	70	0,0248	0,0156	0,8571	3,4426	2,8315	1
	90	0,0429	0,0370	0,9833	4,4435	2,6406	1
RFBT	10	0,0134	0,0372	0,8913	0,4826	9,0941	1
	30	0,0257	0,0377	0,9438	1,4711	4,6831	1
	50	0,0176	0,0361	0,8723	2,4614	5,9587	1
	70	0,0072	0,0110	0,7001	3,4604	9,7444	1
	90	0,0104	0,0142	0,9030	4,4627	6,4127	1
H_2SO_4 -FBD	10	0,0079	0,0390	0,8824	0,4895	15,8572	1
	30	0,0045	0,0287	0,9457	1,4774	20,2263	1
	50	0,0125	0,0385	0,8524	2,4643	9,6981	1
	70	0,0288	0,0210	0,9287	3,4640	3,0172	1
	90	0,0467	0,0422	0,9937	4,4498	2,7841	1
H_2SO_4 -FBG	10	0,0018	0,0222	0,9914	0,4898	45,7060	1
	30	0,0077	0,0326	0,9193	1,4821	13,7620	1
	50	0,0125	0,0189	0,9180	2,4774	6,1740	1
	70	0,0133	0,0457	0,8819	3,4669	10,4520	1
	90	0,0511	0,0484	0,9694	4,4647	2,7855	1
H_2SO_4 -FBT	10	0,0016	0,0043	0,7142	0,4913	33,3029	1
	30	0,0058	0,0285	0,7746	1,4825	17,5666	1
	50	0,0128	0,0249	0,7601	2,4742	7,2089	1
	70	0,0279	0,0367	0,8952	3,4676	4,1292	1
	90	0,0399	0,03887	0,9130	4,4553	3,1040	1
KOH-FBD	10	0,0017	0,0316	0,9908	0,4926	58,5210	1
	30	0,0069	0,0091	0,9303	1,4885	9,0253	1
	50	0,0077	0,0238	0,9736	2,4860	10,8813	1
	70	0,0132	0,0202	0,8218	3,4850	6,7377	1
	90	0,0271	0,0321	0,9444	4,4765	4,0147	1

KOH-FBG	10	0,0023	0,0382	0,9900	0,4923	50,7405	1
	30	0,0032	0,0185	0,9417	1,4882	22,9189	1
	50	0,0120	0,0172	0,9039	2,4912	5,8764	1
	70	0,0208	0,0361	0,8528	3,4801	5,0225	1
	90	0,0225	0,0199	0,9228	4,4978	2,8376	1
KOH-FBT	10	0,0035	0,0460	0,9537	0,4948	38,7769	1
	30	0,0065	0,0240	0,7352	1,4881	14,1337	1
	50	0,0135	0,0144	0,8278	2,4771	5,4506	1
	70	0,0078	0,020	0,5164	3,4717	10,2682	1
	90	0,0193	0,0080	0,7660	4,4677	3,0964	1

IV.2.4. Adsorption mechanism

The intraparticle and external film diffusion models were employed to comprehend the phenomenon restricting the adsorption mechanism, as the pseudo-first and pseudo-second order models were unable to explain the mechanism. These aspects were investigated through diffusion plots, with key parameters summarized in Tables IV.8 and IV.9. Additionally, Figures IV.30-IV.35 provide visual confirmation of the kinetic behaviors exhibited by various adsorbent cultivars and modifications.

The obtained data showed that both types of diffusion contributed to the overall adsorption, with diffusion parameters varying according to the type and cultivar of adsorbent, chemical modification applied, and initial dye concentration. Specifically, chemical treatments with acids and alkalis influence both external mass transfer and internal pore accessibility, as indicated by changes in the diffusion rate constants. However, neither intraparticle nor external film diffusion alone fully accounted for the observed kinetics.

The high correlation coefficients and persistent non-zero intercepts in the fitted models suggest that the dye uptake followed a multistep pathway involving surface adsorption, external film diffusion, and intraparticle pore diffusion. Moreover, increasing the initial dye concentration tended to increase the driving force for diffusion, yet also introduced more competition for adsorption sites, reflecting a delicate balance between kinetics and capacity in these systems and an increasing boundary layer influence [205; 206]. Modifications improved pore accessibility and surface functionality.

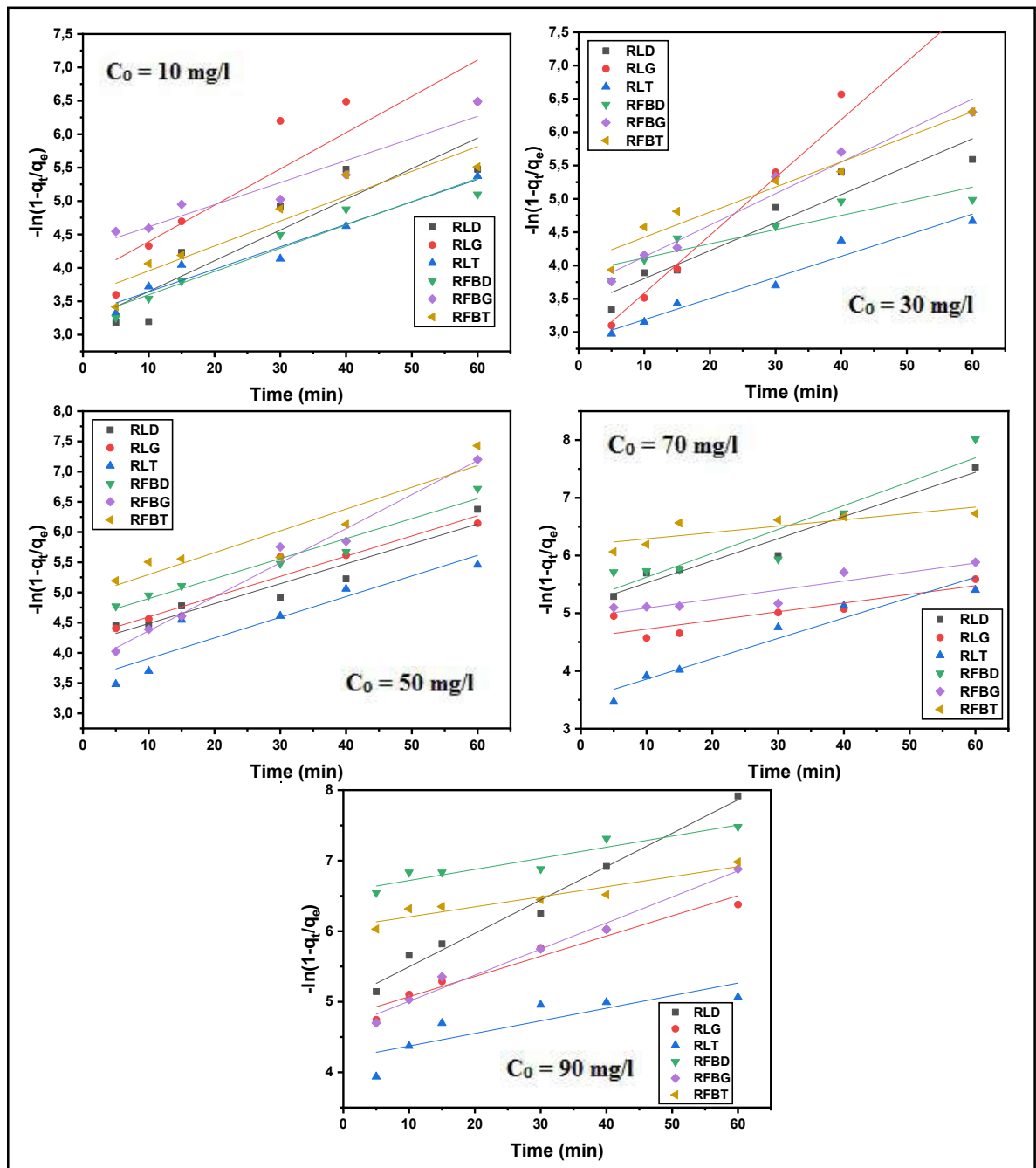


Figure IV.30: External film diffusion plot for adsorption of MB onto raw leafy fronds and empty fruit bunch of three cultivars

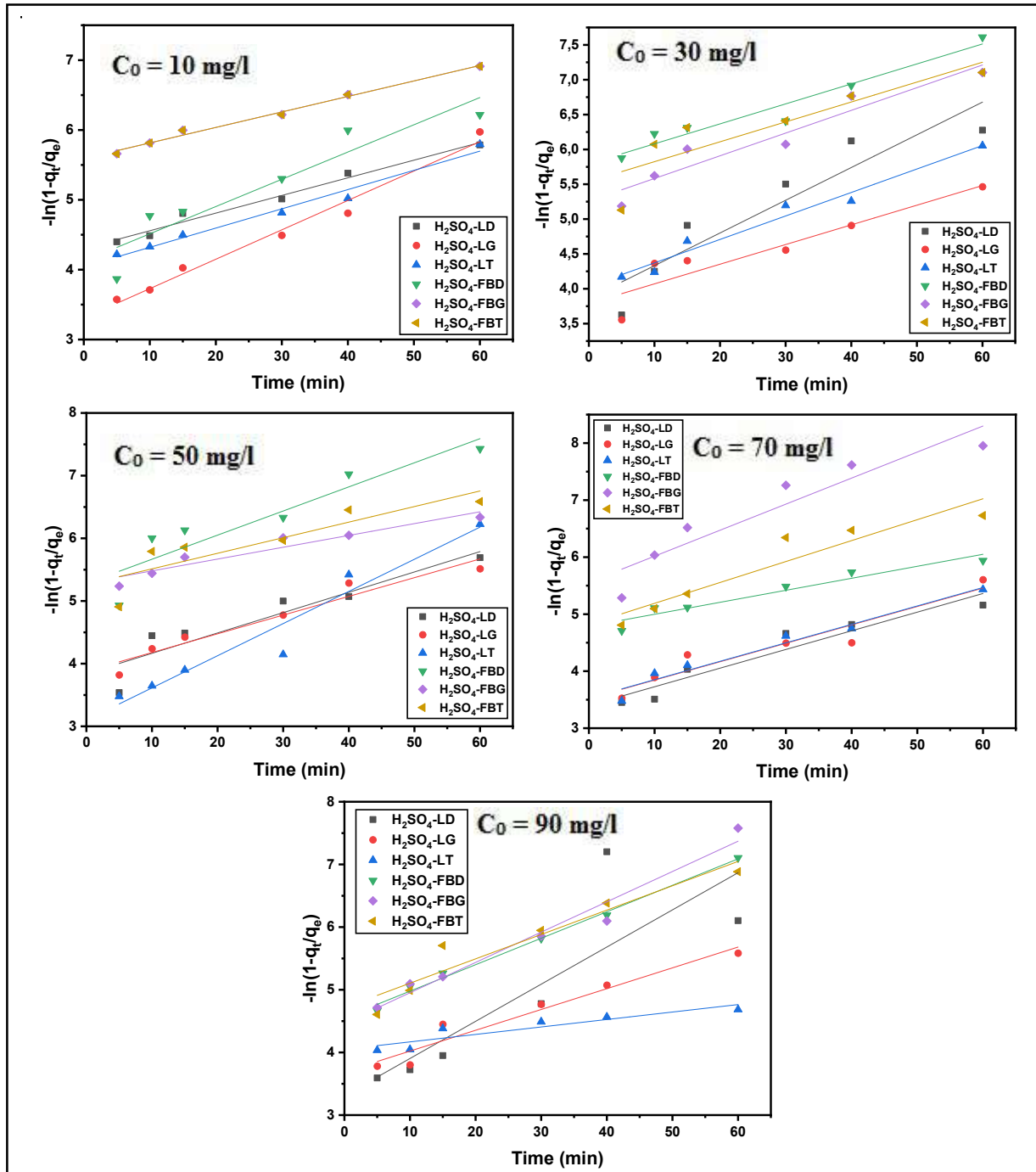


Figure IV.31: External film diffusion plot for adsorption of MB onto H_2SO_4 -modified leafy fronds and empty fruit bunch of three cultivars

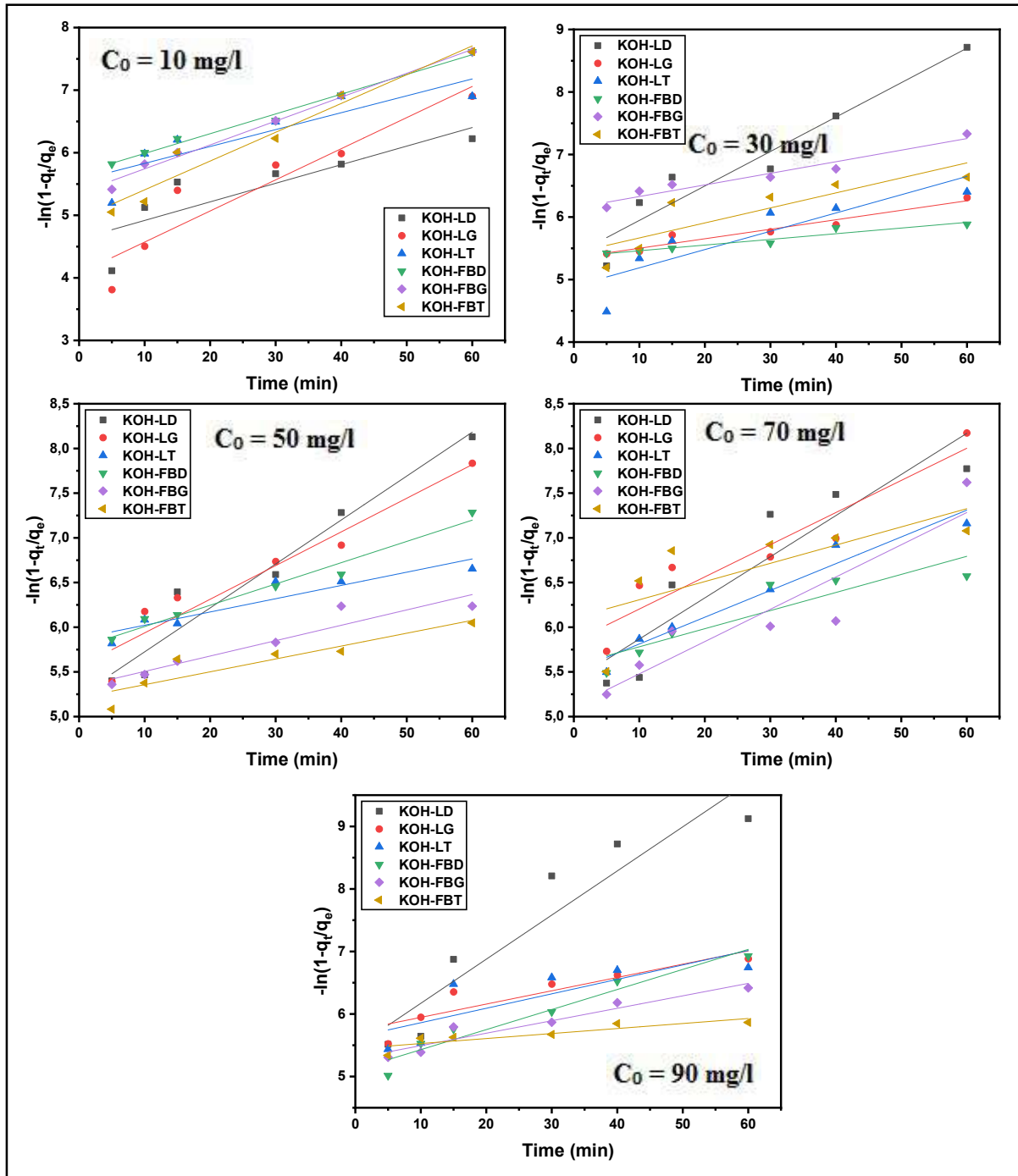


Figure IV.32: External film diffusion plot for adsorption of MB onto KOH-modified leafy fronds and empty fruit bunch of three cultivars

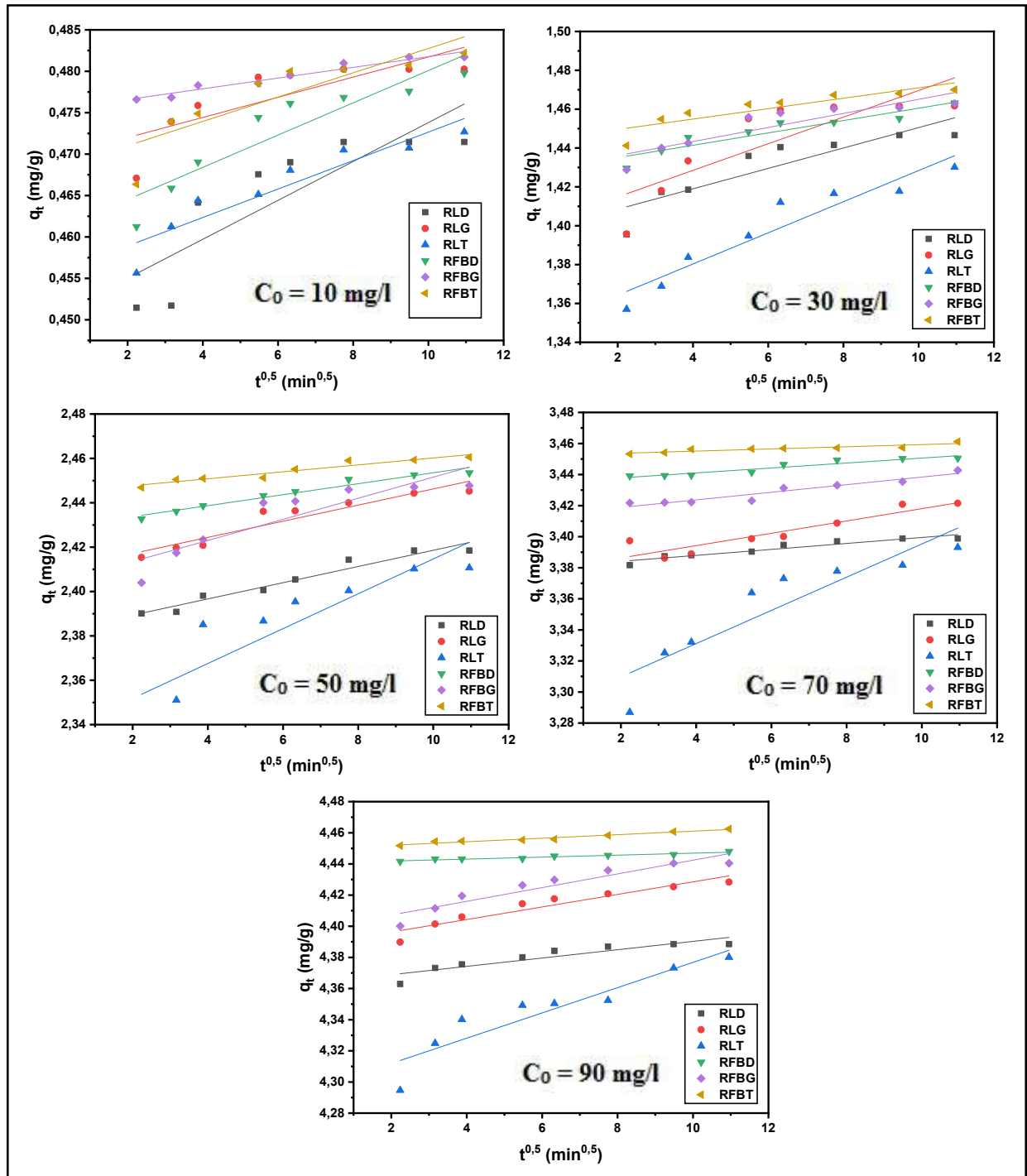


Figure IV.33: Intraparticle diffusion plot for adsorption of MB onto raw leafy fronds and empty fruit bunch of three cultivars

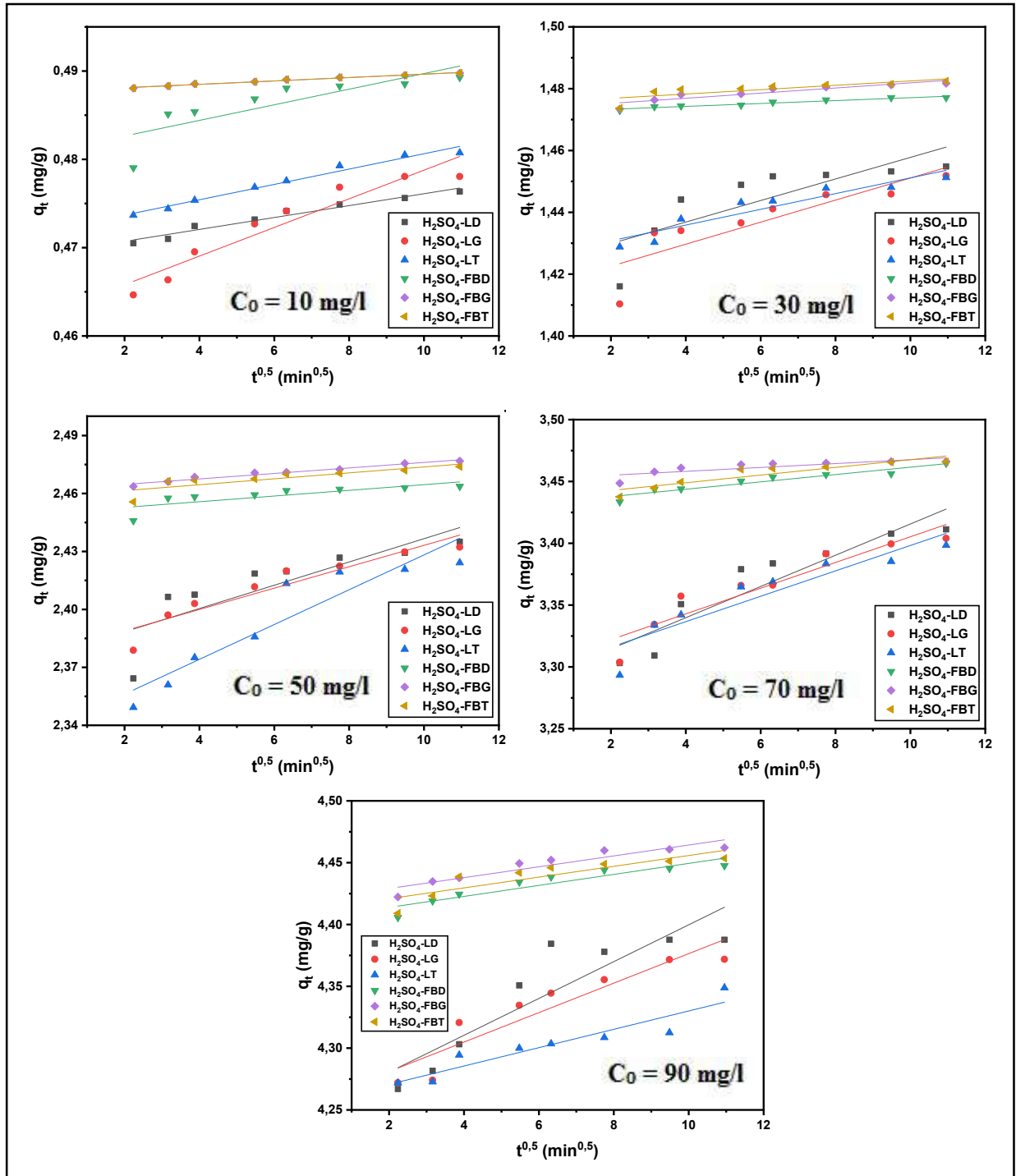


Figure IV.34: Intraparticle diffusion plot for adsorption of MB onto H_2SO_4 -modified leafy fronds and empty fruit bunch of three cultivars

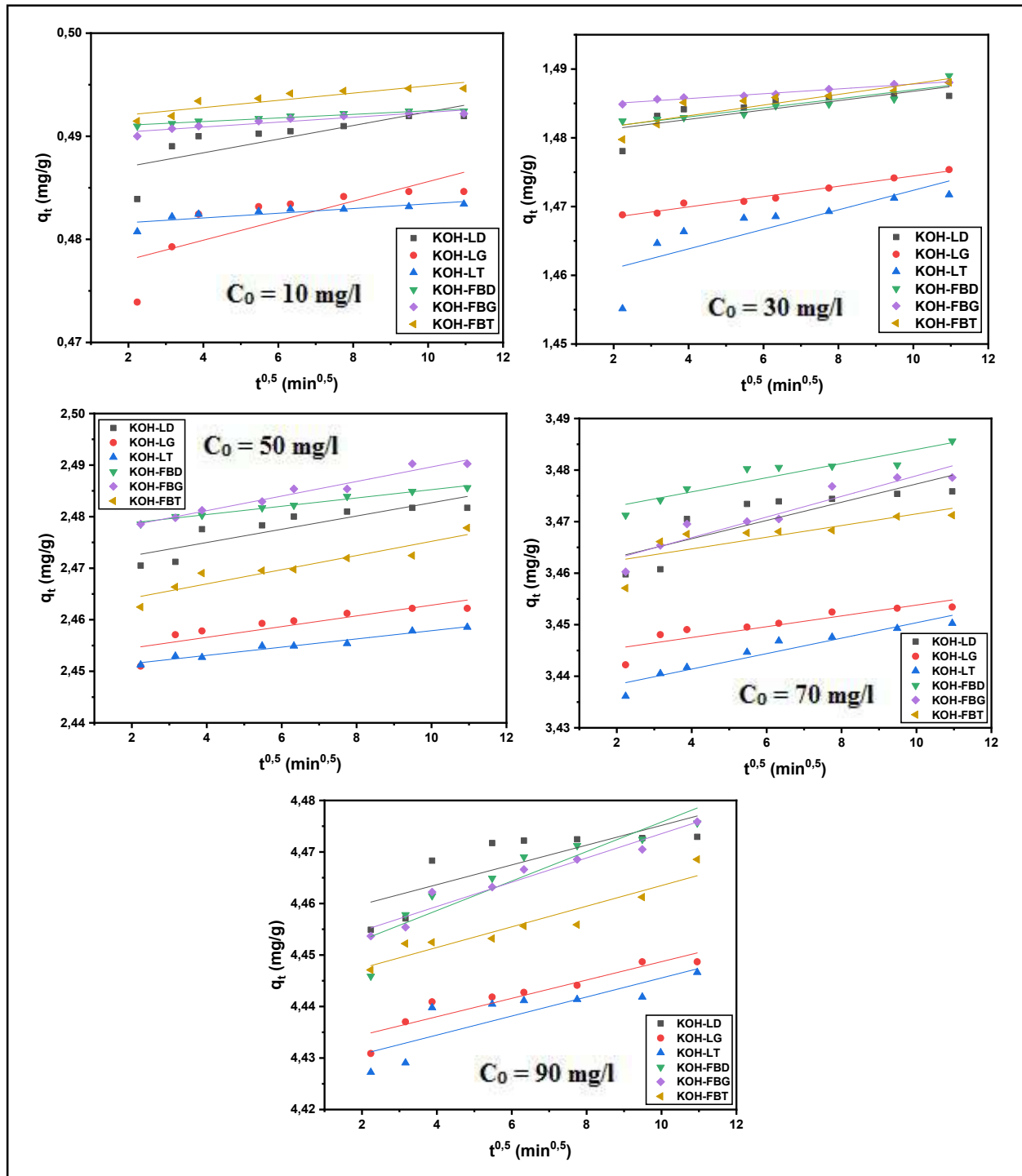


Figure IV.35: Intraparticle diffusion plot for adsorption of MB onto KOH-modified leafy fronds and empty fruit bunch of three cultivars

Table IV.8: External film and intraparticle diffusion parameters of MB adsorption onto raw and modified leafy frond of three cultivars at 25 °C

Adsorbents	External film diffusion				Intraparticule diffusion		
	C_0 (mg/l)	K_{efl} (min^{-1})	C	R^2	K_{id} (mg/g. $\text{min}^{0.5}$)	C (mg/g)	R^2
RLD	10	0,0459	3,1876	0,8318	0,0024	0,4503	0,7232
	30	0,0420	3,3836	0,9182	0,0052	1,3981	0,7970
	50	0,0329	4,1561	0,9189	0,0037	2,3820	0,9512
	70	0,0384	5,1412	0,9614	0,0019	3,3803	0,9090
	90	0,0473	5,0235	0,9826	0,0028	4,3635	0,8403
RLG	10	0,0543	3,8509	0,8212	0,0012	0,4696	0,6488
	30	0,0867	2,7183	0,9862	0,0068	1,4011	0,7131
	50	0,0335	4,2610	0,9290	0,0036	2,4098	0,9026
	70	0,0151	4,5740	0,7555	0,0040	3,3784	0,8503
	90	0,0286	4,7860	0,9577	0,0040	4,3882	0,9064
RLT	10	0,0336	3,3065	0,9541	0,017	0,4555	0,8736
	30	0,0317	2,8702	0,9594	0,0080	1,3482	0,9104
	50	0,0342	3,5640	0,8737	0,0079	2,3361	0,7996
	70	0,0353	3,5045	0,9378	0,0107	3,2880	0,8358
	90	0,0179	4,1942	0,7180	0,0081	4,2956	0,8624
H_2SO_4 -LD	10	0,0253	4,3048	0,9798	0,0077	0,4694	0,9623
	30	0,0469	3,8623	0,8714	0,0035	1,4229	0,6601
	50	0,0324	3,8461	0,8620	0,0060	2,3764	0,7002
	70	0,0327	3,3998	0,9165	0,0126	3,2893	0,8629
	90	0,0593	3,3107	0,7331	0,0149	4,2508	0,8164
H_2SO_4 -LG	10	0,0421	3,3075	0,9822	0,0016	0,4625	0,9161
	30	0,0282	3,7884	0,8656	0,0036	1,4154	0,7546
	50	0,0299	3,8792	0,9391	0,0055	2,3778	0,8906
	70	0,0323	3,5210	0,9097	0,0104	3,3013	0,8832
	90	0,0332	3,6849	0,9305	0,0119	4,2572	0,8452
H_2SO_4 -LT	10	0,0275	4,0445	0,9815	0,0009	0,4719	0,9776
	30	0,0337	4,0344	0,9695	0,0025	1,4257	0,8878
	50	0,0513	3,1008	0,9451	0,0090	2,3381	0,8774
	70	0,0323	3,5280	0,9634	0,0102	3,2955	0,8567
	90	0,0119	4,0491	0,8400	0,0074	4,2558	0,8800
KOH-LD	10	0,0297	4,6204	0,7214	0,0007	0,4857	0,6257
	30	0,0551	5,3952	0,9253	0,0006	1,4800	0,6167
	50	0,0492	5,3228	0,9502	0,0013	2,4698	0,7740
	70	0,0460	5,4074	0,8474	0,0018	3,4596	0,7006
	90	0,0706	5,4649	0,8858	0,0019	4,4560	0,6322
KOH-LG	10	0,0497	4,0740	0,8872	0,0009	0,4761	0,6299
	30	0,0152	5,3492	0,9403	0,0007	1,4669	0,9768
	50	0,0377	5,5598	0,9251	0,0010	2,4524	0,7585
	70	0,0360	5,8437	0,8847	0,0010	3,4433	0,7858
	90	0,0213	5,7329	0,8181	0,0018	4,4309	0,8473
KOH-LT	10	0,0270	5,5594	0,7633	0,0002	0,4812	0,7133
	30	0,0292	4,8950	0,7684	0,0014	1,4582	0,6868

	50	0,0148	5,8738	0,8656	0,0008	2,4500	0,9645
	70	0,0299	5,5131	0,9523	0,0015	3,4354	0,9080
	90	0,0231	5,6287	0,6541	0,0018	4,4271	0,7260

Table IV.9: External film and intraparticle diffusion parameters of MB adsorption onto raw and modified empty fruit bunch of three cultivars at 25 °C

Adsorbents	External film diffusion				Intraparticle diffusion		
	C_0 (mg/l)	K_{efl} (min^{-1})	C	R^2	K_{id} (mg/g. $\text{min}^{0.5}$)	C (mg/g)	R^2
RFBD	10	0,0349	3,2480	0,9350	0,0019	0,4606	0,8526
	30	0,0213	3,9005	0,8493	0,0032	1,4287	0,8772
	50	0,0331	4,5673	0,9642	0,0025	2,4288	0,9613
	70	0,0414	5,2106	0,8836	0,0016	3,4347	0,9050
	90	0,0157	6,5621	0,8974	0,0006	4,4406	0,9370
RFBG	10	0,0331	4,2834	0,9236	0,0006	0,4753	0,9453
	30	0,0473	3,6575	0,9692	0,0036	1,4288	0,8093
	50	0,0564	3,8009	0,9832	0,0050	2,4040	0,8075
	70	0,0156	4,9333	0,8571	0,0024	3,4139	0,9185
	90	0,0370	4,6384	0,9833	0,0044	4,3984	0,8717
RFBT	10	0,0372	3,5829	0,8913	0,0015	0,4681	0,7545
	30	0,0377	4,0472	0,9438	0,0079	1,4543	0,9323
	50	0,0361	4,9368	0,8723	0,0016	2,4446	0,9226
	70	0,0110	6,1794	0,7001	0,0007	3,4523	0,8194
	90	0,0142	6,0614	0,9030	0,0011	4,4497	0,9624
H₂SO₄-FBD	10	0,0390	4,1234	0,8824	0,0009	0,4809	0,6835
	30	0,0287	5,7933	0,9460	0,0005	1,4724	0,9425
	50	0,0385	5,2815	0,8524	0,0015	2,4499	0,6322
	70	0,0210	4,7880	0,9287	0,0030	3,4318	0,9077
	90	0,0422	4,5557	0,9940	0,044	4,4049	0,8644
H₂SO₄-FBG	10	0,0222	5,5931	0,9914	0,0002	0,4877	0,9842
	30	0,0326	5,2571	0,9193	0,0008	1,4736	0,8475
	50	0,0189	5,2915	0,9180	0,0014	2,4618	0,9632
	70	0,0457	5,5605	0,8819	0,0016	3,4519	0,6630
	90	0,0484	4,4690	0,9694	0,0044	4,4203	0,8600
H₂SO₄-FBT	10	0,0222	5,5931	0,9914	0,0002	0,4877	0,9842
	30	0,0285	5,5385	0,7746	0,0007	1,4755	0,6493
	50	0,0249	5,2641	0,7601	0,0015	2,4584	0,7189
	70	0,0367	4,8227	0,8952	0,0031	3,4365	0,8440
	90	0,0389	4,7158	0,9130	0,0044	4,4121	0,7627
KOH-FBD	10	0,0316	5,6726	0,9908	0,0002	0,4907	0,9537
	30	0,0091	5,3698	0,9303	0,0007	1,4804	0,8738
	50	0,0238	5,7696	0,9736	0,0008	2,4772	0,9844
	70	0,0202	5,5786	0,8218	0,0014	3,4703	0,8678
	90	0,0321	5,1079	0,9444	0,0029	4,4472	0,8376
KOH-FBG	10	0,0382	5,3607	0,9900	0,0002	0,4899	0,8810
	30	0,0185	6,1427	0,9417	0,0003	1,4843	0,9751
	50	0,0172	5,3336	0,9039	0,0014	2,4755	0,9668

	<i>70</i>	<i>0,0361</i>	<i>5,1173</i>	<i>0,8528</i>	<i>0,0020</i>	<i>3,4589</i>	<i>0,8970</i>
	<i>90</i>	<i>0,0199</i>	<i>5,2938</i>	<i>0,9228</i>	<i>0,0024</i>	<i>4,4500</i>	<i>0,9420</i>
	<i>10</i>	<i>0,0460</i>	<i>4,9464</i>	<i>0,9537</i>	<i>0,0003</i>	<i>0,4914</i>	<i>0,7968</i>
	<i>30</i>	<i>0,0240</i>	<i>5,4254</i>	<i>0,7352</i>	<i>0,0008</i>	<i>1,4801</i>	<i>0,7820</i>
<i>KOH-FBT</i>	<i>50</i>	<i>0,0144</i>	<i>5,2130</i>	<i>0,8278</i>	<i>0,0014</i>	<i>2,4614</i>	<i>0,8873</i>
	<i>70</i>	<i>0,0204</i>	<i>6,1034</i>	<i>0,5164</i>	<i>0,0011</i>	<i>3,4602</i>	<i>0,6262</i>
	<i>90</i>	<i>0,0080</i>	<i>5,4464</i>	<i>0,7660</i>	<i>0,0020</i>	<i>4,4434</i>	<i>0,8964</i>

Conclusion

In conclusion, this chapter demonstrated that the chemical modification of date palm biomass, particularly through alkaline treatment, significantly improved its structural, surface, and adsorption characteristics, as confirmed by FTIR, XRD, XRF, and SEM analyses. Adsorption experiments further revealed that the performance of the biosorbents was not only dependent on the type of chemical treatment but also varied with the cultivar and anatomical origin of the biomass. Notably, KOH-modified samples from select cultivars exhibited superior removal efficiencies, along with more favorable isotherm and kinetic behaviors. The adsorption data were best described by the Freundlich and Temkin models, indicating a heterogeneous and cooperative adsorption process with chemical interaction. These findings highlight the critical roles of biomass provenance and surface chemistry in optimizing biosorption performance. Building on these results, the next chapter explores the practical implementation of the most effective biosorbent incorporated into a sodium alginate-based membrane. This membrane was integrated into a continuous filtration system for the treatment of agricultural drainage water to assess its environmental applicability and scalability under real-world conditions.

Chapter 5

Application of Modified Date Palm Biomass for Wastewater Treatment

Introduction

Building upon the findings of the previous chapter, which established that chemical modification (particularly alkaline treatment) of date palm biomass markedly enhances its structural, surface, and adsorption properties, this chapter discusses the practical application of these results in wastewater treatment. Prior experimental studies have identified that optimal adsorption performance was achieved by incorporating chemically modified biomass into sodium alginate to fabricate composite adsorptive membranes. Accordingly, this chapter focuses on the development and synthesis of a novel biomembrane composed of alkali-treated date palm waste and sodium alginate. The design of a continuous filtration system was discussed, and the effectiveness of the membrane for treating agricultural drainage water under realistic operating conditions in the *Wadi Righ* region was evaluated. This study represents a significant step towards the practical implementation of low-cost biotechnological solutions for wastewater remediation, with particular emphasis on the environmental and technical feasibility of this innovation in arid areas experiencing water scarcity.

I. Degradation and Pollution of Water Resources in Ouargla Region

In the Sahara, mobilizing aquifers is crucial for development. However, the utilization of these water resources requires a thorough, individualized assessment of post-use water management strategies. Unfortunately, the development of Saharan oases has often come at the cost of previously well-preserved natural balances, which are now severely compromised [207].

In the *Ouargla* region, rapid demographic and industrial growth has intensified the pressure on water resources, leading to a continuous increase in water demand and heightened pollution levels. These environmental challenges are particularly pronounced as urban areas expand and industrial activities increase. Groundwater recharge in *Ouargla* primarily results from several interconnected processes: the discharge of untreated domestic wastewater, excessive and inefficient irrigation of palm groves, runoff from surrounding elevated areas, and floodwaters from three main Oueds (*N'sa*, *M'zab*, and *M'ya*) that drain into the sedimentary basin of *Ouargla*. These inputs, combined with the notably flat topography of the region and the lack of natural drainage outlets, lead to a chronic surplus of water in the subsurface. This persistent rise in the water table contributes directly to the degradation of water quality and explains why groundwater in the *Ouargla* Valley is becoming increasingly polluted [208; 209].

To mitigate these issues and protect groundwater from further deterioration, experts recommend a multi-pronged approach to water management. These include systematic monitoring and treatment of groundwater, a strict prohibition on the use of untreated wastewater for irrigation, and the enforcement of wastewater treatment for all industrial discharges [209]. The implementation of such strategies is essential for restoring ecological balance and ensuring the long-term sustainability of water resources in this arid region.

II. Advances in Adsorptive Membranes for Wastewater Treatment and Desalination

In recent years, various strategies have been explored to develop cost-effective and efficient technologies aimed at reducing wastewater generation and enhancing treated effluent quality. Among these, adsorption has emerged as a promising alternative, particularly through the search for low-cost adsorbent materials. Additionally, membrane separation is gaining popularity in the treatment of inorganic effluents because of its operational simplicity and effectiveness [210]. Adsorptive membranes represent a significant advancement in water treatment technologies, combining membrane filtration with adsorption. They offer advantages such as easy modification, high flexibility, large porosity, and high specific surface area. These membranes are highly effective in removing contaminants, including heavy metals, from water and wastewater, making them ideal for desalination and wastewater treatment applications. Their performance is further enhanced by incorporating advanced materials, such as ionic liquids, deep eutectic solvents, graphene oxide, and nanomaterials, which improve permeability, selectivity, and pollutant rejection while reducing energy consumption and operational costs [211].

Adsorptive membranes have gained considerable attention for enhancing seawater desalination efficiency. The integration of advanced materials, such as ionic liquids and graphene oxide, has resulted in membranes with improved separation performance, enhanced stability, and reduced energy consumption [212].

In addition to their role in desalination, adsorptive membranes have proven effective in removing a broad spectrum of contaminants, including synthetic dyes, pharmaceutical compounds, and toxic inorganic pollutants such as ammonia, nitrogen, and phosphorus. This is largely attributed to their dual adsorption/filtration mechanism, which provides versatility in various environmental applications [212-216].

In wastewater treatment, these membranes have demonstrated significant efficacy in capturing heavy metals, persistent organic pollutants, and other emerging contaminants from industrial and municipal wastewater. Their high adsorption capacity and chemical selectivity make them particularly suitable for treating complex effluents [217-219].

In light of the advancements highlighted above, the subsequent section focuses on the experimental application of a bioadsorptive membrane synthesized from KOH-modified date palm biomass and sodium alginate. The effectiveness of this membrane in treating real drainage water collected from *Ouargla* region was evaluated under continuous filtration conditions.

III. Materials and methods

III.1. Materials

The adsorbent selected for this section is KOH-FBG, chosen for its superior performance compared to the other tested adsorbents, as demonstrated by the findings presented in the previous chapter. Na-alginate, which was used (low viscosity Min 45 cps +/- 2 cps, BIOCHEM Chemopharma), is a natural polymer extracted from brown seaweed and is valued for its biocompatibility, nontoxicity, and biodegradability. Its distinctive physicochemical characteristics, such as gel formation, thickening capability, and encapsulation, make it highly versatile. These properties support its widespread use in fields such as biomedicine, food technology, and environmental management. Calcium chloride was used as a crosslinking agent (CaCl₂ molecular weight 110.99 g/mole, BIOCHEM Chemopharma).

III.2. Preparation of alginate-KOH-FBG adsorptive membrane

The method for producing the alginate-KOH-FBG membrane is well-documented in the literature (alginate membrane). To prepare a 2% sodium alginate solution, 2 g of Na-alginate powder was dissolved in 100 ml of distilled water using a magnetic stirrer at room temperature. Once fully dissolved, approximately 2 g of KOH-treated FBG was added, and the solution was stirred until a uniform mixture was achieved. The alginate-KOH-FBG blend was then poured into Petri dishes to form a membranes (10 ml for each membrane), which were subsequently frozen in a refrigerator for 24 h. Following freezing, a 5% calcium chloride solution was added to the Petri dishes and left for 24 h to fully crosslink the membranes. The resulting membranes were rinsed several times with distilled water to remove residual calcium chloride from its surfaces. The final products, referred to as a date palm-based alginate-KOH-

FBG adsorptive membranes, were dried in a lyophilizer at 0.0207 mbar pressure for 72 h. The resulting membranes exhibited a mass of 0.67 g, with a diameter of 4.5 cm and a thickness of 2.75 mm (see figure V.1).

III.3. Location of sampling point

The water sample was collected manually on May 26, 2025, from irrigation water used for palm grove cultivation at a location where the irrigation stream flows into a wastewater drainage channel prior to the point of confluence (figure V.2). The sampling site was situated between *Said Otba* and *Ain El Beida* (31°59'25.0"N, 5°22'02.6"E), in the Wilaya of *Ouargla, Algeria* (figure V.3). To ensure the representativeness and reliability of subsequent analyses, a homogeneous sample was carefully obtained and preserved under appropriate storage conditions before being subjected to filtration and laboratory analyses.

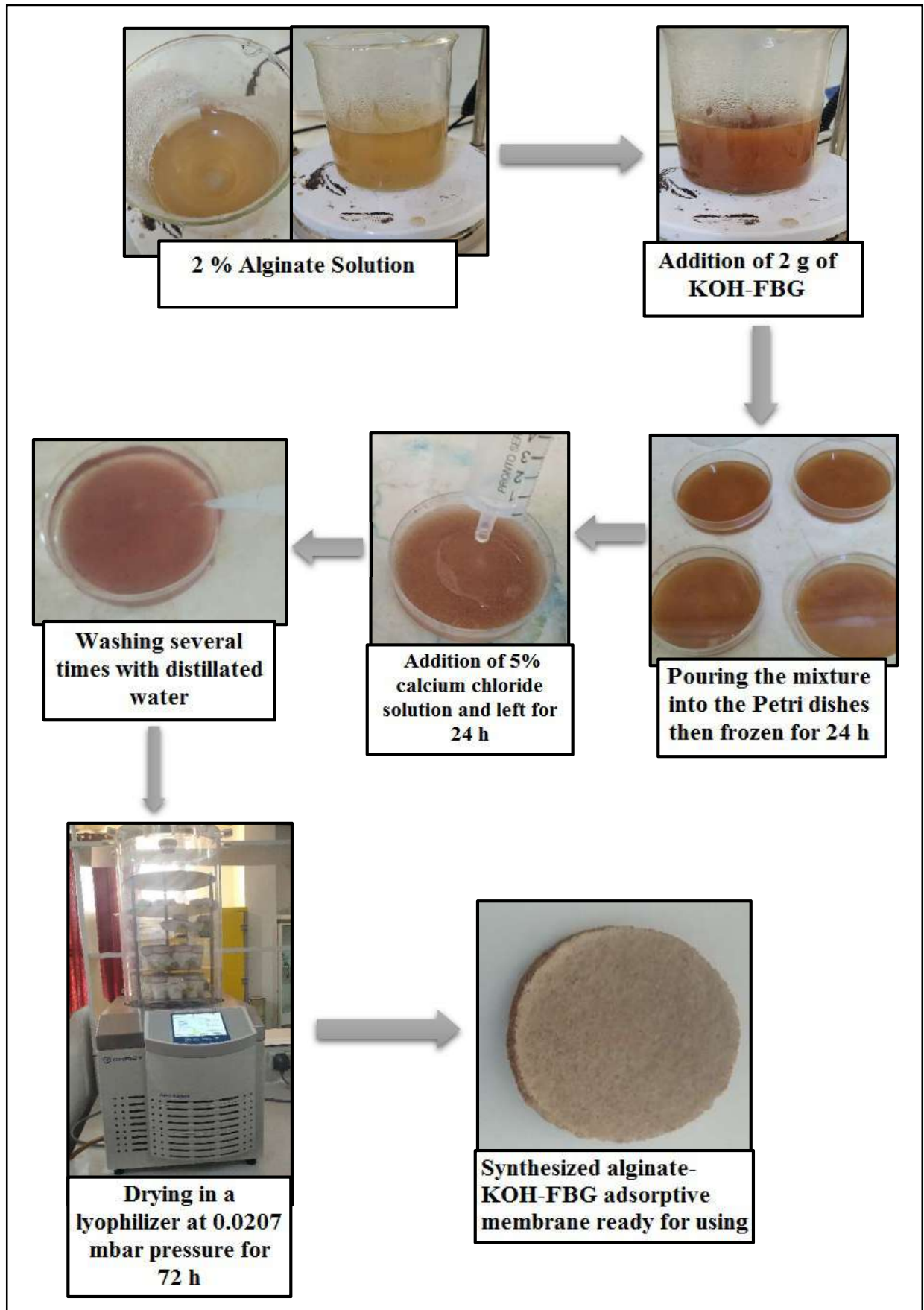


Figure V.1: Preparation of alginate-KOH-FBG adsorptive membrane plan



Figure V.2: Sampling point of drainage water

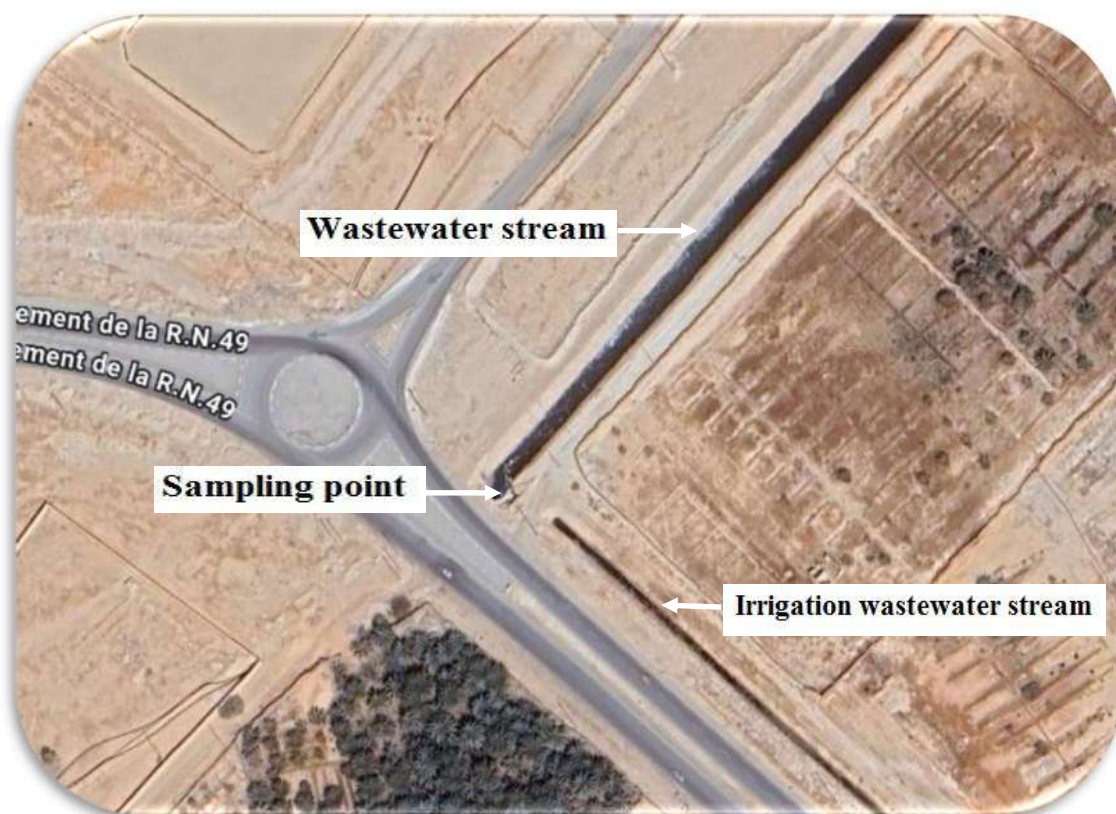


Figure V.3: Location of sampling point [220].

III.4. Filtration system design

The experimental filtration system, as depicted in figure (V.4), was designed to evaluate the performance of a composite membrane for water purification in a laboratory setting. The assembly comprised a laboratory retort stand, an effluent storage bottle, a filtrate storage bottle, and a peristaltic pump to regulate the flow.

Seven alginate-KOH-FBG adsorptive membranes were individually tested during the experiment. Each membrane was subjected to a fixed volume of effluent: 200 ml per membrane, yielding a cumulative treated volume of 1400 ml across all samples. The effluent was initially stored in a designated bottle, from which it was delivered to the membrane surface using a peristaltic pump at a controlled flow rate of 3 ml/min. After filtration through the adsorptive membrane, the filtrate was collected in a separate storage bottle for further analysis.

This setup ensured a consistent and reproducible hydraulic regime, allowing for an accurate comparison of the membrane performance. The modular arrangement also facilitates the easy replacement of membranes between trials and minimises the risk of contamination. Each filtration cycle was performed under identical operational parameters to maximise the reliability and comparability of the experimental results.

IV. Results and discussion

The experimental study investigated the efficiency of a bioadsorptive membrane, synthesized from KOH-modified date palm biomass and sodium alginate, for the treatment of real irrigation water from the Ouargla region. Laboratory analyses were performed at the National Agency for Water Resources (ANRH), and the results are summarized in the table (V.1).

- **BOD₅ Decrease (50%):** The biochemical oxygen demand was halved after filtration, reflecting the effective removal of biodegradable organic matter. While this demonstrates substantial improvement, it is slightly below the removal rates reported for advanced filtration systems in the recent literature [221].
- **COD Reduction (23.34%):** The chemical oxygen demand, which represents both organic and inorganic oxidizable materials, was moderately reduced. This modest efficiency suggests the presence of more recalcitrant compounds in the water, consistent with the reported COD/BOD₅ ratio, which indicates persistent pollutants [221].

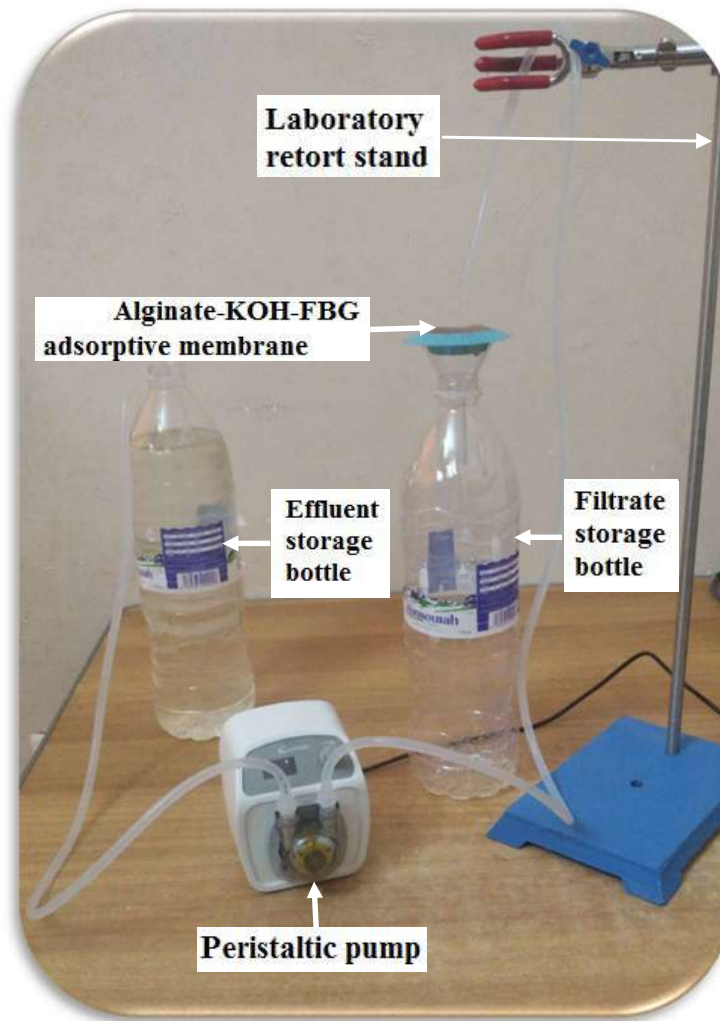


Figure V.4: Filtration system setup

- **TSS Removal (35.55%):** The removal of Total Suspended Solids was achieved at a rate of 35.55% through filtration, which effectively eliminated a substantial portion of suspended solids. However, the efficiency of this method was moderate when compared to other bioadsorptive membranes or granular filtration techniques, which can attain higher removal rates contingent upon the media and operational conditions [222]. The reduction in TSS levels diminishes the risk of soil and crop contamination, thereby enhancing crop safety and potentially increasing yields. This is particularly vital in regions experiencing water scarcity, where treated wastewater serves as a crucial resource for irrigation [223].

- **TDS Reduction (7.49%) and EC Reduction (0.83%):** Total dissolved solids and electrical conductivity parameters showed minimal reduction, which is consistent with expectations, as conventional filtration mostly targets particulate matter rather than dissolved ions. For substantial dissolved solids removal, advanced processes such as reverse osmosis or ion exchange are necessary [224; 225]. Persistently high TDS and EC indicate that treated water may still present challenges for sensitive applications.
- **Nitrate:** No nitrate was detected in either the influent or the filtrate.
- **pH and Temperature:** Both pH and temperature remained stable before and after filtration, indicating that the filtration process did not substantially alter the chemical equilibrium or thermal status of the water column. This is typical for physical filtration processes and aligns with published observations [226].

These findings confirm that bioadsorptive membranes composed of modified date palm biomass and sodium alginate can achieve moderate reductions in organic load and suspended solids in irrigation water. The modest BOD₅, COD, and TSS removal rates highlight the potential of the KOH-FBG/alginate system, although optimization may be necessary to achieve the performance targets observed in high-efficiency membrane or advanced filtration studies. The negligible change in TDS and EC is consistent with the conventional filtration theory and underscores the need for additional treatment steps if dissolved salt removal is required.

The results support the suitability of low-cost, bio-based adsorptive materials for decentralized or pretreatment applications, particularly in regions where conventional treatment infrastructure is limited. However, achieving consistently high purification for all physicochemical parameters necessitates a multistage or hybrid treatment approach.

Table V.1: Physicochemical parameters of effluent and filtrate

<i>Parameters</i>	<i>Before filtration</i>	<i>After filtration</i>	<i>Filtration efficiency rate %</i>
<i>Temperature (°C)</i>	25	25	-
<i>pH</i>	8.5	8.26	-
<i>BOD₅ (mg/l)</i>	10	5	50

<i>COD (mg/l)</i>	288	220.8	23,34
<i>TSS (mg/l)</i>	526	339	35,55
<i>TDS (mg/l)</i>	21116	19534	7,49
<i>EC (μs/cm)</i>	34185	33902	0,83
<i>NO₃⁻ (mg/l)</i>	00	00	-

Conclusion

In conclusion, this chapter demonstrated the efficacy of the fabricated composite membranes, consisting of chemically modified date palm biomass and sodium alginate, in removing a range of contaminants from drainage water, including recalcitrant organic compounds and total suspended solids. The results of continuous filtration experiments showed high removal efficiencies for BOD₅, TSS, and COD, underscoring the promising potential of this system to enhance water quality for agricultural use. Furthermore, the experimental design exhibited reusability and operational flexibility, highlighting the role of this technology in pollution control and promoting environmental sustainability. These findings reinforce the importance of developing locally sourced, cost-effective solutions tailored to the needs of arid and semi-arid regions, paving the way for the broader adoption of such bio-membranes in agricultural wastewater management. Further studies are recommended to enhance the system efficiency and expand its applicability in future large-scale operations.

General conclusion

This doctoral research presents a significant scientific contribution to the field of water pollution remediation by systematically exploring the potential of date palm by-products as sustainable and low-cost biosorbents for methylene blue dye removal. Through an integrated experimental approach encompassing detailed physicochemical characterization, targeted chemical modifications, and controlled adsorption studies, this study provides profound insights into the critical factors and underlying mechanisms governing pollutant uptake efficiency.

Furthermore, this study demonstrates the successful enhancement of the functional properties of date palm biomass to maximize the contaminant removal capacity. The findings establish a robust scientific foundation for the practical application of these abundant agro-industrial byproducts in industrial wastewater treatment, highlighting their environmental and economic viability as promising alternatives to conventional adsorbents.

A core achievement of this study is demonstrating that chemical modification significantly augments the adsorption capacity and kinetics of raw date palm biomass from various cultivars and anatomical parts.

Specifically, alkaline treatment with potassium hydroxide (KOH) yielded superior improvements compared to sulfuric acid (H_2SO_4) treatment and unmodified biomass. The maximum adsorption capacities (q_{max}) for the KOH-modified samples were approximately 4.476 mg/g for KOH-FBG, where the efficiency removal of dye exceeded 99 %.

This enhancement is attributed to the introduction and exposure of oxygen-containing functional groups, such as hydroxyl and carboxyl moieties, and the structural alterations that increase the surface roughness and porosity, as confirmed by FTIR, XRD, and SEM analyses. For example, the crystallinity index increased by up to 20% upon modification, indicating a rearrangement of the lignocellulosic matrix that is favorable for adsorption.

The highest levels of adsorption were predominantly detected within the moderately alkaline pH range (pH 7–11).

Thermodynamic evaluations revealed negative Gibbs free energy changes (ΔG°) ranging from approximately 0.68 to -5.3 kJ/mol for various modified samples, confirming the spontaneity and favorable nature of adsorption under ambient conditions. In the case of RLD, RLG, KOH-LD, KOH-LG, KOH-LT, RFBD, RFBG, H_2SO_4 -FBG, KOH-FBG, RFBT, and KOH-FBT, the

values of the Gibbs free energy change exhibited a trend of becoming less negative or may even transition to positive as the temperature increased from 298 K to 328 K, thereby signifying a reduction in the spontaneity of the adsorption process at elevated temperatures.

Furthermore, the adsorption processes were characterized as exothermic, with ΔH° values often below zero, except for the acid-modified leafy frond samples and KOH-FBD, implying that an increased temperature adversely affects dye uptake, which is a critical consideration for practical application environments.

Negative ΔS° values for the raw and KOH-modified adsorbents indicate decreased randomness at the interface during adsorption, which is consistent with an exothermic process. The positive ΔS° values for some H_2SO_4 -modified samples suggest increased disorder, likely due to structural changes or water molecule desorption.

The process conforms well to the Freundlich and Temkin isotherm models, indicating a heterogeneous and cooperative adsorption process.

Notably, the kinetics consistently aligned with the pseudo-second-order model across all samples, suggesting that chemisorption, likely involving electron sharing or exchange, is the predominant controlling mechanism rather than mere physical adsorption.

The adsorption kinetics involve a multistep process, including surface adsorption, external film diffusion, and intraparticle diffusion, with chemical modifications affecting both mass transfer and pore accessibility. Higher initial dye concentrations increase the diffusion driving force but also cause more site competition and boundary layer effects, highlighting the complex balance between kinetics and capacity.

The study also highlighted significant variability among the three date palm cultivars examined *Degla*, *Ghars*, and *Takermost* illustrating the influence of genetic and anatomical factors on biosorbent efficacy. For instance, *Degla* and *Takermost* cultivars generally exhibited higher adsorption performance than *Ghars*, especially in empty fruit bunches compared to leafy fronds. These differences underscore the importance of cultivar selection and suggest that tailored biomass processing can optimise the biosorbent properties for specific contaminants or environmental conditions.

This study notably applied KOH-modified empty fruit bunch biomass (*Ghars* cultivar) to create a sodium alginate-based bioadsorptive membrane, which effectively reduced organic pollutants

and suspended solids in irrigation water from the Ouargla region, addressing local salinity and pollution challenges.

Quantitatively, the biochemical oxygen demand (BOD₅) was reduced by 50%, chemical oxygen demand (COD) by 23.3%, and total suspended solids (TSS) by approximately 36%. Parameters such as pH and temperature remained stable during filtration. Although the membrane's effectiveness in reducing total dissolved solids (TDS) and electrical conductivity (EC) was modest (7.5% and 0.8% decreases, respectively), these results validate the feasibility of integrating date palm biomass as a functional adsorbent within membrane technologies for decentralised water treatment in arid and resource-limited settings.

Building on the findings of this study, several perspectives are suggested for continued investigation:

1. Develop environmentally friendly and scalable modification methods that minimise the use of harmful chemicals.
2. A wide range of date palm cultivars should be evaluated, considering seasonal and geographic variations, to optimise adsorbents.
3. Investigate adsorbent regeneration, durability, and life cycle impacts to ensure practical and economic feasibility of the proposed technology.
4. The adsorption behaviour in complex multi-pollutant wastewaters was studied to understand the competitive effects.
5. Combining adsorption with complementary treatments and conducting pilot-scale trials to validate real-world applications is recommended.
6. Conduct economic and social assessments to promote adoption, considering costs, acceptance, and regulations.

In conclusion, these outcomes collectively advance the dual objectives of waste valorization and environmental remediation, aligning with sustainable development goals and circular economy principles by converting abundant agricultural residues into high-value water treatment materials. The successful adoption of this biowaste not only mitigates the environmental burdens associated with date palm industry by-products but also provides accessible technological solutions for the challenging water quality issues faced in semi-arid regions.

References

- [1] Baztan, J., Bremer, S., da Cunha, C., de Rudder, A., Jaffrès, L., Jorgensen, B., Krauß, W., Marschütz, B., Peeters, D., Jensen, E. S., Vanderlinden, J. P., Wardekker, A., & Zhu, Z. (2022). Local representations of a changing climate. In *Water and Climate Change: Sustainable Development, Environmental and Policy Issues* (pp. 343–363). Elsevier. <https://doi.org/10.1016/B978-0-323-99875-8.00005-7>
- [2] Singh, V. (2024). Water Pollution. In *Textbook of Environment and Ecology* (pp. 253–266). Springer Nature Singapore. https://doi.org/10.1007/978-981-99-8846-4_17
- [3] Mehra, S., Singh, M., & Chadha, P. (2021). Adverse impact of textile dyes on the aquatic environment as well as on human beings. In *Toxicology International* (Vol. 28, Issue 2, pp. 165–176). <https://doi.org/10.18311/ti/2021/v28i2/26798>
- [4] Siddiqui, S. I., Fatima, B., Tara, N., Rathi, G., & Chaudhry, S. A. (2018). Recent advances in remediation of synthetic dyes from wastewaters using sustainable and low-cost adsorbents. In *The Impact and Prospects of Green Chemistry for Textile Technology* (pp. 471–507). Elsevier. <https://doi.org/10.1016/B978-0-08-102491-1.00015-0>
- [5] Piaskowski, K., Świdorska-Dąbrowska, R., & Zarzycki, P. K. (2018). Dye removal from water and wastewater using various physical, chemical, and biological processes. *Journal of AOAC International*, 101(5), 1371–1384. <https://doi.org/10.5740/jaoacint.18-0051>
- [6] EL-Mously, H., Midani, M., & Darwish, E. A. (2023). *Date Palm Byproducts for Green Fuels and Bioenergy Production* (pp. 271–343). https://doi.org/10.1007/978-981-99-0475-4_11
- [7] Djaafri, M., Salem, F., Kalloum, S., Desideri, U., Bartocci, P., Khelafi, M., Atabani, A. E., & Baldinelli, A. (2024). A Route for Bioenergy in the Sahara Region: Date Palm Waste Valorization through Updraft Gasification. *Energies*, 17(11). <https://doi.org/10.3390/en17112520>
- [8] Agoudjil, B., Benchabane, A., Boudenne, A., Ibos, L., & Fois, M. (2011). Renewable materials to reduce building heat loss: Characterization of date palm wood. *Energy and Buildings*, 43(2–3), 491–497. <https://doi.org/10.1016/j.enbuild.2010.10.014>
- [9] Siva Kumar, N., Asif, M., Poulouse, A. M., Al-Ghurabi, E. H., Alhamed, S. S., & Koduru, J. R. (2023). Preparation, Characterization, and Chemically Modified Date Palm Fiber Waste Biomass for Enhanced Phenol Removal from an Aqueous Environment. *Materials*, 16(11). <https://doi.org/10.3390/ma16114057>
- [10] Kaur, J. (2020). *Date Palm as a Potential Candidate for Environmental Remediation* (pp. 171–190). https://doi.org/10.1007/978-3-030-17724-9_8
- [11] <https://pubchem.ncbi.nlm.nih.gov/compound/Water> consulted on 30/07/2025

- [12] <https://en.wikipedia.org/wiki/Water> consulted on 30/07/2025
- [13] Kontogeorgis, G. M., Holster, A., Kottaki, N., Tsochantaris, E., Topsøe, F., Poulsen, J., Bache, M., Liang, X., Blom, N. S., & Kronholm, J. (2022). Water structure, properties and some applications – A review. In *Chemical Thermodynamics and Thermal Analysis* (Vol. 6). Elsevier B.V. <https://doi.org/10.1016/j.ctta.2022.100053>
- [14] https://en.wikipedia.org/wiki/Properties_of_water consulted on 30/07/2025
- [15] Brini, E., Fennell, C. J., Fernandez-Serra, M., Hribar-Lee, B., Lukšič, M., & Dill, K. A. (2017). How Water's Properties Are Encoded in Its Molecular Structure and Energies. *Chemical Reviews*, 117(19), 12385–12414. <https://doi.org/10.1021/acs.chemrev.7b00259>
- [16] Jeffrey, G. A., & Saenger, W. (1994). Hydrogen-Bonding Patterns in Water, Ices, the Hydrate Inclusion Compounds, and the Hydrate Layer Structures. In *Hydrogen Bonding in Biological Structures* (pp. 425–451). Springer Berlin Heidelberg. https://doi.org/10.1007/978-3-642-85135-3_21
- [17] Li, Q., Li, X., Yang, S., Gu, P., & Yang, G. (2019). Structure, Dynamics, and Stability of Water Molecules during Interfacial Interaction with Clay Minerals: Strong Dependence on Surface Charges. *ACS Omega*, 4(3), 5932–5936. <https://doi.org/10.1021/acsomega.9b00401>
- [18] [https://chem.libretexts.org/Bookshelves/Physical_and_Theoretical_Chemistry_Textbook_Maps/Supplemental_Modules_\(Physical_and_Theoretical_Chemistry\)/Physical_Properties_of_Matter/All_About_Water](https://chem.libretexts.org/Bookshelves/Physical_and_Theoretical_Chemistry_Textbook_Maps/Supplemental_Modules_(Physical_and_Theoretical_Chemistry)/Physical_Properties_of_Matter/All_About_Water) consulted on 31/07/2025
- [19] Maheshwary, S., Patel, N., Sathyamurthy, N., Kulkarni, A. D., & Gadre, S. R. (2001). Structure and stability of water clusters (H₂O)_n, n = 8-20: An ab initio investigation. *Journal of Physical Chemistry A*, 105(46), 10525–10537. <https://doi.org/10.1021/jp013141b>
- [20] <https://www.britannica.com/science/water> consulted on 31/07/2025
- [21] <https://pubs.rsc.org/en/content/articlelanding/2025/cp/d5cp00725> a consulted on 31/07/2025
- [22] Dargaville, B. L., & Hutmacher, D. W. (2022). Water as the often neglected medium at the interface between materials and biology. *Nature Communications*, 13(1). <https://doi.org/10.1038/s41467-022-31889-x>
- [23] Davron Khurshidovich, T. (2024). *SCIENCE TOPIC: WATER IS LIFE* (Vol. 2, Issue 5).
- [24] Robayo-Amortegui, H., Quintero-Altare, A., Florez-Navas, C., Serna-Palacios, I., Suárez-Saavedra, A., Buitrago-Bernal, R., & Casallas-Barrera, J. O. (2024). Fluid dynamics of life: exploring the physiology and importance of water in the critical illness. In *Frontiers in Medicine* (Vol. 11). Frontiers Media SA. <https://doi.org/10.3389/fmed.2024.1368502>

- [25] <https://www.unr.edu/nevada-today/news/2023/atp-why-is-water-uniqueconsulted31/07/2025>
- [26] Popkin, B. M., D’Anci, K. E., & Rosenberg, I. H. (2010). Water, hydration, and health. In *Nutrition Reviews* (Vol. 68, Issue 8, pp. 439–458). Blackwell Publishing Inc. <https://doi.org/10.1111/j.1753-4887.2010.00304.x>
- [27] Ball, P. (2017). Water is an activematrix of life for cell and molecular biology. In *Proceedings of the National Academy of Sciences of the United States of America* (Vol. 114, Issue 51, pp. 13327–13335). National Academy of Sciences. <https://doi.org/10.1073/pnas.1703781114>
- [28] Bertoluzzaa’, A., Fagnanoa, C., Morellib, M. A., Tintia, A., & Tosic, M. R. (1993). The role of water in biological systems’. In *Journal of Molecular Structure* (Vol. 291).
- [29] Griebler, C., & Avramov, M. (2015). Groundwater ecosystem services: A review. In *Freshwater Science* (Vol. 34, Issue 1, pp. 355–367). North American Benthological Society. <https://doi.org/10.1086/679903>
- [30] Vári, Á., Podschun, S. A., Erős, T., Hein, T., Pataki, B., Iojă, I. C., Adamescu, C. M., Gerhardt, A., Gruber, T., Dedić, A., Ćirić, M., Gavrilović, B., & Báldi, A. (2022). Freshwater systems and ecosystem services: Challenges and chances for cross-fertilization of disciplines. *Ambio*, 51(1), 135–151. <https://doi.org/10.1007/s13280-021-01556-4>
- [31] Muminova, R. N., & Charos, E. (2025). *THE ROLE OF WATER IN NATURE AND IN HUMAN LIFE*. <https://ijmri.de/index.php/jmsi>
- [32] do Nascimento Vieira, A., Kleinermanns, K., Martin, W. F., & Preiner, M. (2020). The ambivalent role of water at the origins of life. In *FEBS Letters* (Vol. 594, Issue 17, pp. 2717–2733). Wiley Blackwell. <https://doi.org/10.1002/1873-3468.13815>
- [33] <https://www.biotopics.co.uk/A15/water.htmlconsulted01/08/2025>
- [34] Boyd, C. E. (2015). Physical Properties of Water. In *Water Quality* (pp. 1–19). Springer International Publishing. https://doi.org/10.1007/978-3-319-17446-4_1
- [35] Harvey, A. H., & Friend, D. G. (2004). Physical properties of water. In *Aqueous Systems at Elevated Temperatures and Pressures* (pp. 1–27). Elsevier. <https://doi.org/10.1016/B978-012544461-3/50002-8>
- [36] Novák, V., & Hlaváčiková, H. (2019). Physical properties of water. In *Theory and Applications of Transport in Porous Media* (Vol. 32, pp. 29–36). Springer International Publishing. https://doi.org/10.1007/978-3-030-01806-1_3
- [37] Kirkham, M. B. (2014). Structure and Properties of Water. In *Principles of Soil and Plant Water Relations* (pp. 27–40). Elsevier. <https://doi.org/10.1016/b978-0-12-420022-7.00003-3>

- [38] Mishchuk, N. A., & Goncharuk, V. v. (2017). On the nature of physical properties of water. *Journal of Water Chemistry and Technology*, 39(3), 125–131. <https://doi.org/10.3103/S1063455X17030018>
- [39] Allen, L. C. (1974). *Physical Chemistry of Water: Water. A Comprehensive Treatise*. Felix Franks, Ed. Plenum, New York, 1973. Vol. 1, The Physics and Physical Chemistry of Water. xx, 596 pp., illus.; by subscription, 32.50. *Science*, 184(4133), 152-152.
- [40] Sharp, K. A., & Johnson, E. R. (2001). *Water: Structure and Properties*. www.els.net
- [41] Geiger, A., & Paschek, D. (2008). Water, Properties of. In *Wiley Encyclopedia of Chemical Biology* (pp. 1–9). Wiley. <https://doi.org/10.1002/9780470048672.weceb627>
- [42] Debenedetti, P. G., & Klein, M. L. (2017). Chemical physics of water. In *Proceedings of the National Academy of Sciences of the United States of America* (Vol. 114, Issue 51, pp. 13325–13326). National Academy of Sciences. <https://doi.org/10.1073/pnas.1719350115>
- [43] Truskett, T. M., & Dill, K. A. (2002). A simple statistical mechanical model of water. *Journal of Physical Chemistry B*, 106(45), 11829–11842. <https://doi.org/10.1021/jp021418h>
- [44] Sarkis, V. D. (1974). A study of water pollution. An undergraduate chemistry laboratory experience. *Journal of Chemical Education*, 51(11), 745.
- [45] Schweitzer, L., & Noblet, J. (2018). Water Contamination and Pollution. In *Green Chemistry: An Inclusive Approach* (pp. 261–290). Elsevier Inc. <https://doi.org/10.1016/B978-0-12-809270-5.00011-X>
- [46] Yadav, S. C. (2024). Water Pollution: The Problems and Solutions. *Science Insights*, 44(2), 1245–1251. <https://doi.org/10.15354/si.24.re905>
- [47] Foran, J. A., & Griggs, A. (2017). *Water Contamination* (Vol. 1). Oxford University Press. <https://doi.org/10.1093/oso/9780190662677.003.0019>
- [48] Schwarzenbach, R. P., Egly, T., Hofstetter, T. B., von Gunten, U., & Wehrli, B. (2010). Global water pollution and human health. *Annual Review of Environment and Resources*, 35, 109–136. <https://doi.org/10.1146/annurev-environ-100809-125342>
- [49] Kaur, A. (2021). Water pollution of world and human health. *Asian Journal of Research in Social Sciences and Humanities*, 11(10), 146-152.
- [50] Tarazona, J. v. (2024). Pollution, water. In *Encyclopedia of Toxicology* (pp. 809–815). Elsevier. <https://doi.org/10.1016/B978-0-12-824315-2.00188-3>
- [51] Ramakanth Reddy Tetali, Salomi K, BNV Sai Durga G, Sharon Pushpa P, & Edward Raju Gope. (2024). Analysis of Water Quality Parameters Across Diverse Sources. *Journal of Pharma Insights and Research*, 2(3), 210–216. <https://doi.org/10.69613/3jxm7e23>

- [52] Shukla, B. K., Teeli, M. A., Shukla, S. K., Chandra, R., Bharti, N., & Singh, U. (2024). A Comprehensive Overview of Vital Water Quality Parameters. *Lecture Notes in Civil Engineering*, 439, 1–20. https://doi.org/10.1007/978-981-99-6762-9_1
- [53] Roy, R., Sarkar, S., Kotak, R., Nandi, D., Shil, S., Singha, S., Sharma, K., & Tarafdar, S. (2022) Evaluation of the Water Quality Parameters from Different Point Sources: A Case Study of West Bengal. In *American Journal of Applied Bio-Technology Research (AJABTR)* (Vol. 1).
- [54] Kumar, J., Irineu Da, G., & Editors, S. (2018). *Engineering Select Proceedings of ICGCE*. <http://www.springer.com/series/15087>
- [55] Zangmo, P., Singh, D., Raza, Y., & Narayan, R. (2021). *Issue 4 www.jetir.org (ISSN-2349-5162) JETIR2104280 Journal of Emerging Technologies and Innovative Research (JETIR) www.jetir* (Vol. 8). www.jetir.org
- [56] Gorde, S. P., & Jadhav, M. v. (2013). Assessment of Water Quality Parameters: A Review. In *Journal of Engineering Research and Applications www.ijera.com* (Vol. 3). www.ijera.com
- [57] Dr. Amit Krishan, Dr. Shweta Yadav, & Ankita Srivastava. (2023). Water Pollution's Global Threat to Public Health : A Mini-Review. *International Journal of Scientific Research in Science, Engineering and Technology*, 321–334. <https://doi.org/10.32628/ijrsrset2310643>
- [58] Lin, L., Yang, H., & Xu, X. (2022). Effects of Water Pollution on Human Health and Disease Heterogeneity: A Review. In *Frontiers in Environmental Science* (Vol. 10). Frontiers Media S.A. <https://doi.org/10.3389/fenvs.2022.880246>
- [59] Dr. Vandana Rathore. (2021). IMPACTS OF WATER POLLUTION ON HUMAN HEALTH. *Journal of Science Innovations and Nature of Earth*, 09–10. <https://doi.org/10.59436/s9334m94>
- [60] V, K., N, K., T, P., J, S., & P, K. (2020). Advances in Environmental Pollution Management: Wastewater Impacts and Treatment Technologies. In *Advances in Environmental Pollution Management: Wastewater Impacts and Treatment Technologies* (pp. 1–244). Agro Environ Media - Agriculture and Environmental Science Academy, Haridwar, India. <https://doi.org/10.26832/aesa-2020-aepm>
- [61] Ali Mohamed Baba, F. (2023). *الكترونية محكمة المرج-مجلة العلوم والدراسات الإنسانية جامعة بنغازي* مجلة علمية. *Water Pollution: Causes, Impacts, and Solutions: a critical review*
- [62] Shah, M. P. (2022). *Microbial remediation of azo dyes with prokaryotes*. CRC Press.
- [63] Glover, B. (2000). Dyes, Application and Evaluation. In *Kirk-Othmer Encyclopedia of Chemical Technology*. Wiley. <https://doi.org/10.1002/0471238961.0425051907121522.a01>

- [64] Sekar, N. (2013). UV-absorbent, antimicrobial, water-repellent and other types of functional dye for technical textile applications. In *Advances in the Dyeing and Finishing of Technical Textiles* (pp. 47–77). Elsevier Inc. <https://doi.org/10.1533/9780857097613.1.47>
- [65] Slama, H. ben, Bouket, A. C., Pourhassan, Z., Alenezi, F. N., Silini, A., Cherif-Silini, H., Oszako, T., Luptakova, L., Golińska, P., & Belbahri, L. (2021). Diversity of synthetic dyes from textile industries, discharge impacts and treatment methods. *Applied Sciences (Switzerland)*, 11(14). <https://doi.org/10.3390/app11146255>
- [66] Sabnis, R. W. (2017). Manufacture of Dye Intermediates, Dyes, and Their Industrial Applications. In *Handbook of Industrial Chemistry and Biotechnology* (pp. 581–676). Springer International Publishing. https://doi.org/10.1007/978-3-319-52287-6_9
- [67] Carmen, Z., & Daniela, S. (n.d.). *Textile Organic Dyes-Characteristics, Polluting Effects and Separation/Elimination Procedures from Industrial Effluents-A Critical Overview*. www.intechopen.com
- [68] Al Prol, A. E. (2019). Study of Environmental Concerns of Dyes and Recent Textile Effluents Treatment Technology: A Review. *Asian Journal of Fisheries and Aquatic Research*, 1–18. <https://doi.org/10.9734/ajfar/2019/v3i230032>
- [69] Chan, A., Rubiyatno, & Akhmetov, Z. (2024). Environmental Impact of Synthetic Dyes on Groundwater in Malaysia: Sources, Distribution, Transport Mechanisms, and Mitigation Strategies. *Tropical Aquatic and Soil Pollution*, 4(2), 87–99. <https://doi.org/10.53623/tasp.v4i2.476>
- [70] Srivastava, R., & Sofi, I. R. (2019). Impact of synthetic dyes on human health and environment. In *Impact of Textile Dyes on Public Health and the Environment* (pp. 146–161). IGI Global. <https://doi.org/10.4018/978-1-7998-0311-9.ch007>
- [71] Sarwar, T., & Khan, S. (2022). *Textile Industry: Pollution Health Risks and Toxicity* (pp. 1–28). https://doi.org/10.1007/978-981-19-2832-1_1
- [72] Akter, T., Protity, A. T., Shaha, M., al Mamun, M., & Hashem, A. (2023). *The Impact of Textile Dyes on the Environment* (pp. 401–431). https://doi.org/10.1007/978-981-99-3901-5_17
- [73] Freeman, H. (2013). Colorant, Environmental Aspects. In *Encyclopedia of Color Science and Technology* (pp. 1–11). Springer New York. https://doi.org/10.1007/978-3-642-27851-8_151-1
- [74] Gürses, A., Açıkıldız, M., Güneş, K., & Gürses, M. S. (2016). *Colorants in Health and Environmental Aspects* (pp. 69–83). https://doi.org/10.1007/978-3-319-33892-7_5
- [75] Lekhak, U. M. (2023). Ecotoxicity of synthetic dyes. In *Current Developments in Bioengineering and Biotechnology* (pp. 45–67). Elsevier. <https://doi.org/10.1016/B978-0-323-91235-8.00021-8>

- [76] Singh, S., & Kumar, N. (2024). Removal of Dyes from Waste Water Using Low-Cost Adsorbents. *Macromolecular Symposia*, 413(5). <https://doi.org/10.1002/masy.202400156>
- [77] Kandisa, R. V., & Saibaba KV, N. (2016). Dye Removal by Adsorption: A Review. *Journal of Bioremediation & Biodegradation*, 07(06). <https://doi.org/10.4172/2155-6199.1000371>
- [78] Solayman, H. M., Hossen, Md. A., Abd Aziz, A., Yahya, N. Y., Leong, K. H., Sim, L. C., Monir, M. U., & Zoh, K.-D. (2023). Performance evaluation of dye wastewater treatment technologies: A review. *Journal of Environmental Chemical Engineering*, 11(3), 109610. <https://doi.org/10.1016/j.jece.2023.109610>
- [79] Rathinam, R., Brindha, T., Dheenadhayalan, S., & Sunitha, M. (2023). Removal of Colours in Textile Wastewater by Electrochemical Methods. *Asian Journal of Chemistry*, 35, 1291-1295.
- [80] N Lotha, T., Sorhie, V., Bharali, P., & Jamir, L. (2024). Advancement in Sustainable Wastewater Treatment: A Multifaceted Approach to Textile Dye Removal through Physical, Biological and Chemical Techniques. *ChemistrySelect*, 9(11). <https://doi.org/10.1002/slct.202304093>
- [81] Gawande, S. M., Belwalkar, N. S., & Mane, A. A. (2017). Adsorption and its Isotherm – Theory. *International Journal of Engineering Research*, 6(6), 312. <https://doi.org/10.5958/2319-6890.2017.00026.5>
- [82] Abraham, M. A. (2019). Adsorption as a waste management strategy. *Environmental Progress and Sustainable Energy*, 38(s1), S5–S6. <https://doi.org/10.1002/ep.13194>
- [83] Perry, S. G., Amos, R., & Brewer, P. I. (1973). Adsorption Chromatography: Mechanism and Materials. In *Practical Liquid Chromatography* (pp. 41–73). Springer US. https://doi.org/10.1007/978-1-4757-6226-6_3
- [84] Patterson, H. B. W. (2009). Adsorption. In *Bleaching and Purifying Fats and Oils: Theory and Practice* (pp. 53–67). Elsevier Inc. <https://doi.org/10.1016/B978-1-893997-91-2.50008-0>
- [85] Spanjaard, D., & Desjonquères, M. C. (1990). Electronic Theory of Chemisorption. In *Interaction of Atoms and Molecules with Solid Surfaces* (pp. 255–323). Springer US. https://doi.org/10.1007/978-1-4684-8777-0_9
- [86] Todres, Z. V. (2013). Effects of Sorption. In *Organic Chemistry in Confining Media* (pp. 115–127). Springer International Publishing. https://doi.org/10.1007/978-3-319-00158-6_6
- [87] Bleam, W. (2017). Surface Chemistry and Adsorption. In *Soil and Environmental Chemistry* (pp. 385–443). Elsevier. <https://doi.org/10.1016/b978-0-12-804178-9.00008-2>

- [88] Lowell, S., Shields, J. E., Thomas, M. A., & Thommes, M. (2004). *Chemisorption: Site Specific Gas Adsorption* (pp. 213–233). https://doi.org/10.1007/978-1-4020-2303-3_12
- [89] RIDEAL, E. K. (1948). Adsorption and Heterogeneous Catalysis. *Nature*, *161*(4091), 461–462. <https://doi.org/10.1038/161461a0>
- [90] Borodin, D., Rahinov, I., Shirhatti, P. R., Huang, M., Kandratsenka, A., Auerbach, D. J., Zhong, T., Guo, H., Schwarzer, D., Kitsopoulos, T. N., & Wodtke, A. M. (n.d.). *Following the microscopic pathway to adsorption through chemisorption and physisorption wells*. <http://science.sciencemag.org/>
- [91] Khan, A. H., Peikert, K., Hoffmann, F., Fröba, M., & Bertmer, M. (2019). Nitric Oxide Adsorption in Cu₃btc₂-Type MOFs - Physisorption and Chemisorption as NONOates. *Journal of Physical Chemistry C*, *123*(7), 4299–4307. <https://doi.org/10.1021/acs.jpcc.8b11919>
- [92] Long, C., Lu, Z., Li, A., Liu, W., Jiang, Z., Chen, J., & Zhang, Q. (2005). Adsorption of reactive dyes onto polymeric adsorbents: Effect of pore structure and surface chemistry group of adsorbent on adsorptive properties. *Separation and Purification Technology*, *44*(1), 91–96. <https://doi.org/10.1016/j.seppur.2004.11.007>
- [93] Birniwa, A. H., Mahmud, H. N. M. E., Abdullahi, S. S., Habibu, S., Jagaba, A. H., Ibrahim, M. N. M., Ahmad, A., Alshammari, M. B., Parveen, T., & Umar, K. (2022). Adsorption Behavior of Methylene Blue Cationic Dye in Aqueous Solution Using Polypyrrole-Polyethylenimine Nano-Adsorbent. *Polymers*, *14*(16). <https://doi.org/10.3390/polym14163362>
- [94] Zubareva, N. A., Roshchina, T. M., Khokhlova, T. D., & Shoniya, N. K. (2008). Chemistry of the surface and structural and adsorption properties of fluorinated carbon fiber and an adsorbent based on it. *Russian Journal of Physical Chemistry A*, *82*(12), 2126–2133. <https://doi.org/10.1134/S0036024408120273>
- [95] Rápó, E., & Tonk, S. (2021). Factors affecting synthetic dye adsorption; desorption studies: A review of results from the last five years (2017–2021). In *Molecules* (Vol. 26, Issue 17). MDPI. <https://doi.org/10.3390/molecules26175419>
- [96] Faizal, A. N. M., Putra, N. R., & Zaini, M. A. A. (2023). Insight into the adsorptive mechanisms of methyl violet and reactive orange from water—a short review. *Particulate Science and Technology*, *41*(5), 730–739. <https://doi.org/10.1080/02726351.2022.2140462>
- [97] Memon, S. S., Topare, N. S., Bokil, S. A., Gadekar-Shinde, S., Khedkar, S. v., & Khan, A. (2023). A Review on Effects of Operating Parameters in Batch and Column Mode for Adsorption of Methyl Violet Dye. In *International Journal of Membrane Science and Technology* (Vol. 10, Issue 3).

- [98] Mckay, G. (1982). Adsorption of Dyestuffs from Aqueous Solutions with Activated Carbon I: Equilibrium and Batch Contact-Time Studies. In *J. Chem. Tech. Biotechnol* (Vol. 32).
- [99] Ibrahim, M. M. (2019). Cr 2 O 3 /Al 2 O 3 as adsorbent: Physicochemical properties and adsorption behaviors towards removal of Congo red dye from water. *Journal of Environmental Chemical Engineering*, 7(1). <https://doi.org/10.1016/j.jece.2018.102848>
- [100] Foo, K. Y., & Hameed, B. H. (2010). Insights into the modeling of adsorption isotherm systems. In *Chemical Engineering Journal* (Vol. 156, Issue 1, pp. 2–10). <https://doi.org/10.1016/j.cej.2009.09.013>
- [101] Ho, Y. S., & Mckay, G. (1998). Chemical Engineering Journal ELSEVIER Sorption of dye from aqueous solution by peat. In *Chemical Engineering Journal* (Vol. 70).
- [102] Wang, J., & Guo, X. (2020). Adsorption isotherm models: Classification, physical meaning, application and solving method. In *Chemosphere* (Vol. 258). Elsevier Ltd. <https://doi.org/10.1016/j.chemosphere.2020.127279>
- [103] Baari, M. J., Rudi, L., & Harimu, L. (2025). Adsorption isotherms, thermodynamics, and kinetics of activated carbon as adsorbent to water pollutants: a review. In *Chimica Techno Acta* (Vol. 12). Ural Federal University. <https://doi.org/10.15826/chimtech.2025.12.2.14>
- [104] Munagapati, V. S., Yarramuthi, V., Kim, Y., Lee, K. M., & Kim, D. S. (2018). Removal of anionic dyes (Reactive Black 5 and Congo Red) from aqueous solutions using Banana Peel Powder as an adsorbent. *Ecotoxicology and Environmental Safety*, 148, 601–607. <https://doi.org/10.1016/j.ecoenv.2017.10.075>
- [105] Aichour, A., Zaghouane-Boudiaf, H., Mohamed Zuki, F. B., Kheireddine Aroua, M., & Ibbora, C. V. (2019). Low-cost, biodegradable and highly effective adsorbents for batch and column fixed bed adsorption processes of methylene blue. *Journal of Environmental Chemical Engineering*, 7(5). <https://doi.org/10.1016/j.jece.2019.103409>
- [106] Giles, C. H., MacEwan, T. H., Nakhwa, S. N., & Smith, D. (1960). 786. Studies in adsorption. Part XI. A system of classification of solution adsorption isotherms, and its use in diagnosis of adsorption mechanisms and in measurement of specific surface areas of solids. *Journal of the Chemical Society (Resumed)*, 3973–3993. <https://doi.org/10.1039/jr9600003973>
- [107] Theoretical, I., & U I T S O N, A. H. (1973). *A General Treatment and Classification of the Solute Adsorption Isotherm*.
- [108] Ragadhita, R., & Nandiyanto, A. B. D. (2021). How to calculate adsorption isotherms of particles using two-parameter monolayer adsorption models and equations. *Indonesian Journal of Science and Technology*, 6(1), 205–234. <https://doi.org/10.17509/ijost.v6i1.32354>

- [109] Dąbrowski, A. (2001). Adsorption — from theory to practice. *Advances in Colloid and Interface Science*, 93(1–3), 135–224. [https://doi.org/10.1016/S0001-8686\(00\)00082-8](https://doi.org/10.1016/S0001-8686(00)00082-8)
- [110] Ho, Y. S., & McKay, G. (1999). Pseudo-second order model for sorption processes. *Process Biochemistry*, 34(5), 451–465. [https://doi.org/10.1016/S0032-9592\(98\)00112-5](https://doi.org/10.1016/S0032-9592(98)00112-5)
- [111] Blanchard, G., Maunaye, M., & Martin, G. (1984). REMOVAL OF HEAVY METALS FROM WATERS BY MEANS OF NATURAL ZEOLITES. In *Water Res* (Vol. 18, Issue 12).
- [112] Walter, J., Weber, J. J., & Morris, J. C. (1963). SA 6 53 KINETICS OF ADSORPTION ON CARBON FROM SOLUTIONa Closure by. In *Journal of the Sanitary Engineering Division* (Vol. 89, Issue 6).
- [113] Wang, X. S., Tang, Y. P., & Tao, S. R. (2008). Removal of Cr (VI) from aqueous solutions by the nonliving biomass of Alligator weed: Kinetics and equilibrium. *Adsorption*, 14(6), 823–830. <https://doi.org/10.1007/s10450-008-9145-6>
- [114] Boyd, G. E., Adamson, A. W., & Myers, L. S. (1947). The Exchange Adsorption of Ions from Aqueous Solutions by Organic Zeolites. II. Kinetics ¹. *Journal of the American Chemical Society*, 69(11), 2836–2848. <https://doi.org/10.1021/ja01203a066>
- [115] Bakalis, E., & Zerbetto, F. (2025). Adsorption Kinetics: Classical, Fractal, or Fractional? *Langmuir*, 41(30), 19834–19844. <https://doi.org/10.1021/acs.langmuir.5c01726>
- [116] Plazinski, W., Rudzinski, W., & Plazinska, A. (2009). Theoretical models of sorption kinetics including a surface reaction mechanism: A review. In *Advances in Colloid and Interface Science* (Vol. 152, Issues 1–2, pp. 2–13). <https://doi.org/10.1016/j.cis.2009.07.009>
- [117] Hubbe, M. A., Azizian, S., & Douven, S. (2019). *Implications of Apparent Pseudo-Second-Order Adsorption Kinetics onto Cellulosic Materials: A Review*.
- [118] Chao, C. T., & Krueger, R. R. (2007). *The Date Palm (Phoenix dactylifera L.): Overview of Biology, Uses, and Cultivation*.
- [119] Al-Khayri, J. M., Mohan, S., Dennis, J., & Johnson, V. (n.d.). *Compendium of Plant Genomes The Date Palm Genome, Vol. 1 Phylogeny, Biodiversity and Mapping*. <http://www.springer.com/series/11805>
- [120] Barrow, S. C., & Barrow, S. C. (1998). A Monograph of Phoenix L. (Palmae: Coryphoideae) A Monograph of Phoenix L. (Palmae: Coryphoideae. In *Bulletin* (Vol. 53, Issue 3).
- [121] Yildiz, N., & Sohrabi, M. (2019). Hurma Ağacının (Phoenix dactylifera L.) İklim ve Toprak İstekleri Climate and Soil Requirements of Date Palm (Phoenix dactylifera L.). In *International Journal of Engineering, Design and Technology* (Vol. 1, Issue 2). <http://dergipark.gov.tr/ijedt>
- [122] Jain, S. M., & Johnson, D. V. (2015). *Date palm genetic resources and utilization* (Vol. 1). J. M. Al-Khayri (Ed.). Dordrecht, The Netherlands: Springer.

- [123] ben Salah, M., Amira, J., & SALAH Mohamed, B. (2014). Architecter Study of the Young Date Palm (*Phoenix dactylifera* L.) Root System. In *Journal of Life Sciences* (Vol. 8, Issue 5). <https://www.researchgate.net/publication/281624920>
- [124] Belarbi-Halli, R., & Dexheimer, J. (1983). *Le pneumatode chez Phoenix dactylifera L. I. Structure et ultrastructure*. www.nrcresearchpress.com
- [125] Zango, O., Pintaud, J.-C., & Rey, H. (n.d.). *Comparative Study of Architecture and Geometry of the Date Palm Male and Females Inflorescences*.
- [126] Rahmania, F., & Huon, A. (1997). Structure des cires épicuticulaires des feuilles du palmier-dattier, *Phoenix dactylifera* L. *Acta Botanica Gallica*, 144(3), 327–332. <https://doi.org/10.1080/12538078.1997.10515377>
- [127] Pintaud, J., Ludeña, B., Aberlenc-Bertossi, F., Zehdi, S., Gros-Balthazard, M., Ivorra, S., Terral, J., Tengberg Archeozoologie, C. M., Abdoukader, S., Daher, A., Nabil, M., Saro Hernández, I., González-Pérez, M., Sosa, P., Moussouni, S., Si-Dehbi, F., & Bouguedoura, N. (2013). *Biogeography of the Date Palm (Phoenix dactylifera L., Arecaceae): Insights on the Origin and on the Structure of Modern Diversity*.
- [128] Franzisky, B. L., Mueller, H. M., Du, B., Lux, T., White, P. J., Carpentier, S. C., Winkler, J. B., Schnitzler, J.-P., Kudla, J., Kangasjärvi, J., Reichelt, M., Mithöfer, A., Mayer, K. F. X., Rennenberg, H., Ache, P., Hedrich, R., Messerer, M., & Geilfus, C.-M. (2024). *Date palm acclimates to aridity by diverting organic osmolytes for root osmotic adjustment in parallel with leaf membrane remodeling and ROS scavenging*. <https://doi.org/10.1101/2024.06.07.597900>
- [129] Du, B., Kruse, J., Winkler, J. B., Alfarraj, S., Albasher, G., Schnitzler, J. P., Ache, P., Hedrich, R., & Rennenberg, H. (2021). Metabolic responses of date palm (*Phoenix dactylifera* L.) leaves to drought differ in summer and winter climate. *Tree Physiology*, 41(9), 1685–1700. <https://doi.org/10.1093/treephys/tpab027>
- [130] Yaish, M. W., & Kumar, P. P. (2015). Salt tolerance research in date palm tree (*Phoenix dactylifera* L.), past, present, and future perspectives. *Frontiers in Plant Science*, 6(MAY), 1–5. <https://doi.org/10.3389/fpls.2015.00348>
- [131] Akenous, F. Z., Anli, M., & Meddich, A. (2022). Biostimulants as Innovative Tools to Boost Date Palm (*Phoenix dactylifera* L.) Performance under Drought, Salinity, and Heavy Metal(Oid)s' Stresses: A Concise Review. In *Sustainability (Switzerland)* (Vol. 14, Issue 23). MDPI. <https://doi.org/10.3390/su142315984>
- [132] Meddich, A., Ait El Mokhtar, M., Bourzik, W., Mitsui, T., Baslam, M., & Hafidi, M. (2018). *Optimizing Growth and Tolerance of Date Palm (Phoenix dactylifera L.) to Drought, Salinity, and Vascular Fusarium-Induced Wilt (Fusarium oxysporum) by Application of Arbuscular Mycorrhizal Fungi (AMF)* (pp. 239–258). https://doi.org/10.1007/978-3-319-75910-4_9

- [133] Garcia-Maquilon, I., Coego, A., Lozano-Juste, J., Messerer, M., de Ollas, C., Julian, J., Ruiz-Partida, R., Pizzio, G., Belda-Palazón, B., Gomez-Cadenas, A., Mayer, K. F. X., Geiger, D., Alquraishi, S. A., Alrefaei, A. F., Ache, P., Hedrich, R., & Rodriguez, P. L. (2021). PYL8 ABA receptors of *Phoenix dactylifera* play a crucial role in response to abiotic stress and are stabilized by ABA. *Journal of Experimental Botany*, 72(2), 757–774. <https://doi.org/10.1093/jxb/eraa476>
- [134] Djerouni, A., Chala, A., Simozrag A, A., Benmehaia, R., & Baka, M. (2015). EVALUATION OF MALE PALMS USED IN POLLINATION AND THE EXTENT OF ITS RELATIONSHIP WITH CULTIVARS OF DATE-PALMS (PHOENIX DACTYLIFERA L.) GROWN IN REGION OF OUED RIGH, ALGERIA. In *Pak. J. Bot* (Vol. 47, Issue 5).
- [135] Benamor, B., Ghenbazi, K., Berramdane, M., Gheraissa, N., Retima, L., Cherrada, N., Chemsas, A. E., Ghemam Amara, D., & Chala, A. (2024). Chemical profiling of male date palm (*Phoenix dactylifera* L.) leaflets in El M’Ghair region, Algeria: Insights into total phenols, flavonoids, proteins, and total sugars. *Acta Agriculturae Slovenica*, 120(1). <https://doi.org/10.14720/aas.2024.120.1.16578>
- [136] ALLAM, A., DJAFRI, K., BERGOUIA, M., KHEMISSAT, E.-H., TAMA, M., & TALEB, B. (2021). MORPHOLOGICAL AND PHYSICO-CHEMICAL CHARACTERISATION OF DATE PALM CULTIVARS FROM GHARDAÏA (SOUTHEAST ALGERIA). *Journal of Applied Life Sciences and Environment*, 54(1), 12–24. <https://doi.org/10.46909/journalalse-2021-002>
- [137] Bertossi, A. (2010). *Biotechnologies du palmier dattier : actes du 3ème séminaire du réseau AUF-BIOVEG*.
- [138] Al-Obaid, R., Al-Sakran, A. A., & Muneer, S. E. (1996). Adoption of Date Palm Tissue Culture Technology Among Date Palm Producers in the Central Region of Saudi Arabia. In *Agricultural Research Center, Faculty of Food Sciences and Agriculture* (Vol. 2, Issue 145). <http://qf-research-division.org/>
- [139] Tabassum-Abbasi, M., Abbasi, S. A., & Abbasi, T. (2022). Date Palm Waste and Attempts to Use it as an Energy Source: State-of-the-Art. *Advances in Behavioral Based Safety: Proceedings of HSFEA 2020*, 43.
- [140] Benyagoub, E. (2023). An overview of *Phoenix dactylifera* L. Date Varieties in the Province of Bechar (Southwest of Algeria): Productivity and Challenges of the Date Palm Sector. *Al-Qadisiyah Journal For Agriculture Sciences*, 0(0), 166–176. <https://doi.org/10.33794/qjas.2023.145284.1150>
- [141] Burezq, H. A. (2024). Sustainable Biochar Production from Date Palms: A Scoping Review of Solutions for Arab Regions. In *International Journal of Agriculture and Natural Resources* (Vol. 51, Issue 3, pp. 157–175). Pontificia Universidad Católica de Chile, Facultad de Agronomía e Ingeniería Forestal. <https://doi.org/10.7764/ijanr.v51i3.2526>

- [142] Kumar, N. S., Asif, M., Poulouse, A. M., Al-Ghurabi, E. H., Alhamed, S. S., & Koduru, J. R. (2024). Remediation of 2,4,6-Trichlorophenol from Aqueous Solution by Raw and Chemical Modified Date Palm Stone Biomass: Kinetics and Isotherms Studies. *BioResources*, 19(2), 3543–3570. <https://doi.org/10.15376/biores.19.2.3543-3570>
- [143] Alhawtali, S., El-Harbawi, M., el Blidi, L., Alrashed, M. M., Alzobidi, A., & Yin, C. Y. (2024). Date Palm Leaflet-Derived Carbon Microspheres Activated Using Phosphoric Acid for Efficient Lead (II) Adsorption. *C-Journal of Carbon Research*, 10(1). <https://doi.org/10.3390/c10010026>
- [144] Alghamdi, A. G., & Alasmay, Z. (2023). Efficient Remediation of Cadmium- and Lead-Contaminated Water by Using Fe-Modified Date Palm Waste Biochar-Based Adsorbents. *International Journal of Environmental Research and Public Health*, 20(1). <https://doi.org/10.3390/ijerph20010802>
- [145] Aloud, S. S., Alharbi, H. A., Hameed, B. H., Giesy, J. P., Almady, S. S., & Alotaibi, K. D. (2023). Production of activated carbon from date palm stones by hydrothermal carbonization and microwave assisted KOH/NaOH mixture activation for dye adsorption. *Scientific Reports*, 13(1). <https://doi.org/10.1038/s41598-023-45864-z>
- [146] O., O. I., & E., O. (2014). Comparison of Effectiveness of Raw Okra (*Abelmoschus esculentus* L) and Raw Sugarcane (*Saccharum officinarum*) Wastes as Bioadsorbent of Heavy Metal in Aqueous Systems. *Environment and Pollution*, 4(1). <https://doi.org/10.5539/ep.v4n1p1>
- [147] Thaçi, B., Daci-Ajvazi, M., Daci, N., & Gashi, S. (2016). Valorization of Some Untreated Low Cost Adsorbents for Water Pollution Control. *Current World Environment*, 11(3), 728–736. <https://doi.org/10.12944/cwe.11.3.06>
- [148] Gupta, N., Kushwaha, A. K., & Chattopadhyaya, M. C. (2016). Application of potato (*Solanum tuberosum*) plant wastes for the removal of methylene blue and malachite green dye from aqueous solution. *Arabian Journal of Chemistry*, 9, S707–S716. <https://doi.org/10.1016/j.arabjc.2011.07.021>
- [149] El-Shafie, A. S., Hassan, S. S., Akther, N., & El-Azazy, M. (n.d.). *CIRCULAR ECONOMY FOR GLOBAL WATER SECURITY Watermelon rinds as cost-efficient adsorbent for acridine orange: a response surface methodological approach*. <https://doi.org/10.1007/s11356-021-13652-9/Published>
- [150] Mirizadeh, S., al Arni, S., Elwaheidi, M., Salih, A. A. M., Converti, A., & Casazza, A. A. (2023). Adsorption of Tetracycline and Ciprofloxacin from Aqueous Solution on Raw Date Palm Waste. *Chemical Engineering and Technology*, 46(9), 1957–1964. <https://doi.org/10.1002/ceat.202300193>

- [151] Al-Haidary, A. M. A., Zanganah, F. H. H., Al-Azawi, S. R. F., Khalili, F. I., & Al-Dujaili, A. H. (2011). A study on using date palm fibers and leaf base of palm as adsorbents for Pb(II) ions from its aqueous solution. *Water, Air, and Soil Pollution*, 214(1–4), 73–82. <https://doi.org/10.1007/s11270-010-0405-1>
- [152] Amin, M. T., Alazba, A. A., & Shafiq, M. (2016). Adsorption of copper (Cu²⁺) from aqueous solution using date palm trunk fibre: isotherms and kinetics. *Desalination and Water Treatment*, 57(47), 22454–22466. <https://doi.org/10.1080/19443994.2015.1131635>
- [153] Zeghoud, L., Gouamid, M., ben Mya, O., Rebiai, A., & Saidi, M. (2019). Adsorption of Methylene Blue Dye from Aqueous Solutions Using Two Different Parts of Palm Tree: Palm Frond Base and Palm Leaflets. *Water, Air, and Soil Pollution*, 230(8). <https://doi.org/10.1007/s11270-019-4255-1>
- [154] Dhar, R., Kim, B. S., Alblooshi, A., & Ahmad, I. (2018). Removal of synthetic cationic dye from aqueous solution using date palm leaf fibers as an adsorbent. *International Journal of Engineering and Technology (UAE)*, 7(4), 3007-3013.
- [155] Natrayan, L., Kaliappan, S., Dheeraj Kumar Reddy, C. N., Karthick, M., Sivakumar, N. S., Patil, P. P., Sekar, S., & Thanappan, S. (2022). Development and Characterization of Carbon-Based Adsorbents Derived from Agricultural Wastes and Their Effectiveness in Adsorption of Heavy Metals in Waste Water. *Bioinorganic Chemistry and Applications*, 2022. <https://doi.org/10.1155/2022/1659855>
- [156] Nguyen, H. N., Le, P. T., Nguyen, T. P., Do, T. H., Nguyen, T. D., Dinh, T. M. T., & Tran, Q. M. (2025). Removing emerging organic pollutants (oxytetracycline) by engineered biochars originated from agricultural wastes. *Environmental Progress & Sustainable Energy*, 44(1). <https://doi.org/10.1002/ep.14512>
- [157] He, Q., Qi, B., Zhang, D., & Yi, X. (2024). *Adsorption Characteristics of Methylene Blue onto Biochar Derived from Lavender Straws* (pp. 23–36). https://doi.org/10.1007/978-3-031-52901-6_3
- [158] Remmani, R., Papini, M. P., Amanat, N., & Canales, A. R. (2024). Superior Adsorption of Chlorinated VOC by Date Palm Seed Biochar: Two-Way ANOVA Comparative Analysis with Activated Carbon. *Environments - MDPI*, 11(12). <https://doi.org/10.3390/environments11120288>
- [159] Mahmoud, E. R. I., Aly, H. M., Hassan, N. A., Aljabri, A., Khan, A. L., & El-Labban, H. F. (2024). Biochar from Date Palm Waste via Two-Step Pyrolysis: A Modified Approach for Cu (II) Removal from Aqueous Solutions. *Processes*, 12(6). <https://doi.org/10.3390/pr12061189>
- [160] Zubair, M., Mu'azu, N. D., Jarrah, N., Blaisi, N. I., Aziz, H. A., & A. Al-Harthi, M. (2020). Adsorption Behavior and Mechanism of Methylene Blue, Crystal Violet, Eriochrome Black T, and Methyl Orange Dyes onto Biochar-Derived Date Palm Fronds Waste Produced at

Different Pyrolysis Conditions. *Water, Air, and Soil Pollution*, 231(5). <https://doi.org/10.1007/s11270-020-04595-x>

[161] Aichour, A., Zaghouane-Boudiaf, H., & Djafer Khodja, H. (2022). Highly removal of anionic dye from aqueous medium using a promising biochar derived from date palm petioles: Characterization, adsorption properties and reuse studies. *Arabian Journal of Chemistry*, 15(1). <https://doi.org/10.1016/j.arabjc.2021.103542>

[162] Khadhri, N., el Khames Saad, M., ben Mosbah, M., & Moussaoui, Y. (2019). Batch and continuous column adsorption of indigo carmine onto activated carbon derived from date palm petiole. *Journal of Environmental Chemical Engineering*, 7(1). <https://doi.org/10.1016/j.jece.2018.11.020>

[163] Liu, G., Dai, Z., Liu, X., Dahlgren, R. A., & Xu, J. (2022). Modification of agricultural wastes to improve sorption capacities for pollutant removal from water – a review. In *Carbon Research* (Vol. 1, Issue 1). Springer Nature. <https://doi.org/10.1007/s44246-022-00025-1>

[164] Park, D., Yun, Y. S., & Park, J. M. (2010). The past, present, and future trends of biosorption. In *Biotechnology and Bioprocess Engineering* (Vol. 15, Issue 1, pp. 86–102). <https://doi.org/10.1007/s12257-009-0199-4>

[165] Fathy, N. A., El-Shafey, O. I., & Khalil, L. B. (2013). Effectiveness of Alkali-Acid Treatment in Enhancement the Adsorption Capacity for Rice Straw: The Removal of Methylene Blue Dye. *ISRN Physical Chemistry*, 2013, 1–15. <https://doi.org/10.1155/2013/208087>

[166] Kovacova, Z., Demcak, S., Balintova, M., Pla, C., & Zinicovscaia, I. (2020). Influence of wooden sawdust treatments on Cu(II) and Zn(II) removal from water. *Materials*, 13(16). <https://doi.org/10.3390/MA13163575>

[167] Castro, D., Rosas-Laverde, N. M., Aldás, M. B., Almeida-Naranjo, C. E., Guerrero, V. H., & Pruna, A. I. (2021). Chemical Modification of Agro-Industrial Waste-Based Bioadsorbents for Enhanced Removal of Zn(II) Ions from Aqueous Solutions. *Materials*, 14(9). <https://doi.org/10.3390/ma14092134>

[168] Jawad, A. H., Abdulhameed, A. S., & Mastuli, M. S. (2020). Acid-fractionalized biomass material for methylene blue dye removal: a comprehensive adsorption and mechanism study. *Journal of Taibah University for Science*, 14(1), 305–313. <https://doi.org/10.1080/16583655.2020.1736767>

[169] Hafeez, Ainy, et al. "Optimization of Zinc Ions Removal by Modified Phoenix Dactylifera L. Seeds Using Response Surface Methodology." *Journal of the Chemical Society of Pakistan*, vol. 41, no. 1, 28 Feb. 2019, p. 78. *Gale Academic OneFile*, link.gale.com/apps/doc/A579553450/AONE?u=anon~f9e45d10&sid=googleScholar&xid=84f549ca. Accessed 10 Aug. 2025.

[170] Rajamohan, N., Rajasimman, M., & Dilipkumar, M. (2014). Parametric and kinetic studies on biosorption of mercury using modified Phoenix dactylifera biomass. *Journal of the*

Taiwan Institute of Chemical Engineers, 45(5), 2622–2627.
<https://doi.org/10.1016/j.jtice.2014.07.004>

[172] Yadav, S. K., Sinha, S., & Singh, D. K. (2015). Chromium(VI) removal from aqueous solution and industrial wastewater by modified date palm trunk. *Environmental Progress and Sustainable Energy*, 34(2), 452–460. <https://doi.org/10.1002/ep.12014>

[173] https://d-maps.com/carte.php?num_car=4429&lang=frconsulted29/06/2025

[174] Al-Ghouti, M. A., Li, J., Salamh, Y., Al-Laqtah, N., Walker, G., & Ahmad, M. N. M. (2010). Adsorption mechanisms of removing heavy metals and dyes from aqueous solution using date pits solid adsorbent. *Journal of Hazardous Materials*, 176(1–3), 510–520. <https://doi.org/10.1016/j.jhazmat.2009.11.059>

[175] Alsenani, G. (2014). Removal of Congo red dye from aqueous solution by date palm leaf base. *American Journal of Applied Sciences*, 11(9), 1553–1557. <https://doi.org/10.3844/ajassp.2014.1553.1557>

[176] Aichour, A., & Zaghouane-Boudiaf, H. (2020). Single and competitive adsorption studies of two cationic dyes from aqueous mediums onto cellulose-based modified citrus peels/calcium alginate composite. *International Journal of Biological Macromolecules*, 154, 1227–1236. <https://doi.org/10.1016/j.ijbiomac.2019.10.277>

[177] Ameh, E. S. (2019). A review of basic crystallography and x-ray diffraction applications. *International Journal of Advanced Manufacturing Technology*, 105(7–8), 3289–3302. <https://doi.org/10.1007/s00170-019-04508-1>

[178] Andersen, L. K., Morgan, T. J., Boulamanti, A. K., Álvarez, P., Vassilev, S. v., & Baxter, D. (2013). Quantitative X-ray fluorescence analysis of biomass: Objective evaluation of a typical commercial multi-element method on a WD-XRF spectrometer. *Energy and Fuels*, 27(12), 7439–7454. <https://doi.org/10.1021/ef4015394>

[179] Cheah, Y. S., & Masaharu, K. (2023). Comparison of crystallinity index computational methods based on lignocellulose X-ray diffractogram. *Materials Research Proceedings*, 29, 128–134. <https://doi.org/10.21741/9781644902516-16>

[180] kumari, P., Veerangouda, M., Palled, V., Anantachar, M., Hiregoudar, S., M. Naik, N., & Beladadhi, R. V. (2019). Effect of Potassium Hydroxide (KOH) Pretreatment on Solids Recovery, Delignification and Total Sugars of Cotton Stalk. *International Journal of Current Microbiology and Applied Sciences*, 8(02), 2457–2467. <https://doi.org/10.20546/ijcmas.2019.802.286>

[181] Liu, Y., Xie, J., Wu, N., Ma, Y., Menon, C., & Tong, J. (2019). Characterization of natural cellulose fiber from corn stalk waste subjected to different surface treatments. *Cellulose*, 26(8), 4707–4719. <https://doi.org/10.1007/s10570-019-02429-6>

- [182] Siddiqui, S. H., Uddin, M. K., Isaac, R., & Aldosari, O. F. (2022). An Effective Biomass for the Adsorption of Methylene Blue Dye and Treatment of River Water. *Adsorption Science and Technology*, 2022. <https://doi.org/10.1155/2022/4143138>
- [183] Boumediene, M., Benaïssa, H., George, B., Molina, S., & Merlin, A. (2018). Effects of pH and ionic strength on methylene blue removal from synthetic aqueous solutions by sorption onto orange peel and desorption study. *J. Mater. Environ. Sci*, 9(6), 1700–1711. <https://doi.org/10.26872/jmes.2018.9.6.190>
- [184] Galloni, M. G., Bortolotto, V., Falletta, E., & Bianchi, C. L. (2022). pH-Driven Selective Adsorption of Multi-Dyes Solutions by Loofah Sponge and Polyaniline-Modified Loofah Sponge. *Polymers*, 14(22). <https://doi.org/10.3390/polym14224897>
- [185] Aziam, R., Chiban, M., Eddaoudi, E., Soudani, A., Zerbet, M., & Sinan, F. (2016). Factors controlling the adsorption of acid blue 113 dye from aqueous solution by dried *C. edulis* plant as natural adsorbent. *Arabian Journal of Geosciences*, 9(15). <https://doi.org/10.1007/s12517-016-2675-4>
- [186] Shukla, A., Zhang, Y.-H., Dubey, P., Margrave, J. L., & Shukla, S. S. (2002). The role of sawdust in the removal of unwanted materials from water. In *Journal of Hazardous Materials* (Vol. 95).
- [187] Abdelrazek, E. J. E., Gahlan, A. A., Gouda, G. A., & Ahmed, A. S. A. (2025). Cost-effective adsorption of cationic dyes using ZnO nanorods supported by orange peel-derived carbon. *Scientific Reports*, 15(1). <https://doi.org/10.1038/s41598-025-86209-2>
- [188] Ma, L., Jiang, C., Lin, Z., & Zou, Z. (2018). Microwave-hydrothermal treated grape peel as an efficient biosorbent for methylene blue removal. *International Journal of Environmental Research and Public Health*, 15(2). <https://doi.org/10.3390/ijerph15020239>
- [189] Shafiq, M., Alazba, A. A., & Amin, M. T. (2018). Removal of heavy metals from wastewater using date palm as a biosorbent: A comparative review. In *Sains Malaysiana* (Vol. 47, Issue 1, pp. 35–49). Penerbit Universiti Kebangsaan Malaysia. <https://doi.org/10.17576/jsm-2018-4701-05>
- [190] Hammari, A. M., Abubakar, H., Misau, M. I., Aroke, U. O., & Hamza, U. D. (2020). Adsorption Equilibrium and Kinetic Studies of Methylene Blue Dye Using Groundnut Shell and Sorghum Husk Biosorbent. In *JEBAT* (Vol. 3, Issue 2). <http://journal.hibiscuspublisher.com/index.php/JEBAT/index>
- [191] Li, N., Zhu, X., Miao, Y., Wang, Z., Lin, C. S. K., & Li, C. (2025). Meta-analysis and empirical research on the effectiveness of biochar in remediating tetracyclines pollution in water bodies. *Bioresource Technology*, 435. <https://doi.org/10.1016/j.biortech.2025.132917>
- [192] Mohammadzadeh, F., Golshan, M., Haddadi-Asl, V., & Salami-Kalajahi, M. (2023). Adsorption kinetics of methylene blue from wastewater using pH-sensitive starch-based hydrogels. *Scientific Reports*, 13(1). <https://doi.org/10.1038/s41598-023-39241-z>

- [193] Kaveeshwar, A. R. (2018). Removal of Barium (II), Iron (II), and Strontium (II) from Fracking Wastewater Using Pecan Shell-Based Activated Carbon: Modelling of Adsorption Kinetics, Isotherms, and Thermodynamic Analysis. *University of Louisiana at Lafayette*.
- [194] Aichour, A., Zaghouane-Boudiaf, H., Iborra, C. V., & Polo, M. S. (2018). Bioadsorbent beads prepared from activated biomass/alginate for enhanced removal of cationic dye from water medium: Kinetics, equilibrium and thermodynamic studies. *Journal of Molecular Liquids*, 256, 533–540. <https://doi.org/10.1016/j.molliq.2018.02.073>
- [195] Lian, Q. (2018). Adsorption of Lead (II) onto Phosphate Modified Ordered Mesoporous Carbon: Kinetics, Isotherm, Mechanism, Thermodynamic and Diffusion-Controlled Study. *University of Louisiana at Lafayette*.
- [196] Ahmad, T., Danish, M., Rafatullah, M., Ghazali, A., Sulaiman, O., Hashim, R., & Ibrahim, M. N. M. (2012). The use of date palm as a potential adsorbent for wastewater treatment: A review. In *Environmental Science and Pollution Research* (Vol. 19, Issue 5, pp. 1464–1484). <https://doi.org/10.1007/s11356-011-0709-8>
- [197] Chigbundu, E. C., & Adebawale, K. O. (2017). Equilibrium and fractal-like kinetic studies of the sorption of acid and basic dyes onto watermelon shell (*Citrullus vulgaris*). *Cellulose*, 24(11), 4701–4714. <https://doi.org/10.1007/s10570-017-1488-2>
- [198] Mahmoud, M. A. (2013). Kinetics and Thermodynamics of Date Palm Fibers (DPF) as Agricultural Waste Materials. *Journal of Chromatography & Separation Techniques*, 04(07). <https://doi.org/10.4172/2157-7064.1000194>
- [199] Al-Rub, F. A. A. (2006). Biosorption of zinc on palm tree leaves: Equilibrium, kinetics, and thermodynamics studies. *Separation Science and Technology*, 41(15), 3499–3515. <https://doi.org/10.1080/01496390600915015>
- [200] Bouafia, H., Lamine Sekrifa, M., & Touil, Y. (2024). Removal of Methylene Blue from Aqueous Solutions Using Date Palm By-Products from Algerian Sahara: Cultivar Variations Effect. *ChemistrySelect*, 9(17). <https://doi.org/10.1002/slct.202303978>
- [201] Zou, W., Bai, H., Gao, S., & Li, K. (2013). Characterization of modified sawdust, kinetic and equilibrium study about methylene blue adsorption in batch mode. *Korean Journal of Chemical Engineering*, 30(1), 111–122. <https://doi.org/10.1007/s11814-012-0096-y>
- [202] Soltani, A., Faramarzi, M., & Parsa, S. A. M. (2021). A review on adsorbent parameters for removal of dye products from industrial wastewater. In *Water Quality Research Journal* (Vol. 56, Issue 4, pp. 181–193). IWA Publishing. <https://doi.org/10.2166/wqrj.2021.023>
- [203] Oetjik, W., & Aida Ibrahim, S. (2021). A Review: The Effect of Initial Dye Concentration and Contact Time on The Process of Dye Adsorption using Agricultural Wastes Adsorbent. *Progress in Engineering Application and Technology*, 2(2), 1051–1059. <https://doi.org/10.30880/peat.2021.02.02.094>
- [204] Yilmaz, P., Gunduz, D., & Ozbek, B. (2021). Utilization of low-cost bio-waste adsorbent for methylene blue dye removal from aqueous solutions and optimization of process variables

- by response surface methodology approach. *Desalination and Water Treatment*, 224, 367–388. <https://doi.org/10.5004/dwt.2021.27206>
- [205] Hasani, S., Ardejani, F. D., & Olya, M. E. (2017). Equilibrium and kinetic studies of azo dye (Basic Red 18) adsorption onto montmorillonite: Numerical simulation and laboratory experiments. *Korean Journal of Chemical Engineering*, 34(8), 2265–2274. <https://doi.org/10.1007/s11814-017-0110-5>
- [206] Dharmarathna, S. P., & Priyantha, N. (2024). Investigation of boundary layer effect of intra-particle diffusion on methylene blue adsorption on activated carbon. *Energy Nexus*, 14, 100294. <https://doi.org/10.1016/j.nexus.2024.100294>
- [207] Idider, T. (2007). *Article scientifique Le problème des excédents hydriques à Ouargla : situation actuelle et perspectives d'amélioration**. <https://doi.org/10.1684/sec.2007.0085>
- [208] Hamdi, W., Youcefi, M., Touil, Y., Bougrinat, R., Ferhi, N., & Ould El Hadj, M. D. (2012). CONTRIBUTION À L'ÉTUDE DE QUELQUES CARACTÉRISTIQUES PHYSICO-CHIMIQUES ET HYGIÉNIQUES DES EAUX USÉES ISSUES DE REJETS DE CERTAINES LOCALITÉS DE LA CUVETTE DE OUARGLA (SAHARA SEPTENTRIONAL EST ALGÉRIEN): IMPACT SUR LE MILIEU RÉCEPTEUR. *Algerian Journal of Arid Environment "AJAE"*, 2(1), 56-63.
- [209] Sofiane, S., Bachi, O. E. K., & Yamina, G. (2013). Etude de la Qualité Physico-chimique des Eaux de la Nappe Phréatique de la Région de Ouargla (Sahara Septentrional de L'Algérie). *Tunis. J. Med. Plants Nat. Prod*, 9, 44-48.
- [210] Barakat, M. A. (2011). New trends in removing heavy metals from industrial wastewater. In *Arabian Journal of Chemistry* (Vol. 4, Issue 4, pp. 361–377). <https://doi.org/10.1016/j.arabjc.2010.07.019>
- [211] Guan, X., Zhang, B., Li, D., Ren, J., Zhu, Y., Han, Q., & Rao, P. (2023). Adsorption-based filtration membranes for wastewater treatment. In *Adsorption through Advanced Nanoscale Materials* (pp. 259–285). Elsevier. <https://doi.org/10.1016/B978-0-443-18456-7.00012-2>
- [212] Qalyoubi, L., Zuburtikudis, I., Abu Khalifeh, H., & Nashef, E. (2023). Adsorptive Membranes Incorporating Ionic Liquids (ILs), Deep Eutectic Solvents (DESs) or Graphene Oxide (GO) for Metal Salts Extraction from Aqueous Feed. *Membranes*, 13(11), 874. <https://doi.org/10.3390/membranes13110874>
- [213] Guan, K., Fang, S., Zhou, S., Fu, W., Li, Z., Gonzales, R. R., Xu, P., Mai, Z., Hu, M., Zhang, P., & Matsuyama, H. (2023). Thin film composite membrane with improved permeance for reverse osmosis and organic solvent reverse osmosis. *Journal of Membrane Science*, 688, 122104. <https://doi.org/10.1016/j.memsci.2023.122104>
- [214] Durrani, W. Z., Nasrullah, A., Khan, A. S., Fagieh, T. M., Bakhsh, E. M., Akhtar, K., Khan, S. B., Din, I. U., Khan, M. A., & Bokhari, A. (2022). Adsorption efficiency of date palm

- based activated carbon-alginate membrane for methylene blue. *Chemosphere*, 302. <https://doi.org/10.1016/j.chemosphere.2022.134793>
- [215] Taheran, M. (2018). *Développement d'un module membranaire imprégné par des enzymes ligninolytiques et de biochar pour la dégradation de composés pharmaceutiques* (Doctoral dissertation, Institut National de la Recherche Scientifique (Canada)).
- [216] Li, Q., Li, Y., Ma, X., Du, Q., Sui, K., Wang, D., Wang, C., Li, H., & Xia, Y. (2017). Filtration and adsorption properties of porous calcium alginate membrane for methylene blue removal from water. *Chemical Engineering Journal*, 316, 623–630. <https://doi.org/10.1016/j.cej.2017.01.098>
- [217] Rijal, M. S., Nasir, M., Purwasasmita, B. S., & Asri, L. A. T. W. (2023). Cellulose nanocrystals-microfibrils biocomposite with improved membrane performance. *Carbohydrate Polymer Technologies and Applications*, 5, 100326. <https://doi.org/10.1016/j.carpta.2023.100326>
- [218] Vo, T. S., Hossain, M. M., Jeong, H. M., & Kim, K. (2020). Heavy metal removal applications using adsorptive membranes. In *Nano Convergence* (Vol. 7, Issue 1). Korea Nano Technology Research Society. <https://doi.org/10.1186/s40580-020-00245-4>
- [219] Zhu, M., Zhu, L., Wang, J., Yue, T., Li, R., & Li, Z. (2017). Adsorption of Cd(II) and Pb(II) by in situ oxidized Fe₃O₄ membrane grafted on 316L porous stainless steel filter tube and its potential application for drinking water treatment. *Journal of Environmental Management*, 196, 127–136. <https://doi.org/10.1016/j.jenvman.2017.02.073>
- [220] https://goo.gl/maps/wEu6DVQavBtoGV2JA?g_st=amconsulted29/06/2025
- [221] al Kholif, M., Nurhayati, I., Sugito, Sari, D. A., Sutrisno, J., Pungut, & Mujiyanti, D. R. (2023). Removal of BOD₅ and COD from Domestic Wastewater by Using a Multi-Media-Layering (MML) System. *Environment and Natural Resources Journal*, 21(6), 534–544. <https://doi.org/10.32526/ennrj/21/20230202>
- [222] Josse, R. G., Toklo, R. M., Dossou-Yovo, P., & Fatombi, J. K. (2017). Valorisation des sciures du bois de *Moringa oleifera* dans le traitement physico-chimique des lixiviats du lieu d'enfouissement sanitaire (LES) de Ouèssè/Ouidah (Sud Bénin). *Journal of Applied Biosciences*, 96(1), 9109. <https://doi.org/10.4314/jab.v96i1.8>
- [223] Christou, A., Beretsou, V. G., Iakovides, I. C., Karaolia, P., Michael, C., Benmarhnia, T., Chefetz, B., Donner, E., Gawlik, B. M., Lee, Y., Lim, T. T., Lundy, L., Maffettone, R., Rizzo, L., Topp, E., & Fatta-Kassinos, D. (2024). Sustainable wastewater reuse for agriculture. In *Nature Reviews Earth and Environment* (Vol. 5, Issue 7, pp. 504–521). Springer Nature. <https://doi.org/10.1038/s43017-024-00560-y>
- [224] Pushpalatha, N., Sreeja, V., Karthik, R., & Saravanan, G. (2022). Total Dissolved Solids and Their Removal Techniques. *International Journal of Environmental Sustainability and Protection*, 2(2), 13–20. <https://doi.org/10.35745/ijesp2022v02.02.0002>

[225] Wu, S. (Xiao), & Maskaly, J. (2018). Study on the effect of total dissolved solids (TDS) on the performance of an SBR for COD and nutrients removal. *Journal of Environmental Science and Health - Part A Toxic/Hazardous Substances and Environmental Engineering*, 53(2), 146–153. <https://doi.org/10.1080/10934529.2017.1383130>

[226] Nasir Laghari, A., das Walasai, G., Rehman Jatoi, A., Akhtar Shaikh, F., & Ali Siyal, Z. (2018). www.etasr.com Laghari et al.: Performance Analysis of Water Filtration Units for Reduction of pH. In *Technology & Applied Science Research* (Vol. 8, Issue 4). Turbidity. www.etasr.com